

Decomposition Reactions in Aromatic Nitration

Dissertation presented for the Doctor of Philosophy degree in
Refining, Petrochemical and Chemical Engineering

by

Diogo Manuel Nobre Afonso

Supervision: Doctor Alejandro França Gomes Ribeiro

Professor Luís Miguel Madeira

Professor Joaquim Silvério Marques Vital

Porto, July 2019

Trabalho financiado pela Fundação para a Ciência e Tecnologia e pela Bondalti Chemicals S.A., no âmbito do Programa Doutoral em Engenharia da Refinação, Petroquímica e Química
(PD/BDE/113546/2015)



Agradecimentos

Finda uma nova etapa do meu percurso académico, gostaria de expressar o meu agradecimento a todos que partilharam comigo esta experiência.

O meu primeiro agradecimento vai para os meus orientadores, Alejandro Ribeiro, Professor Luís Miguel Madeira e Professor Joaquim Vital, por todo o tempo, paciência e empenho que dedicaram para que este trabalho chegasse a um bom porto. Agradeço todos os conhecimentos partilhados e por acreditaram no sucesso deste trabalho. Gostaria de deixar um agradecimento ao Paulo Araújo pelo acompanhamento do trabalho e um agradecimento especial ao Alejandro Ribeiro por todo o esforço e dedicação que colocou neste trabalho e pela amizade com que me recebeu na Bondalti e com que sempre me ajudou.

Agradeço à Bondalti Chemicals, S.A. por ter permitido que este douramento se tivesse realizado em ambiente industrial e pela disponibilização de todo o material necessário à realização deste.

À Fundação para a Ciência e Tecnologia (FCT) pelo apoio financeiro concedido através da bolsa de doutoramento em ambiente empresarial ao abrigo do Programa Doutoral em Engenharia da Refinação, Petroquímica e Química (PD/BDE/113546/2015). À unidade de investigação UID/EQU/005511/2019 – Laboratório de Engenharia de Processos, Ambiente, Biotecnologia e Energia – LEPABE – financiado por fundos nacionais através da FCT/MCTES (PIDDAC).

A todos os companheiros da Bondalti, principalmente: Ana Afonso, Hugo Pedreiras, Rui Andrade. Não poderia deixar de escrever um agradecimento à Dulce Silva, Susana Caldas e ao Leonardo Sequeira pela boa disposição e companheirismo diários nas nossas viagens Porto – Estarreja – Porto.

Ao pessoal do contentor / palacete em especial à Joana Duarte, Filipa Franco, Pedro Gonçalves, Rui Churro.

À minha família agradeço todo o apoio e ajuda ao longo desta longa caminhada. Aos meus pais pela educação que me inculcaram, pelo apoio e pelas oportunidades que me deram e que permitiram que chegasse ao fim desta etapa. Às minhas irmãs por me terem sempre acompanhado e dado força, tanto a nível pessoal como académico e profissional.

À Diana, que me incentivou a aceitar este desafio, pela fantástica pessoa que és, pelo apoio incondicional que sempre me deste, por estares ao meu lado ao longo de todos estes anos, por tudo o que já vivemos e iremos viver e por sempre teres confiado que era capaz de finalizar esta etapa.

Abstract

Mononitrobenzene (MNB) is an important chemical commodity used mainly in the production of aniline, although having numerous other applications. Due to MNB importance to our daily lives, benzene nitration has been subject to continuous improvements and studies aiming the increase of the reaction productivity and, consequently, the reduction of the reaction by-products formation. Currently, the state-of-the-art process for producing MNB is the adiabatic one. In this process, benzene is mixed with a mixture of sulfuric and nitric acid, the so-called mixed acid. MNB formation results from the reaction between benzene and nitric acid catalysed by sulfuric acid. Moreover, sulfuric acid acts also as a heat sink absorbing the heat released during the strongly exothermic reaction.

However, despite all the improvements achieved in benzene nitration, there are still some gaps regarding the formation of the reaction by-products that were meant to be suppressed with the present work. Some studies have already been performed focused in the minimization of the typical benzene nitration by-products, nitrophenols and dinitrobenzene. In this work it was intended to study and justify the appearance of carbon dioxide (under the form of ammonium carbonate) in the MNB production process, aiming to determine if the source of this gas is the raw material (i.e., benzene), the typical impurities present in the nitration grade benzene (*n*-hexane, methylcyclohexane, toluene, etc.), the reaction by-products or the chemical species present in the reaction medium and unknown to date.

The performed studies in the benzene nitration plant allowed detecting carbon dioxide in the reaction stage and evidenced that the gas is formed in the mentioned plant section. Such finding suggests the occurrence of oxidation reactions during benzene nitration, which is corroborated by the detection of oxidized compounds in the reaction medium that were found to be dicarboxylic acids, namely oxalic acid, mesoxalic acid, fumaric acid, maleic acid, succinic acid, and adipic acid. The detection of these dicarboxylic acids allowed postulating a CO₂ formation path, based in oxidation processes and in the compounds present in the nitration media, which involved phenol formation and oxidation.

During this work, it was found for the first time that phenol is present in the benzene nitration medium of both industrial and laboratory samples and that this compound is the nitrophenols precursor, as theoretically suggested in the literature. Additionally, phenol detection in the nitration media supports the postulated formation path of the dicarboxylic acids and carbon dioxide.

Besides phenol detection, it was evidenced that nitrophenols are formed by consecutive reactions, i.e., mononitrophenols are nitrated to dinitrophenols, which, in turn, origin trinitrophenol; the different reactivities of these compounds was also evidenced. The impact of the main reaction parameters on the nitrophenols formation was evaluated and their temporal concentration profiles

exhibited upon experiments carried out in a batch reactor, an unusual aspect in benzene nitration studies. Furthermore, the obtained results allowed the construction of kinetic models (with good adherence to experimental data), one that demonstrated phenol's high reactivity while supporting its role as the nitrophenols precursor, and another that described nitrophenols interconversion for different operation conditions.

While searching for unknown chemical compounds in the nitration media, seeking to explain CO₂ origin and formation path, a new class of reaction by-products was detected, to date not mentioned in studies focused on benzene nitration. These compounds, detected in industrial samples, were found to be sulfonic acids, namely, benzenesulfonic acid, 2-mononitrobenzenesulfonic acid, 3-mononitrobenzenesulfonic acid and 4-mononitrobenzenesulfonic acid. The formation of such chemical species was then studied in lab scale benzene nitrations, being shown that they are formed during benzene nitration, either by benzene sulfonation followed by benzenesulfonic acid nitration or by benzene nitration followed by mononitrobenzene sulfonation. A parametric study was carried out to assess the effect of some operation conditions on the sulfonic acids genesis, which enabled concluding that the reaction temperature and the sulfuric acid concentration are important parameters affecting their formation. It was also evidenced that the studied sulfonic acids have a higher affinity into the reaction aqueous phase than to the organic one.

Other lab scale reactions were conducted, in the range of the industrial operating conditions, in which pure benzene, benzene enriched in typical impurities from the production process (toluene, *n*-hexane, methylcyclohexane, etc.) and benzene enriched in the reaction by-products, known or detected during this work, were nitrated. The obtained results enabled revealing that the organic species responsible for the generation of the decomposition products (CO and CO₂) is the reaction's raw material, benzene. Such finding is opposite to what is stated in the literature, which is that CO₂ is formed due to the decomposition of the aliphatic compounds present in the reaction medium. The effect of some operating conditions on carbon dioxide, nitrophenols, and oxalic acid formation was also studied while conducting pure benzene nitrations, having been verified that the formation of these chemical compounds is influenced by the reaction temperature, sulfuric and nitric acid concentration, and by the benzene / nitric acid ratio. Furthermore, the conducted tests evidenced the occurrence of oxidation reactions during benzene nitration to mononitrobenzene, responsible for phenol formation and the subsequent nitrophenols generation by consecutive nitrations, and by phenol oxidation, yielding thus dicarboxylic acids which are decomposed into CO and CO₂.

Resumo

O mononitrobenzeno é um importante intermediário químico usado essencialmente como matéria-prima na produção de anilina, podendo também ser utilizado numa diversidade de outras aplicações. Dada a importância do mononitrobenzeno, a reação de nitração de benzeno tem sido alvo de diversos estudos e melhorias que visam o aumento da produtividade e a consequente redução dos subprodutos formados. Atualmente, o processo produtivo de referência para a síntese de mononitrobenzeno baseia-se na tecnologia de nitração adiabática. De acordo com esta tecnologia processual, o benzeno é misturado com ácido sulfúrico e ácido nítrico, sendo a mistura destes ácidos conhecida como ácido misto. A formação de mononitrobenzeno resulta da reação entre o benzeno e o ácido nítrico. Para além de ser o catalisador da reação, o ácido sulfúrico tem também a função de absorver a energia libertada pela nitração de benzeno, uma reação extremamente exotérmica.

Apesar de todos os avanços alcançados relativos à nitração de benzeno, existem ainda algumas lacunas relacionadas com a formação dos subprodutos da reação que se pretenderam esclarecer com a realização do presente trabalho. Anteriormente realizaram-se estudos focados na formação dos subprodutos típicos da reação, nomeadamente nitrofenóis e dinitrobenzeno, tendo como objetivo minimizar a sua formação. Neste trabalho pretendeu-se estudar e justificar o aparecimento de CO₂ (sob a forma de carbonato de amónia) no processo produtivo de mononitrobenzeno, procurando-se determinar se este gás tem origem na própria matéria prima da reação, em contaminações típicas do benzeno (*n*-hexano, metilciclohexano, tolueno, etc.), nos subprodutos conhecidos da reação ou em espécies químicas presentes no meio reacional e até à data desconhecidas.

Os estudos realizados na fábrica de nitração de benzeno permitiram detetar dióxido de carbono na etapa reacional e evidenciar que o gás se forma nesta secção, o que é indicativo da ocorrência de reações de oxidação durante a nitração de benzeno. Tal facto é suportado pela deteção de espécies químicas oxidadas no meio reacional que revelaram ser ácidos dicarboxílicos, nomeadamente ácido oxálico, ácido mesoxálico, ácido fumárico, ácido maleico, ácido succínico e ácido adípico. A descoberta destes compostos permitiu postular um mecanismo de formação de CO₂, baseado em processos de oxidação e envolvendo a formação e oxidação de fenol.

No decorrer deste trabalho foi possível demonstrar, pela primeira vez, que o fenol está presente no meio reacional da nitração de benzeno, tanto em amostras industriais como em amostras resultantes de nitrações conduzidas à escala laboratorial, e que este composto é o precursor dos nitrofenóis, conforme postulado e referido na literatura. Adicionalmente, a deteção de fenol no meio reacional sustenta o esquema postulado para a formação de CO₂ e de ácidos dicarboxílicos.

Além da deteção de fenol no meio reacional, foi evidenciado que os nitrofenóis são formados por reações consecutivas, ou seja, o mononitrofenol é nitrado a dinitrofenol que por sua vez leva à formação de trinitrofenol; evidenciou-se também as diferentes reatividades destas espécies

nitrofenólicas. O impacto dos principais parâmetros da nitração de benzeno na formação dos nitrofenóis também foi alvo de estudo através da realização de uma série de reações descontínuas. Os testes realizados permitiram obter e exibir os perfis de concentração das diferentes espécies nitrofenólicas ao longo do tempo reacional, um aspeto incomum em estudos de nitração de benzeno. Adicionalmente, os resultados dos testes possibilitaram a construção de modelos cinéticos, um que demonstrou a elevada reatividade do fenol e permitiu suportar o papel desta espécie aromática como precursor dos nitrofenóis, e outro capaz de descrever a interconversão dos nitrofenóis em diferentes condições operacionais.

Na sequência da procura de espécies desconhecidas presentes no meio reacional tendo em vista explicar a origem e formação de CO_2 , foi detetada uma nova classe de subprodutos, até à data não referida na literatura relativa à nitração de benzeno. Estes compostos foram detetados em amostras recolhidas do processo industrial de nitração e revelaram ser ácidos sulfónicos, nomeadamente, ácido benzenossulfónico, ácido 2-mononitrobenzenossulfónico, ácido 3-mononitrobenzenossulfónico e ácido 4-mononitrobenzenossulfónico. De modo a estudar a formação destes ácidos orgânicos durante a nitração, foi realizado um conjunto de nitrações de benzeno à escala laboratorial tendo-se verificado que estes compostos são realmente formados durante a reação, quer através da sulfonação de benzeno a ácido benzenossulfónico seguida da nitração deste a ácido mononitrobenzenossulfónico, quer pela nitração de benzeno a MNB e a sua subsequente sulfonação a ácido mononitrobenzenossulfónico. A influência de alguns parâmetros operacionais na génese destes compostos sulfonados também foi analisada o que permitiu concluir que a temperatura de reação e a concentração de ácido sulfúrico são parâmetros que afetam a formação dos ácidos sulfónicos durante a nitração de benzeno. Os testes realizados mostraram também que os ácidos sulfónicos têm uma maior afinidade para a fase aquosa do que para a fase orgânica.

Foram ainda realizados testes de nitração à escala laboratorial, na gama das condições industriais, com benzeno puro, benzeno enriquecido em impurezas tipicamente presentes no processo industrial (tolueno, metilciclohexano, *n*-hexano), e benzeno aditivado com os subprodutos conhecidos da reação, ou detetados do decorrer do presente trabalho. Estes ensaios permitiram demonstrar que a espécie responsável pelo aparecimento dos produtos de decomposição (CO e CO_2) na nitração é a própria matéria prima orgânica da reação, o benzeno. Esta conclusão é contrária ao que é defendido na literatura, onde se refere ser a decomposição das espécies alifáticas presentes no meio reacional a causa da formação de CO_2 . As nitrações realizadas permitiram ainda avaliar o efeito de algumas condições reacionais na geração de CO_2 , de ácido oxálico e de nitrofenóis, tendo-se verificado que a formação dos compostos enumerados é influenciada pela temperatura, pela concentração de ácido sulfúrico e nítrico, e pela razão molar entre benzeno e ácido nítrico. Adicionalmente, os testes laboratoriais possibilitaram evidenciar a ocorrência de reações de oxidação de benzeno durante a nitração a mononitrobenzeno, responsáveis pela formação de fenol

com a subsequente formação de nitrofenóis por reações consecutivas de nitratação, e em que o fenol, após ser formado, é novamente oxidado, levando à formação de ácidos dicarboxílicos que se decompõem em CO e CO₂.

Table of contents

Abstract	iii
Resumo	v
List of figures	xiii
List of tables	xxiii
Thesis outline	1
Chapter 1 – State of the art	3
1.1. Nitration	3
1.2. Aromatic nitration.....	4
1.2.1. Mononitrobenzene.....	5
1.2.2. Mononitrotoluene.....	6
1.3. Mononitrobenzene market	7
1.4. MNB production technologies	9
1.5. Aromatic nitration.....	13
1.5.1. Reaction rate	15
1.5.2. Interfacial area.....	17
1.5.3. Mixed acid composition	18
1.5.4. Temperature	19
1.5.5. Organic substrate / nitric acid ratio.....	19
1.5.6. Residence time	19
1.6. By-products formation.....	20
1.7. Decomposition in aromatic nitration.....	23
1.8. References	32
Chapter 2 – Carbon dioxide generation in nitrobenzene production	41
2.1. Introduction	42
2.2. Material and methods	44
2.2.1. Sampling	44
2.2.2. CO ₂ quantification.....	45

2.3.	Results and discussion.....	47
2.4.	Conclusions.....	49
2.5.	References.....	51
Chapter 3 – Oxidation by-products in nitrobenzene production.....		53
3.1.	Introduction.....	54
3.2.	Materials and methods	55
3.2.1.	Sampling and samples preparation	55
3.2.2.	HPLC analytical method.....	56
3.2.3.	UHPLC-MS analytical method.....	56
3.2.4.	Decomposition gases quantification in dicarboxylic acids oxidation.....	57
3.3.	Results and discussion.....	58
3.3.1.	Identification of oxidation by-products in the benzene nitration.....	58
3.3.1.1.	Identified by-products	61
3.3.1.2.	Unidentified by-products.....	63
3.3.2.	Proposed oxidation pathway	74
3.3.3.	Oxidation by-products decomposition	76
3.4.	Conclusions.....	81
3.5.	References.....	82
Chapter 4 – Phenol in mixed acid benzene nitration systems.....		87
4.1.	Introduction.....	88
4.2.	Experimental section.....	90
4.3.	Analytical methods	91
4.3.1.	Developed methods for phenol detection.....	91
4.4.	Results and discussion.....	92
4.4.1.	Developed method for phenol detection in laboratory phenol-added benzene solutions nitration	92
4.4.2.	Phenol detection in the industrial plant.....	97
4.4.3.	Phenol detection in phenol-free laboratory nitrations	100
4.5.	Conclusions.....	105

4.6.	References	107
Chapter 5 – (Nitro)Phenols reactivity in mixed acid benzene nitration systems		111
5.1.	Introduction	112
5.2.	Material and methods	114
5.2.1.	Organic phase analysis	116
5.2.2.	Acid phase characterization.....	117
5.3.	Results and discussion	117
5.3.1.	Phenol-added benzene nitrations in soft conditions.....	117
5.3.2.	Phenol-free benzene nitrations	123
5.3.2.1.	Modelling	125
5.3.2.2.	Effect of the sulfuric acid strength	129
5.3.2.3.	Effect of the temperature	131
5.3.2.4.	Effect of the nitric acid concentration	134
5.4.	Conclusions	137
5.5.	References	139
Chapter 6 – (Nitro)benzenesulfonic acids in nitrobenzene production		143
6.1.	Introduction	144
6.2.	Material and methods	145
6.2.1.	Laboratorial tests.....	146
6.2.2.	Samples preparation	147
6.2.3.	HPLC-DAD analytical method	147
6.2.4.	UHPLC-MS analytical method	148
6.3.	Results and discussion	148
6.3.1.	Identification of (nitro)benzenesulfonic acids in mixed acid industrial benzene nitration medium	148
6.3.2.	Laboratorial tests.....	154
6.4.	Conclusions	165
6.5.	References	166
Chapter 7 – Benzene deep oxidation in mixed acid nitration.....		169

7.1.	Introduction.....	170
7.2.	Material and methods.....	171
7.2.1.	Laboratorial reactor	171
7.2.2.	Gaseous phase analysis.....	173
7.2.3.	Organic phase analysis	173
7.2.4.	Acid phase characterization	174
7.3.	Results and discussion.....	174
7.3.1.	Impurities and by-products added-benzene nitration	174
7.3.2.	Effect of the operation conditions.....	181
7.4.	Conclusions.....	187
7.5.	References.....	189
Chapter 8 – Conclusions and future work		193
8.1.	Conclusions.....	193
8.2.	Future work.....	196
Appendix A – Laboratorial unit		197
Appendix B – Carbon dioxide generation in nitrobenzene production.....		205
Appendix C – Oxidation by-products in nitrobenzene production		207
Appendix D – Phenol in mixed acid benzene nitration systems		221
Appendix E – (Nitro)benzenesulfonic acids in nitrobenzene production		225

List of figures

Figure 1.1 – a) Nitration of an aromatic molecule, adapted from [2]. b) Nitration of aliphatic molecules, adapted from [6].	3
Figure 1.2 – Mononitrobenzene structure.	5
Figure 1.3 - Key intermediates derived from MNB. Adapted from [2].	6
Figure 1.4 – Global MNB installed capacity by producer in 2011. Adapted from [17].	8
Figure 1.5 – Worldwide share of MNB production in 2010. Adapted from [27].	8
Figure 1.7 – General MNB continuous production process.	10
Figure 1.8 – Benzene nitration mechanism. Adapted from [30]	14
Figure 1.9 – Raman spectroscopy study for HNO_3 dissociation into $\text{NO}_2 +$ at 293 K and different $\text{H}_2\text{O}/\text{H}_2\text{SO}_4/\text{HNO}_3$ compositions. The lines are representative of HNO_3 dissociation into $\text{NO}_2 +$: A – 100%; B – 80%; C – 60%; D -40%; E – 20%; F – 10%; G – 5%; H – 0%. Adapted from [71].	16
Figure 1.10 – Benzene oxidation mechanism by the NO^+ ion. Adapted from [35, 80].	20
Figure 1.11 – Phenolic by-products formation mechanism proposed by [80]. Adapted from [80, 84].	21
Figure 1.12 – Benzene by-products formation mechanism. Adapted from [25, 30, 85].	22
Figure 1.13 – Phenol nitrosation, isomerization and oxidation. Adapted from [3].	23
Figure 1.14 – Phenol oxidation pathway. Adapted from [92].	24
Figure 1.15 – MNB oxidation, isomerization and ring cleavage. Adapted from [3].	24
Figure 1.16 – Toluene nitration by-products. Adapted from [83].	25
Figure 1.17 – Chromatograms for benzene and toluene nitration products. Adapted from [83].	26
Figure 1.18 – Toluene nitration products at different reaction temperatures. Adapted from [83].	27
Figure 1.19 – a) Cyclohexane nitration. b) Cyclohexane C – C break. c) Paraffin oxidation and nitration. Adapted from [15, 106].	29
Figure 1.20 – Oxidation by nitric acid. Adapted from [110].	29
Figure 1.21 – Possible reaction pathway of organic compounds oxidation by Fenton's reagent. Adapted from [101, 116, 118].	31

Figure 2.1 – General flow-sheet of the mononitrobenzene production process and sampling points.	42
Figure 2.2 – Scheme of the sampling apparatus.	45
Figure 2.3 – Scheme of the CO ₂ capturing apparatus for the developed quantification method.	46
Figure 3.1 – Scheme of the apparatus for the dicarboxylic acids oxidation.	57
Figure 3.2 – Produced MNB a) HPLC-DAD chromatogram; b) Total Ion Chromatogram.	59
Figure 3.3 – a) Produced MNB HPLC chromatogram. Black line – industrial sample; red line – oxalic acid-added industrial sample. UV-Vis spectrum from: b) industrial sample, c) oxalic acid-enriched industrial sample.	61
Figure 3.4 – Known compounds detected in the performed analysis.	63
Figure 3.5 – a) Produced MNB HPLC chromatogram. Black line – industrial sample; red line – mesoxalic acid-added industrial sample. UV-Vis spectrum from the first chromatographic peak in the: b) industrial sample, c) mesoxalic acid-added industrial sample. d) Mesoxalic acid standard UV-Vis spectrum.	64
Figure 3.6 – Oxalic acid UV-Vis spectrum of a benzene nitration sample.	65
Figure 3.7 – Possible U2 analyte identification.	65
Figure 3.8 – Possible U3 analyte identification.	66
Figure 3.9 – a) Produced MNB HPLC chromatogram. Black line – industrial sample; red line – enriched industrial sample. Fumaric acid UV-Vis spectrum from: b) industrial sample, c) enriched industrial sample.	67
Figure 3.10 – a) Produced MNB HPLC chromatogram. Black line – industrial sample; red line – maleic acid-added industrial sample. UV-Vis spectrum from: b) industrial sample, c) maleic acid-added industrial sample.	68
Figure 3.11 – Possible U5 peak identification.	69
Figure 3.12 – Possible U6 peak identification.	69
Figure 3.13 – Possible U7 peak identification.	70
Figure 3.14 – a) Produced MNB HPLC chromatogram. Black line – industrial sample; red line – enriched industrial sample in succinic acid; green line – enriched industrial sample in fumaric acid. UV-Vis spectrum of the analyte with 6.6	

minutes of retention time from a: b) industrial sample, c) succinic-added industrial sample.	71
Figure 3.15 – a) Acid water HPLC chromatogram. Black line – industrial sample; red line – adipic acid-added industrial sample. UV-Vis spectrum from: b) industrial sample, c) adipic acid-added industrial sample.	72
Figure 3.16 – Possible U9 analyte identification.	72
Figure 3.17 – Possible reaction pathway for the decomposition of organic compounds present in Bz nitration medium. Adapted from [1, 30, 33, 36, 38-39].	75
Figure 3.18 – Carbon monoxide and carbon dioxide formation by oxalic acid decomposition. Oxalic acid concentration: 2000 ppm; mixed acid composition: 66% wt. H ₂ SO ₄ ; 5% wt. HNO ₃ . Reaction temperature: 100 °C. Lines are added just for a better visualization of the trends.....	76
Figure 3.19 – Carbon monoxide vs. carbon dioxide formation in oxalic acid decomposition. Reaction conditions: T = 100 °C; Oxalic acid concentration = 2000 ppm; mixed acid composition: 66% wt. H ₂ SO ₄ ; 5% wt. HNO ₃	77
Figure 3.20 – Carbon dioxide formed amounts for different temperatures. Mixed acid composition: 66% wt. H ₂ SO ₄ ; 5% wt. HNO ₃ . Lines are added just for better visualization of the trends.....	78
Figure 3.21 – Nitric acid influence on oxalic acid decomposition. Mixed acid composition: 66% wt. H ₂ SO ₄ ; 5% wt. HNO ₃ for nitric acid run; reaction temperature: 135 °C. Lines are added just for better visualization of the trends.	79
Figure 3.22 – Decomposition of different dicarboxylic acids at adiabatic benzene nitration conditions in the absence of benzene. Mixed acid composition: 66% wt. H ₂ SO ₄ ; 5% wt. HNO ₃ . Reaction temperature [130; 140] °C. Lines are added just for better visualization of the trends.....	80
Figure 4.1 – Proposed nitrophenolic by-products formation mechanism. Adapted from [15, 17].	89
Figure 4.2 – Effect of the sample preparation procedure on the HPLC chromatogram (a) and c) and on the corresponding Ph UV-Vis spectrum (b) and d); a) and b) acidified sample (pH < 2); c) and d) alkaline sample (pH > 10). Samples' reaction time = 0.5 min. Reaction conditions: T _{initial} = 5 °C, H ₂ SO ₄ = 39 wt.%; HNO ₃ = 2 wt.%.	93

Figure 4.3 – Run E3 – HPLC chromatograms (a, c, e, g) and UV-vis spectra of phenol peak (b, d, f, h). a) and b) 3 min reaction time, organic phase. c) and d) 3 min reaction time, acid phase. e) and f) 10 min reaction time, organic phase. g) and h) 10 min reaction time, acid phase. Reaction conditions: $T_{\text{initial}} = 15\text{ }^{\circ}\text{C}$, $\text{H}_2\text{SO}_4 = 39\text{ wt.}\%$; $\text{HNO}_3 = 2\text{ wt.}\%$	95
Figure 4.4 – Run E3. Phenol and nitrophenols concentration profiles. a) Ph, b) 2-MNP, and c) 4-MNP concentration profiles in the acid (right axis) and organic (left axis) phases; d) Ph, 2-MNP, and 4-MNP profiles (both phases analysed). Reaction conditions: $T_{\text{initial}} = 15\text{ }^{\circ}\text{C}$, $\text{H}_2\text{SO}_4 = 39\text{ wt.}\%$; $\text{HNO}_3 = 2\text{ wt.}\%$	96
Figure 4.5 – 2-MNP intramolecular and 4-MNP intermolecular hydrogen bonds.....	97
Figure 4.6 – Bz nitration in industrial reactor. a) Organic phase HPLC chromatogram. b) Corresponding Ph's UV-Vis spectrum. c) Acid phase HPLC chromatogram. d) Corresponding Ph's UV-Vis spectrum. e) GC-FID chromatogram of the organic phase.....	98
Figure 4.7 – Run E6. a) Organic phase HPLC chromatogram. b) Corresponding Ph's UV-Vis spectrum. c) Acid phase HPLC chromatogram. d) Corresponding Ph's UV-Vis spectrum. Sample collected 5 minutes after the reaction start. Reaction conditions: $T_{\text{initial}} = 90\text{ }^{\circ}\text{C}$, $\text{H}_2\text{SO}_4 = 60\text{ wt.}\%$; $\text{HNO}_3 = 5\text{ wt.}\%$	100
Figure 4.8 – E6 concentration profiles obtained from: a) the HPLC analysis of the organic phase samples; b) the HPLC analysis of the acid phase samples; c) the GC analysis of the organic phase samples. Reaction conditions: $T_{\text{initial}} = 90\text{ }^{\circ}\text{C}$, $\text{H}_2\text{SO}_4 = 60\text{ wt.}\%$; $\text{HNO}_3 = 5\text{ wt.}\%$	102
Figure 4.9 – Run E7. a) Organic phase HPLC chromatogram. b) Corresponding Ph's UV-Vis spectrum. Sample's reaction time = 10 min. Reaction conditions: $T_{\text{initial}} = 89\text{ }^{\circ}\text{C}$, $\text{H}_2\text{SO}_4 = 32\text{ wt.}\%$; $\text{HNO}_3 = 9\text{ wt.}\%$, $\text{Bz} \approx 50\text{ wt.}\%$; $\text{MNB} \approx 50\text{ wt.}\%$	104
Figure 4.10 – Ph concentration profile for run E7. Organic phase analysis. Reaction conditions: $T_{\text{initial}} = 89\text{ }^{\circ}\text{C}$, $\text{H}_2\text{SO}_4 = 32\text{ wt.}\%$; $\text{HNO}_3 = 9\text{ wt.}\%$; $\text{Bz} \approx 50\text{ wt.}\%$; $\text{MNB} \approx 50\text{ wt.}\%$	104
Figure 4.11 – Run E8. a) Organic phase HPLC chromatogram. b) Corresponding Ph's UV-Vis spectrum. c) GC-FID chromatogram from the retrieved sample. Sample's reaction time = 1 min. Reaction conditions: $T_{\text{initial}} = 89\text{ }^{\circ}\text{C}$, $\text{H}_2\text{SO}_4 = 33\text{ wt.}\%$; $\text{HNO}_3 = 9\text{ wt.}\%$, $\text{Bz} \approx 50\text{ wt.}\%$; $\text{MNB} \approx 50\text{ wt.}\%$	105

Figure 5.1 – Nitrophenols interconversion scheme. Adapted from refs [15, 19].....	113
Figure 5.2 – Scheme of the laboratory reactor used in the batch reactions.	116
Figure 5.3 – Phenol concentration profiles at different reaction temperatures. Analysis of the organic phase. Mixed acid composition: % wt. $\text{H}_2\text{SO}_4 = 40$; % wt. $\text{HNO}_3 = 2$. $X_{\text{HNO}_3} < 2\%$, $X_{\text{Bz}} < 1\%$, at the reaction end. Lines are added just for better visualization of the trends.....	118
Figure 5.4 – a) Phenol, b) 2-MNP, and c) 4-MNP profiles in the acid and organic phase from run E4. Reaction conditions: $T = 15\text{ }^\circ\text{C}$, % wt. $\text{H}_2\text{SO}_4 = 40$; % wt. $\text{HNO}_3 = 2$. $X_{\text{HNO}_3} < 2\%$ at the reaction end. Lines are added just for better visualization of the trends.	119
Figure 5.5 – Postulated Ph nitration scheme in mixed acid phenol-added benzene nitration.	120
Figure 5.6 – a) Phenol, b) 2-MNP, and c) 4-MNP profiles for runs E4 (1204 r.p.m) and E5 (1422 r.p.m). Reaction conditions: $T = 15\text{ }^\circ\text{C}$, % wt. $\text{H}_2\text{SO}_4 = 40$; % wt. $\text{HNO}_3 = 2$. Lines are added just for a better visualization of the trends.	121
Figure 5.7 – Total concentration profiles and fitting of the proposed model to experimental data. Reaction conditions (run E4): $T = 15\text{ }^\circ\text{C}$, % wt. $\text{H}_2\text{SO}_4 = 40$; % wt. $\text{HNO}_3 = 2$. $X_{\text{HNO}_3} < 2\%$ at the reaction end.	123
Figure 5.8 – a) Temperature evolution; and b) nitric acid; c) 2-MNP; d) 4-MNP; e) 2,4-DNP; f) 2,6-DNP; g) TNP; and h) total NPs concentration profiles for different runs. $T_{\text{initial}} = 70\text{ }^\circ\text{C}$; % wt. $\text{H}_2\text{SO}_4 = 66$; % wt. $\text{HNO}_3 = 5$. The data points represent the average values for the different runs (E6, E7 and E8) while the vertical lines are related with the population standard deviation between the data (determined with a confidence interval of 95%). Lines are added just for better visualization of the trends.....	124
Figure 5.9 – Scheme of Bz nitration and NPs formation. Ph was intentionally not considered as the NPs precursor.	126
Figure 5.10 – Effect of sulfuric acid concentration and fitting of the proposed model to experimental data on the: a) Temperature history; b) Nitric acid conversion; and c) 2-MNP; d) 4-MNP; e) 2,4-DNP; f) 2,6-DNP; g) TNP; and h) total NPs concentration profiles for the average values of runs E6, E7, E8 (66 wt.% H_2SO_4) and E9 (61 wt.% H_2SO_4); $T_{\text{initial}} = 70\text{ }^\circ\text{C}$, wt.% $\text{HNO}_3 = 5$. The solid lines represent the adjusted values for run E9 while the dashed lines refer to the adjusted values for the average of the runs E6, E7 and E8.	130

Figure 5.11 – Effect of initial the reaction temperature and fitting of the proposed model to experimental data on: a) Temperature history; b) Nitric acid conversion; and c) 2-MNP; d) 4-MNP; e) 2,4-DNP; f) 2,6-DNP; g) TNP; and h) total NPs concentration profiles for runs E9 (70 °C) and E10 (90 °C); % wt. H ₂ SO ₄ = 61. % wt. HNO ₃ = 5. The dashed lines represent the adjusted values for run E10 while the solid lines refer to the adjusted values for run E9.....	133
Figure 5.12 – Effect of nitric acid concentration and fitting of the proposed model to experimental data on: a) Temperature history; b) Nitric acid conversion; and c) 2-MNP; d) 4-MNP; e) 2,4-DNP; f) 2,6-DNP; g) TNP; and h) total NPs concentration profiles for runs E11 (5 % wt. HNO ₃) and E12 (9 % wt. HNO ₃); T _{initial} = 90 °C; wt.% H ₂ SO ₄ = 51. The dashed lines represent the adjusted values for run E12 while the solid lines refer to the adjusted values for run E11.....	135
Figure 6.1 – Possible by-products of the mixed acid (HNO ₃ +H ₂ SO ₄) benzene nitration reaction.....	144
Figure 6.2 – Scheme of the laboratorial reactor used in the batch reactions.....	146
Figure 6.3 – a) Crude MNB HPLC-DAD chromatogram. b), c), d) and e) UV-Vis spectra of different detected chemical species.	149
Figure 6.4 – Crude MNB a) Total Ion Chromatogram. b), c), d) and e) mass and UV-Vis spectra of different analytes.	150
Figure 6.5 – HPLC chromatograms of a) crude MNB, and crude MNB added with b) BSA, d) 2-MNBSA, f) 3-MNBSA or h) 4-MNBSA. UV-Vis spectra of c) BSA, e) 2-MNBSA, g) 3-MNBSA and i) 4-MNBSA.....	153
Figure 6.6 – a) Temperature evolution; b) Nitric acid conversion; and c) BSA; d) 2-MNBSA; e) 3-MNBSA; f) 4-MNBSA and g) total sulfonic acids concentration profiles for runs E1 (90 °C) and E2 (70 °C) in both reaction phases. % wt. H ₂ SO ₄ = 66; % wt. HNO ₃ = 5. Lines are added just for a better visualization of the trends.	155
Figure 6.7 – a) HPLC-DAD chromatogram for run E1 (at the reaction end). b) BSA; c) 2-MNBSA; d) 3-MNBSA; d) 4-MNBSA UV-Vis spectra.....	156
Figure 6.8 – a) Temperature evolution; b) Nitric acid conversion; and c) BSA; d) 2-MNBSA; e) 3-MNBSA; f) 4-MNBSA; and g) total sulfonic acids concentration profiles for runs E1 (66% wt. H ₂ SO ₄) and E3 (60% wt. H ₂ SO ₄) in both reaction	

phases. $T_{\text{initial}} = 90\text{ }^{\circ}\text{C}$; % wt. $\text{HNO}_3 = 5$. Lines are added just for a better visualization of the trends.....	158
Figure 6.9 – a) Temperature evolution; b) Nitric acid conversion; and c) BSA; d) 2-MNBSA; e) 3-MNBSA; f) 4-MNBSA; and g) total sulfonic acids concentration profiles for runs E1 (organic substrate: Bz) and E4 (organic substrate: MNB) in both reaction phases. $T_{\text{initial}} = 90\text{ }^{\circ}\text{C}$; % wt. $\text{H}_2\text{SO}_4 = 66$; % wt. $\text{HNO}_3 = 5$. Lines are added just for a better visualization of the trends.....	160
Figure 6.10 – a) Temperature evolution; b) Nitric acid conversion; and c) BSA; d) 2-MNBSA; e) 3-MNBSA; f) 4-MNBSA; and g) total sulfonic acids concentration profiles for runs E4 (organic substrate: MNB) and E5 and E6 (organic substrate: MNB+BSA (150 ppm in the organic phase)) in both reaction phases. For runs E5 and E6 the data points represent the average values for the performed runs while the vertical lines are related with the population standard deviation between the data. $T_{\text{initial}} = 90\text{ }^{\circ}\text{C}$; % wt. $\text{H}_2\text{SO}_4 = 66$; % wt. $\text{HNO}_3 = 5$. Lines are adjusted for a better visualization of the trends.	162
Figure 6.11 – Possible MNBSAs formation routes.	163
Figure 7.1 – Sketch of the laboratorial unit.....	172
Figure 7.2 – Organic compounds present in the benzene nitration medium.....	175
Figure 7.3 – CO_2 formation in nitration as function of the different compounds incorporated in benzene (except for MNB). $m_{\text{CO}_2 \text{ ref}}$ refers to the CO_2 formed amounts in the nitration of pure benzene. Reaction conditions: $T_{\text{initial}} = 90\text{ }^{\circ}\text{C}$; % wt. $\text{H}_2\text{SO}_4 = 66$; % wt. $\text{HNO}_3 = 5$; reaction time = 1 h; concentration of the organic species in benzene = 2500 ppm. Aliphatics concentration in recycled benzene = 3% wt..	176
Figure 7.4 – Amounts of CO_2 formed in the nitration of mixtures of recycled benzene and pure benzene. $m_{\text{CO}_2 \text{ ref}}$ is referent to CO_2 amounts formed in the nitration of pure Bz. Reaction conditions: $T_{\text{initial}} = 90\text{ }^{\circ}\text{C}$; % wt. $\text{H}_2\text{SO}_4 = 66$; % wt. $\text{HNO}_3 = 5$; Reaction time = 1 h. Aliphatics concentration in recycled benzene = 3% wt..	178
Figure 7.5 – Carbon monoxide concentration profile in pure benzene nitration. Reaction conditions: $T_{\text{initial}} = 90\text{ }^{\circ}\text{C}$; % wt. $\text{H}_2\text{SO}_4 = 66$; % wt. $\text{HNO}_3 = 5$. The line is added just for better visualization of the trend.....	180
Figure 7.6 – a) Carbon dioxide and carbon monoxide concentration profile; b) carbon monoxide vs. carbon dioxide formation in a pure benzene nitration. Reaction	

conditions: $T_{\text{initial}} = 90\text{ }^{\circ}\text{C}$; % wt. $\text{H}_2\text{SO}_4 = 61$; % wt. $\text{HNO}_3 = 5$. Dashed lines are added just for a better visualization of the trends.	180
Figure 7.7 – CO_2 formed amounts in Bz nitration at the following reaction conditions: $T_{\text{initial}} = 90\text{ }^{\circ}\text{C}$; % wt. $\text{H}_2\text{SO}_4 = 66$; % wt. $\text{HNO}_3 = 5$; reaction time = 1 h. Bz was fed in excess (11% mol) except for the stoichiometric feed run in which Bz / nitric acid = 1, $P = P_{\text{atm}}$. The reference test was conducted at atmospheric pressure, maintaining the remaining reaction conditions unchanged.	181
Figure 7.8 – Nitrophenols vs. carbon dioxide formation in Bz nitration. Reaction conditions: $T = [70; 90]\text{ }^{\circ}\text{C}$; % wt. $\text{H}_2\text{SO}_4 = [60; 70]$; % wt. $\text{HNO}_3 = [3; 5]$	184
Figure 7.9 – Experimental vs. predicted values for CO_2 formation as function of the reaction conditions.	185
Figure 7.10 – Oxalic acid vs. NPs formation in Bz nitration. Reaction conditions: $T = 90\text{ }^{\circ}\text{C}$; % wt. $\text{H}_2\text{SO}_4 = [60; 70]$; % wt. $\text{HNO}_3 = [3; 5]$	186
Figure 7.11 – Reaction (by-)products from benzene nitration. Elaborated based on info taken from refs [7-9, 26, 29, 32] and in the Chapters 3.	187
Figure 8.1 – Reaction product and by-products from the benzene nitration.	195
Figure A.1 – Nitration reactor developed by Santos [2]. Adapted from [2].	197
Figure A.2 – Corroded reactor components. Adapted from [2].	198
Figure A.3 – a) Reactor glass cylinders before being assembled. b) Reactor diameters, thickness and height.	198
Figure A.4 – a) Reactor's bottom. b) Reactor's top.	199
Figure A.5 – Steel and tantalum stirrers.	199
Figure A.6 – Reactor's top connections.	200
Figure A.7 – Aqueous phase reagents feed.	201
Figure A.8 – Organic substrate feed.	201
Figure A.9 – Sampling point of liquid samples.	202
Figure A.10 – Scheme of the laboratorial nitration unit.	202
Figure B.1 – CO_2 quantification method validation.	205

Figure C.1 – Ammonia effect on an acid water sample. Red line – sample without dilution; Blue line – Sample diluted with an ammonia solution.	207
Figure C.2 – Organic phase (produced MNB) / aqueous phase separation.	208
Figure C.3 – Produced MNB chromatogram at 210 nm. Mobile phase (KH_2PO_4) flow = 0.7 mL.min ⁻¹	209
Figure C.4 – Produced MNB chromatogram at 210 nm. Mobile phase (KH_2PO_4) flow = 1 mL min ⁻¹	209
Figure C.5 – Produced MNB HPLC chromatogram at 210 nm (using Table C.1 conditions).	210
Figure C.6 – Produced MNB HPLC chromatogram. Eluent: formic acid. Gradient feed of methanol.....	212
Figure C.7 – Produced MNB HPLC chromatogram. Isocratic feed. Eluent: formic acid.	212
Figure C.8 – Acid water HPLC chromatogram using Table C.2 conditions.	213
Figure C. 9 – MS spectra of analyte: a) U2; b) U3; c) U4; d) U5; e) U6; f) U7; g) U8; h) U9; i) K6; j) K7 and k) K8. See Table's 3.1 nomenclature.	214
Figure C.10 – Acid water HPLC chromatogram. Red line – industrial sample; black line – 5-nitro-2-furoic acid-added industrial sample.	215
Figure C.11 – Acid water HPLC chromatogram. Black line – industrial sample; Red line – industrial sample + KMnO_4	215
Figure C.12 – Fumaric acid standard curve.	216
Figure D.1 – Scheme of the laboratorial reactor used in the batch reactions.	221
Figure D.2 – Phenol concentration profiles for the runs E3, E4 and E5 ($T_{\text{initial}} = 15\text{ }^\circ\text{C}$; $\text{H}_2\text{SO}_4 = 39\text{ wt.}\%$; $\text{HNO}_3 = 2\text{ wt.}\%$). Analysis of the organic phase.....	222
Figure D.3 – GC analysis for run E3. Reaction conditions: $T_{\text{initial}} = 15\text{ }^\circ\text{C}$, $\text{H}_2\text{SO}_4 = 39\text{ wt.}\%$, $\text{HNO}_3 = 2\text{ wt.}\%$	223
Figure D.4 – Run E6. a) Organic phase HPLC chromatogram. b) Corresponding Ph's UV- Vis spectrum. c) Acid phase HPLC chromatogram. d) Corresponding Ph's UV- Vis spectrum. Sample collected 30 minutes after the reaction start. Reaction conditions: $T_{\text{initial}} = 90\text{ }^\circ\text{C}$, $\text{H}_2\text{SO}_4 = 60\text{ wt.}\%$; $\text{HNO}_3 = 5\text{ wt.}\%$	224

Figure E.1 – Total ion chromatogram for **a)** crude MNB sample, **c)** crude MNB sample added with BSA. Mass spectra from BSA in **b)** crude MNB sample, **d)** crude MNB sample added with BSA.....225

List of tables

Table 1.1 – Comparison of different mononitrobenzene production processes. Adapted from [57, 64].	18
Table 1.2 – Typical industrial nitrating conditions. Adapted from [2, 13, 38].	27
Table 1.3 – Typical impurities present in nitration grade benzene. Adapted from [103].	28
Table 2.1 – Carbon dioxide quantification in the reaction section of the nitration plant. The disclosed values are normalized.	47
Table 3.1 – MS/MS fragmentation pattern of the detected chromatographic peaks.	60
Table 3.2 – Identification of the chromatographic peaks detected in Figure 3.2.	73
Table 4.1 – Reaction conditions of the performed nitration tests.	90
Table 5.1 – Reaction conditions of the performed nitration tests.	115
Table 5.2 – Kinetic parameters estimated for the reaction network presented in Figure 5.9.	128
Table 6.1 – Reaction conditions of the performed nitration tests. Reaction time: 30 minutes; stirring speed: 1200 r.p.m; $\text{HNO}_3 = 5\%$ wt.	147
Table 6.2 – Mass fragmentation pattern of some of the detected species.	151
Table 6.3 – Distribution coefficients determined at the reaction end. ^{a)}	164
Table 7.1 – Aliphatic compounds at the inlet and outlet of the industrial nitration section.	178
Table 7.2 – Formation of benzene (and mononitrobenzene) nitration by-products at different reaction conditions. Reaction time = 1 h; Operation pressure = 1.8 bar(g).	183
Table A.1 – Reactor dimensions.	198
Table C.1 – Eluent feed composition.	210
Table C.2 – Eluent feed composition for the HPLC-MS method.	212

Table C.3 – p -value of the analysed samples from different plant locations. Samples collected in March 17 th	217
Table C.4 – p -value of the analysed crude MNB samples collected in March 9 th	218

Thesis outline

Benzene nitration is a well-known and intensively studied chemical reaction used for the production of mononitrobenzene, a chemical commodity that finds application in the production of aniline, drugs such as paracetamol, and dyes, among others. However, despite the importance of this chemical reaction and all the performed studies addressing it, some issues have to be clarified, namely those related to the formation of the oxidized reaction by-products; this was the main goal of this PhD thesis.

Firstly, a review of benzene nitration production processes, nitration mechanism and by-products formation was done (Chapter 1) to contextualize the focus of the present work and to provide the reader with sufficient information about the process under study. An assessment of the mononitrobenzene industry demonstrates the importance of benzene nitration on a global scale. Additionally, in the first chapter, the motivation for this work is revealed, which is also related to carbon dioxide detection in the nitration plant under the form of ammonium carbonate. The formation of carbon dioxide in benzene nitration suggests the occurrence of decomposition reactions in parallel to benzene nitration, an unexplored topic in the context of this process. Consequently, determining the CO₂ formation path and understanding how the reaction conditions affect this and other compounds generation were the main driving forces that led to the development of the present work.

Chapter 2 is dedicated to the detection of carbon dioxide in the reaction stage of a mononitrobenzene production process. For quantifying carbon dioxide in liquid streams, an analytical method was specifically developed. The main objective of this chapter was to verify if carbon dioxide, which appears under the form of ammonium carbonate in the nitration plant, was being formed in the reaction section.

In Chapter 3, the detection and identification of unknown chemical species present in the benzene nitration medium, which were suspected to be oxidation intermediate products, is addressed. The detection of these compounds required the development of a new high-performance liquid chromatography analytical method while their identification demanded mass spectrometry analysis. Besides that, oxidation of dicarboxylic acids under benzene nitration conditions is also assessed. The main goal was to demonstrate if the dicarboxylic acids could yield carbon dioxide at the industrial benzene nitration conditions.

In this work, one could not neglect the formation of the typical benzene nitration by-products (nitrophenols). Therefore, Chapter 4 is related to the efforts made for detecting phenol in benzene nitration media, from both industrial and lab samples. Phenol detection in benzene nitration medium was very important because enabled evidencing experimentally, for the first time, that this species plays a role on nitrophenols genesis; moreover, it allowed suggesting that it may also be further

oxidized yielding dicarboxylic acids by the aromatic ring opening, carbon dioxide and carbon monoxide, as discussed in Chapter 7.

Chapter 5 is focused on nitrophenols formation and their interconversion. In this chapter, phenol-added benzene nitrations were carried out in a batch reactor under mild conditions for recording phenol consumption and the consequent 2-mononitrophenol and 4-mononitrophenol formation. The results enabled the construction of a kinetic model that supports phenol role as the mononitrophenols precursor while evidencing its high reactivity. Phenol-free benzene nitrations were also conducted at conditions closer to the industrial ones, in which some operation parameters such as the reaction temperature, sulfuric acid and nitric acid concentration were changed, being analysed their effect on the nitrophenols formation and interconversion. The collected data allowed demonstrating nitrophenols interconversion and enabled the construction of a kinetic model for describing such reactions.

In Chapter 6 (mononitro)benzenesulfonic acids formation during nitration is addressed. These chemical species are not reported in benzene nitration studies and were identified by mass spectrometry analysis. In order to have a better know-how about these compounds' formation in benzene nitration, some operation parameters such as the reaction temperature, sulfuric acid concentration, and the organic substrate composition were changed, being assessed their impact on the formation of the sulfonic acids.

In Chapter 7, the precursor for the origin of the detected decomposition gaseous products (carbon dioxide and carbon monoxide) is presented. For that, several benzene nitrations were conducted at the typical industrial conditions, in which diverse chemical species, typically present in the reaction medium, were added (individually and separately) to a benzene matrix and then nitrated. Additionally, some reaction parameters such as the reaction temperature, mixed acid composition and benzene / nitric acid ratio, among others, were changed in order to evaluate their impact on the oxidized by-products.

Chapter 8 summarises the main conclusions that were achieved during this work, and particularly those that address both the formation mechanism associated to nitrophenols generation as well as the one behind benzene oxidation which comprises phenol oxidation to dicarboxylic acids and then to carbon monoxide and carbon dioxide. Conclusions related to sulfonic acids formation during benzene nitration are also presented. Additionally, some suggestions for future work are given.

Chapter 1 – State of the art

1.1. Nitration

Nitration can be defined as the irreversible reaction between an organic compound and a nitrating agent [1-2]. This reaction, one of the earliest to be operated in the chemical industry [3-5], can be employed to produce mononitrobenzene (MNB), but it can also be used, for example, in the mononitrotoluene (MNT) synthesis or in the nitration of other hydrocarbons. A nitration reaction leads to the introduction of one or more nitro groups ($-\text{NO}_2$) of the nitrating agent, generally nitric acid or its derivatives [6], into the aromatic or aliphatic organic molecule by replacing a hydrogen atom [1-2], as represented in Figure 1.1.

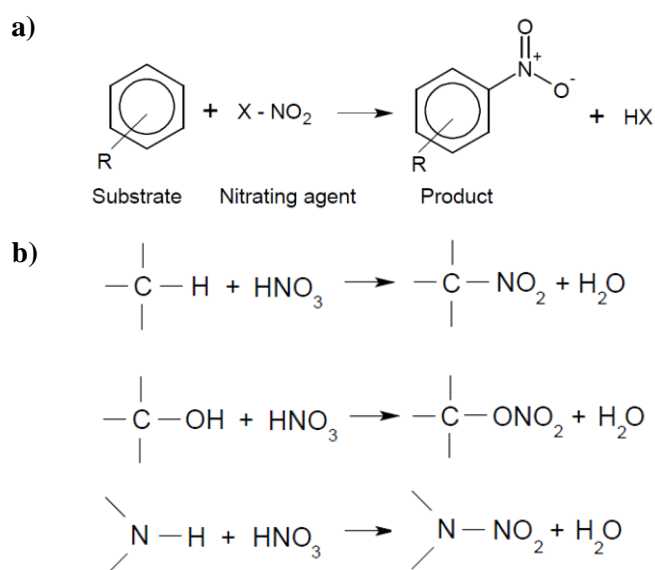


Figure 1.1 – a) Nitration of an aromatic molecule, adapted from [2]. **b)** Nitration of aliphatic molecules under severe reaction conditions, adapted from [6].

However, in addition to the hydrogen, other atoms can be replaced by the nitro groups. For instance, in the Victor Meyer reactions the nitro group is responsible for the substitution of a bromine ($-\text{Br}$) or an iodine ($-\text{I}$) atom [1, 7].

Nitration reactions are highly exothermic, being that the heat of reaction depends on the hydrocarbon to be nitrated, which, together with the reaction temperature, influences the nitration mechanism [1].

Nitration can be carried out directly or indirectly [3]. If a nitro group is directly introduced in the organic compound the nitration is direct, being nitric acid, mixed acid (a mixture of nitric acid and sulfuric acid) and nitrogen dioxide, with or without catalyst, the main nitration agents used [3].

Alternatively, if a functional group is introduced in the organic compound, being subsequently readily replaced by the nitro group, the nitration is indirect [3]. There are two widely used indirect nitration methods, of which one consists in the sulfonation of an organic compound ($R-SO_3H$) with the subsequent substitution of the sulfonic by the nitro group, through reaction with nitric acid. The other method employed implies the introduction of a nitroso group in the organic compound ($R-NO$) with subsequent oxidation to the nitro group [3].

Electrophilic, nucleophilic and free radical nitration are the three categories in which nitration mechanisms can be splitted [7], being the reaction mechanism dependent on the reactants and on the operating conditions [1]. Free radical nitration is usually employed for low molecular weight nitroalkanes synthesis while nucleophilic nitration is used for the production of nitro and polynitro alkanes [7]. Electrophilic nitration, the main method used for nitro aromatic compounds synthesis [7], is the method by which MNB is prepared [8] at industrial level. Aromatic substrates can also be nitrated by free radical nitration, however, this method is not very successful for the aromatic nitration [1].

Due to its highly exothermic nature, nitration is considered one of the most potentially hazardous processes of the chemical industry [2]. This potential hazard is also related with the feedstocks and reaction products high flammability, with the use of highly hazardous chemicals [9] and with the possibility of temperature runaway (responsible for some industrial accidents [9-10]). This reaction can be carried out on a continuous or batch basis accordingly to the produced quantities required [2], however since the 1990s continuous flow units are widely used [1].

1.2. Aromatic nitration

Aromatic nitration has been widely studied; it has been a precursor of theoretical organic chemistry and it is an important chemical reaction for the chemical industry [11].

In 1834 the german chemist Eilhard Mitscherlich discovered the nitration of organic substances, being the first to synthesize MNB through a reaction between benzene and fuming nitric acid [12-14]. Nevertheless, it is believed that already in 1825 Faraday had accomplished benzene nitration [15] without recognizing his discovery [6]. Nitration was found suitable for being applied to a variety of aromatic compounds (equation 1.1) [6].



A few years after Mitscherlich discovery it was introduced an important method to accomplish nitration with a mixture of sulfuric and nitric acid, known as mixed acid [15]. The mixed acid concept was introduced by a Mansfield's patent [12] despite the previous Hofmann and Muspratt work on benzene nitration. In their work, Hofmann and Muspratt managed to produce mono and

dinitrobenzene resorting to a mixture of nitric and sulfuric acids [2, 15-16]. The discovery of mixed acid use for nitration was so important that even nowadays industrial nitrations are performed employing that mixture of acids. That is the case of MNB synthesis, which was first commercially produced in England, in 1856 [13], and since then nitration has been continuously studied [12, 15] and subject to continuous improvements.

Industrially, the nitroaromatics of greater interest are MNB and MNT since they are precursors of the polyurethane industry, which supports various applications (e.g. insulation materials for automotive and construction sectors, coatings and elastomers, among others [17]).

1.2.1. Mononitrobenzene

Among the possible hydrocarbons that can be nitrated, benzene is the most important to Bondalti Chemicals once it is a raw material for the MNB production, a nitrocompound produced at Bondalti's plant.

MNB ($C_6H_5NO_2$ – displayed in Figure 1.2) is an important organic compound used mainly as feedstock for aniline production [13]. At room temperature MNB is a yellow liquid, and it has a typical odour of bitter almonds [2, 13, 18]. Mononitrobenzene, also known as oil of mirbane [2, 13], is soluble in several organic solvents, slightly soluble in water and completely miscible in benzene [13, 18]. Despite being soluble in many organic solvents, MNB can also be used as a solvent, namely in Friedel-Crafts reactions, once it is a good solvent of aluminium trichloride ($AlCl_3$) [2, 13], which is used as the reaction catalyst [8].

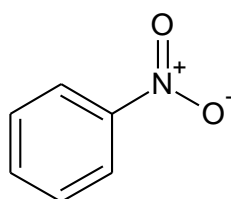


Figure 1.2 – Mononitrobenzene structure.

A variety of products can be produced from MNB, as shown in Figure 1.3. These products can be obtained by different reactions [2], being MNB hydrogenation the most important reaction for Bondalti Chemicals once it is responsible for the aniline production. The formation of 4-aminophenol through MNB, and then of acetaminophen is also an important reaction since acetaminophen is a widely used analgesic (paracetamol).

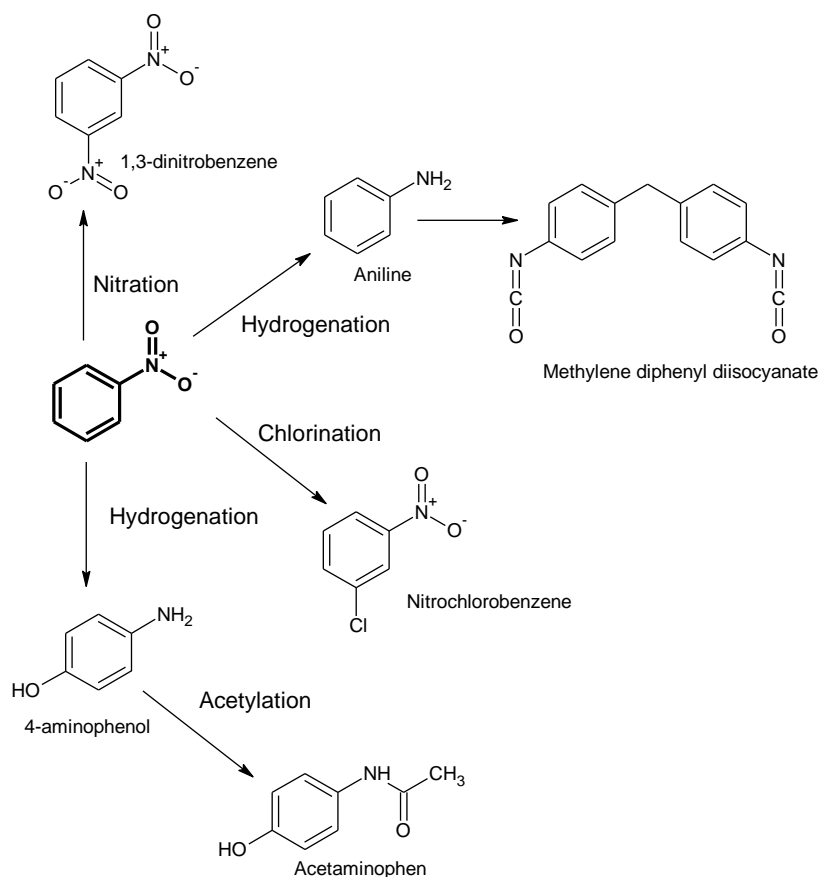


Figure 1.3 - Key intermediates derived from MNB. Adapted from [2].

MNB is a very toxic substance [13] and it is anticipated to be a human carcinogen based on the experimental studies performed on animals [18]. It can be absorbed by contacting the skin or by inhalation [13, 18-19], leading to the conversion of haemoglobin into methaemoglobin, which may cause cyanosis (if the methaemoglobin level reaches 15%) [13] due to the lower ability of blood (haemoglobin) to carry oxygen. Exposure to MNB may also cause eye irritation [13]; therefore, it is very important to use the adequate safety equipment when working with this organic compound.

1.2.2. Mononitrotoluene

Toluene nitration results in the formation of ortho, meta and para isomers of MNT [13]. *Ortho*-nitrotoluene is the dominant isomer produced by conventional mixed acid nitration of toluene [2]; therefore, it is the only isomer to be addressed in the present work.

The presence of the methyl group on the aromatic ring of toluene molecule facilitates the nitration reaction [13] and that is why toluene nitration is much faster, when compared with the benzene nitration [2]. However, the nitration temperature must be lower than the temperature of benzene nitration in order to reduce by-products formation, once the presence of the methyl group increases the easiness of oxidation side reactions [13].

Ortho-MNT is a clear yellow liquid, soluble in most organic solvents and slightly soluble in water [13]. It is used as an intermediate in the synthesis of azo dyes, rubber chemicals, agriculture chemicals, explosives and foams [13]. Toluene can be dinitrated to produce dinitrotoluene (DNT), a starting material for toluene diisocyanate (TDI) synthesis, which is a basic chemical commodity [20].

Toluene is a known impurity present in the benzene nitration feed stream; therefore, due to the easy toluene oxidation, it can be one of the causes for the unknown by-products appearing during benzene nitration.

1.3. Mononitrobenzene market

MNB hasn't a known natural source and so it has to be manufactured before being used in the different industrial applications [21]. Since a great percentage of the produced MNB (about 98 % [22]) is used as feedstock in aniline synthesis, which is itself greatly used (about 80 %) for methylene diphenyl diisocyanate (MDI) production [17], it can be stated that the MDI and aniline production are the main driving forces for the mononitrobenzene manufacture. MDI is used in the preparation of polyurethane rigid foams for construction, insulation, and packaging, and it can also be used in sealants and elastomers applications [17, 23].

MNB can also be used to produce explosives, dyes, pesticides, drugs, rubber chemicals or as a solvent [17, 24]. In 2010, about 60% of Europe's produced paracetamol was obtained with MNB synthesised at Bondalti Chemicals [25].

From an economical point of view, the main vectors to be taking into account in MNB synthesis are the operation costs, like wastes treatment, raw materials and energy costs, and the world demand for MNB or MNB-related products (such as aniline and MDI) [13]. Typically, about 85% of the operation costs are associated to the raw materials costs [13], which make it the most significant cost in MNB production.

Worldwide, in 2011, there was a MNB installed capacity of about 6.4 million tons per year, being predicted an annual growth of 6.3 % in the following years [17]. There are about 30 companies responsible for the MNB production, wherein BASF, DuPont, Bayer, Tosoh Corporation, Huntsman and Rubicon are representative of about 60 % of world's production capacity [17] – Figure 1.4.

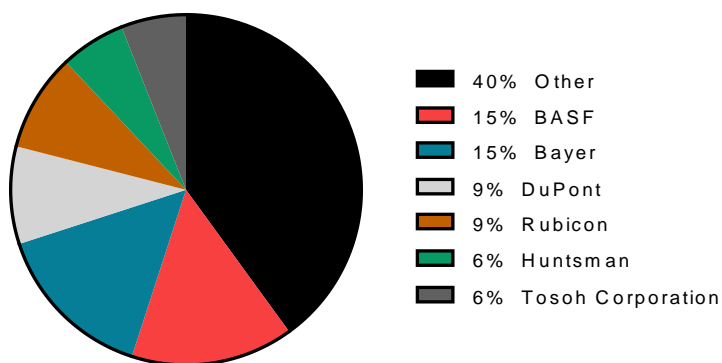


Figure 1.4 – Global MNB installed capacity by producer in 2011. Adapted from [17].

At national level, Bondalti has a production capacity of 300 000 tons per year, which represents approximately 5 % of 2011's world production capacity.

Over the past years the MNB manufacture has been increasing due to the high demand of developing regions, such as China and Middle East, while Europe's and North America's demand has been growing slowly [26]. Until 2022 is expected an annual growth of about 5% [26].

Together with China, Western Europe and the United States are responsible for the majority of worldwide MNB consumption. These regions, besides being the greater MNB consumers, are also the greater MNB producers as can be seen in Figure 1.5.

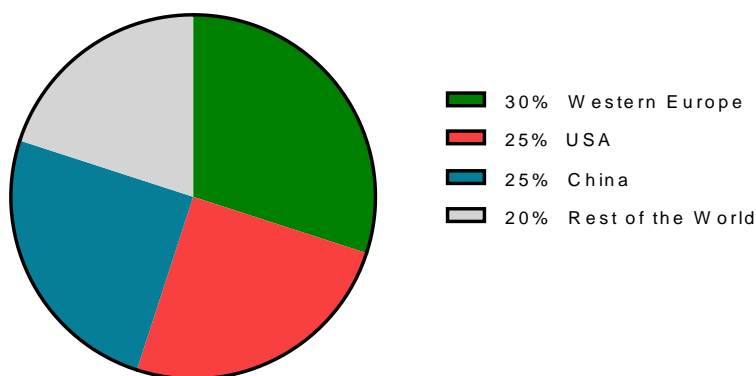


Figure 1.5 – Worldwide share of MNB production in 2010. Adapted from [27].

China is expected to become the largest MNB producer, if it is not already, with a production share over 50%, due to the implementation of some projects for the integrated production of MDI [27]. In Europe, Bondalti has a MNB production capacity share of about 15 % and most of the Bondalti's MNB is converted to aniline, which is sold to Dow (also located in Estarreja) as raw material for the MDI synthesis. The high production capacity of Bondalti Chemicals makes it one of the biggest European MNB production companies (Figure 1.6).

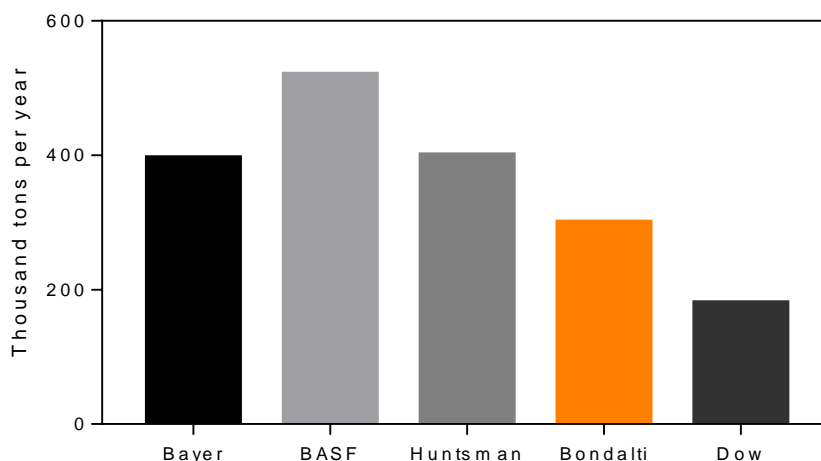


Figure 1.6 – West European installed MNB production capacity by producer in 2011. Adapted from [17].

Between 1974 and 2012, the world's MNB production increased about 10 times, allowing to state that MNB has become a commodity chemical [27]. In Portugal, Bondalti recently doubled its MNB production capacity and has increased its annual production consecutively [28-29], becoming, by this way, one of the most important MNB industrial players in Europe and in the world.

Although the presented data is not the most updated, it allows to recognize the importance of MNB production for the chemical industry, particularly for the Portuguese organic chemical industry, and for our daily lives.

1.4. MNB production technologies

Mononitrobenzene can be produced continuously or by a batch process. Due to the lower capital costs and higher efficiency of the continuous nitration, almost all the MNB producers use this production process instead of the batch one [13]. There are two main methodologies in the continuous nitration process which are the adiabatic nitration, the present state of the art process, and the isothermal nitration, usually employed in the past [13].

Over the years significant process changes have been occurring in nitration plants. In the 1940s nitrations were essentially conducted in batch reactors but, due to technology developments and higher production demand, in the 1990s continuous flow nitration technology became widely used [1]. Typically in the benzene nitration batch process the reaction time is comprehended between 2 and 4 hours, low reaction temperatures are employed (50 – 90 °C) and the obtained MNB yields are about 95 – 98 % [13, 30]. Continuous nitration reactors can reach higher yields using higher

temperatures (in adiabatic nitration) than the batch ones and became the present state of the art in nitration due to the higher produced quantities with lower production costs.

Similarly to MNB production, MNT can be produced continuously (by adiabatic or isothermal nitration) or by batch processes. Some patents [31-34] cover benzene and toluene nitration, although the reference to toluene has the objective of strengthen and enlarge the patent scope [13].

MNB production technology is licensed by a few companies such as Chematur, DuPont, Meissner, Noram and Biazzi. All these companies, except Biazzi (that uses isothermal nitration), resort to adiabatic nitration for the MNB synthesis. Biazzi's technology is no longer available because the isothermal process cannot compete economically with the adiabatic nitration offered by the other technology licensors [17]. Indeed, the average production cost of the adiabatic process is 25 % lower by tonne of MNB produced than the isothermal one [17].

Noram is the licensor of the following MNB production companies: Bondalti Chemicals, Bayer, Hunstman, DuPont / First Chemical, HuChem, Tianji and Shandong Jinling [17]. Noram's technology is considered the most competitive large scale MNB process, with low maintenance, proven product quality and process reliability [17].

The MNB adiabatic production process can be represented by the flowsheet shown in Figure 1.7, although it also represents the isothermal nitration process if the diluted sulfuric acid re-concentration is carried out. The general adiabatic nitration process has the following sections: nitration, phase separation, MNB washing system, MNB purification and sulfuric acid re-concentration. The major difference between both processes is that in the isothermal one the temperature is kept constant in the nitrator reactors whereas in the adiabatic process the heat transfer to the surroundings is minimal [35].

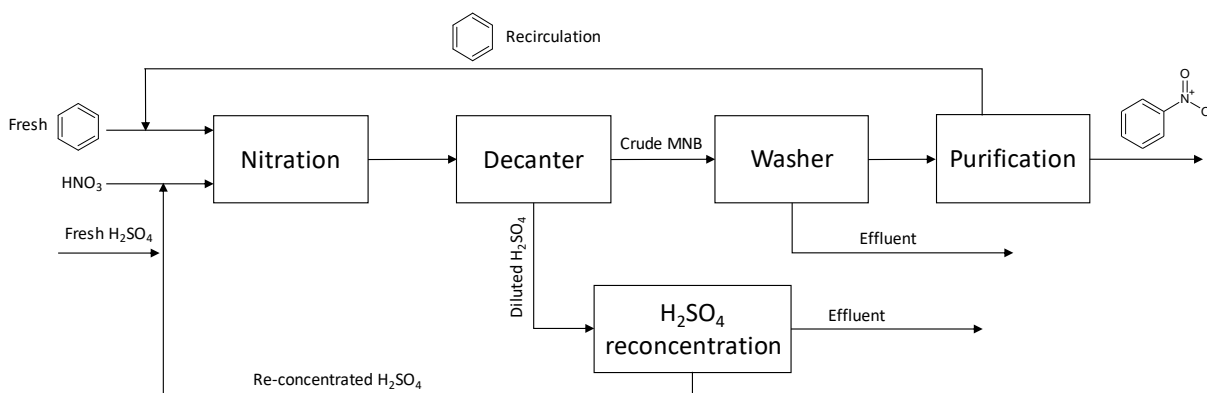


Figure 1.7 – General MNB continuous production process.

In the Biazzi's isothermal nitration process benzene and mixed acid are fed to a series of three nitrators, each equipped with high speed agitation and helical cooling coils to maintain and control the reaction temperature ($\approx 50\text{ }^{\circ}\text{C}$) [36]. In this technology the fresh mixed acid is fed only to the

third nitrator and benzene is charged in the initial one, meaning that benzene reacts with the spent / recirculated mixed acid in the first two reactors. Downstream the second nitrator there is a process unit responsible for separation of unconverted benzene and MNB from the spent mixed acid. The organic phase from the separator is fed to the third reactor and the spent mixed acid is sent to a sulfuric acid concentration unit [36]. Fresh mixed acid is fed to the third reactor in order to complete the reaction, being the residence time in the range of 15 to 20 minutes [36].

Until 1941 the state of the art on nitration was the isothermal process. The transition from the isothermal to the adiabatic nitration began in 1941 with Castner work [37]; however it was only after the 1980s that the isothermal process stopped being the main commercial route for the MNB production [17]. Castner was the first to patent an adiabatic process for aromatic nitration and the first to suggest the possibility of continuous operation [30, 37] alternatively to the discontinuous isothermal process. With some improvements over time, the adiabatic process proposed by Castner became the present state of the art for the industrial production of MNB.

In Castner's adiabatic process the heat of reaction is not removed as it happens in the isothermal process. Instead it is dissipated in the aqueous phase (mixed acid), allowing sulfuric acid to reach the acid concentration unit with a higher temperature, therefore favouring the re-concentration step and minimizing the energetic costs allocated to the unit. However, Castner's patent lacks information regarding by-products originated during nitration. In 1977 Alexanderson *et al.* [32] patented a process based on Castner's invention with some improved operational parameters in order to make the adiabatic nitration a successful commercial production process. Accordingly to Alexanderson *et al.* [32], the operational conditions proposed by Castner ($\approx 90\text{ }^{\circ}\text{C}$ and 2 – 6 % nitric acid in the mixed acid) favours by-products formation (dinitrobenzene – DNB – and nitrophenols – NPs) and may be hazardous. In order to improve the gaps of Castner work, Alexanderson *et al.* [32] proposed an initial reaction temperature between 40 and 80 $^{\circ}\text{C}$, a residence time on the order of 0.5 to 3 minutes and 5 to 8.5 % of HNO_3 in the mixed acid composition to obtain less than 500 ppm of dinitrated products. Besides benzene, these authors claim that other aromatic hydrocarbons such as toluene may be nitrated by their process.

One year later Alexanderson *et al.* [38] registered another patent improving their previous work. They propose that the adiabatic nitration occurs in a series of four continuous stirred tank reactors (CSTRs) wherein benzene (at room temperature) and mixed acid (80 – 120 $^{\circ}\text{C}$) are fed to the first nitrator and then the reaction mixture flows successively to the second, third and fourth reactor. All the reactors have the same residence time (either 0.3; 2; 2.8 or 5 minutes each) and operate under super-atmospheric pressure and at a maximum temperature below 145 $^{\circ}\text{C}$ [38].

At Bondalti the MNB production is based in the process patented by Alexanderson *et al.* [38] in 1978. Nitration occurs in two CSTR batteries, wherein each reactor battery is fed by two independent streams, one containing mixed acid and the other containing benzene [39]. The residence time in each nitrator is about 1 minute and the reaction mixture exiting the reaction section

is sent to a decanter to proceed to the phase separation. Then crude MNB is subjected to washing and other purification steps. Before resorting to adiabatic nitration, Bondalti's MNB production process was the isothermal one (Meissner). The nitration technology shift happened when it was no longer possible to use the diluted sulfuric acid for fertilizers, which has turned the isothermal nitration process to MNB economically unviable.

Accordingly to Guenkel *et al.* [34], and despite the improvements introduced by Alexanderson *et al.* [32, 38], some enhancements regarding by-products formation minimization, conversion efficiencies and reaction rates should be made. Guenkel *et al.* [31, 34] resort to a pipe nitrator, which allows to disperse benzene uniformly in the acid phase, to perform the adiabatic benzene nitration continuously and at atmospheric pressure. A more desirable reactor, namely the jet impingement reactor patented by Rae and Hauptmann [40], is referred by Guenkel *et al.* [34] to perform adiabatic the nitration. The jet impingement reactor enhances benzene dispersion in the mixed acid, increasing by this way the interfacial area. This method enables to reach higher reaction rates, higher yields and lower by-products formation [13].

Both the jet impingement reactor and pipe nitrator are Noram's technologies and are considered second generation adiabatic processes [27]. Other companies such as Chematur and Meissner have also their own nitration processes. Chematur's adiabatic process is based in Henke *et al.* [41] while Meissner process uses a tubular reactor with a special annular mixer injector to get the nitrating acid completely surrounded by the benzene feed [17].

Given the environmental problem associated to the large sulfuric acid quantities employed in the benzene nitration some vapor phase nitration processes, which do not require the use of this mineral acid, have been developed [42-43]. Most of the vapor phase nitrations resort to metal oxides catalysts [13, 44] to favour the reaction [3]. The biggest disadvantage of these processes is the lack of long term stability of the catalyst [13]. The use of ionic liquids was also studied being achieved promising results regarding MNB production accordingly to Earle and Katdare [45].

Despite all the improvements achieved so far, MNB production is still subject to continuous studies in order to increase the reaction productivity, decrease the by-products formation and improve the plants' operability [46-52]. However, even with all the performed studies regarding benzene nitration, the adiabatic technology is still the state-of-the-art process for producing MNB.

In the future, this paradigm can be changed because of the efforts made for producing aniline directly from benzene (benzene amination [53]) or due to the bio-process that is being developed for producing aniline directly from biomass [54]. The industrialization of both these processes would affect seriously MNB production since it is mainly used as an aniline precursor.

1.5. Aromatic nitration

Since about 1950, due to the work of Hughes *et al.* [55], it is accepted that nitration of most aromatic hydrocarbons, glycols and amines, in which mixed acid or highly concentrated nitric acid are employed, occurs by NO_2^+ attack [1, 9]. The Ingold-Hughes mechanism for aromatic nitration is depicted in the following equations [6, 55]:



The first two steps of Ingold mechanism (equations 1.2 and 1.3) involve the HNO_3 dissociation and the NO_2^+ formation, the reactive electrophile. Then the NO_2^+ ion reacts with the aromatic substrate (equation 1.4) and the Wheland intermediate (ArHNO_2^+) is formed. Finally (equation 1.5), the Wheland intermediate is deprotonated and the nitration is completed by regeneration of the system aromaticity and of the acid catalyst (HA) [6]. Other mechanisms for nitration of aromatics are described in the literature, such as those proposed by Olah or by Schofield [6], but none of the mechanisms is completely conclusive [56]. Nevertheless, the Ingold-Hughes mechanism is still the most consensual for the aromatic nitration [30].

The MNB production reaction is a highly exothermic reaction ($145 \text{ kJ}\cdot\text{mol}^{-1}$ [57]) between benzene and nitric acid, catalysed by a strong acid such as, for example, sulphuric acid [1]. Usually, in industrial nitration plants sulphuric acid is used as catalyst due to its relatively low price [1] and its catalytic efficiency [58]. The sulphuric acid function is to donate a proton to nitric acid [59], which will be protonated and dissociated forming, by this way, the nitration agent, the nitronium ion (NO_2^+) [2, 60] (equation 1.6).



The major drawback associated with mixed acid used is the recovery and regeneration of sulfuric acid, which becomes diluted with water [9]. Benzene nitration can also be accomplished by using only concentrated nitric acid, however the reactivity is lower than the one obtained with mixed acid [60].

The reaction mechanism for the MNB formation can be represented by equations 1.7 and 1.8 [35].



Nitration reactions have some associated problems because they involve heterogeneous liquid-liquid dispersions, with chemical reaction and mass transfer phenomena occurring simultaneously [4]. The low solubility of organic compounds such as benzene, toluene or chlorobenzene [4] in the mixed acid leads to the formation of two distinct liquid phases during nitration. Therefore, the reaction medium is composed by an organic rich phase and by an acid rich phase. The reagents immiscibility implies that the reaction occurs on a heterogeneous medium, making difficult to determine accurately the reaction mechanism [31, 35].

Once benzene and MNB have low solubility in the mixed acid, it is expected that benzene nitration occurs near the interface between the organic and the acid phase [31, 61]. The accepted aromatic reaction mechanism is represented in Figure 1.8, specifically for benzene nitration.

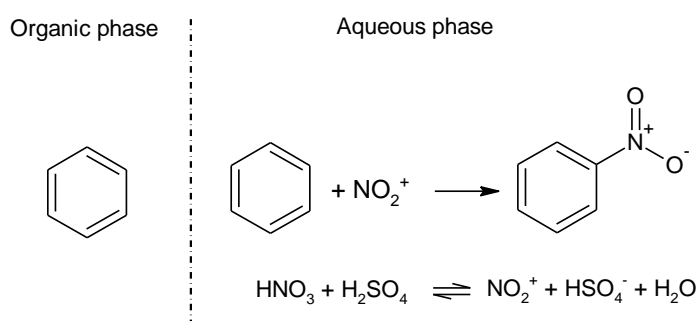


Figure 1.8 – Benzene nitration mechanism. Adapted from [30]

The aromatic nitration mechanism, described herein for benzene nitration, can be disclosed by the following steps [30-31, 35] – Figure 1.8:

- Benzene diffusion from the organic phase to the interface and then from the interface to the aqueous phase;
- On the interface or on the aqueous phase, benzene reacts with the nitronium ion to form MNB;
- MNB diffuses from the aqueous phase to the interface, and then to the organic phase.

The presented reaction mechanism is based on Giles *et al.* [62] work. Giles *et al.* [62] proposed a reaction model for aromatic nitration, based on the fast reaction regime taking place in the aqueous phase near the interface.

Based in this reaction mechanism, Santos [30] was able to develop mechanistic models for the continuous nitration of benzene in the range of the industrial conditions. These mathematical models were focused on the film model and on the Danckwerts penetration model, considered

benzene diffusion to the acid phase and its nitration in the latter [30, 35], and enabled obtaining a quite good agreement between the predicted and the experimental values even for the simplest model approach (based on the film model) [5]. The film model was latter the basis for optimization studies in Bondalti's nitration plant [35, 63].

1.5.1. Reaction rate

Nitration reaction rate depends on sulphuric acid concentration, more precisely nitration rates are generally proportional to the nitronium ion concentration [1]. An increase of H_2SO_4 concentration leads to an increase in the NO_2^+ ion production [57, 64]; however, for the occurrence of a maximum in the rate of nitration, the H_2SO_4 concentration should be lower than 90% [3, 12]. For higher H_2SO_4 concentrations the rate of nitration decreases due to the formation of the $HSO_4^-NO_2^+$ ion pair, which affects the generation of the electrophilic species [58].

Nitration rates are also influenced by the substituents on the aromatic ring. For instance, aromatics with attached alkyl groups like toluene or cumene are more reactive than benzene due to a ring electron density increase established by the alkyl group [1]. On the other hand, aromatics with attached nitro groups such as MNB are not so easily nitrated once the nitro group reduces the electron density of the ring [1].

After kinetic studies in homogeneous medium it has been established that the nitration of aromatic compounds, in dilute or concentrated aqueous sulphuric acid, has a second order kinetics [55, 65-67], first order for each reagent [6, 68], as presented in equation 1.9 [30]. Depending on the organic substrate to be nitrated, the reaction rate limiting step can be the electrophilic species formation or the electrophilic attack on the organic reactant [69]. If the reaction rate limiting step is the nitronium ion formation, the nature and concentration of the organic substrate does not influence the observed rate, so different compounds may undergo nitration at the same rate corresponding to the rate of NO_2^+ ion formation [69].

$$r = k_{2obs}[HNO_3][ArH] \quad (1.9)$$

The parameter k_{2obs} (observed rate constant) is a function of temperature [58], and in the benzene nitration case, k_{2obs} is strongly and positively affected by the increase of sulphuric acid concentration [58, 70] due to the consequent higher HNO_3 dissociation. Given that the nitrating agent is the NO_2^+ ion, the reaction rate can be rewritten as shown in equation 1.10 [30].

$$r = k_2[NO_2^+][ArH] \quad (1.10)$$

Oppositely to k_{2obs} , the rate constant k_2 doesn't depend on the H_2SO_4 concentration, it is only affected by temperature [58]. However, the use of equation 1.10 has a disadvantage when compared with equation 1.9 that lies in the difficulty of measuring the NO_2^+ concentration. This quantification implies the use of Raman spectroscopy techniques, as proposed by Edwards and Fawcett [71] and by Deno *et al.* [72].

The dependence of the reaction rate from the sulphuric acid concentration lies in the H_2SO_4 capacity to dissociate HNO_3 and form NO_2^+ . In general the rates of nitration are proportional to the nitronium ion concentration [1]. Edwards and Fawcett [71] studied the mixed acid dissociation into the nitronium ion as function of temperature and of the mixed acid composition. Due to their work they were able to construct a ternary diagram indicative of HNO_3 dissociation at 20 °C for the different mixed acid compositions (Figure 1.9).

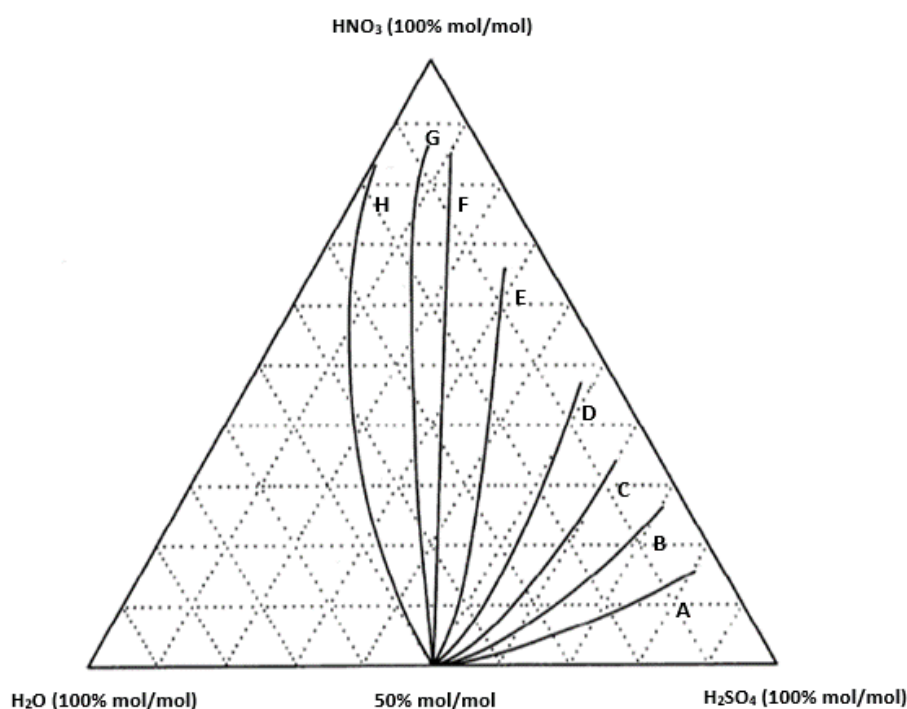


Figure 1.9 – Raman spectroscopy study for HNO_3 dissociation into NO_2^+ at 293 K and different $H_2O/H_2SO_4/HNO_3$ compositions. The lines are representative of HNO_3 dissociation into NO_2^+ : A – 100%; B – 80%; C – 60%; D – 40%; E – 20%; F – 10%; G – 5%; H – 0%. Adapted from [71].

Below line A of Figure 1.9 nitric acid is not detected by Raman spectroscopy meaning that it is totally dissociated in NO_2^+ ions. As the mixed acid composition is gradually modified, by increasing the H_2O and HNO_3 concentrations and, consequently, by decreasing the H_2SO_4 concentration, the HNO_3 dissociation is lowered reaching a point where the NO_2^+ ion is not detected (in the left of line

H). Contrary to what would be expected, the mixed acid employed in the industrial nitrations has a composition that fits in the region where the nitronium ion is not detected [11]. This fact led to the suggestion that another nitrating species such as the H_2NO_3^+ ion may be responsible for nitration [71], or to the possible presence of too low NO_2^+ ion concentrations to be measured by Raman spectroscopy [1]. Notwithstanding, Edwards and Fawcett don't reject the NO_2^+ nitration mechanism [30, 71, 73]. Moreover, it should be noted that the H_2NO_3^+ ion is a weaker nitrating agent than the NO_2^+ ion [30].

Recently, the effect of sulfuric acid on nitric acid dissociation was confirmed by Russo *et al.* [74] who developed a simplified model for predicting nitric acid dissociation in ternary HNO_3 - H_2SO_4 - H_2O systems.

Edwards and Fawcett [71] concluded that the temperature increase has a negative effect on the HNO_3 dissociation and, consequently, on nitration. Nevertheless, the temperature rise leads to an increase on the reaction rate (Arrhenius equation), which is expected to be the controlling factor on the nitration reaction rate.

Organic nitration can be influenced by various parameters. The knowledge of the impact of the different parameters on the reaction rate and selectivity is important for the reaction optimization, although in heterogeneous systems it is of the highest difficulty to describe the effect of a single parameter on the reaction [30].

1.5.2. Interfacial area

The interfacial area between the organic and the acid phases is an important parameter in benzene and other hydrocarbons nitration since the main reactions occur near or at the interface [1, 62]. By increasing the interfacial area reactants mass transfer is favoured, resulting in the production of more reaction products, less quantities of by-products [75] and higher reaction rates [76]. The simplest way to achieve a good interfacial area in a CSTR is by increasing the stirring speed. Indeed, the stirring speed can influence the results obtained in benzene [5] or toluene nitration [20].

Aware of the importance of the interfacial area, nitration technology licensors are replacing the traditional reactors by reactors with complex dispersion mechanisms in order to enhance the interfacial area and, consequently, the reaction rate and selectivity [30]. Microreactors can also be used to achieve better mass transfer and temperature control [57, 77-78]. In addition, and accordingly to Burns and Ramshaw [57, 64], this technology allows to obtain, for benzene nitration, lower dinitrophenol (DNP) concentrations but higher dinitrobenzene concentrations when compared with the traditional nitration (Table 1.1).

Table 1.1 – Comparison of different mononitrobenzene production processes. Adapted from [57, 64].

Source	T _{inlet} (°C)	Technology	T _{outlet} (°C)	% H ₂ SO ₄ (wt.)	% MNB (wt.)	DNB (ppm)	DNP (ppm)
Alexanderson <i>et al.</i> [38]	80	Adiabatic nitration	128	60.6	89.5	<100	1000
	80		134	65.2	99.1	290	1800
Guenkel <i>et al.</i> [34]	95		120	69.5	90	50	1700
Burns and Ramshaw [57, 64]	90	Microreaction	90	77.7	94	4000	350
	90		90	72.7	60.7	<1000	<100

Nevertheless, so far, microreactor technology does not present better results for benzene nitration than those achieved in the industrial reactors [57, 64], and so MNB production by microreactors must be object of further study and improvement. Furthermore, to be able to synthesize industrial quantities of MNB it would be necessary thousands of microreactors working in parallel [64], which would imply a high investment cost.

1.5.3. Mixed acid composition

Mixed acid composition affects also the by-products formation as well as the reaction rate. For instance, if the HNO₃ concentration in mixed acid is lower than 3 % (wt.%), benzene conversion decreases as well as the reaction rate but, if the HNO₃ concentration is higher than 7.5 % (wt.%), the heat generated favours the dinitration [38]. For toluene nitration low sulfuric acid content in the mixed acid increases the oxidation tendency of nitric acid, yielding nitration by-products [79]. Oppositely, the increase of sulfuric acid concentration leads to the decrease of organic by-products during toluene nitration [80].

As it is accepted that the NO₂⁺ ion is the nitrating agent, it is important that the mixed acid composition ensures the total dissociation of HNO₃. The incomplete HNO₃ dissociation leads to an acid accumulation and consequently the by-products concentration increases, mainly oxidation products [64]. Also, the H₂SO₄ concentration is relevant given that it affects strongly the reaction rate [58, 70].

The mixed acid composition is also important because it is known to affect the solubility of the aromatic reagents in the reaction's aqueous phase [81]. Accordingly to Schiefferle *et al.* [81], the increase of nitric acid and sulfuric acid concentration (and the consequent decrease of water concentration) enhances the solubility of the aromatic hydrocarbons in the aqueous phase.

1.5.4. Temperature

As stated before, the temperature increase has a negative effect on the NO_2^+ ion formation [71] and thus on the hydrocarbon nitration. Moreover, the increase of this parameter contributes also for the presence of larger amounts of nitration by-products on the crude reaction products [38, 82-83]. However, the temperature rise is beneficial for the nitration rate [5, 58]. This temperature dependence can be explained by the exponential temperature effect in the kinetics (according to the Arrhenius law).

Likewise a temperature increase contributes for the organic compounds solubility in mixed acid (in a lesser extent than the contribution of mixed acid composition) [81]. The temperature affects also the viscosity, density and surface tension of the reactional phases (organic and acid phase) and, consequently, the interfacial area between the two phases [1].

1.5.5. Organic substrate / nitric acid ratio

Another important parameter affecting nitration reactions is the organic substrate / nitric acid ratio on the feed composition. In the MNB production process, benzene commonly is fed in stoichiometric excess relatively to HNO_3 [34, 38, 46]. This allows to minimize the by-products formation because of the lower nitric acid content in the organic phase [75], avoids the HNO_3 accumulation on the process [13] and improves benzene mass transfer for the acid phase, enhancing MNB production [75]. On the other hand, an excess of organic substrate relatively to HNO_3 in toluene nitration has a negative effect once it originates a dark coloured spent acid referred to as black acid [83].

1.5.6. Residence time

Residence time is likewise a key parameter affecting the overall reaction performance. Normally, a higher residence time leads to higher conversion, but an excessive residence time can have a negative effect on the reaction culminating on the formation of the unwanted nitration by-products [30]. To minimize the by-products formation short residence times should be employed, which can be compensated by increasing the interfacial area, improving by this way the mass transfer phenomena [76]. Nonetheless, it is essential that the residence time is long enough to complete the reaction without favoring the by-products. Typically the residence times are between 5 seconds to 15 minutes [68].

After this short analysis it is possible to state that aromatic (benzene, toluene, etc.) nitration reaction is influenced by a set of parameters that should be controlled and optimized in order to achieve the greatest reagents conversion and the lowest by-products formation.

1.6. By-products formation

Nitration reactions are always followed by side reactions that are influenced by different factors like the composition of the nitrating mixture, the nature of the compound to be nitrated and the general nitration conditions [3]. It is important to minimize these side reactions due to their negative environmental, safety and economic impacts [80].

An aromatic compound present in the reaction medium that hasn't been nitrated can be oxidized to form phenol or cresol that may originate, respectively, nitrophenols during benzene nitration or nitrocresols when nitrating toluene [3]. If the aromatic feed is contaminated with some aliphatic compounds, these molecules may also be subject to oxidation reactions leading, ultimately, to CO₂ release during nitration (which has been industrially observed).

Over the years the formation mechanism of nitration by-products has been subject of investigation [35]. However, despite the studies made, among the proposed mechanisms there is none completely accepted [35]. In 1958, Titov postulated a reaction mechanism between an aromatic compound and the nitrosonium ion (NO⁺) [80], as depicted in Figure 1.10 (specified for benzene). Titov proposed this mechanism after having found di- and tri-nitrophenol in benzene nitration reaction products, trinitrocresol in toluene nitration and trinitrochlorophenol in chlorobenzene nitration [3].

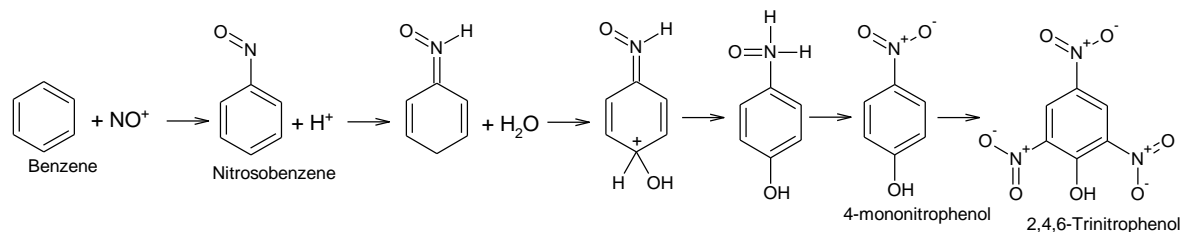


Figure 1.10 – Benzene oxidation mechanism by the NO⁺ ion. Adapted from [35, 80].

Accordingly to the presented mechanism, the first step is the formation of a nitroso compound by reaction between benzene and NO⁺. Then, by rearrangements the nitroso compound originates a phenolic compound which may undergo successive nitration to form nitro, dinitro or trinitrophenol [80]. This mechanism was abandoned when it was found that it couldn't well explain by-products formation [80].

Titov suggested another mechanism in which a nitronium ion becomes attached to the aromatic ring through one of its oxygen atoms instead of the nitrogen atom forming an aryl nitrite (ArONO) (equation 1.11) [3, 80].





Then the nitrite compound is decomposed to yield a phenol and a nitrosonium ion (equation 1.12) [3, 80] and by nitration reactions the organic compound can form mononitro, dinitro or trinitro phenolic compounds [80]. However, there is no evidence that NO_2^+ ion may react with the aromatic ring accordingly with this mechanism [80].

Hanson *et al.* [80] proposed a different mechanism in which the aromatic substrate is initially attacked by the nitronium ion, then by water and finally the nitrous acid formed is eliminated [84] (Figure 1.11).

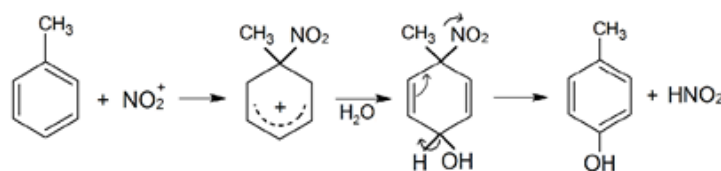


Figure 1.11 – Phenolic by-products formation mechanism proposed by [80]. Adapted from [80, 84].

As in the Titov's mechanism, the nitrophenolic by-products are obtained by subsequent nitration of the phenolic compound [84].

Once benzene nitration reaction occurs in a heterogeneous medium, mass transfer limitations are observed, leading to by-product formation [57] and lower reaction selectivity and yield [30]. The main impurities originated in the industrial production of MNB are nitrophenols (DNP and TNP) and dinitrobenzene [82], which are thought to form tar-like deposits on hydrogenation catalysts used in aniline synthesis [17]. Moreover, the presence of reaction by-products is potentially hazardous [32] and requires purification and waste treatment steps [27], increasing the MNB production cost.

Benzene oxidation to phenol is assumed to take place within the organic phase, by action of nitric acid, while nitration reactions occurs in the acid phase [57]. After benzene oxidation, phenol is transferred from the organic to the aqueous phase where it is nitrated [34], returning to the organic phase in the form of a nitrophenolic compound [35]. Dummann *et al.* [85] proved that the nitrophenolic compounds are formed by a parallel reaction to the nitration of the substrate, and that the di- and tri-nitrated products are formed by consecutive nitrations of the main reaction product. Thus, the formation of di- and tri-nitrobenzene starts with the diffusion of benzene to the aqueous phase, where it is mono or poly nitrated, and finishes with the diffusion of the nitro products back to the organic phase. Figure 1.12 outlines the benzene by-products formation reactions.

Decomposition Reactions in Aromatic Nitration

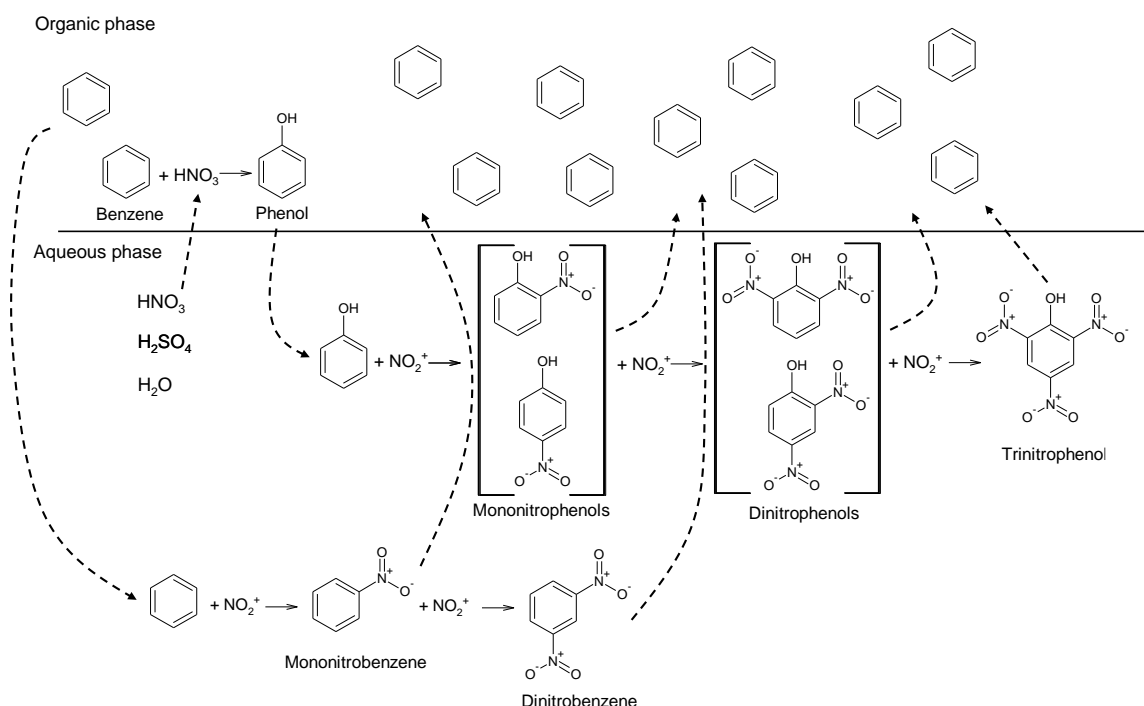


Figure 1.12 – Benzene by-products formation mechanism. Adapted from [25, 35, 85].

Despite all the studies already performed addressing benzene nitration nitrophenolic by-products, there is information lacking in the literature, namely the demonstration of nitrophenols interconversion, i.e., mononitrophenols (MNPs) originating DNPs and DNPs being converted into trinitrophenol (TNP). For instance, in Berretta and Louie [82] work only the total nitrophenols formed amounts are presented for different reaction conditions. In the work by Quadros *et al.* [75], the authors consider only 2,4-DNP and TNP. On the other hand, Burns and Ramshaw [64] refer the formation of MNPs, DNPs and TNPs, but the individual isomers concentration is not presented.

Other studies are focused in predicting nitrophenols formation considering the reaction conditions [30, 86-87]. However, these studies were driven for the construction of statistical models for nitrophenols formation, being focused only in the most representative species (2,4-DNP and TNP) and neglecting the formation of their precursors.

Regarding the nitrophenols distribution in both reaction phases, some studies were recently conducted showing that these compounds, namely 2,4-DNP and TNP have a much higher affinity into the organic than to the aqueous acid phase [88-89]. These conclusions are in accordance with the proposed nitrophenols formation mechanism, which states that after phenol diffusion to the acid phase and its subsequent di- or tri-nitration, dinitrophenol and trinitrophenol are diffused back to the organic phase (Figure 1.12). Knowing the partition of these compounds and the remaining nitrophenolic by-products is important to model these species in a two liquid phases system.

1.7. Decomposition in aromatic nitration

Oxidation reactions are widely used in industrial wastewater treatments for degrading organic contaminants [90], typically yielding CO_2 and water as reaction products (if the oxidation is complete). During industrial benzene nitration it is suspected that oxidation reactions are occurring, being this the reason for CO_2 detection under the form of ammonium carbonate. The formation of this salt occurs due to the contact between CO_2 and an ammonium solution, as described in equation 1.13.



The ammonia solution is used in the nitration process, more precisely in the washing section (Figure 1.7) for removing nitrophenols from the produced MNB. Ammonium carbonate formation and build-up can lead to the plugging of different industrial equipment [91], being thus crucial to minimize or even suppress CO_2 formation in nitration plants to avoid the use of another alkaline agent in the washing section for capturing and removing carbon dioxide from the plant as described by Buchi and Guenkel [91]. However, there is no concrete information regarding the compound that is being oxidised. It can be benzene, MNB, some oxidized by-products such as nitrophenols, or some of the impurities present in the benzene feed stream. Consequently, determining the CO_2 formation path and understanding how the reaction conditions affect this and others compounds generation are crucial aspects.

Having in consideration that benzene can be oxidized to phenol during nitration, and that this compound can undergo nitrosation, isomerization and oxidation reactions leading to mesoxalic acid and its oxime formation (Figure 1.13), whom can then be further oxidized yielding CO , CO_2 and water [3], phenol formation can explain, partially or totally, the CO_2 formation during nitration.

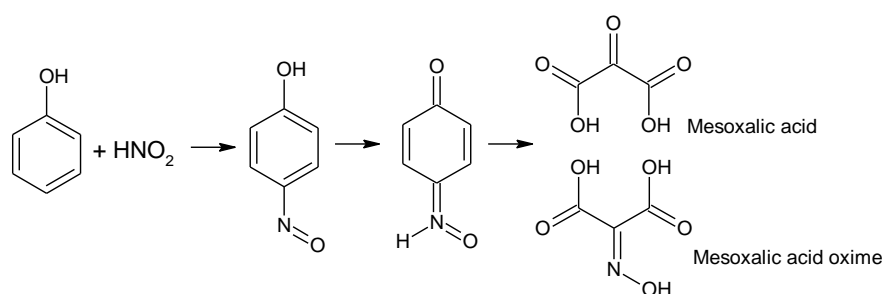


Figure 1.13 – Phenol nitrosation, isomerization and oxidation. Adapted from [3].

Due to the harsh conditions of benzene nitration (high temperature in a highly oxidizing system), after being generated, phenol can also be further oxidized to catechol or hydroquinone, originating

then benzoquinones which by ring cleavage give origin to carboxylic acids and, ultimately, to CO₂ as exemplified in Figure 1.14.

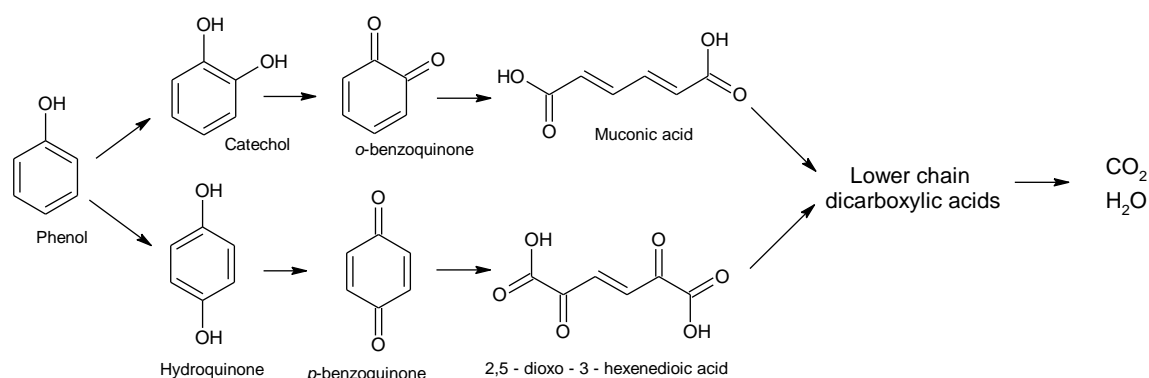


Figure 1.14 – Phenol oxidation pathway. Adapted from [92].

In addition to phenol, the MNB aromatic ring can also be cleaved through a sequence of oxidation and isomerization reactions, which lead to mesoxalic acid and its oxime generation, as described by Urbański [3] based on Seyewetz and Poizat [93] work and illustrated in Figure 1.15.

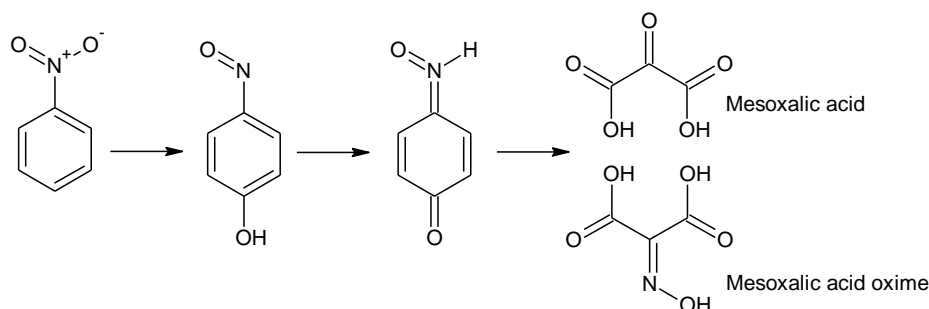


Figure 1.15 – MNB oxidation, isomerization and ring cleavage. Adapted from [3].

However, the CO₂ source may not be limited to phenol or MNB, it can also result from the oxidation of other aliphatic or aromatic hydrocarbons. For instance, Ross and Kirshen [94] state, based in the work developed by Bennett *et al.* [95], that in the nitration of DNT the major oxidation products are CO, CO₂ and nitrous acid. Ross and Kirshen [94] have also detected these carbon oxides formation and found that they represented 15 to 20% of the oxidized substrate. Additionally, the authors have also found that among the DNT isomers, 3,5-DNT was the one which yielded higher amounts of gaseous by-products during nitration [94]. While nitrating DNT Hill *et al.* [96] have also detected the formation of both CO and CO₂. However, is important to mention that in the referred DNT nitration studies, nitric acid was fed in excess contrarily to what is verified in benzene nitration.

Once toluene can be present in nitration grade benzene and because this compound undergoes nitration [3] and oxidation [13, 83] more easily than benzene, it can be thought that toluene, or toluene derivatives, may contribute for the detected CO₂ amounts in industrial plants.

Some of the reaction routes and oxidation by-products of toluene nitration are represented in Figure 1.16.

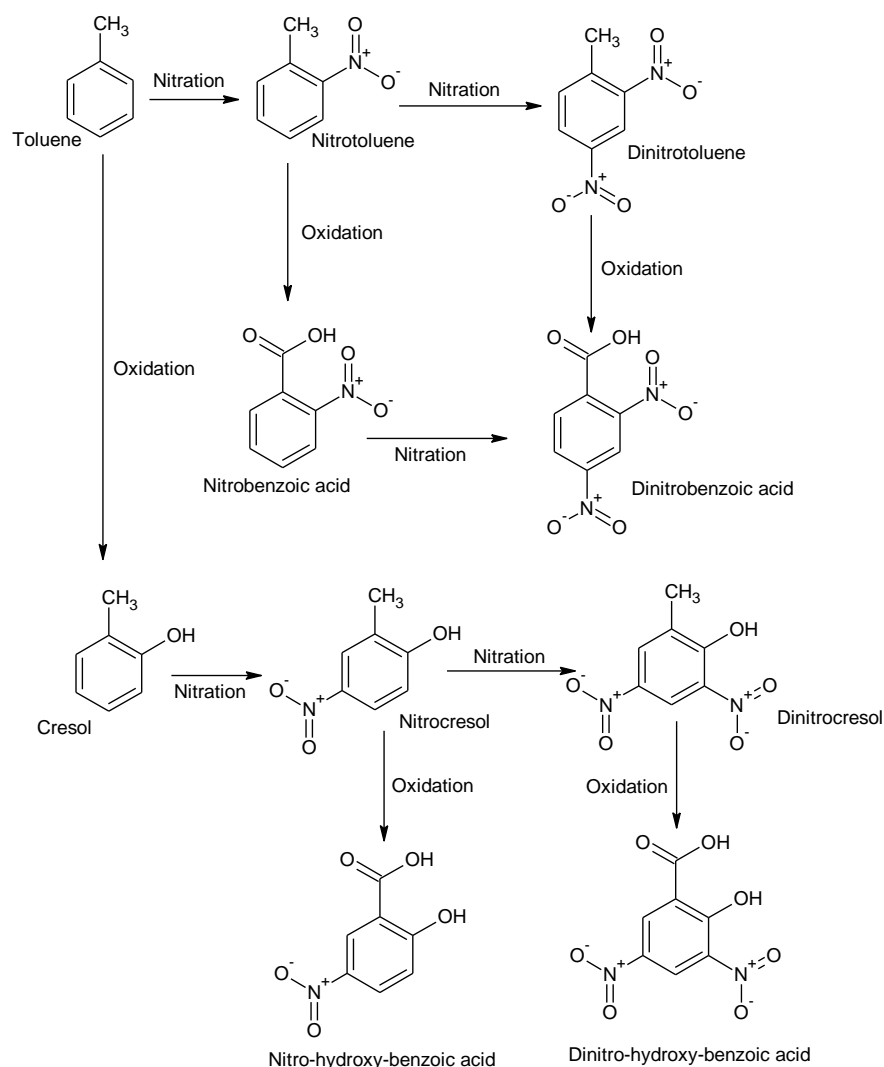
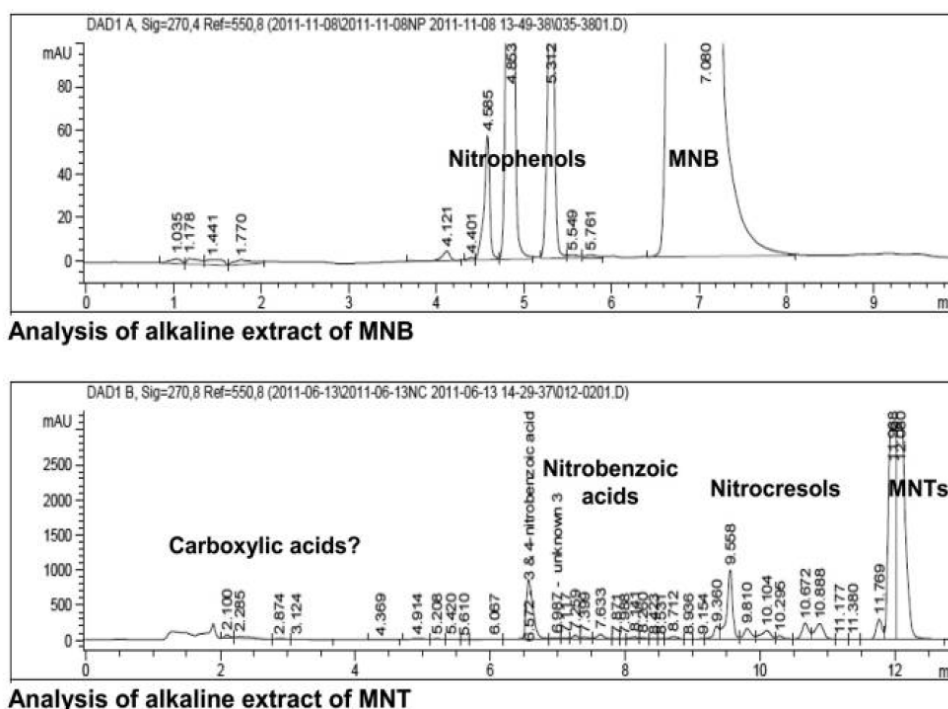


Figure 1.16 – Toluene nitration by-products. Adapted from [83].

The presented by-products can suffer further oxidation reactions. It is possible to notice, by comparing Figures 1.12 and 1.16, that toluene nitration is a more prone reaction for by-products formation than benzene nitration. Moreover, if the nitrating conditions employed are harsher, by-products formation should be enhanced. Thus, the presence of traces of toluene on the benzene feed stream may be responsible for the appearance of unidentified compounds in the reaction medium. As an example, Figure 1.17 shows a comparison between benzene and toluene nitration products,

which allows to corroborate that toluene nitration is more susceptible towards by-products formation.



some impurities formation during benzene nitration because the employed reaction temperature is higher than that employed in toluene nitration (cf. Table 1.2).

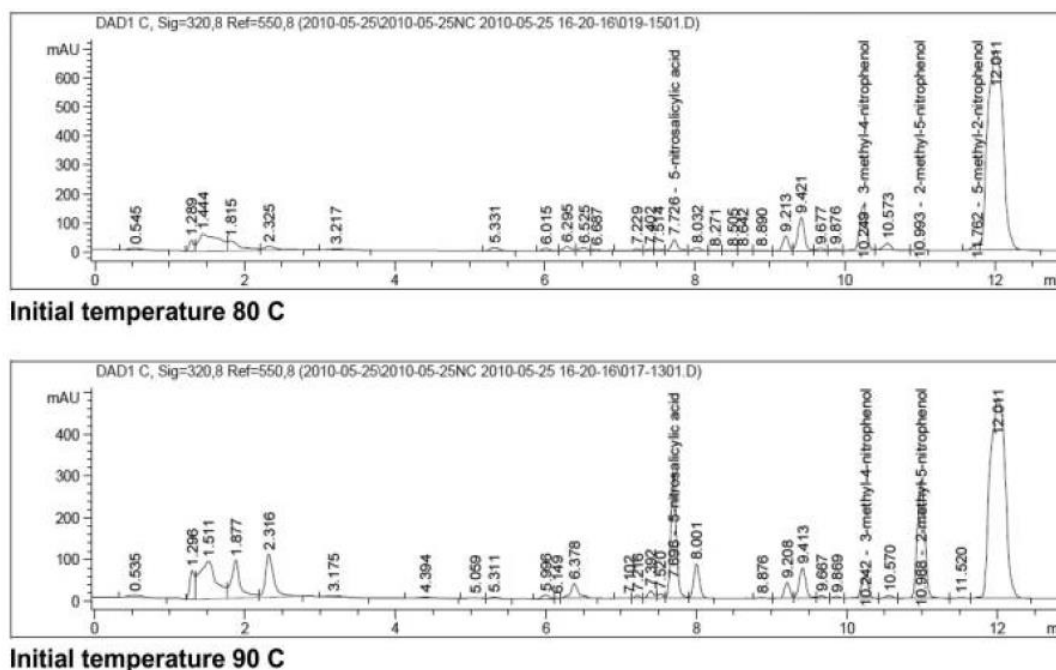


Figure 1.18 – Toluene nitration products at different reaction temperatures. Adapted from. [83].

In benzene nitration the increase of the reaction temperature is known to enhance nitrophenols formation [75], as well as phenol generation since it is the nitrophenols precursor [100]. As seen before, phenol can also be in the genesis of carboxylic acids and carbon dioxide (Figure 1.13 and 1.14); consequently, the temperature rise can also imply the increase of these compounds' formation. In fact, the dependence of the reaction temperature in oxidation reactions is well known and studied in advanced oxidation processes [101-102].

Table 1.2 shows industrial and general conditions relatively to benzene and toluene nitration.

Table 1.2 – Typical industrial nitrating conditions. Adapted from [2, 13, 38].

Substrate	% H ₂ SO ₄ (wt.)	% HNO ₃ (wt.)	% H ₂ O (wt.)	T (°C)
Benzene	62 - 64	4 - 8	24 - 34	80 – 120
Toluene	52 - 67	17 - 32	12 - 20	25 – 40

Scrutinizing Table 1.2 it is possible to see that there is a difference in the nitric acid content in mixed acid for benzene and toluene nitration. That can be explained because toluene industrial nitration is done resorting to the isothermal process [44], which uses lower reaction temperatures. Consequently, in order to promote the reaction, higher HNO₃ content is required (see equation 1.9).

Besides toluene, nitration grade benzene typically contains small amounts of other impurities (Table 1.3) that can build-up in the recycled benzene stream [31]. When this phenomena is observed an aliphatic purge to the system is industrially carried out [27]. However, if such phenomenon is not verified this can mean that the impurities are being slowly oxidised in the organic phase yielding carbon dioxide and carboxylic acids [103].

Table 1.3 – Typical impurities present in nitration grade benzene. Adapted from [103].

Compound	Typical concentration (ppm)
Cyclopentane	100
Methylcyclopentane	50
Cyclohexane	200
Methylcyclohexane	100
Toluene	100

Regarding the presented impurities, the one of great interest is toluene since it produces more by-products than the others [84]. However, the presence of aliphatic compounds in the feed stream should not be neglected.

It is known that nitrated aliphatic compounds in contact with hot sulphuric acid are hydrolysed [6, 104] and that the contact between concentrated nitric acid and aliphatics yield both nitrated compounds and oxidized species [104]. However, in contact with mixed acid aliphatics nitration occurs very slowly [104]. This is because these species nitration is accomplished through a free radical mechanism [84, 105], which requires harsher conditions than those of benzene nitration. Therefore, if occurring, the nitration of aliphatic compounds should be in a small extent, meaning that their role on the formation of oxidized species should be neglectable. Nevertheless, if nitroaliphatics formation in aromatic nitration is not insignificant, species such as nitrocyclohexane may be produced (Figure 1.19 a)), oxidation steps may also occur and C – C bonds can be broken [84] – Figure 1.19 b). It is also possible, in the presence of linear paraffins, the formation of nitrocarboxylic acids, which are then converted into lower nitroparaffins releasing carbon dioxide (Figure 1.19 c)).

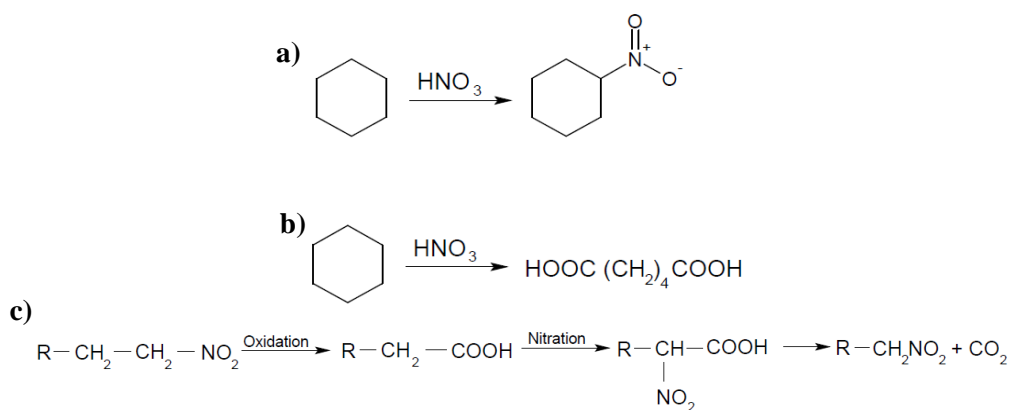


Figure 1.19 – a) Cyclohexane nitration. b) Cyclohexane C – C break. c) Paraffin oxidation and nitration. Adapted from [15, 106].

Aliphatic nitration studies at 25 °C with nitronium salts were performed and it was concluded that alkane's C – C bonds are more reactive than C – H bonds, meaning that these compounds preferably undergo nitrolysis instead of nitration [6]. Furthermore, if the alkane is nitrated it becomes more soluble in nitric acid, becoming more readily attacked by the acid so that the ultimate products are oxides of nitrogen, water and carbon dioxide [106-107].

Despite the possible decomposition of aliphatics or aromatic impurities (or of their nitrated derivatives), it is important to have in mind that the amounts of these compounds in benzene nitration medium are low, thus, their contribution for CO₂ release, if verified, should be minimal.

Regarding the oxidizing agent responsible for the oxidative degradation of organic compounds, that ultimately lead to CO₂ release, nitric acid (or nitric acid derivatives), which is used as raw material on the nitration of aromatic chemicals, appears to be capable of triggering such reactions. Indeed, while nitrating aliphatic compounds it was seen that the decrease of nitric acid concentration led to the reduction of the amounts of oxidized species [104], being thus evidenced the nitric acid influence on the formation of the oxidized compounds. Additionally, nitric acid is also pointed as a powerful oxidizing agent [108-109], responsible for benzene oxidation to phenol [57, 100]. Moreover, when a phenolic impurity is heated to 50 °C in HNO₃ it can be nearly completely oxidised [110], as depicted in Figure 1.20.

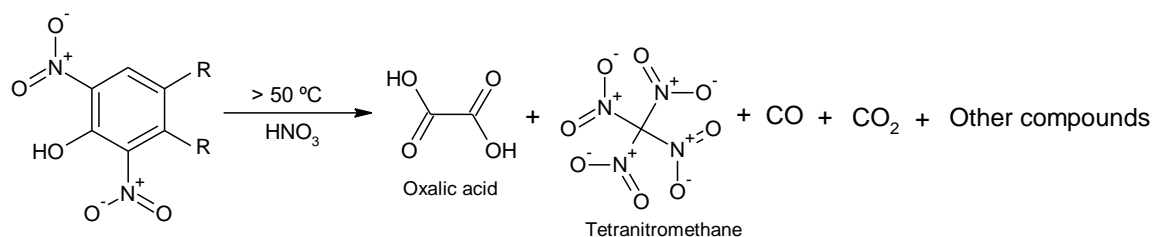


Figure 1.20 – Oxidation by nitric acid. Adapted from [110].

Due to its oxidizing properties, nitric acid can be used as an oxidizing agent for removing precipitates mainly composed by carbon, hydrogen, oxygen and nitrogen produced during benzene nitration with satisfactory results according to Mairata and Knauff [51]. Rodger and Mcirvine [111] refer nitric acid suitability for destroying organic matter present in spent acids from pentaerythritol nitration. Furthermore, to enable the re-concentration of sulfuric acid from the spent acid of nitrotoluene nitration process, nitric acid can be used as the oxidizing agent for removing dissolved organic compounds [98-99].

Under drastic conditions, i.e., under high temperature, high water content and high amounts of nitrogen oxides in nitric acid, the nitric acid oxidising effect is enhanced and the breakdown of the organic molecules may occur [14]. Thus, it is possible that within aromatic nitration conditions, nitric acid is responsible for oxidizing organic matter, leading ultimately to oxalic acid, CO₂ and CO formation as represented in Figure 1.20.

As previously mentioned (section 1.5), HNO₃ decomposes to form the nitronium ion, but it can also be decomposed in nitric oxides that may act as powerful oxidants. The thermal decomposition of nitric acid may be an important factor to be considered because nitric acid does decompose within the benzene nitration conditions and, therefore, may yield potential oxidizers [84, 112-113]. Accordingly to Ross and Kirshen [94] and Kazakov *et al.* [114], a possible route for the nitric acid decomposition is the following (equations 1.13 and 1.14):



Ross and Kirshen [94] suggest that the formed NO₂ is the active oxidizing species in mixed acid systems. According to Hermann *et al.* [20] the presence of NO₂ in the reaction medium of nitrotoluene nitration is believed to be the responsible for the degradative oxidation of nitrocresols yielding water, CO₂ and short chain carboxylic acids such as formic acid, acetic acid and oxalic acid. This is indicative that nitric acid or nitric acid derivatives have an oxidizing function in nitration as (for instance) ozone has in advanced oxidation processes, although in a smaller extent. If by chance in the reaction medium are present other oxidants, oxidation reactions can be further promoted.

Numerous investigations have dealt with oxidative degradation of organic compounds from nitration processes [101, 115-119] being found that nitrated compounds can be oxidized to short-chain carboxylic acids, water, CO₂ and even CO (Figure 1.21).

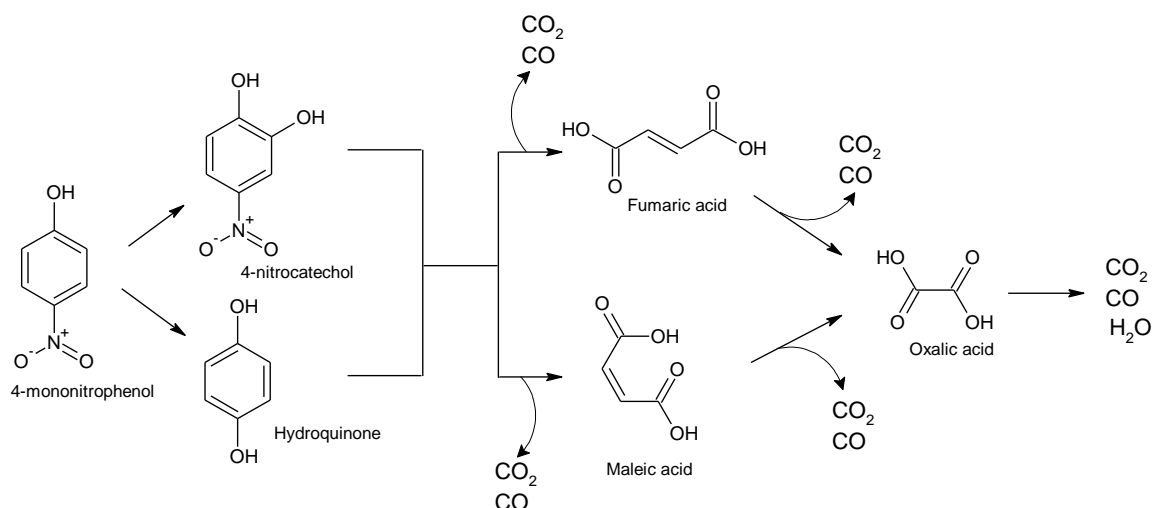


Figure 1.21 – Possible reaction pathway of organic compounds oxidation by Fenton's reagent. Adapted from [101, 116, 118].

Despite the fact that there is no information regarding the formation of hydroxyl radicals in nitration reactions, the harsh nitration conditions together with the oxidizing potential of nitric acid (or nitric acid derivatives) may lead to the oxidative degradation of the organic matter present in the benzene nitration medium as described in advanced oxidation processes and illustrated in Figure 1.21. These oxidative degradation reactions are suspected to be those responsible for the formation of the detected carbon dioxide (in the form of ammonium carbonate) in the nitration plant.

Nomenclature

Abbreviations

Bz	Benzene
CSTR	Continuous stirred tank reactor
DNB	Dinitrobenzene
DNP	Dinitrophenol
DNT	Dinitrotoluene
MNB	Mononitrobenzene
MNT	Mononitrotoluene
MNP	Mononitrophenol
NP	Nitrophenol
Ph	Phenol
TNP	Trinitrophenol

1.8. References

- [1]. Albright, L. F., Nitration. In *Kirk-Othmer Encyclopedia of Chemical Technology*, John Wiley & Sons, Inc., 2000, 10.1002/0471238961.1409201801120218.a01.
- [2]. Booth, G., Nitro Compounds, Aromatic. In *Ullmann's Encyclopedia of Industrial Chemistry*, Wiley-VCH, Weinheim, 2000, doi:10.1002/14356007.a17_411.
- [3]. Urbański, T., *Chemistry and Technology of Explosives*. Pwn-Polish Scientific Publishers, Vol. 1, Warszawa, Poland, 1964.
- [4]. Zaldívar, J. M.; Molga, E.; Alós, M. A.; Hernández, H.; Westerterp, K. R., Aromatic nitrations by mixed acid. Fast liquid-liquid reaction regime. *Chemical Engineering and Processing: Process Intensification* **1996**, 35 (2), 91-105, [https://doi.org/10.1016/0255-2701\(95\)04119-2](https://doi.org/10.1016/0255-2701(95)04119-2).
- [5]. Quadros, P. A.; Oliveira, N. M. C.; Baptista, C. M. S. G., Continuous adiabatic industrial benzene nitration with mixed acid at a pilot plant scale. *Chemical Engineering Journal* **2005**, 108 (1), 1-11, <http://dx.doi.org/10.1016/j.cej.2004.12.022>.
- [6]. Olah, G. A.; Malhotra, R.; Narang, S. C., *Nitration: Methods and Mechanisms*. Wiley-VCH, 1989.
- [7]. Agrawal, J. P.; Hodgson, R. D., *Organic Chemistry of Explosives*. John Wiley & Sons, West Sussex, UK, 2007.
- [8]. Carey, F., *Organic Chemistry*. 4th edition, McGraw-Hill, New York, 2000.
- [9]. Albright, L. F.; Carr, R. V. C.; Schmitt, R. J., Nitration: An Overview of Recent Developments and Processes. In *Nitration*, American Chemical Society, Washington, DC. ACS Symposium Series, 1996; Vol. 623, pp 1-9, doi:10.1021/bk-1996-0623.ch001
10.1021/bk-1996-0623.ch001.
- [10]. am Ende, D. J.; Clifford, P. J.; Northrup, D. L., The role of reaction calorimetry in the development and scale-up of aromatic nitrations. *Thermochimica Acta* **1996**, 289 (2), 143-154, [https://doi.org/10.1016/S0040-6031\(96\)03065-1](https://doi.org/10.1016/S0040-6031(96)03065-1).
- [11]. Hanson, C.; Pratt, M. W. T.; Sohrabi, M., Some Aspects of Aromatic Nitration in Aqueous Systems. In *Industrial and Laboratory Nitrations*, American Chemical Society, Washington, DC. ACS Symposium Series, 1976; Vol. 22, pp 225-242, doi:10.1021/bk-1976-0022.ch015
10.1021/bk-1976-0022.ch015.
- [12]. Hoggett, J. G.; Moodie, R. B.; Penton, J. R.; Schofield, K., Nitration and aromatic reactivity. Cambridge University Press, Cambridge, UK, 1971,
- [13]. Dugal, M., Nitrobenzene and Nitrotoluenes. In *Kirk-Othmer Encyclopedia of Chemical Technology*, John Wiley & Sons, Inc., 2000, 10.1002/0471238961.1409201801041109.a01.pub2.

- [14]. Topchiev, A. V., Introduction. In *Nitration of Hydrocarbons and Other Organic Compounds*, Pergamon Press, London UK, 1959; pp 1-10, <https://doi.org/10.1016/B978-0-08-009154-9.50003-6>.
- [15]. Schofield, K., Aromatic Nitration. Cambridge University Press, Cambridge, UK, 1980,
- [16]. Muspratt, J. S.; Hofmann, A. W., Ueber das Nitranilin, ein neues Zersetzungsproduct des Dinitrobenzols. *Justus Liebigs Annalen der Chemie* **1846**, 57 (2), 201-224, doi:10.1002/jlac.18460570208.
- [17]. CUF-QI, Internal Report. 2012,
- [18]. National Toxicology Program *Report on Carcinogens*; 13th edition, U.S. Department of Health and Human Services: 2014.
- [19]. Patnaik, P., *A Comprehensive Guide to the Hazardous Properties of Chemical Substances*. 3rd edition, John Wiley & Sons, New Jersey, 2007.
- [20]. Hermann, H.; Gebauer, J.; Konieczny, P., Industrial Nitration of Toluene to Dinitrotoluene. In *Nitration*, American Chemical Society, Washington, DC. ACS Symposium Series, 1996; Vol. 623, pp 234-249,
- [21]. European Chemicals Bureau *European Union Risk Assessment Report, Nitrobenzene, Part I - Environment*; 2007.
- [22]. Kent, J. A., *Kent and Riegel's Handbook of Industrial Chemistry and Biotechnology*. 11th edition, Springer, New York, USA, 2007; Vol. 1.
- [23]. Eiermann, M.; Ebel, K. Nitration of Aromatic Hydrocarbons. US Patent 2002/0038060 A1, March 28, 2002.
- [24]. Lee, B.-S.; Chung, K.-H.; Lee, Y.-S.; Kim, Y.-G. Process for Nitration of Aromatic Compounds Using a Non-Acid Type Nitration Process. US Patent 6,291,726 B1, September 18, 2001.
- [25]. Nogueira, A. In *Optimização da Nitração de Aromáticos*, Seminário: Os Desafios da Indústria Petroquímica e de Refinação e o Papel do Sistema Científico e Tecnológico, Lisboa, 2010.
- [26]. IHS Markit, Nitrobenzene. <<https://ihsmarkit.com/products/nitrobenene-chemical-economics-handbook.html>>, 2017, accessed February 5th, 2019.
- [27]. Guenkel, A., The Adiabatic Mononitrobenzene Process from the Bench Scale in 1974 to a Total World Capacity Approaching 10 Million MTPY in 2012. In *Chemistry, Process Design, and Safety for the Nitration Industry*, American Chemical Society, Washington, DC. ACS Symposium Series, 2013; Vol. 1155, pp 1-11, doi:10.1021/bk-2013-1155.ch001 10.1021/bk-2013-1155.ch001.
- [28]. CUF-QI, Relatório e Contas. 2017.
- [29]. CUF-QI, Management Report. 2016.
- [30]. Santos, P. A. Q. d. O. Nitração de Compostos Aromáticos: Transferência de Massa e Reação Química. PhD Thesis, Universidade de Coimbra, Portugal, 2004.

- [31]. Guenkel, A.; Rae, J. M.; Hauptmann, E. G. Nitration process. EP 0 436 443 B1, 1996.
- [32]. Alexanderson, V.; Trecek, J. B.; Vanderwaart, C. M. Adiabatic Process for Nitration of Nitratable Aromatic Compounds. US Patent 4021498, May 3, 1977.
- [33]. Evans, C. M. Manufacture of Organic Nitro Compounds. US Patent 4973770, November 27, 1990.
- [34]. Guenkel, A.; Rae, J. M.; Hauptmann, E. G. Nitration Process. US Patent 5313009, May 17, 1994.
- [35]. Nogueira, A. Optimização da Nitração de Aromáticos. PhD thesis, Universidade de Coimbra, Portugal, 2014.
- [36]. Nexant, PERP 02/03-2, Nitrobenzene/Aniline. 2003.
- [37]. Castner, J. B. Nitration of Organic Compounds. US Patent 2256999, September 23, 1941.
- [38]. Alexanderson, V.; Trecek, J. B.; Vanderwaart, C. M. Continuous Adiabatic Process for the Mononitration of Benzene. US Patent 4091042, May 23, 1978.
- [39]. Bondalti Chemicals, Internal Report. 2014.
- [40]. Rae, J. M.; Hauptmann, E. G. Jet Impingement Reactor. US Patent 4994242, February 19, 1991.
- [41]. Henke, L.; Winterbauer, H.; Hetzel, J. Verfahren zur adiabatischen Nitrierung von Benzol. DE 102009005324 A1, July 22, 2010.
- [42]. Sato, I. H.; Nakamura, T. S. Process for Nitration of Benzene. US Patent 4551568, November 5, 1985.
- [43]. Dongare, M. K.; Patil, P. T.; Malshe, K. M. Process for Vapor Phase Nitration of Benzene Using Nitric Acid Over Molybdenum Silica Catalyst. US Patent 6791000 B2, September 14, 2004.
- [44]. Duehr, J., Nitration Technology for Aromatics As Described in the Patent Literature. In *Chemistry, Process Design, and Safety for the Nitration Industry*, American Chemical Society, Washington, DC. ACS Symposium Series, 2013; Vol. 1155, pp 71-82,
- [45]. Earle, M. J.; Katdare, S. P. Aromatic Nitration Reactions. US Patent 6906231 B2, June 14, 2005.
- [46]. Berretta, S. Adiabatic Process for Making Mononitrobenzene. US Patent 8692035 B2, April 8, 2014.
- [47]. Guenkel, A. A.; Berretta, S. Removal of Non-aromatic Impurities from a Nitration Process. US Patent 9139509 B2, September 22, 2015.
- [48]. Knauff, T.; Merkel, M.; Mairata, A. Method for Producing Nitrobenzene by Adiabatic Nitriding. US Patent 9260377 B2, February 16, 2016.
- [49]. Munning, J.; Pennemann, B.; Rausch, A. K. Process for the Continuous Preparation of Nitrobenzene. US Patent 8357827 B2, January 22, 2013.

- [50]. Knauft, T.; Drinda, P. Process for Producing Nitrobenzene. US Patent 2018/0346405 A1, December 6, 2018.
- [51]. Mairata, A.; Knauft, T. Process for the Preparation of Nitrobenzene by Adiabatic Nitration. US Patent 9302978 B1, April 5, 2016.
- [52]. Knauf, T.; Merkel, M. Process for the Production of Nitrobenzene by Adiabatic Nitration. US Patent 9284256 B2, March 15, 2016.
- [53]. Mendes, A. M. M.; Ribeiro, A. F. G.; Dias, M. C.; Félix, A. S. P.; Pinho, M. J. O. Electrodes/Electrolyte Assembly, Reactor and Method for Direct Amination of Hydrocarbons. WO 2014/155360 A1, October 2, 2014.
- [54]. Jaeger, G.; Magnus, J.; Moussa, S. Production of Aniline Via Anthranilate. US Patent 10173969 B2, January 8, 2019.
- [55]. Hughes, E. D.; Ingold, C. K.; Reed, R. I., 493. Kinetics and mechanism of aromatic nitration. Part II. Nitration by the nitronium ion, NO_2^+ , derived from nitric acid. *Journal of the Chemical Society* **1950**, (0), 2400-2440, 10.1039/JR9500002400.
- [56]. Cardoso, S. P.; Carneiro, J. W. d. M., Nitração aromática: substituição eletrofílica ou reação com transferência de elétrons? *Química Nova* **2001**, 24, 381-389,
- [57]. Burns, J. R.; Ramshaw, C., Development of a Microreactor for Chemical Production. *Chemical Engineering Research and Design* **1999**, 77 (3), 206-211, <http://dx.doi.org/10.1205/026387699526106>.
- [58]. C. Marziano, N.; Tomasin, A.; Tortato, C.; M. Zaldivar, J., Thermodynamic nitration rates of aromatic compounds. Part 4. Temperature dependence in sulfuric acid of HNO_3 - NO_2^+ equilibrium, nitration rates and acidic properties of the solvent. *Journal of the Chemical Society, Perkin Transactions 2* **1998**, (9), 1973-1982, 10.1039/A802521E.
- [59]. Halder, R.; Lawal, A.; Damavarapu, R., Nitration of toluene in a microreactor. *Catalysis Today* **2007**, 125 (1-2), 74-80, <http://dx.doi.org/10.1016/j.cattod.2007.04.002>.
- [60]. Carey, F. A.; Sundberg, R. J., *Advanced Organic Chemistry: Part B: Reaction and Synthesis*. Springer, 2007.
- [61]. Quadros, P. A.; Reis, M. S.; Baptista, C. M. S. G., Different Modeling Approaches for a Heterogeneous Liquid-Liquid Reaction Process. *Industrial & Engineering Chemistry Research* **2005**, 44 (25), 9414-9421, 10.1021/ie050205m.
- [62]. Giles, J.; Hanson, C.; Ismail, H. A. M., A Model for Rate of Nitration of Toluene Under Heterogeneous Conditions. In *Industrial and Laboratory Nitrations*, American Chemical Society, Washington, DC. ACS Symposium Series, 1976; Vol. 22, pp 190-209, doi:10.1021/bk-1976-0022.ch012
10.1021/bk-1976-0022.ch012.
- [63]. Silva, D. C. M., Optimização da Etapa de Nitração do Benzeno. In *Projecto em Consórcio Aroma*, Coimbra, Portugal, 2006,

- [64]. Burns, J. R.; Ramshaw, C., A Microreactor for the Nitration of Benzene and Toluene. *Chemical Engineering Communications* **2002**, 189 (12), 1611-1628, 10.1080/00986440214585.
- [65]. Coombes, R. G.; Moodie, R. B.; Schofield, K., Electrophilic aromatic substitution. Part I. The nitration of some reactive aromatic compounds in concentrated sulphuric and perchloric acids. *Journal of the Chemical Society B: Physical Organic* **1968**, (0), 800-804, 10.1039/J29680000800.
- [66]. Marziano, N. C.; Sampoli, M.; Pinna, F.; Passerini, A., Thermodynamic nitration rates of aromatic compounds. Part 2. Linear description of rate profiles for the nitration of aromatic compounds in the range 40-98 wt% sulphuric acid. *Journal of the Chemical Society, Perkin Transactions 2* **1984**, (7), 1163-1166, 10.1039/P29840001163.
- [67]. Smith, M. B.; March, J., *March's Advanced Organic Chemistry: Reactions, Mechanisms, and Structure*. 6th edition, John Wiley & Sons, New Jersey, 2007.
- [68]. Kulkarni, A. A., Continuous flow nitration in miniaturized devices. *Beilstein Journal of Organic Chemistry* **2014**, 10, 405-424, 10.3762/bjoc.10.38.
- [69]. Carey, F. A.; Sundberg, R. J., *Advanced Organic Chemistry: Part A: Structure and Mechanisms*. 5th edition, Springer, New York, 2007.
- [70]. Zaldivar, J. M.; Molga, E.; Alós, M. A.; Hernández, H.; Westerterp, K. R., Aromatic nitrations by mixed acid. Slow liquid-liquid reaction regime. *Chemical Engineering and Processing: Process Intensification* **1995**, 34 (6), 543-559, [http://dx.doi.org/10.1016/0255-2701\(95\)04111-7](http://dx.doi.org/10.1016/0255-2701(95)04111-7).
- [71]. Edwards, H. G. M.; Fawcett, V., Quantitative Raman spectroscopic studies of nitronium ion concentrations in mixtures of sulphuric and nitric acids. *Journal of Molecular Structure* **1994**, 326, 131-143, [http://dx.doi.org/10.1016/0022-2860\(94\)85013-5](http://dx.doi.org/10.1016/0022-2860(94)85013-5).
- [72]. Deno, N. C.; Peterson, H. J.; Sacher, E., Nitric Acid Equilibria in Water—Sulfuric Acid. *The Journal of Physical Chemistry* **1961**, 65 (2), 199-201, 10.1021/j100820a002.
- [73]. Edwards, H. G. M.; Turner, J. M. C.; Fawcett, V., Raman spectroscopic study of nitronium ion formation in mixtures of nitric acid, sulfuric acid and water. *Journal of the Chemical Society, Faraday Transactions* **1995**, 91 (10), 1439-1443, 10.1039/FT9959101439.
- [74]. Russo, D.; Marotta, R.; Commodo, M.; Andreozzi, R.; Somma, I. D., Ternary HNO₃-H₂SO₄-H₂O Mixtures: A Simplified Approach for the Calculation of the Equilibrium Composition. *Industrial & Engineering Chemistry Research* **2018**, 57 (5), 1696-1704,
- [75]. Quadros, P. A.; Castro, J. A. A. M.; Baptista, C. M. S. G., Nitrophenols Reduction in the Benzene Adiabatic Nitration Process. *Industrial & Engineering Chemistry Research* **2004**, 43 (15), 4438-4445, 10.1021/ie034263o.

- [76]. Lyle, F. A.; Sood, M. K.; Roger, E. E., Modeling Nitronium Ion Concentrations in HNO₃-H₂SO₄-H₂O Mixtures. In *Nitration*, American Chemical Society, 1996; Vol. 623, pp 201-213, doi:10.1021/bk-1996-0623.ch018
10.1021/bk-1996-0623.ch018.
- [77]. Antes, J.; Boskovic, D.; Krause, H.; Loebbecke, S.; Lutz, N.; Tuercke, T.; Schweikert, W., Analysis and Improvement of Strong Exothermic Nitrations in Microreactors. *Chemical Engineering Research and Design* **2003**, *81* (7), 760-765, <http://dx.doi.org/10.1205/026387603322302931>.
- [78]. Shen, J.; Zhao, Y.; Chen, G.; Yuan, Q., Investigation of Nitration Processes of iso-Octanol with Mixed Acid in a Microreactor. *Chinese Journal of Chemical Engineering* **2009**, *17* (3), 412-418, [http://dx.doi.org/10.1016/S1004-9541\(08\)60225-6](http://dx.doi.org/10.1016/S1004-9541(08)60225-6).
- [79]. Muennig, J.; Pennemann, B.; Wastian, D.; Michele, V.; Caravaggio, J.; Jr., J. F. G. Process for the Production of Dinitrotoluene. US Patent 7041858 B1, May 9, 2006.
- [80]. Hanson, C.; Kaghazchi, T.; Pratt, M. W. T., Side Reactions During Aromatic Nitration. In *Industrial and Laboratory Nitrations*, American Chemical Society, Washington, DC. ACS Symposium Series, 1976; Vol. 22, pp 132-155, doi:10.1021/bk-1976-0022.ch008
10.1021/bk-1976-0022.ch008.
- [81]. Schiefferle, D. F.; Hanson, C.; Albright, L. F., Heterogeneous Nitration of Benzene. In *Industrial and Laboratory Nitrations*, American Chemical Society, Washington, DC. ACS Symposium Series, 1976; Vol. 22, pp 176-189, doi:10.1021/bk-1976-0022.ch011
10.1021/bk-1976-0022.ch011.
- [82]. Berretta, S.; Louie, B., Effect of Reaction Conditions on the Formation of Byproducts in the Adiabatic Mononitration of Benzene into Mononitrobenzene (MNB). In *Chemistry, Process Design, and Safety for the Nitration Industry*, American Chemical Society, Washington, DC. ACS Symposium Series, 2013; Vol. 1155, pp 13-26, doi:10.1021/bk-2013-1155.ch002
10.1021/bk-2013-1155.ch002.
- [83]. Gattrell, M.; Louie, B., Adiabatic Nitration for Mononitrotoluene (MNT) Production. In *Chemistry, Process Design, and Safety for the Nitration Industry*, American Chemical Society, Washington, DC. ACS Symposium Series, 2013; Vol. 1155, pp 27-48, doi:10.1021/bk-2013-1155.ch003
10.1021/bk-2013-1155.ch003.
- [84]. Lowenbach, W.; Schlesinger, J.; King, J. A., *Toxic Pollutant Identification: Nitrobenzene/aniline Manufacturing*. U.S. Environmental Protection Agency, 1979.
- [85]. Dumann, G.; Quittmann, U.; Gröschel, L.; Agar, D. W.; Wörz, O.; Morgenschweis, K., The capillary-microreactor: a new reactor concept for the intensification of heat and mass transfer in liquid-liquid reactions. *Catalysis Today* **2003**, *79-80*, 433-439, [http://dx.doi.org/10.1016/S0920-5861\(03\)00056-7](http://dx.doi.org/10.1016/S0920-5861(03)00056-7).

- [86]. Nogueira, A. G.; Silva, D. C. M.; Reis, M. S.; Baptista, C. M. S. G., Prediction of the By-products Formation in the Adiabatic Industrial Benzene Nitration Process. *Chemical Engineering Transactions* **2013**, 32, 1249-1254,
- [87]. Portugal, P. A. G.; Reis, M. S.; Baptista, C. M. S. G., Extending model prediction ability for the formation of nitrophenols in benzene nitration. *Chemical Engineering Transactions* **2009**, 17, 117-122,
- [88]. Lopes, A. L. C. V.; Ribeiro, A. F. G.; Reis, M. S.; Silva, D. C. M.; Portugal, I.; Baptista, C. M. S. G., Modelling the Distribution of Nitrophenols in a Liquid-Liquid System Representative of an Industrial Nitration Process. *Chemical Engineering Transactions* **2017**, 57, 1033-1038,
- [89]. Lopes, A. L. C. V.; Ribeiro, A. F. G.; Reis, M. P. S.; Silva, D. C. M.; Portugal, I.; Baptista, C. M. S. G., Distribution models for nitrophenols in a liquid-liquid system. *Chemical Engineering Science* **2018**, 189, 266-276,
- [90]. Herney-Ramirez, J.; Vicente, M. A.; Madeira, L. M., Heterogeneous photo-Fenton oxidation with pillared clay-based catalysts for wastewater treatment: A review. *Applied Catalysis B: Environmental* **2010**, 98 (1–2), 10-26, <http://dx.doi.org/10.1016/j.apcatb.2010.05.004>.
- [91]. Buchi, S. D.; Guenkel, A. A., Method of purifying nitrated aromatic compounds from a nitration process. WO 2016198921 A1, December 15, 2016.
- [92]. Devlin, H. R.; Harris, I. J., Mechanism of the oxidation of aqueous phenol with dissolved oxygen. *Industrial & Engineering Chemistry Fundamentals* **1984**, 23 (4), 387-392,
- [93]. Seyewetz, A.; Poizat, L., Sur l'oxydation des dérivés nitrés et nitrosés aromatiques par le persulfate d'ammoniaque. *Comptes rendus hebdomadaires des séances de l'Académie des sciences* **1909**, 148,
- [94]. Ross, D. S.; Kirshen, N. A., Nitration and Oxidative Side Reactions of Dinitrotoluenes. In *Industrial and Laboratory Nitrations*, American Chemical Society, Washington, DC. ACS Symposium Series, 1976; Vol. 22, pp 114-131, doi:10.1021/bk-1976-0022.ch007 10.1021/bk-1976-0022.ch007.
- [95]. Bennett, G. M.; Brand, J. C. D.; James, D. M.; Saunders, T. G.; Williams, G., 94. Nitration in sulphuric acid. Part IV. Kinetics of the nitration of 2 : 4-dinitrotoluene. *Journal of the Chemical Society* **1947**, (0), 474-492, 10.1039/JR9470000474.
- [96]. Hill, M. E.; Coon, C. L.; Blucher, W. G.; McDonald, G. J.; Marynowski, C. W.; Tolberg, W.; Peters, H. M.; Simon, R. L.; Ross, D. L., Low Temperature Process for TNT Manufacture Part 1. Laboratory Development. In *Industrial and Laboratory Nitrations*, American Chemical Society, Washington, DC. ACS Symposium Series, 1976; Vol. 22, pp 253-271,
- [97]. Milligan, B.; Huang, D.-S. Process for Refining Aqueous Acid Mixtures Utilized in Nitration of Aromatics. US Patent 4257968, March 24, 1981.

- [98]. Evans, C. M., Practical Considerations in Concentration and Recovery of Nitration-Spent Acids. In *Nitration*, American Chemical Society, Washington, DC. ACS Symposium Series, 1996; Vol. 623, pp 250-268,
- [99]. Mater, G. B. D. L.; Milligan, B. Purification of Spent Sulfuric Acid. US Patent 3856673, December 24, 1974.
- [100]. Afonso, D.; Ribeiro, A. F. G.; Araújo, P.; Vital, J.; Madeira, L. M., Phenol in Mixed Acid Benzene Nitration Systems. *Industrial & Engineering Chemistry Research* **2018**, 57 (46), 15942-15953,
- [101]. Carbajo, J.; Quintanilla, A.; Casas, J. A., Assessment of carbon monoxide formation in Fenton oxidation process: The critical role of pollutant nature and operating conditions. *Applied Catalysis B: Environmental* **2018**, 232, 55-59,
- [102]. Zazo, J. A.; Pliego, G.; Blasco, S.; Casas, J. A.; Rodriguez, J. J., Intensification of the Fenton Process by Increasing the Temperature. *Industrial & Engineering Chemistry Research* **2011**, 50 (2), 866-870, 10.1021/ie101963k.
- [103]. Guenkel, A. A.; Maloney, T. W., Recent Advances in the Technology of Mononitrobenzene Manufacture. In *Nitration*, American Chemical Society, Washington, DC. ACS Symposium Series, 1996; Vol. 623, pp 223-233, doi:10.1021/bk-1996-0623.ch020
10.1021/bk-1996-0623.ch020.
- [104]. Topchiev, A. V., Nitration of Saturated, Aromatic-Aliphatic and Unsaturated Hydrocarbons With Nitric Acid. In *Nitration of Hydrocarbons and Other Organic Compounds*, Pergamon Press, London UK, 1959
- [105]. Markofsky, S. B., Nitro Compounds, Aliphatic. In *Ullmann's Encyclopedia of Industrial Chemistry*, Wiley-VCH, Weinheim, 2000, 10.1002/14356007.a17_401.pub2.
- [106]. Asinger, F., The Nitration and Nitration Products of the Paraffins. In *Paraffins Chemistry and Technology*, Asinger, F., Ed. Pergamon Press, Oxford, 1968; pp 365-482, <http://dx.doi.org/10.1016/B978-0-08-011318-0.50009-4>.
- [107]. Hodge, E. B., Process of nitrating paraffin hydrocarbon and product thereof. US Patent 1967667, July 24, 1934.
- [108]. Albright, L. F.; Schiefferle, D. F.; Hanson, C., Reactions occurring in the organic phase during aromatic nitrations. *Journal of Applied Chemistry and Biotechnology* **1976**, 26, 522-525, 10.1002/jctb.5020260174.
- [109]. Clarke, S. I.; Mazzafro, W. J.; Updated by, S., Nitric Acid. In *Kirk-Othmer Encyclopedia of Chemical Technology*, John Wiley & Sons, Inc., 2000, 10.1002/0471238961.1409201803120118.a01.pub2.
- [110]. Odle, R. R.; Guggenheim, T. L.; DeLong, L. M., Solubility, Equilibrium, Behavior, and Analytical Characterization of Tetranitromethane, Trinitromethane, Methyl Amine, and Ammonia in a Nitration Facility. In *Chemistry, Process Design, and Safety for the Nitration*

- Industry*, American Chemical Society, Washington, DC. ACS Symposium Series, 2013; Vol. 1155, pp 203-228, doi:10.1021/bk-2013-1155.ch014
10.1021/bk-2013-1155.ch014.
- [111]. Rodger, I.; Mcirvine, J. D., The decomposition of spent PETN nitration acids. *Canadian Journal of Chemical Engineering* **1963**, *41*, 87-90,
- [112]. Somma, I. D.; Marotta, R.; Andreozzi, R.; Caprio, V., Nitric Acid Decomposition Kinetics in Mixed Acid and their Use in the Modelling of Aromatic Nitration *Chemical Engineering Transactions* **2014**, *36*, 127-132,
- [113]. Di Somma, I.; Marotta, R.; Andreozzi, R.; Caprio, V., Nitric acid decomposition kinetics in mixed acid and their use in the modeling of aromatic nitration. *Chemical Engineering Journal* **2013**, *228*, 366-373, <https://doi.org/10.1016/j.cej.2013.04.100>.
- [114]. Kazakov, A. I.; Rubtsiv, Y. I.; Andrienko, L. P.; Manelis, G. B., Kinetics and mechanism of thermal decomposition of nitric acid in sulfuric acid solutions. *Russian Chemical Bulletin* **1987**, *36* (10), 1999-202,
- [115]. Chen, W.-S.; Juan, C.-N.; Wei, K.-M., Mineralization of dinitrotoluenes and trinitrotoluene of spent acid in toluene nitration process by Fenton oxidation. *Chemosphere* **2005**, *60* (8), 1072-1079, <http://dx.doi.org/10.1016/j.chemosphere.2005.01.021>.
- [116]. Rodrigues, C. S. D.; Borges, R. A. C.; Lima, V. N.; Madeira, L. M., *p*-Nitrophenol degradation by Fenton's oxidation in a bubble column reactor. *Journal of Environmental Management* **2018**, *206*, 774-785,
- [117]. Ayoub, K.; Hullebusch, E. D. v.; Cassir, M.; Bermond, A., Application of advanced oxidation processes for TNT removal: A review. *Journal of Hazardous Materials* **2010**, *178* (1-3), 10-28,
- [118]. Carlos, L.; Fabbri, D.; Capparelli, A. L.; Prevot, A. B.; Pramauro, E.; Einschlag, F. S. G., Intermediate distributions and primary yields of phenolic products in nitrobenzene degradation by Fenton's reagent. *Chemosphere* **2008**, *72* (6), 952-958, <http://dx.doi.org/10.1016/j.chemosphere.2008.03.042>.
- [119]. Zazo, J. A.; Casas, J. A.; Mohedano, A. F.; Gilarranz, M. A.; Rodríguez, J. J., Chemical Pathway and Kinetics of Phenol Oxidation by Fenton's Reagent. *Environmental Science and Technologies* **2005**, *39* (23), 9295-9302,

Chapter 2 – Carbon dioxide generation in nitrobenzene production

Abstract

A gravimetric method was developed to detect and quantify carbon dioxide (CO_2) formed by organic matter decomposition during industrial benzene nitration into mononitrobenzene, both in liquid (organic and aqueous) and gas streams. The developed method consisted in removing dissolved CO_2 from the liquid streams by nitrogen (N_2) bubbling, aiming the subsequent gas sequestration through a precipitate formation (barium carbonate – BaCO_3) in an alkaline (barium hydroxide – $\text{Ba}(\text{OH})_2$) solution, followed by gravimetric analysis.

The developed gravimetric method allowed to map CO_2 distribution in the reaction section of a nitration plant and enabled revealing that this gaseous species was being formed during benzene nitration. Such finding evidences the occurrence of side oxidation reactions during benzene nitration, which are responsible for the decomposition of the organic matter in the reaction medium, and justifies the ammonium carbonate appearance in the alkaline (ammonium) washing section. Furthermore, the operation parameters such as the nitric acid concentration in the nitration media are suggested to influence CO_2 formation during benzene nitration.

Keywords: Carbon dioxide, oxidation, benzene nitration, mononitrobenzene, decomposition.

2.1. Introduction

The most commonly employed [1] mononitrobenzene production process (adiabatic technology) has the following sections: nitration or reaction section, phase separation, mononitrobenzene washing system, mononitrobenzene purification, and sulfuric acid re-concentration – Figure 2.1.

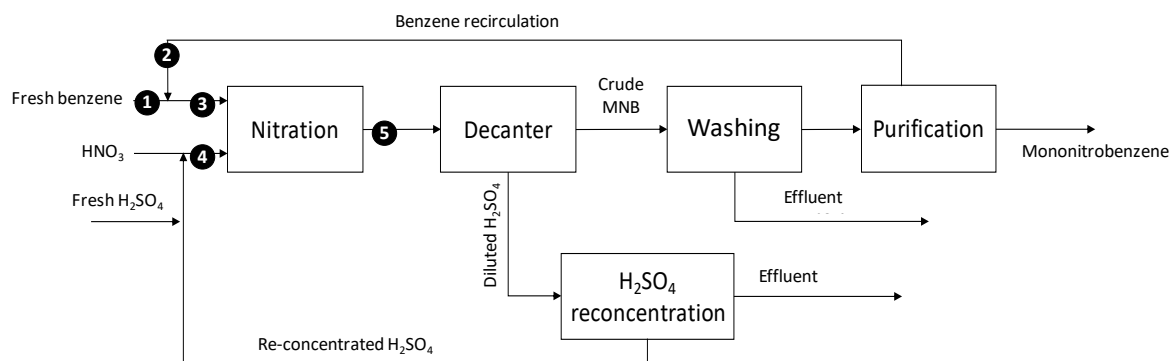


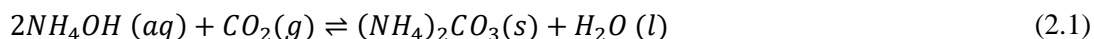
Figure 2.1 – General flow-sheet of the mononitrobenzene production process and sampling points.

In the reaction section, a mixture of fresh benzene (1) and recycled benzene (2) is fed (benzene feed (3)) to the reaction section, together with an aqueous stream composed by nitric and sulfuric acid, the so-called mixed acid (4). In the reaction section, benzene is converted to mononitrobenzene by the action of nitric acid. Besides being the reaction catalyst, sulfuric acid is also a heat sink that absorbs the heat released during the reaction. The reaction mixture exiting the nitration stage (5) is directed to the mononitrobenzene / acid separator (decanter) where the organic phase is separated from the acid (aqueous) one. The acid phase goes to the Sulfuric Acid Concentrators (H₂SO₄ re-concentration) where sulfuric acid is re-concentrated, to then be fed back to the reaction.

The organic stream coming from the decanter is directed to the washing section for the removal of dissolved mineral acids (H₂SO₄ and HNO₃) by liquid-liquid extraction in an acid washer [2]. Then, in a second washing section (alkaline washing stage), nitrophenols, which are typical reaction by-products, are extracted from the organic stream by the action of an alkaline agent such as NH₄OH, NaOH or Na₂CO₃ [3]. Finally, a third washing section, known as neutral washing, may be present to remove the salts coming from the alkaline washing section [3]. After the washing stage, the organic stream is fed to a purification unit where unreacted benzene and aliphatics are removed from the produced mononitrobenzene and fed back to the reaction section, forming thus the recycled benzene (2) stream.

In the second washing section, when NH₄OH is used as the alkaline agent, nitrophenols formed during benzene nitration are removed from mononitrobenzene because in contact with the ammonia solution ammonium nitrophenolates are formed (compounds with higher affinity to the aqueous

phase). Besides extracting nitrophenols from the organic stream, in the presence of CO₂, this alkaline agent is also responsible for the formation of ammonium carbonate ((NH₄)₂CO₃, by CO₂ sequestration), as described by equation (2.1).



Ammonium carbonate is a solid at temperatures up to 60 °C [4], soluble in the aqueous phase, and may form precipitates if CO₂ builds up, leading to the occurrence of operational issues such as piping and equipment plugging. Additionally, CO₂ presence in the alkaline washing section tends to decrease nitrophenols extraction efficiency. Nitration plants in which the alkaline solution used to extract nitrophenols is NaOH do not deal with solids formation problems, however, the use of NaOH disables nitrophenols elimination by incineration [5].

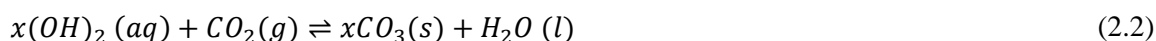
To avoid CO₂ accumulation (ammonium carbonate build-up) in nitration plants it is crucial to check where CO₂ is formed in the plant, its amounts and determine its distribution over the industrial process to allow a proper gas removal from the nitration plant before the alkaline washing section. Accomplishing these objectives would represent an advantage that could enable further optimization of the benzene nitration process since it would allow increasing the nitrophenols extraction efficiency.

The formation of CO₂ (detected by ammonium carbonate generation) in nitration plants [6] is thought to occur during benzene nitration by decomposition of the organic matter present in the reaction medium, although there are no experimental evidences supporting this theory. The decomposition of organic compounds is known to yield CO₂, but CO can also arise, as described in some studies addressing advanced oxidation processes [7-10]. However, to the best of our knowledge, CO was never detected during benzene nitration, neither in laboratory studies nor in industrial production processes.

Incomplete oxidations are known to occur in benzene nitration since nitrophenols, typical reaction by-products, are formed by phenol nitration, which is, in turn, originate *via* benzene oxidation [11]. Similarly, during toluene nitration, incomplete oxidations are also occurring once nitrocresols are formed (by cresol nitration). However, in addition to these reactions, the decomposition of organic compounds can also occur. For instance, according to Guenkel and Maloney [12], at the typical mononitrobenzene adiabatic production process is suggested that aliphatic impurities, incorporated in the feed benzene, are slowly oxidised originating carboxylic acids and carbon dioxide, although without any experimental evidence. Additionally, in the dinitrotoluene production process, carboxylic acids were detected, being their source attributed to the hydrocarbon impurities present in toluene feed or toluene itself [13]. Hermann *et al.* [14] reported also, in the dinitrotoluene production, the formation of carbon dioxide, water, formic acid, acetic acid, and oxalic acid, being suggested that these compounds could be formed by nitrocresols

oxidation [15]. These oxidative side reactions, that lead to CO₂ formation, imply an increase in the plant's specific consumptions because a portion of the fed organic substrate (e.g. benzene for mononitrobenzene production) can be oxidized instead being nitrated, leading to a decrease of the nitration productivity and selectivity.

Aiming to detect (and quantify) CO₂ in industrial streams, known to be present in the nitration plant due to ammonia carbonate formation, it was intended to capture this gas by producing insoluble carbonate salts, a method already used for CO₂ capture [16-17]. However, in these gas capture methods CO₂ is usually already in the gas phase, which is not the case of most of the benzene nitration streams, that are mainly liquid (aqueous or organic). Therefore, a forced convection technique was used to direct CO₂ into the capturing agent. A suitable CO₂ capturing agent is an alkaline earth hydroxide because the CO₂ contact with this solution leads to the formation of a carbonate precipitate, as described by equation (2.2),



in which x corresponds to a chemical element from the alkaline earth metals periodic table group. The chosen capturing agent in the performed studies was barium hydroxide.

2.2. Material and methods

The reagents used in the present study were barium hydroxide octahydrate from Fischer Chemical (> 99%) and nitrogen from Air Liquide (> 99.99%). Three gas absorbers were connected in series and filled with a barium hydroxide solution, previously subjected to a vacuum filtration (using a N 816.1.2 KTP vacuum pump from KNF and borosilicate filters from Whatman), aiming the CO₂ capture. In the first two gas absorbers magnetic stirrers (one in each) were placed to decrease the bubbles size (thus increasing the contact area, and promoting the mass transfer). After each test, the pH of the CO₂ capturing solution was measured with a pH tape to verify if barium hydroxide had been totally consumed. If the solution pH was neutral or acid, it meant that the capturing agent had been completely consumed, which implied that CO₂ was not being entirely captured.

2.2.1. Sampling

Organic and aqueous liquid samples from different locations from the mononitrobenzene production plant were collected to determine CO₂ distribution throughout a nitration plant. The sampling procedure was done with an apparatus that comprised an empty round bottom flask and two gas absorbers (connected in series) filled with the CO₂ capturing agent. By this way, the CO₂

losses during the sample collection were minimal, if not negligible. To avoid a pressure rise in the sampling flask, the second absorber was opened to the atmosphere during the samples collection. The sampling apparatus is illustrated in Figure 2.2.

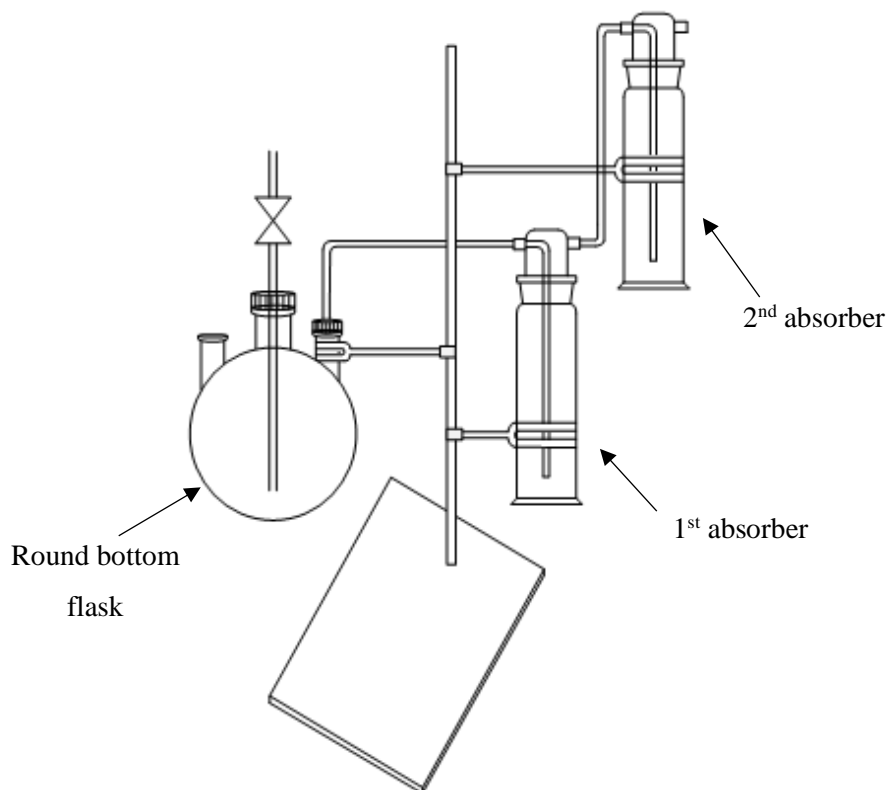


Figure 2.2 – Scheme of the sampling apparatus.

For collecting gaseous streams, the round bottom flask was replaced by a 100 mL gas syringe equipped with a valve and disconnected from the gas absorbers.

2.2.2. CO₂ quantification

The quantification method consisted of bubbling the industrial sample during a determined time to force the release of dissolved CO₂. The turbulence caused by the gas bubbling led to the dissolved CO₂ release, directing it into the alkaline solutions placed in three gas absorbers connected in series (Figure 2.3), where CO₂ capture was intended to occur. Capturing CO₂ by producing insoluble carbonate salts was the settled procedure to detect and quantify this gas in the collected samples. Nitrogen was the chosen bubbling gas due to its inert properties; its flow rate was carefully controlled using a needle valve and a gas rotameter (from King Instrument Company).

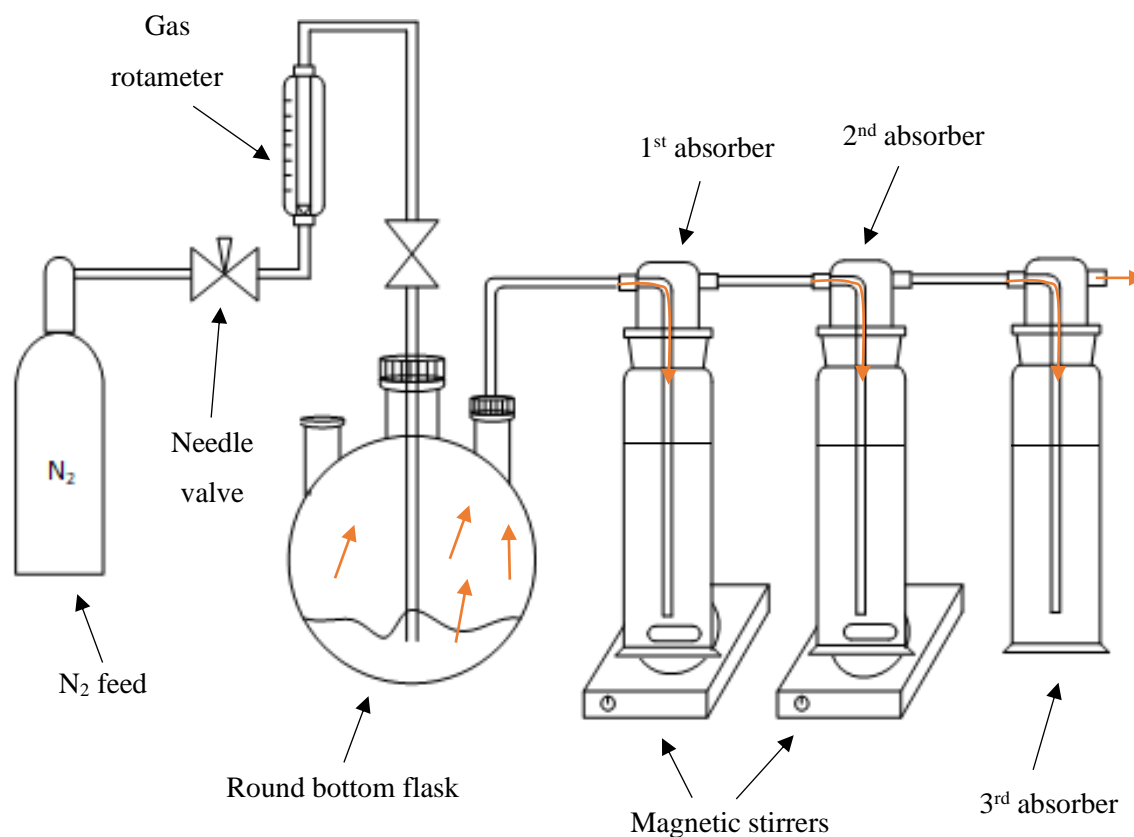


Figure 2.3 – Scheme of the CO₂ capturing apparatus for the developed quantification method.

To determine CO₂ amounts in the analysed samples a gravimetric method was employed in which the formed BaCO₃ was related with the captured CO₂. That was accomplished by removing barium carbonate from the aqueous solution by a solid-liquid separation through vacuum filtration. Then, the filtrate was placed in a hot (> 100 °C) heating plate, until reaching a constant mass, to eliminate the moisture from BaCO₃. By this way, it was assured that only the formed precipitate was accounted for in CO₂ quantification.

This method was preliminarily validated by adding a determined mass of solid CO₂ to an mononitrobenzene matrix (final product), being reached a maximum deviation of 13% between the placed and the collected CO₂ mass (Figure B.1 – Appendix B). The repeatability of the obtained results, together with the performed validation, evidences the suitability of the N₂ bubbling method to quantify dissolved CO₂ in industrial samples.

When analysing gaseous streams, the quantification procedure was slightly simpler since it did not require expelling dissolved CO₂. It was only necessary to bubble the collected gas in the CO₂ capturing solutions. CO₂ quantification was posteriorly done by filtering the alkaline solutions and weighing the formed BaCO₃, as done for the liquid samples.

2.3. Results and discussion

Table 2.1 summarizes the obtained results regarding CO₂ detection and quantification in the sampling points highlighted in Figure 2.1. According to the disclosed results, it is visible that CO₂ concentration and mass flow rate in fresh benzene (1), in benzene feed (2) and recycled benzene (3), runs 1 to 3 respectively, is lower than 0.5 (arbitrary concentration units) and than 8×10^{-4} (arbitrary mass flow rate units). This is indicative that the gas amounts fed into the reaction section dissolved in the raw material are negligible.

Table 2.1 – Carbon dioxide quantification in the reaction section of the nitration plant. The disclosed values are normalized.

Run #	Date	Production rate*	Stream	CO ₂ concentration	CO ₂ mass flow rate
1	21-05-2018 11:20	0.83	Fresh benzene (1)	0.2	8×10^{-4}
2	21-05-2018 12:10	0.83	Benzene feed (2)	0.5	4×10^{-4}
3	21-05-2018 13:00	0.83	Recycled benzene (3)	0.2	8×10^{-4}
4	02-11-2017 12:10	0.99	Mixed acid (4)	0.5	0.04
5	03-11-2017 17:00	0.99		0.6	0.05
6	06-11-2017 10:10	0.62		0.5	0.03
7	21-05-2018 10:00	0.83		0.9	0.07
8	02-11-2017 17:00	0.99	Reactors' outlet (5)	7.0	0.61
9	03-11-2017 10:50	0.99		9.4	0.80
10	07-11-2017 17:00	0.99		9.3	0.79

* The production rate is referred to the MNB produced amounts;

Due to confidentiality requirements the values presented in the Table are normalized.

Another inlet in the reaction section is the mixed acid stream (4). The results (runs 4 to 7) evidence that the gas flow rate (0.03 to 0.07 arbitrary mass flow rate units) is in the same order of magnitude in all the performed analysis, despite the higher values obtained in run 7, which can be explained by the higher mixed acid (4) temperature at the moment of the sample collection. Another factor contributing to the detection of higher amounts of CO₂ in run 7 is related to the nitric acid feed. In runs 4 to 6, the nitric acid feed was distributed along the reaction section while in run 7 nitric acid was being entirely fed at the reaction section inlet. Feeding less nitric acid at the reaction inlet led to a lower temperature rise in the reaction section, which culminated with lower amounts of CO₂ formed and fed back to the reaction, explaining thus the higher gas concentration for run 7. Knowing beforehand that nitric concentration and the reaction temperature have a direct impact on the nitrophenols generation [18-20], and relating such knowledge with the results of mixed acid (4), one might be suspected that nitrophenols and CO₂ formation is related. For run 6 it is visible that despite similar gas concentration values to runs 4 and 5, the CO₂ flow rate is lower, a consequence of the lower mononitrobenzene production at the sampling moment.

The results from mixed acid (4) analysis, when compared with benzene feed ones (runs 1 to 3), are indicative that this stream is the main CO₂ source at the reaction section inlet.

The reaction outlet (5) exhibit a CO₂ flow rate between 0.61 and 0.80, a much higher value than the ones obtained for the reaction section inlets. This revealed that CO₂ is being formed during benzene nitration and allowed to evidence that this gas is formed in the reaction section due to the decomposition of organic compounds. In fact, this is the most likely plant location for occurring such reactions since is where the conditions are harsher (higher temperature and higher sulfuric and nitric acid concentrations). The CO₂ production in the reaction section explains why ammonium carbonate is formed in the alkaline washing section of plants that apply ammonium for extracting nitrophenols from the produced mononitrobenzene. Other industrial streams downstream the reaction section were also analysed (liquid and gaseous), which allowed detecting and quantifying CO₂ and enabled proposing some techniques for the removal of the dissolved gas from liquid streams [21]. Although the results reported in Table 2.1 are not from samples collected at the same moment, they allow estimating the CO₂ flow rate generated in the reaction section, which accordingly to the disclosed results is of about 0.74 (arbitrary mass flow rate units; run 9 – run 5 – run 1).

In what concerns the reactor's outlet (5) results, it is noticeable a slight but acceptable deviation between them (runs 8 to 10). The deviation noticed for run 8 can be explained by the variation of operational parameters such as the reaction temperature, mixed acid composition, reactor's stirring speed, etc., which had contributed for a slight fluctuation of CO₂ amounts.

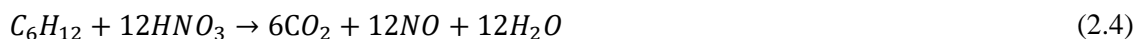
Carbon dioxide is an unwanted by-product in benzene nitration due to the already mentioned operational issues (because of ammonium carbonate formation) and because it contributes for reducing the plant productivity since the gas can be formed by the organic raw material (benzene) decomposition. Additionally, nitric acid (or nitric acid derivatives), the other raw material, can also be consumed in the organic matter decomposition instead of being used in the nitration to produce mononitrobenzene.

Based on Table 2.1 results, it was determined that 0.74 (arbitrary mass flow rate units) of CO₂ were being produced in the plant's reaction section. Despite being reported that in benzene nitration the formed CO₂ source are aliphatic impurities present in the production process [12], it was considered that only benzene is decomposed (oxidised) to CO₂ by the action of nitric acid as described in equation (2.3).

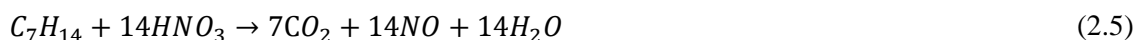


By his way, the potential benzene losses can be determined, although theoretically. Using the determined CO₂ flow rate (0.74), benzene decomposed amounts were found to be 0.22 (arbitrary flow rate units).

In addition to benzene, other organic compounds present in the reaction medium such as cyclohexane, methylcyclohexane, heptane or toluene, typical impurities present in the nitration grade benzene (at ppm scale), can potentially be oxidized to CO₂ by the action of nitric acid. Among these impurities, cyclohexane tends to be the most representative. Therefore, assuming that this compound is the unique CO₂ source, the necessary amounts of cyclohexane for originating 0.74 (arbitrary flow rate units) of CO₂ were determined resorting to equation (2.4).

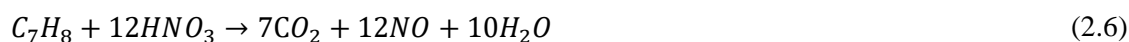


It was found that 0.24 (arbitrary flow rate units) of cyclohexane must be decomposed for yielding 0.74 (arbitrary flow rate units) of CO₂. If methylcyclohexane was to be the only oxidized organic compound, according to equation (2.5), 0.24 (arbitrary flow rate units) were needed to origin 0.74 (arbitrary flow rate units) of CO₂.



In order to verify if these aliphatic compounds could yield CO₂ during benzene nitration, samples from the inlet and outlet of the reaction section were collected, being found that these species amounts were similar in both sampling points. Such results are indicative that the aliphatics are not responsible for the formation of carbon dioxide during benzene nitration, a finding opposite to what is stated in the open literature [12].

Considering now that only toluene was the oxidized compound, 0.22 (arbitrary flow rate units) of this species were necessary to produce 0.74 (arbitrary flow rate units) of CO₂ – equation (2.6).



Regarding toluene, it was not detected after the industrial reaction section because it is a compound easily oxidized and nitrated (when compared to benzene). Therefore, it could be nitrated to mono or dinitrotoluene, to nitrocresols (the typical toluene nitration by-products) or ultimately oxidized to CO₂. Nonetheless, toluene amounts in benzene feed do not justify the formed CO₂ flow rate. Consequently, one can state that benzene should be the (major) CO₂ precursor.

2.4. Conclusions

In the present work, an analytical method for detecting and quantifying CO₂ in the mononitrobenzene production process was developed. The development of this analytical method

allowed mapping the reaction section inlets and outlet of the nitration plant, which enabled evidencing CO₂ formation in the nitration stage. Such study was, to our knowledge, the first to be disclosed in nitration plants with experimental supporting data and reveals the occurrence of oxidation reactions during benzene nitration, justifying the formation of ammonium carbonate in some nitration plants.

The decomposition of benzene and other compounds typically present in the reaction medium was theoretically evaluated being found that benzene should be the main contributor for CO₂ formation while the contribution of toluene, cyclohexane and methylcyclohexane for CO₂ generation should be negligible.

Moreover, it was seen that the operating conditions, namely the nitric acid concentration in the reaction medium may play a role on carbon dioxide generation during benzene nitration.

2.5. References

- [1]. Guenkel, A., The Adiabatic Mononitrobenzene Process from the Bench Scale in 1974 to a Total World Capacity Approaching 10 Million MTPY in 2012. In *Chemistry, Process Design, and Safety for the Nitration Industry*, American Chemical Society, Washington, DC. ACS Symposium Series, 2013; Vol. 1155, pp 1-11, doi:10.1021/bk-2013-1155.ch001
10.1021/bk-2013-1155.ch001.
- [2]. Silva, D. C. M.; Ribeiro, A. F. G.; Terras, S. M. M.; Mendes, F. P. Method and Equipment for Removing Impurities from Nitrated Aromatic Compounds. WO 2014/174499 A1, October 30, 2014.
- [3]. Berretta, S., Washing system for nitroaromatic compounds. EP 2465823 A2, August 18, 2012.
- [4]. House, J. E., Decomposition of ammonium carbonate and ammonium bicarbonate and proton affinities of the anions. *Inorganic and Nuclear Chemistry Letters* **1980**, 16 (4), 185-187, [https://doi.org/10.1016/0020-1650\(80\)80118-8](https://doi.org/10.1016/0020-1650(80)80118-8).
- [5]. Ribeiro, A.; Silva, D.; Gaudêncio, C., Process for the removal of nitrophenolic compounds in the production of nitrobenzene. WO2014122596 A2, August 14, 2014.
- [6]. Buchi, S. D.; Guenkel, A. A., Method of purifying nitrated aromatic compounds from a nitration process. WO 2016198921 A1, December 15, 2016.
- [7]. Carbajo, J.; Quintanilla, A.; Casas, J. A., Assessment of carbon monoxide formation in Fenton oxidation process: The critical role of pollutant nature and operating conditions. *Applied Catalysis B: Environmental* **2018**, 232, 55-59,
- [8]. Devlin, H. R.; Harris, I. J., Mechanism of the oxidation of aqueous phenol with dissolved oxygen. *Industrial & Engineering Chemistry Fundamentals* **1984**, 23 (4), 387-392,
- [9]. Denisov, E. T.; Metelitsa, D. I., Oxidation of Benzene. *Russian Chemical Reviews* **1968**, 37 (9), 656-665, 10.1070/rc1968v037n09abeh001690.
- [10]. Zhang, G.; Hua, I., Supercritical Water Oxidation of Nitrobenzene. *Industrial & Engineering Chemistry Research* **2003**, 42 (2), 285-289, 10.1021/ie010479j.
- [11]. Burns, J. R.; Ramshaw, C., Development of a Microreactor for Chemical Production. *Chemical Engineering Research and Design* **1999**, 77 (3), 206-211, <http://dx.doi.org/10.1205/026387699526106>.
- [12]. Guenkel, A. A.; Maloney, T. W., Recent Advances in the Technology of Mononitrobenzene Manufacture. In *Nitration*, American Chemical Society, Washington, DC. ACS Symposium Series, 1996; Vol. 623, pp 223-233, doi:10.1021/bk-1996-0623.ch020
10.1021/bk-1996-0623.ch020.
- [13]. Quakenbush, A. B.; Pennington, B. T., Commercial Dinitrotoluene Production Process. In *Nitration*, American Chemical Society, 1996; Vol. 623, pp 214-222, doi:10.1021/bk-1996-0623.ch019

10.1021/bk-1996-0623.ch019.

- [14]. Hermann, H.; Gebauer, J.; Konieczny, P., Industrial Nitration of Toluene to Dinitrotoluene. In *Nitration*, American Chemical Society, Washington, DC. ACS Symposium Series, 1996; Vol. 623, pp 234-249,
- [15]. Albright, L. F., Nitration. In *Kirk-Othmer Encyclopedia of Chemical Technology*, John Wiley & Sons, Inc., 2000, 10.1002/0471238961.1409201801120218.a01.
- [16]. Haghnegahdar, M. R.; Hatamipour, M. S.; Rahimi, A., Removal of carbon dioxide in an experimental powder-particle spouted bed reactor. *Separation and Purification Technology* **2010**, 72 (3), 288-293, <https://doi.org/10.1016/j.seppur.2010.02.019>.
- [17]. Han, S.-J.; Yoo, M.; Kim, D.-W.; Wee, J.-H., Carbon Dioxide Capture Using Calcium Hydroxide Aqueous Solution as the Absorbent. *Energy & Fuels* **2011**, 25 (8), 3825-3834, 10.1021/ef200415p.
- [18]. Nogueira, A. G. Optimização da Nitração de Aromáticos. PhD Thesis, Universidade de Coimbra, Portugal, 2014.
- [19]. Quadros, P. A.; Castro, J. A. A. M.; Baptista, C. M. S. G., Nitrophenols Reduction in the Benzene Adiabatic Nitration Process. *Industrial & Engineering Chemistry Research* **2004**, 43 (15), 4438-4445, 10.1021/ie034263o.
- [20]. Afonso, D.; Ribeiro, A. F. G.; Araújo, P.; Vital, J.; Madeira, L. M., (Nitro)Phenols reactivity in mixed acid benzene nitration. *Submitted* **2019**,
- [21]. Diogo Afonso, Bondalti Chemicals, Internal Report. **2019**.

Chapter 3 – Oxidation by-products in nitrobenzene production

Abstract

An analytical methodology was developed allowing to identify and quantify oxidation by-products from benzene nitration besides the typical ones, nitrophenols and dinitrobenzene. This new class of compounds, composed by dicarboxylic acids, was identified in samples from the mononitrobenzene production process by UV-Vis spectrometry and mass spectrometry. Such finding suggests that during benzene nitration organic matter is being oxidized yielding these oxidized species.

The identified dicarboxylic acids were fumaric, succinic, adipic and oxalic acid, being also evidenced the presence of maleic and mesoxalic acid. This was the first time that these compounds (except oxalic acid) were identified in benzene nitration systems.

Laboratory scale tests were performed in which these dicarboxylic acids were added to synthetic mixed acid in the absence of benzene. It was found that oxalic, mesoxalic, fumaric, succinic and adipic acid are decomposed yielding carbon dioxide, being also evidenced carbon monoxide generation. Furthermore, it was also demonstrated that the increase of the reaction temperature and the presence of nitric acid promote oxidation and decomposition reactions.

Keywords: Oxidation, organic matter decomposition, dicarboxylic acids, oxidation intermediates.

3.1. Introduction

Nitration is an important and well-studied chemical reaction, being employed in the chemical industry since the beginning of the last century. It can be used to produce commodity chemicals such as mononitrobenzene (MNB) and mononitrotoluene (MNT), which are then used as precursors in the production of other compounds like aniline or drugs.

Nitration reactions are always accompanied by side reactions that, during benzene (Bz) nitration, are responsible for nitrophenols (NPs) and dinitrobenzene (DNB) formation [1-3]. Studies addressing these reaction by-products have already been performed [2-4]. However, in addition to these secondary reaction products, other by-products are also formed that are suspected to have origin in decomposition reactions occurring in parallel to the main reaction. According to Guenkel and Maloney [5], these by-products are carboxylic acids and carbon dioxide resulting from aliphatics oxidation. Despite pointing that the secondary products are carboxylic acids, Guenkel and Maloney [5] haven't provided any analytical evidence used for identifying them. In addition to the suggested oxidation of paraffinic compounds, the oxidized species can also be formed through aromatics degradation due to the severe nitration conditions (high temperature and oxidizing environment). For instance, phenol (the NPs precursor) can be oxidized to mesoxalic acid or oxalic acid, and methyl groups from aromatic compounds (toluene, xylene, typically present in the nitration grade benzene) can be oxidised to hydroxymethyl and carboxyl groups [1].

When comparing benzene and toluene nitration, Gattrell and Louie [6] noticed that the latter tends to originate a higher oxidation by-products variety, which can be justified by toluene's higher susceptibility towards oxidation. The authors [6] have also shown that the increase of the reaction temperature resulted in the reduction of cresols concentration and an increase of the toluene nitration oxidation by-products (water soluble), pointing that the cresols decomposition rate was faster than its formation.

Ross and Kirshen [7] reported the formation of carbon dioxide and carbon monoxide during the nitration of dinitrotoluene. They have also detected the presence of organic compounds, water-soluble, although the authors weren't able to identify these species successfully. Hanson *et al.* [8] also refer the occurrence of oxidation reactions that can decompose nitrocresols, formed during toluene mononitration, into oxalic acid.

The results obtained and disclosed in the Chapter 2 revealed that during Bz nitration, oxidation reactions are occurring, which ultimately lead to CO₂ formation, as also stated by Guenkel and Maloney [5]. However, our study (Chapter 2) didn't allow to determine which compounds present in the Bz nitration medium (aliphatics and/or aromatics) were the CO₂ precursors. It is known that the Bz stream fed to the reaction section has in its composition some impurities (methylcyclohexane, toluene and xylene), both aliphatic and aromatic, containing methyl groups that are prone to be oxidised, leading to carboxylic acids and carbon dioxide formation.

Notwithstanding, Bz itself can play a role in carboxylic acids and carbon dioxide formation as it is suggested in the previous chapter (Chapter 2).

Regarding the oxidizing agent responsible for the organic matter decomposition, it is also unknown. Nitric acid, usually used together with sulfuric acid (mixed acid) in nitration reactions, is a possible candidate because it is pointed out as the responsible for benzene oxidation to phenol [9] in benzene nitration. During toluene nitrations, nitric acid can promote ring oxidation or decomposition leading to the formation of gaseous by-products [10]. Moreover, Odle *et al.* [11] reported that concentrated nitric acid at 50 °C (a temperature lower than the one employed in benzene nitration) is able to completely oxidize phenolic compounds, evidencing thus its oxidant capacity. At higher temperatures, i.e. within the nitration temperature range, nitric acid can be decomposed yielding potential oxidants [7] that may contribute for the organic matter oxidation during nitration reactions. Additionally, sulfuric acid action as a potential oxidant should not be excluded since it is suggested that it can play a role in oxidation, although in a small extent [7, 12].

Although there are studies addressing oxidation reactions during nitration, this topic needs to be further clarified because the information is very sparse, essentially regarding oxidation during Bz nitration. Therefore, the aim of this study was to develop an analytical methodology able to detect oxidation by-products from Bz nitration because only NPs and DNB are accounted for [3, 13]. The identification of these secondary products is also an objective. Moreover, it is intended to propose a possible oxidation mechanism, which culminates in CO₂ formation.

3.2. Materials and methods

The chemical reagents used in this study were the following: oxalic acid dihydrate (99.5%) from Panreac, sodium mesoxalate monohydrate (> 98%) from Aldrich, fumaric acid (99%) from Alfa Aesar, succinic acid (100%) from VWR Chemicals, adipic acid (> 99%) from Fluka, barium hydroxide octahydrate (> 99%) from Fischer Chemical, sulfuric acid (99%) from Quimitécnica, nitric acid (65 %) from Baker, acetonitrile (HPLC grade) from Fischer Scientific, and potassium dihydrogen phosphate from Merck.

3.2.1. Sampling and samples preparation

The analysed samples were collected from different locations of Bondalti Chemicals nitration plant. As the samples were diverse either organic or aqueous, according to the plant sampling points, a suitable sample preparation procedure was required previously to their analysis. The organic samples were subjected to a liquid-liquid extraction aiming the samples analysis by High Performance Liquid Chromatography (HPLC). The extraction was accomplished by adding a

determined amount of demineralized water to the organic phase, being then the mixture vigorously shaken. The final step was the phase separation, which was done resorting to a centrifuge (1500 r.p.m for 1 minute). The resulting aqueous phase was the one analysed by HPLC. The extraction efficiency was found to be higher than 90% for oxalic and fumaric acid (the tested organic acids).

Regarding the aqueous samples, they were diluted with demineralized water aiming the reduction of the acid concentration and consequently the chromatographic column protection.

3.2.2. HPLC analytical method

The liquid chromatographic analyses were performed in an Elite LaChrom HPLC apparatus from VWR-Hitachi equipped with Diode Array Detector (DAD), a reverse phase column (Purospher® STAR RP-18e LiChroCART®) packed with silica microspheres (5 µm, 250 mm × 4 mm) and a guard column (LiChroCART® - 5 µm, 4 mm × 4 mm). The temperature of the chromatographic column was maintained at 30 °C by the HPLC's oven and the volume of the injected sample was 10 µL. The eluent feed was in gradient mode with a KH₂PO₄ solution (2.5 mM, pH ≈ 2.4) and acetonitrile as follows:

- 0 – 5 minutes: 0.4 mL/min, 88% KH₂PO₄, 12% acetonitrile;
- 5 – 11 minutes: 1.0 mL/min, 88% KH₂PO₄, 12% acetonitrile;
- 11 – 23 minutes: 1.0 mL/min: 50% KH₂PO₄, 50% acetonitrile;
- 23 – 26 minutes: 1.0 mL/min, 88% KH₂PO₄, 12% acetonitrile;
- 26 – 30 minutes: 0.4 mL/min, 88% KH₂PO₄, 12% acetonitrile.

3.2.3. UHPLC-MS analytical method

In order to perform mass spectrometry (MS) analysis, the developed HPLC-DAD analytical method had to be adapted to comply with some restrictions because the use of H₂SO₄ (the eluent's acidifying agent) and of non-volatile buffers is not recommended in MS analysis [14-15]. Therefore, the mobile phase was replaced by a 0.15% (V/V) formic acid aqueous solution because this organic acid can be used both as the acidifying agent and as the KH₂PO₄ salt substitute [16-17].

To separate the different analytes, an Ultimate 3000RSCL U/HPLC from Thermo Scientific equipped with a Thermo Fisher Hypersil GOLD column (100 × 2.1 mm; particle size 1.9 µm) was used. The HPLC was coupled to a LTQ XL Linear Ion Trap 2D mass spectrometer (ThermoFisher Scientific), equipped with an orthogonal electrospray ionization source operating in negative mode. The spray voltage was 5 kV and the capillary voltage temperature was 275 °C.

3.2.4. Decomposition gases quantification in dicarboxylic acids oxidation

The oxidation of some dicarboxylic acids was carried out in a round bottom flask, placed in a heating mantle to maintain the desired temperature throughout the reaction time. For verifying if CO_2 was being formed, a N_2 flow, carefully controlled with a needle valve, was used to direct the generated gases to three gas absorbers, placed in series, and filled with a $\text{Ba}(\text{OH})_2$ solution. The used apparatus is illustrated in Figure 3.1.

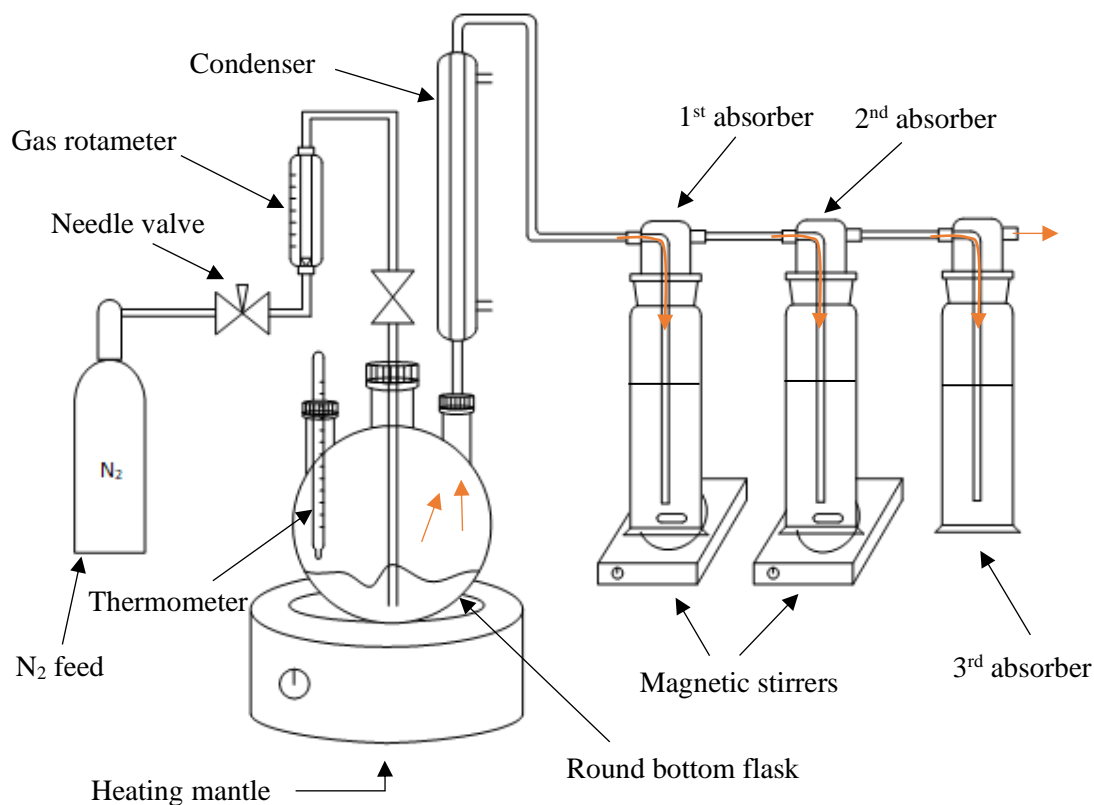


Figure 3.1 – Scheme of the apparatus for the dicarboxylic acids oxidation.

As done in the Chapter 2, the formed amounts of barium carbonate were related with those of carbon dioxide. The condenser was placed at the round bottom flask exit to avoid the loss of NO_x to the gas absorbers.

Dicarboxylic acids were also oxidized in a jacketed laboratory reactor. In this experiment, both carbon monoxide and carbon dioxide formation was verified using a Gas-Pro detector from Crowcon. To that, N_2 was used to expel these gases from the reactor, directing them to the gas detector. Previously to the addition of each dicarboxylic acid, the round bottom flask or the reactor were purged with N_2 to ensure that the detected amounts of CO and CO_2 were only respecting to the oxidation of the organic acids.

3.3. Results and discussion

In the following sections the detection and identification of the oxidation by-products will be addressed, as well as their possible formation path and oxidation at the typical range of benzene nitration conditions.

3.3.1. Identification of oxidation by-products in the benzene nitration

An analytical method for HPLC was developed (please see Appendix C for details) aiming to detect other chemical species besides the typical ones (NPs and DNB) formed through side reactions during Bz nitration. As can be seen in Figure 3.2-a), an HPLC-DAD chromatogram of an industrial sample (produced MNB; collected from the reaction outlet), the developed method enabled the detection of several chromatographic peaks. Such fact is also noticed in the total ion chromatogram (TIC), disclosed in Figure 3.2-b), of another produced MNB sample.

In Figure 3.2, the chromatographic peaks represented as K_i correspond to known compounds present in the reaction medium while those addressed as U_i allude to unknown chemical species. The analysis of the depicted HPLC chromatogram, allows noticing the presence of six chromatographic peaks (U_1 to U_6) corresponding to unknown compounds in the analysed sample. Although the developed method enabled detecting several new chromatographic peaks, it did not enable their identification since it only provided the peaks' UV-Vis spectra, which by themselves cannot be used for identifying chemicals species. Nevertheless, due to the proximity between some of the chromatographic peaks (peaks U_2 to U_5), the corresponding analytes are likely to be species with the same functional groups.

In order to assess the compounds' structure, a UHPLC-MS (Ultra High Performance-Liquid Chromatography - Mass spectrometry) analysis was performed, which allowed obtaining a TIC chromatogram (Figure 3.2 – b)).

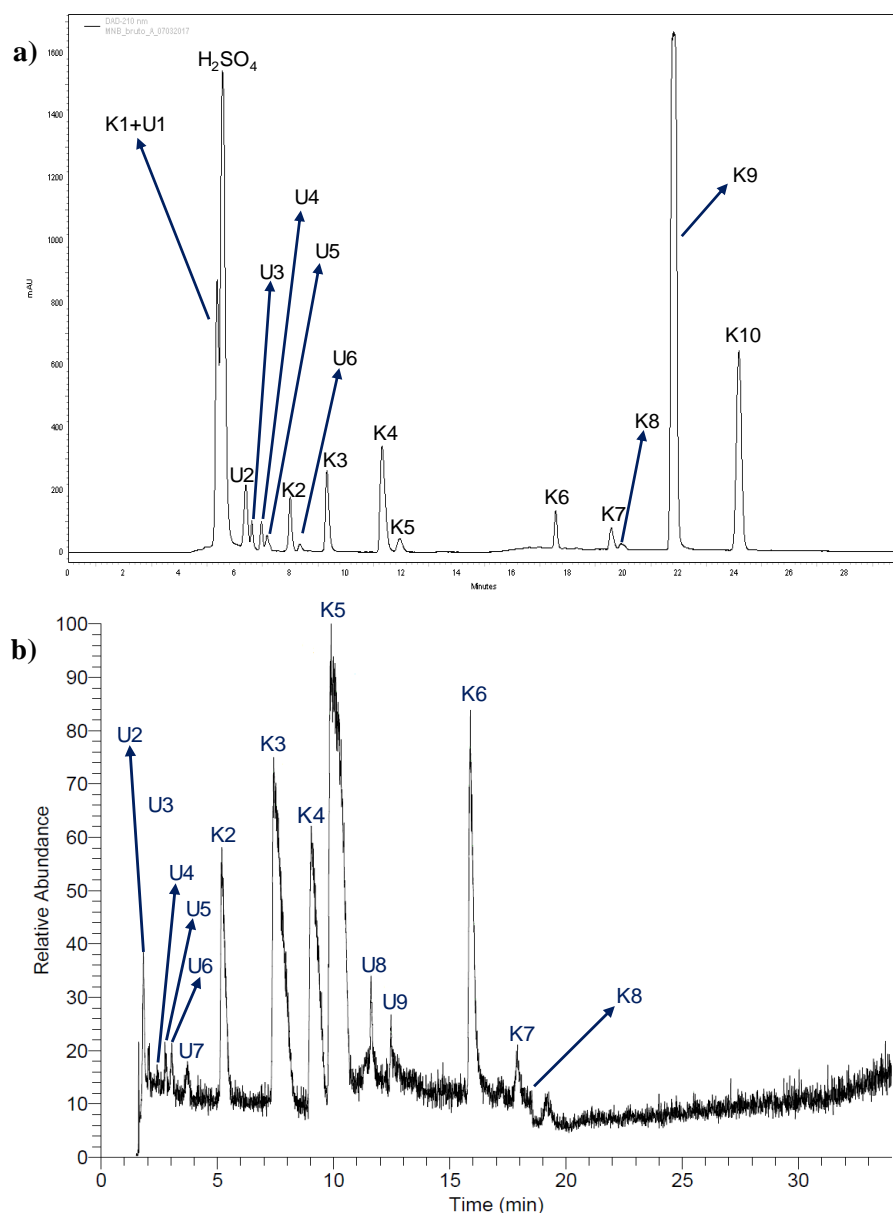


Figure 3.2 – Produced MNB **a)** HPLC-DAD chromatogram; **b)** Total Ion Chromatogram.

As mentioned before, the depicted TIC evidence the presence of several chemical species in the produced MNB. Scrutinizing this chromatogram is visible that some of the detected compounds have higher peaks intensity than others, but any conclusion cannot be withdrawn regarding their identification. That can only be done by studying the mass spectra of the detected compounds (shown in the Appendix C, Figure C.9) and their mass fragmentation patterns, which were also obtained during the MS analysis – Table 3.1. The knowledge of such data enabled assigning some of the detected chromatographic peaks to chemical species because the mass spectra provided both the analyte's molecular ion, which can be related with the compound's molar mass, and its mass fragmentation pattern, that can be linked to the compound's structure [18-19].

The nomenclature used in Table 3.1 for numbering the detected peaks is the same as in Figure 3.2, i.e., the K_i peaks are assigned to known chemical compound while the U_i peaks are referent to unidentified compounds. Nevertheless, it is important to have in mind that the analytical conditions (chromatographic column and eluent) differed between the performed analysis (Figure 3.2-a): HPLC – DAD; Figure 3.2-b) and Table 3.1: HPLC-MS), thus the peaks numeration may have no correspondence between Figure 3.2-a) and Figure 3.2-b) (and Table 3.1).

Table 3.1 – MS/MS fragmentation pattern of the detected chromatographic peaks.

# Peak	Retention time (min)	m/z [M-H] ⁻	Mass fragments		
U2	1.81	156	112		
U3	2.08	229	212		
U4	2.40	115	97	71	
U5	2.74	308	262		
		262	216	182	168
U6	3.04	272	228		
		228	198		
U7	3.71	117	99	73	
		288	270	244	198
K2	5.19	157	129	113*	93*
K3	7.42	202	172	156	138
K4	9.16	202	172	156	138
K5	9.89	202	172	156	138
U8	11.61	145	127	101	83
		201	157	111	66
		344	272	258	
U9	12.47	159	141	117	97
K6	15.88	228	198		
		182	152	136	
K7	17.91	183	153	123	
		137	109	93	
K8	18.34	183	153	123	
		106	65		
		147	62		
		228	198		

* Fragments possibly belonging to another compound.

3.3.1.1. Identified by-products

Since it is suggested that carboxylic acids are present in Bz nitration units [5], as carbon dioxide was found to be formed in a nitration unit (Chapter 2) and because it is known (both by Bondalti and by the nitration technology licensor) that oxalic acid is present in the MNB production process, the existence of this organic acid in the reaction medium was assessed. That was accomplished by collecting an industrial sample and then enriching it in an oxalic acid standard. The obtained results are disclosed in Figure 3.3.

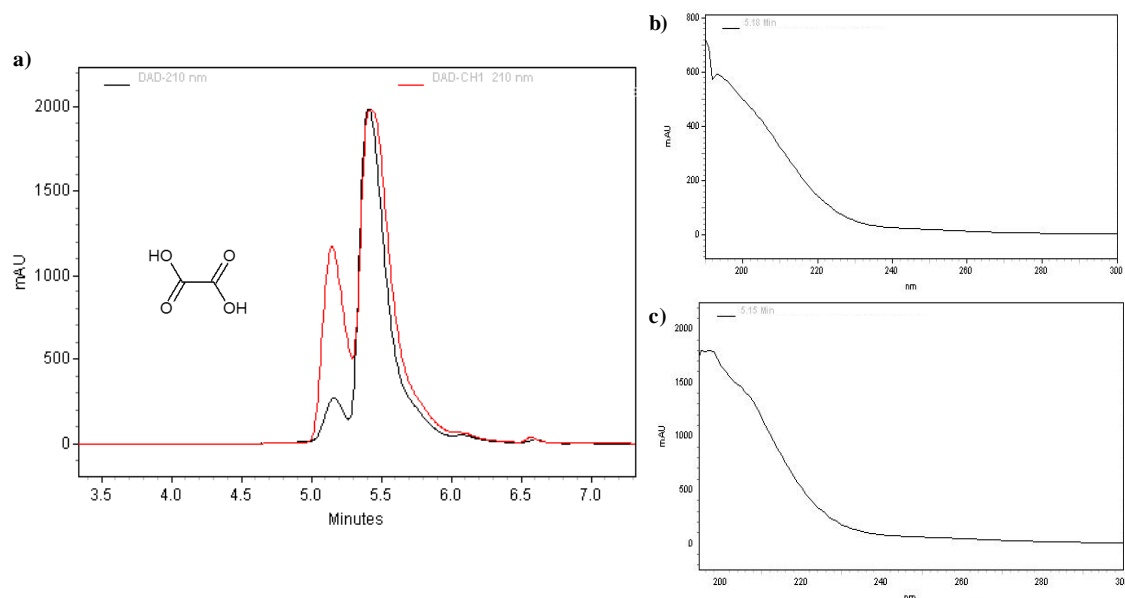


Figure 3.3 – a) Produced MNB HPLC chromatogram. Black line – industrial sample; red line – oxalic acid-added industrial sample. UV-Vis spectrum from: b) industrial sample, c) oxalic acid-enriched industrial sample.

Figure 3.3 shows that the addition of oxalic acid to the industrial sample led to a rise of the first chromatographic peak (Figure 3.2 - a) – K1). This fact, together with the resemblance of the UV-vis spectra (Figure 3.3-b) and c)) allows identifying the K1 chromatographic peak as oxalic acid.

This result shows that oxalic acid can be monitored by HPLC-DAD instead of using ionic chromatography as is done in Bondalti. Additionally, this finding, although not being a novelty, together with the detection of CO₂, supports that during Bz nitration oxidation reactions are occurring which are responsible for the decomposition of the organic matter.

In addition to oxalic acid, other organic acids were detected and identified both by HPLC-DAD and UHPLC-MS namely the compounds identified as K2, K3, K4 and K5 [20] – Figure 3.2-a) and b) and Table 3.1.

The identification of the K2 peak was done considering the compound's molecular ion and its mass fragmentation pattern, data retrieved from Table 3.1. Once the molecular ion was formed by

the removal of positive ions (H^+) from the molecule, it can be stated that this species molar mass is $158\text{ g}\cdot\text{mol}^{-1}$ (molecular ion = $157\text{ }m/z$). Studying the presented mass fragmentation pattern, one can infer that the performed MS analysis led to the formation of mass fragments with the following values: 28 u ($157 - 129$), 44 u ($157 - 113$) and 64 u ($157 - 93$), corresponding to the loss of SO_2 (64 u), CO_2 (44 u) and CO , N_2 or C_2H_4 (28 u). Considering the molecular ion value (and the respective molar mass) and the 64 u mass fragment, the K2 analyte was identified as benzenesulfonic acid. A detailed compound identification is addressed elsewhere [20]. The remaining mass fragments (44 u and 28 u) should belong to another compound, most likely with the same retention time of benzenesulfonic acid, since these fragments are not consistent with the benzenesulfonic acid structure.

Regarding the chromatographic peaks K3 to K5 (Table 3.1), one can see that they exhibit the same molecular ion and the same fragmentation pattern. Such data indicate that these chemical compounds are isomers. The analysis of the obtained molecular ion ($202\text{ }m/z$) enabled to determine that the compounds' molar mass is $203\text{ g}\cdot\text{mol}^{-1}$ and the scrutiny of the mass fragmentation pattern allowed to deduce that these species exhibited mass fragments of 30 u ($202-172$), 46 u ($202-156$) and 64 u ($202-138$) that correspond, respectively, to NO , NO_2 and SO_2 losses. Taking into account these evidences, the analytes K3 to K5 were identified as mononitrobenzenesulfonic acids (2-, 3- and 4-mononitrobenzenesulfonic acid). The identification of these compounds is detailed in [20]. The formation of the mononitrobenzenesulfonic acids was found to occur by Bz sulfonation and nitration and by MNB sulfonation [20], revealing a new class of mixed acid Bz nitration by-products, the sulfonic acids class.

The chromatographic peaks numbered as K6, K7 and K8 were identified as trinitrophenol (K6) and dinitrophenol (K7 and K8). The compounds' identification (peaks K6 and K7) was done considering their molecular ions and the correspondent molar mass (229 and $184\text{ g}\cdot\text{mol}^{-1}$ for trinitrophenol and dinitrophenol, respectively) and the masses of their fragments, which evidenced the loss of NO_2 (46 u) and NO (30 u). The K8 peak's data reveals the presence of several ions in its mass spectrum (Table 3.1; Figure C.9). Once the chromatographic peak K8 is a shoulder peak (Figure 3.2-b)) it may contain some interferences from the peak K7. Other possible justifications are related with interferences of compounds accumulated in the chromatographic column because a $228\text{ }m/z$ ion with a mass fragment of 30 u was detected, data similar to the one of K6 peak, or even with the overlapping of different compounds at peak's K8 retention time. Nevertheless, since the ion $183\text{ }m/z$ showed the higher peak intensity it was considered as the molecular ion to identify the K8 peak as dinitrophenol.

In what concerns to K9 and K10 chromatographic peaks (Figure 3.2-a)) after a UV-Vis spectra analysis, they were found to be respectively, MNB and Bz. Despite the high yield of Bz nitration, Bz was detected together with MNB because it is typically fed in excess at the reaction section.

Summarizing, the known compounds detected in the produced MNB are compiled in Figure 3.4. These compounds were also detected in other plant locations [21].

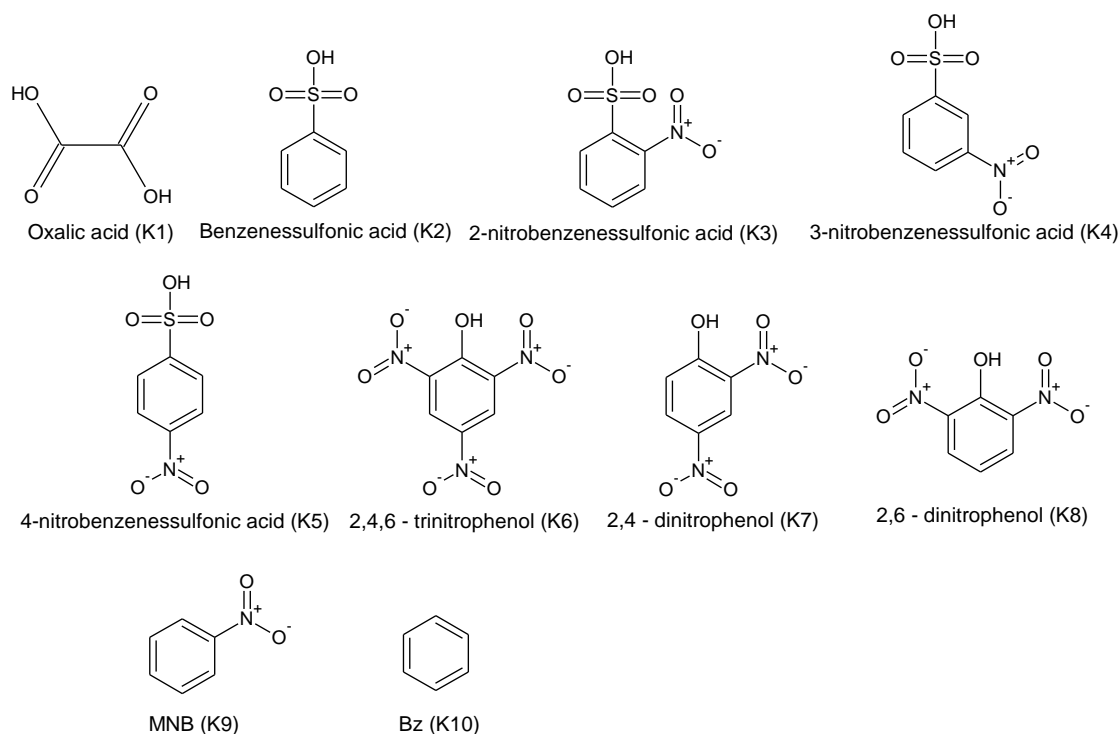


Figure 3.4 – Known compounds detected in the performed analysis.

3.3.1.2. Unidentified by-products

Once oxalic acid was detected in a nitration plant and once that in published works addressing the decomposition of organic compounds both oxalic acid and mesoxalic acid are referred [22-25], the presence of the latter organic acid in the nitration plant was checked. Therefore, an industrial sample was collected, analysed by HPLC and then enriched with a mesoxalic acid standard. The gotten results are illustrated in Figure 3.5.

As shown in Figure 3.5, the addition of mesoxalic acid to the industrial sample led to the area rise of the first chromatographic peak, that has been identified as oxalic acid. This finding suggests that oxalic acid and mesoxalic acid have similar retention times, being thus overlapped. Analysing the obtained UV-Vis spectra it is noticeable that the addition of mesoxalic acid to the industrial sample affected the UV-Vis spectrum corresponding to the first chromatographic peak (comparison of Figure 3.5-b) and c)); however, the spectrum differs from that of mesoxalic acid standard (comparison of Figure 3.5-c) and d)). The main differences, although not very significant, between the UV-Vis spectra of the industrial sample and the one enriched in mesoxalic acid, are noticed by the intensity increase in the absorption band below 200 nm and near 220 nm. At 200 nm oxalic acid, which was assigned to the first chromatographic peak, also has a maximum of absorption,

therefore mesoxalic acid presence in the sample can be screened focusing on the 220 nm band of the UV-Vis spectrum. Nevertheless, depending on mesoxalic acid concentration, the intensity increase at 220 nm may not be perceptible meaning that oxalic acid UV-Vis spectrum conceals mesoxalic acid's spectrum, hindering thus the latter organic acid detection.

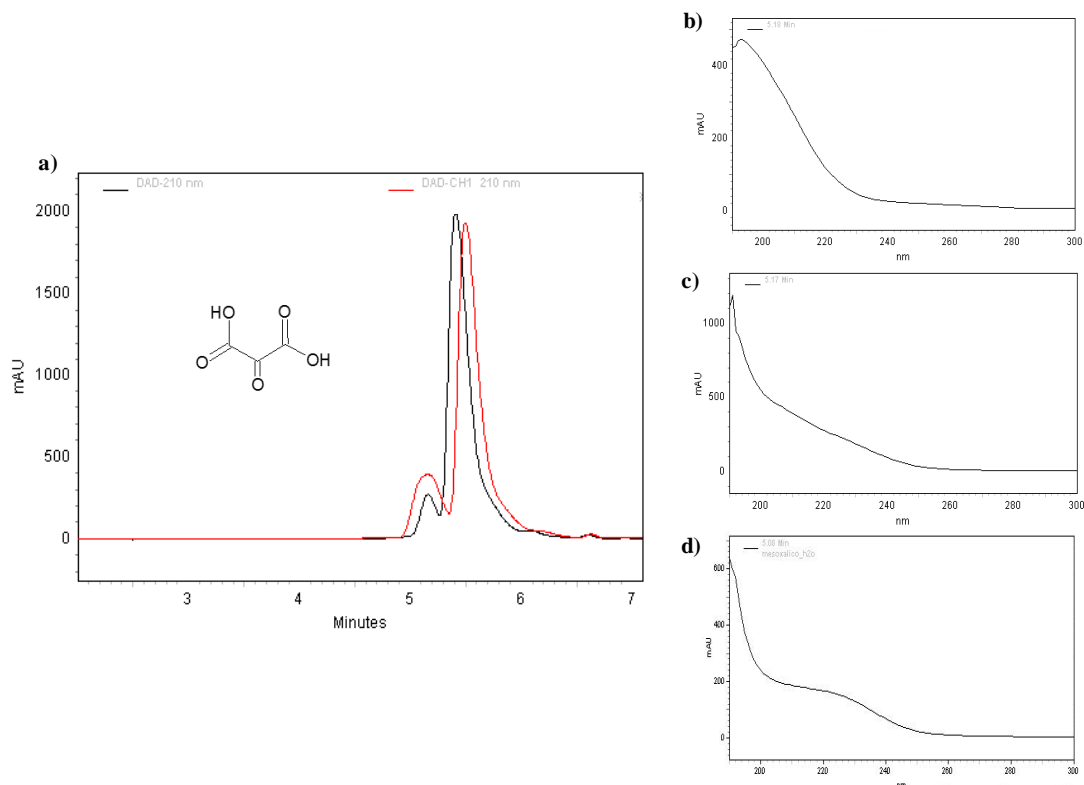


Figure 3.5 – a) Produced MNB HPLC chromatogram. Black line – industrial sample; red line – mesoxalic acid-added industrial sample. UV-Vis spectrum from the first chromatographic peak in the: b) industrial sample, c) mesoxalic acid-added industrial sample. d) Mesoxalic acid standard UV-Vis spectrum.

The fact of oxalic acid and mesoxalic acid have the same retention time together with the mesoxalic acid interference in oxalic acid UV-Vis spectrum may explain the reason why at times oxalic acid UV-Vis spectrum presents slight discrepancies when compared to the UV-Vis of the standard – Figure 3.6.

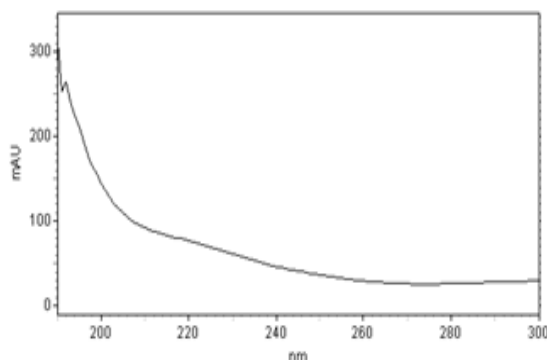


Figure 3.6 – Oxalic acid UV-Vis spectrum of a benzene nitration sample.

Considering these facts and as both oxalic and mesoxalic acids are detected in works addressing the oxidation of organic compounds, one can suggest that the first detected peak (Figure 3.2-a)) corresponds to a mixture of oxalic acid (K1) and mesoxalic acid (U1).

According to Table 3.1 data, the analyte U2 has a molecular ion of 156 m/z which means that the compound's molar mass is 157 $\text{g} \cdot \text{mol}^{-1}$. Since the analyte's molar mass is an odd number and considering the nitrogen rule (odd molar mass = odd number of nitrogen atoms; even molar mass = even number of nitrogen atoms), one can unveil that this compound has an odd number of nitrogen atoms in its structure that are most likely associated to nitro groups ($-\text{NO}_2$). Regarding the gotten fragment mass, the depicted results show the loss of 44 u ($156 - 112$), which is indicative of CO_2 loss. This finding suggests that the analyte is a carboxylic acid since these compounds are characterized by CO_2 loss, and sometimes, by H_2O loss [26]. Compiling the analyte's molecular ion, molar mass, mass fragment and considering the nitrogen rule, such compound can be identified as 4-nitrocyclopentene-1-carboxylic acid, as 5-nitro-2-furoic acid or as 6-nitrohexa-2,4-dienoic acid – Figure 3.7.

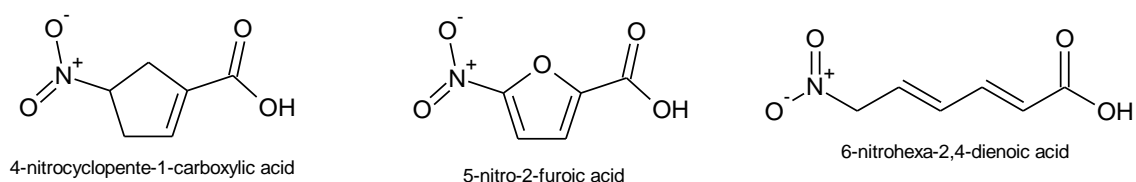


Figure 3.7 – Possible U2 analyte identification.

The 6-nitrohexa-2,4-dienoic acid could be formed by MNB ring cleavage and oxidation or by benzene ring opening and its subsequent nitration while 5-nitro-2-furoic acid and 4-nitrocyclopentene-1-carboxylic acid could be formed through cyclopentane (a typical impurity present in nitration grade Bz [5]) oxidation and nitration. Despite the proposed identifications match the analyte's molar mass, and for 5-nitro-2-furoic acid its mass fragmentation pattern matches also

the one disclosed in Table 3.1 [27], the chromatographic peak U2 was not successfully identified. The resemblance between analyte U2 and 5-nitro-2-furoic acid MS data led to the addition of a 5-nitro-2-furoic acid standard to an industrial sample, however it was found that this standard retention time differed from those of all the detected analytes (cf. the HPLC chromatogram in the Appendix C section, Figure C.10).

In parallel to the UHPLC-MS analysis, a headspace solid phase microextraction (HS-SPME) – gas chromatography (GC) – time-of-flight mass spectrometry (ToFMS) analysis was also performed. This analysis consisted in volatilizing the volatile compounds of an industrial liquid sample, which were then injected in the GC-ToFMS apparatus. The obtained results allowed to detect Bz, MNB, 2-mononitrophenol (a typical by-product formed during Bz nitration), heptane and methylcyclohexane, aliphatic compounds that are typically present in the Bz fed to the MNB production process. However, contrarily to what is evidenced by the interpretation of the analyte U2 mass fragmentation pattern (Table 3.1), the presence of dicarboxylic acids was not verified, which can be justified by these compounds' high boiling point (low volatility). Once the unknown compounds detected in the UHPLC-MS analysis were not found by HS-SPME/GC-ToFMS, together with the detection of CO₂ in the plant, addressed in Chapter 2, reinforces the possible the presence of dicarboxylic acids in the Bz nitration plant.

Analysing the peak U3, it is noticeable that its molecular ion has a value of 229 *m/z*, corresponding to a molar mass of 230 g·mol⁻¹, and that its mass fragmentation pattern evidences the loss of the OH group (229 - 212 = 17 u). Considering the nitrogen rule, this compound may have an even number, or none, nitrogen atoms in its composition. If no nitrogen atoms are present in the molecule, it can be identified as tetrahydroxyphthalic acid, a compound possibly formed by xylene (present in Bz fed to the MNB production process) oxidation. However, one would expect a fragment correspondent to the loss of CO₂ since tetrahydroxyphthalic acid is a carboxylic acid. On the other hand, if the presence of nitrogen atoms is to be considered, the compound can be identified as nitranilic acid. Nitranilic acid can arise from Bz oxidation to quinone, followed by quinone oxidation and nitration. Despite the proposed identifications (Figure 3.8), the presence of these compounds in the nitration medium was not confirmed.

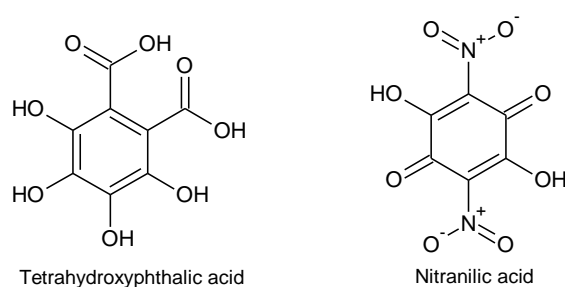


Figure 3.8 – Possible U3 analyte identification.

Examining the U4 peak's MS data, it can be concluded that this chemical species' molar mass is of $116 \text{ g} \cdot \text{mol}^{-1}$ (molecular ion value + 1), that the gotten mass fragments allow deducing the loss of water (18 u; 115-97) and carbon dioxide (44 u; 115-71) and that the number of nitrogen atoms is zero or even. Based on these assumptions the analyte can be identified as fumaric acid, a compound typically detected in oxidation processes of aromatics [28-30], which presents the same molecular ion [31] of the one displayed in Table 3.1. To confirm the proposed identification, an industrial sample was analysed by HPLC-DAD and then enriched with a fumaric acid standard. The obtained results are illustrated in Figure 3.9.

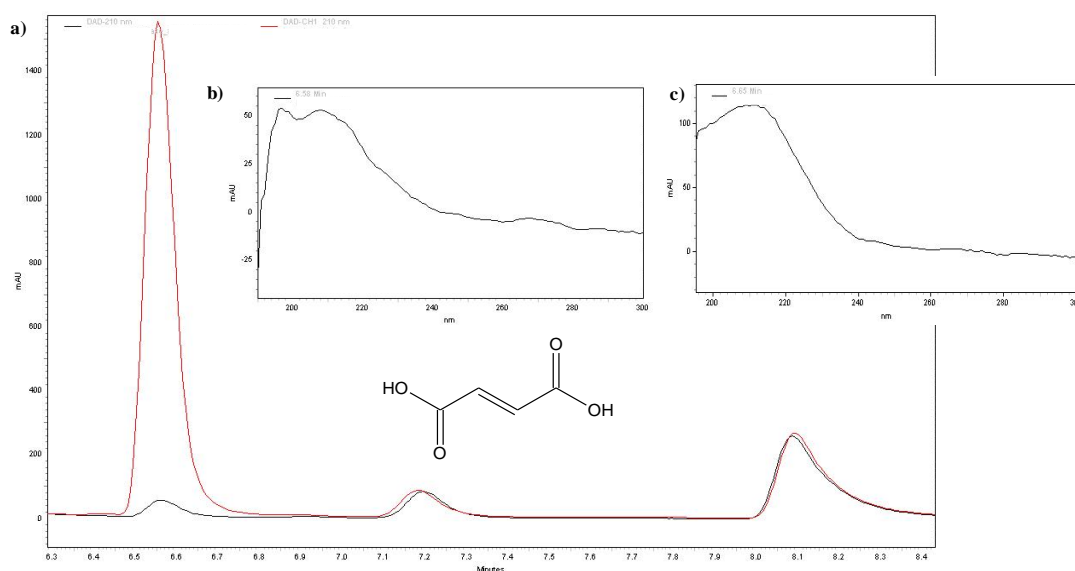


Figure 3.9 – a) Produced MNB HPLC chromatogram. Black line – industrial sample; red line – enriched industrial sample. Fumaric acid UV-Vis spectrum from: b) industrial sample, c) enriched industrial sample.

As it can be clearly seen in Figure 3.9-a), the addition of fumaric acid to the industrial sample led to the area increase of the chromatographic peak with a retention time of 6.55 minutes, indicating that this peak corresponds indeed to fumaric acid. Nevertheless, to identify unequivocally this analyte, the UV-Vis spectra obtained from both the performed analyses (industrial and enriched samples) were compared, being noticed the resemblance between them, and that both spectra present a maximum of absorption at 210 nm. These findings validate the identification of the chromatographic peak identified as U4 as fumaric acid (*trans* isomer of butenedioic acid).

However, this analyte could also be identified as maleic acid (*cis* isomer of butenedioic acid) since it is a geometric isomer of fumaric acid, having the same maximum of absorption (210 nm) and the same retention time, as it can be noticed by examining Figure 3.10.

Despite both compounds' similar properties (molecular formula, mass fragmentation pattern, maximum of absorption wavelength), the third chromatographic peak shown in Table 3.1 was

identified as fumaric acid since it is a more stable compound than maleic acid [32] and because fumaric acid produces a chromatographic peak with higher intensity than maleic acid's one. Nevertheless, maleic acid presence in Bz nitration plant should not be neglected because this compound is typically detected, together with fumaric acid, during the oxidation of organic molecules [23, 33].

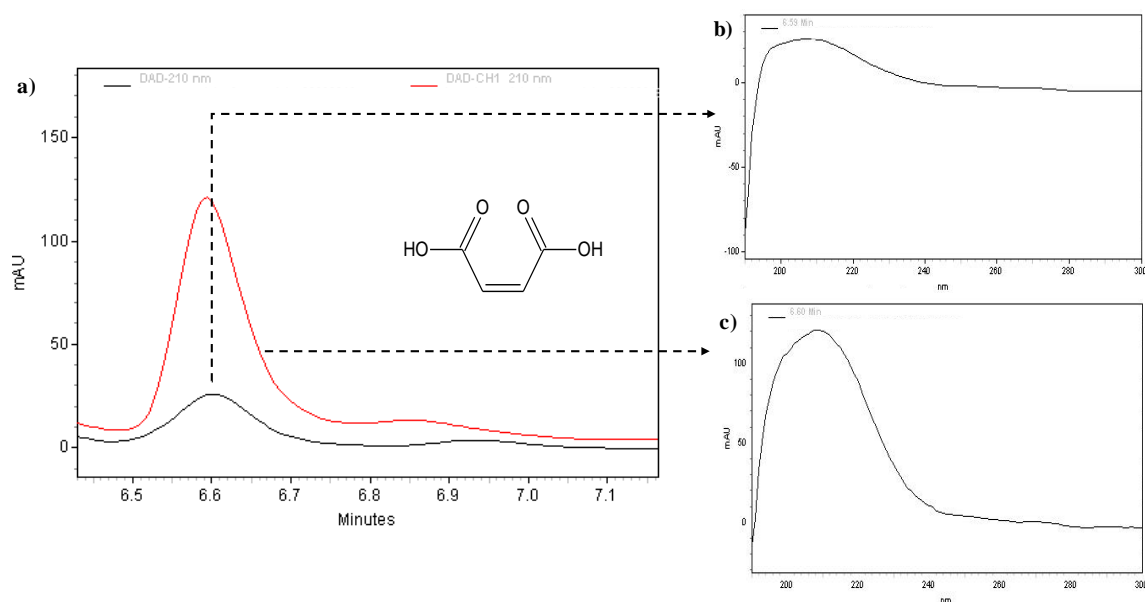
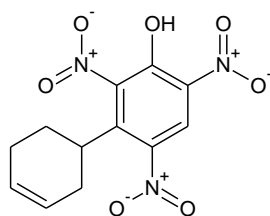


Figure 3.10 – a) Produced MNB HPLC chromatogram. Black line – industrial sample; red line – maleic acid-added industrial sample. UV-Vis spectrum from: **b)** industrial sample, **c)** maleic acid-added industrial sample.

In order to achieve an undoubtable peak identification, standards of fumaric and maleic acid could be added, separately, to the sample, being then analysed by HPLC-MS. Another possibility is the sample's derivatization for improving the compounds separation in the chromatographic column [34] and for introducing changes in their molecular weight and fragmentation pattern [35]. The sample's derivatization would also enable its analysis by GC-MS which could contribute for the enlightenment of both isomers' presence in the sample.

The information exhibited in Table 3.1 concerning the chromatographic peak U5 indicates that the heaviest detected ion has a value of 308 m/z , being possibly a molecular ion. Examining its fragmentation pattern one can deduce that a nitro group (46 u; 308-262) is lost, evidence supported by the nitrogen rule (odd molar mass). Consequently, one can suspect that 2,4,6-trinitro-1',2',3',6'-tetrahydro[1,1'-biphenyl]-3-ol, illustrated in Figure 3.11, may be present in the analysed sample, although its existence was not confirmed.

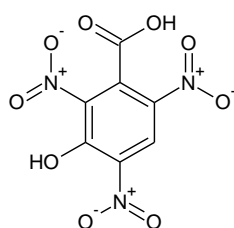


2,4,6-trinitro-1',2',3',6'-tetrahydro[1,1'-biphenyl]-3-ol

Figure 3.11 – Possible U5 peak identification.

Nevertheless, the lost mass fragment (46 u) may also match the formation of an adduct between formic acid (used in the eluent) and the analyte. Considering the adduct formation, the molecular ion of peak U5 would have a value of 262 m/z and its mass fragments allows inferring the loss of NO_2 (46 u; 262-216), of H_2S (34 u; 216-182) and of CH_2 (14 u; 182-168) or $\text{C}_6\text{H}_5\text{O}$ (94 u; 262-168). However, any compound complying with the determined molar mass (263 $\text{g}\cdot\text{mol}^{-1}$) and mass fragments (NO_2 , H_2S and CH_2 or $\text{C}_6\text{H}_5\text{O}$) was found. If the adduct with formic acid is not formed the chromatographic peak U5 may correspond to only one analyte with a molar mass of 309 $\text{g}\cdot\text{mol}^{-1}$, although any compound was found complying deduced mass fragments (NO_2 , H_2S , CH_2 or $\text{C}_6\text{H}_5\text{O}$) and molar mass, or to at least two non-resolved analytes, which are represented by the heavier ions (308 and 262 m/z).

Analysing the U6 peak's data, is noticeable the existence of a molecular ion with a value of 272 m/z , and that the obtained mass fragments allowed assuming the loss of CO_2 (44 u; 272-228) and NO (30 u; 228-198), indicating that this compound is a nitro carboxylic acid, possibly 3-hydroxy-2,4,6-trinitrobenzoic acid – Figure 3.12.



3-hydroxy-2,4,6-trinitrobenzoic acid

Figure 3.12 – Possible U6 peak identification.

The 3-hydroxy-2,4,6-trinitrobenzoic acid could be formed by toluene (typically present in Bz nitration grade) oxidation to benzoic acid, followed by benzoic acid nitration and oxidation; however, its presence in the nitration plant was not confirmed.

Regarding the chromatographic peak numbered as U7, the analysis of the corresponding MS data indicates the presence of a heavy ion (288 m/z), possibly a molecular ion, and allows to infer

the loss of H₂O (18 u; 288-270), CO₂ (44 u; 288-244) and NO₂ (46 u; 244-198). Compiling the gathered information, one can suggest that 3,5-dihydroxy-2,4,6-trinitrobenzoic acid is present in the sample – Figure 3.13.

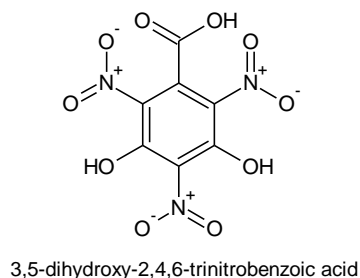


Figure 3.13 – Possible U7 peak identification.

This compound could be generated by toluene oxidation and nitration, however its presence in the reaction medium of benzene nitration was not confirmed.

A further analysis of U7 peak's MS data enables noticing possible losses of H₂O (18 u; 117-99) and of CO₂ (44 u; 117-73) which are characteristic of carboxylic acids. If the ion 117 *m/z* is considered a molecular ion, the compilation of its molar mass (118 g·mol⁻¹) and of the presupposed mass fragments, suggest the presence of succinic acid in the analysed sample, a compound typically detected in oxidation processes of aromatics [23, 36]. The performed data analysis indicate that the chromatographic peak U7 may correspond to at least two non-resolved analytes.

The presence of succinic acid in the nitration plant was verified by collecting and analysing by HPLC-DAD an industrial sample which was then enriched in the acid standard. The results achieved are depicted in Figure 3.14.

According to the mentioned figure, succinic acid's retention time is of about 6.6 minutes, a similar value to that of fumaric acid (Figure 3.9). However, comparing the compounds UV-Vis spectra (industrial sample and succinic acid-added sample) is visible that succinic acid maximum of absorption is 205 nm while the industrial sample chromatogram evidences that the analyte's maximum of absorption is of about 210 nm. This means that in the developed HPLC-DAD method, fumaric acid and succinic acid chromatographic peaks are overlapped, not being possible to quantify the latter if both organic acids are present in the sample. Nevertheless, succinic acid presence in the nitration plant should not be discarded.

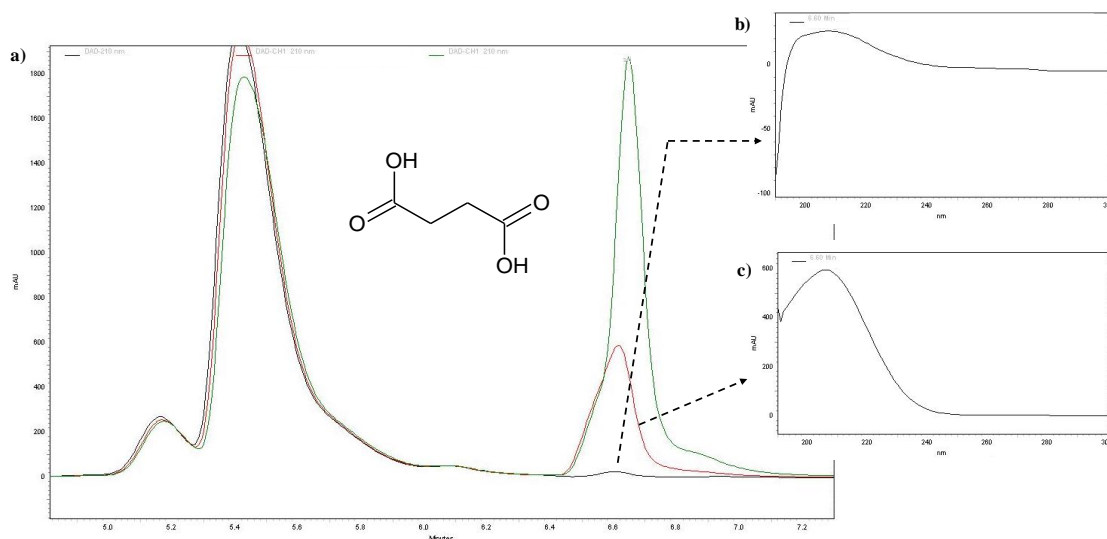


Figure 3.14 – a) Produced MNB HPLC chromatogram. Black line – industrial sample; red line – enriched industrial sample in succinic acid; green line – enriched industrial sample in fumaric acid. UV-Vis spectrum of the analyte with 6.6 minutes of retention time from a: b) industrial sample, c) succinic-added industrial sample.

The results obtained for the peak U8 reveal the existence of three ions that have generated different fragments during the analysis. This may be indicative of the presence of several non-resolved analytes at the same retention time. On the other hand, the detected ions can also be characteristic of only one compound being the molecular ion the heaviest detected ion ($344\ m/z$). However, any chemical compound was found complying with this possible molecular ion ($344\ m/z$) and all the detected mass fragmentation pattern. Considering the ion $201\ m/z$ and the corresponding mass fragmentation pattern, which suggests the loss of CO_2 ($44\ \text{u}$; $201-157$), NO_2 , $\text{C}_2\text{H}_4+\text{H}_2\text{O}$ or $\text{C}_2\text{H}_5\text{OH}$ ($46\ \text{u}$; $157-111$), and of COOH ($45\ \text{u}$; $111-66$) one can allude to the presence of a carboxylic acid in the sample, although its identification was not successfully accomplished.

The presence of a carboxylic acid is also noticeable when studying the fragmentation pattern of the ion $145\ m/z$, which points to the loss of H_2O ($18\ \text{u}$; $145-127$), CO_2 ($44\ \text{u}$; $145-101$) and successively H_2O and CO_2 ($62\ \text{u}$; $145-83$). Assuming that the $145\ m/z$ ion is a molecular ion and bearing in mind the deduced mass fragments, adipic acid presence in the analysed sample can be proposed. This identification is supported by Frauendorf and Herzsuh [26] work once the authors reported the same molecular ion and fragmentation pattern for identifying adipic acid.

Aiming to confirm the adipic acid presence in the nitration plant, an industrial sample was analysed by HPLC-DAD and then enriched with the referred carboxylic acid. The results achieved are shown in Figure 3.15.

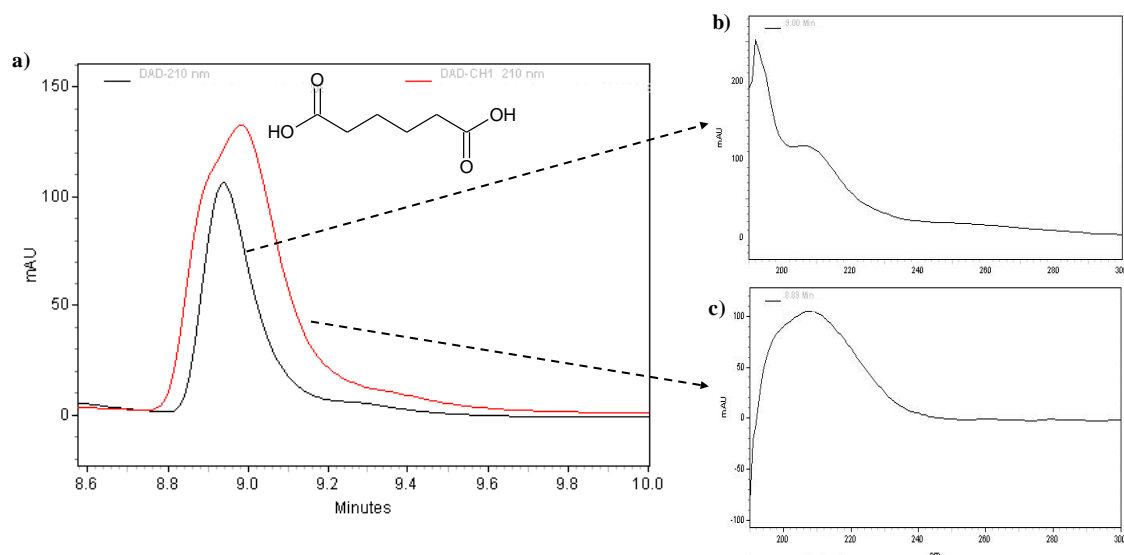


Figure 3.15 – a) Acid water HPLC chromatogram. Black line – industrial sample; red line – adipic acid-added industrial sample. UV-Vis spectrum from: b) industrial sample, c) adipic acid-added industrial sample.

Observing Figure 3.15 is perceptible that adipic acid's retention time is 8.9 minutes in the developed HPLC-DAD analytical method. However, this retention time is alike the one of other species (K3, 2-mononitrobenzenesulfonic acid) – Figure 3.2-a). This means that the developed analytical method is not suitable for detecting adipic acid, and consequently to confirm its presence in the plant. Nevertheless, adipic acid should be present in the plant once it was detected during the oxidation of aromatic compounds [23] and it can be the precursor of smaller carboxylic acids as succinic, mesoxalic and oxalic acid, and also of carbon dioxide (compounds found in the nitration plant).

As for the peak numbered as U9, the corresponding mass spectrum displays a molecular ion of 159 m/z and a mass fragmentation pattern that suggests the loss of H_2O (18 u; 159-141), C_3H_6 (42 u; 159-117) and of CO_2 and H_2O (62 u; 159-97). The data retrieved from the performed analysis indicates that this compound has a molar mass of 160 $g \cdot mol^{-1}$ and that it is a carboxylic acid, possibly butylpropanedioic acid – Figure 3.16 – which can have its genesis in methyl hexane (impurity possibly present in Bz feed) oxidation.. However, the presence of this organic acid in the nitration plant was not confirmed.

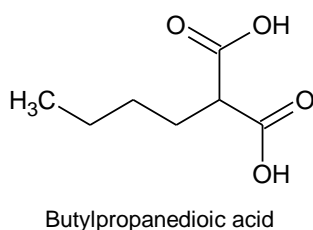


Figure 3.16 – Possible U9 analyte identification.

Despite not having successfully identified all the detected compounds a conclusion can be withdrawn from the exhibited MS data, which is that during Bz nitration in addition to the typical formed by-products, dicarboxylic acids are also formed.

The detection of these organic acids in the nitration plant, species that are usually detected in oxidation processes of aromatic compounds [23, 37-39], together with the detection of CO₂ allows to state unequivocally that the dicarboxylic acids arise from the oxidation of the organic matter in Bz nitration. Compiling the identified compounds and relating this information with the chromatographic peaks detected in Figure 3.2-a), Table 3.2 was constructed.

Table 3.2 – Identification of the chromatographic peaks detected in Figure 3.2.

Chromatographic peak	Compound
K1+U1	Oxalic acid + Mesoxalic acid
U2	Unidentified
U3	Succinic acid, Fumaric acid, Maleic acid
U4	Unidentified
U5	Unidentified
K2	Benzenesulfonic acid
U6	Unidentified
K3	2-mononitrobenzenesulfonic acid + adipic acid
K4	3-mononitrobenzenesulfonic acid
K5	4-mononitrobenzenesulfonic acid
K6	2,4,6 – trinitrophenol
K7	2,4 – dinitrophenol
K8	2,6 – dinitrophenol
K9	MNB
K10	Bz

Although there are still chemical species to be identified, the number of unknown compounds was reduced to four (U2, U4, U5 and U6). Aiming to determine the nature of these compounds, a simple test was performed which consisted in diluting an industrial sample with KMnO₄. By this way, it was expected to verify if the unknown compounds were dicarboxylic acids once KMnO₄ is a known carboxylic acid oxidizing agent, capable of decomposing such compounds [40-42]. The findings achieved in this test have shown that compounds U4 and U6 are most likely dicarboxylic acids, consequently oxidation intermediates, because their chromatographic peaks have disappeared after the KMnO₄ addition. Moreover, their maximum wavelength of absorption is comprised between 200 and 215 nm, the typical range of organic acids [43]. The chromatographic

peaks disappearance was also verified for the oxalic acid + mesoxalic acid (K1+U1) and fumaric + succinic + maleic acid (U3) peaks. The chromatogram obtained for this test is given in the Appendix C (Figure C.11).

It is worth to mention that the chromatographic peak areas of compounds K2, K3, K4 and K5 remained unchanged after KMnO_4 addition. Such evidence was expected because these compounds are not carboxylic acids. As the analytes U2 and U5 showed a behaviour similar to that of compounds K2 to K5, one can suggest that these compounds have substituent groups containing sulphur or nitrogen atoms.

The detected compounds during this study were found to be present in different plant locations [21].

3.3.2. Proposed oxidation pathway

The detection and identification of oxidized compounds (dicarboxylic acids), together with CO_2 finding in the nitration plant (addressed in Chapter 2), allowed to propose a formation pathway for the organic compounds present in the Bz nitration medium. The proposed pathway, illustrated in Figure 3.17, was based on the open literature related with oxidation processes and focused in compounds present in the benzene nitration media.

According to Figure 3.17, phenol is formed through Bz oxidation, reaction known to be in the nitrophenols genesis [4, 9], but it can also be further oxidized leading to catechol or hydroquinone formation, compounds that can be responsible for the appearance of *o*-benzoquinone and *p*-benzoquinone, respectively [30, 33]. Then, due to the benzoquinone ring cleavage, muconic acid or 2,5-dioxo-3-hexenedioic acid can be formed, which, by successive oxidations lead to fumaric acid, maleic acid, oxalic acid, and ultimately to CO and CO_2 formation [24, 30, 33, 36, 38-39, 44]. Although not being represented in the proposed oxidation pathway, ketones and aldehydes may also be formed through the decomposition of aromatic compounds [23, 33].

Besides being a catechol and hydroquinone precursor, phenol can be decomposed to mesoxalic acid (ring cleavage), also a possible CO_2 precursor [1]. Additionally, phenol can also be nitrated originating mononitrophenols which in turn can then undergo ring-cleavage reactions to form dicarboxylic acids as muconic, maleic, fumaric or oxalic acids, which ultimately will lead to CO_2 [39, 45] and CO formation [44].

Another possible pathway for CO_2 formation arises from toluene (or toluene derivatives such as nitro or dinitrotoluene, nitroresols, etc.) oxidation, as referred by Ross and Kirshen [7], Hanson *et al.* [8]. For instance, toluene can be oxidized to benzoic acid, which in turn can originate phenol, leading ultimately to carbon dioxide formation.

Decomposition Reactions in Aromatic Nitration

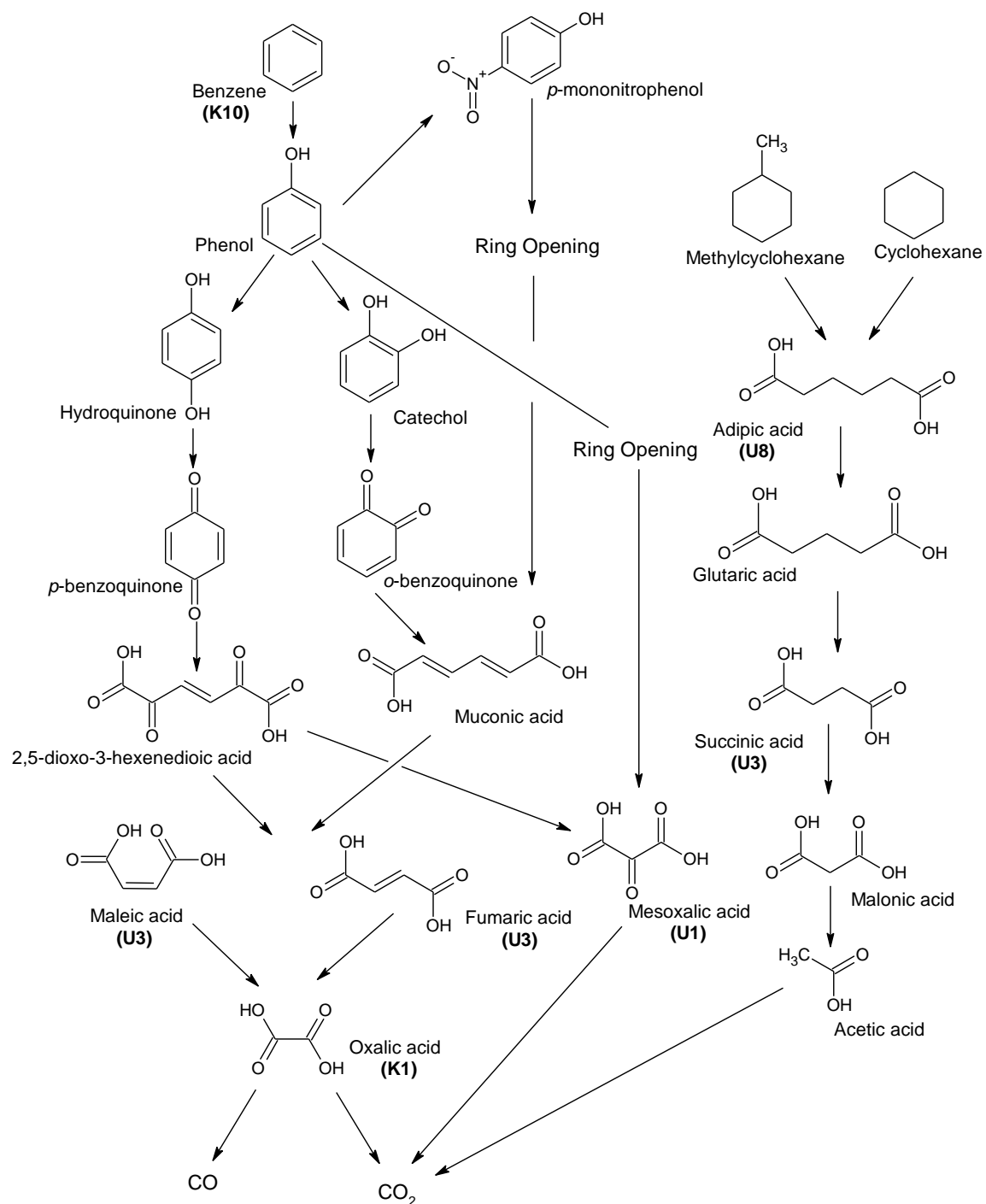


Figure 3.17 – Possible reaction pathway for the decomposition of organic compounds present in Bz nitration medium. Adapted from [1, 30, 33, 36, 38-39].

Carbon dioxide can also appear through the decomposition of adipic acid which originates then glutaric acid, succinic acid, malonic and acid acetic acid by successive decarboxylation and oxidation reactions. Adipic acid could be formed by cyclohexane or methylcyclohexane (typical Bz nitration grade impurities) oxidation and ring cleavage.

Despite the different displayed CO_2 formation paths, it is expected that the majority of the detected oxidation by-products (and of CO_2) have origin in Bz oxidation because Bz (together with MNB) is the major constituent of the nitration media while the aliphatic species are only present in low concentrations (ppm levels) in the reaction medium.

3.3.3. Oxidation by-products decomposition

The analysis (HPLC-DAD and HPLC-MS) performed to the industrial samples didn't allowed determining if the detected oxidation by-products were intermediate precursors of the spotted CO_2 (Chapter 2) in the nitration plant. Moreover, and given that oxalic acid is a recalcitrant molecule, it was intended to check if this compound could be decomposed within the typical Bz nitration conditions, leading to CO and CO_2 formation.

To check this hypothesis, a determined amount of oxalic acid was added to synthetic mixed acid at different temperatures (in the range of the industrial values), being the molecule decomposition verified by checking CO and CO_2 formation with a gas detector. The results obtained are depicted in Figure 3.18.

According to Figure 3.18, it is seen that within Bz nitrating conditions, oxalic acid is decomposed both to CO and CO_2 . However, the reaction conditions differ from those of Bz nitration because in the absence of Bz, nitric acid consumption is low, while during Bz nitration this acid is rapidly depleted from the system. This means that nitric acid may have been decomposed instead being consumed, yielding potential oxidants such as NO_2 [7, 46] that may have contributed for the decomposition of oxalic acid.

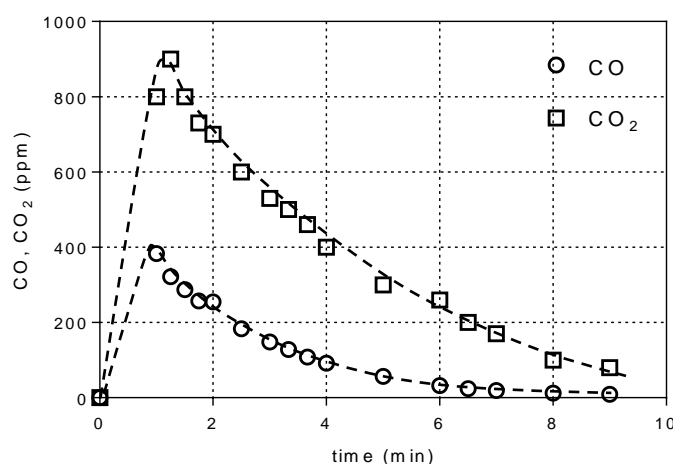


Figure 3.18 – Carbon monoxide and carbon dioxide formation by oxalic acid decomposition. Oxalic acid concentration: 2000 ppm; mixed acid composition: 66% wt. H_2SO_4 ; 5% wt. HNO_3 . Reaction temperature: 100 °C. Lines are added just for a better visualization of the trends.

Analysing CO and CO₂ concentration profiles, it is seen that in less than 10 minutes their amounts became vestigial, indicating that oxalic acid decomposition was finished. Nevertheless, the detected gas amounts corresponded only to about 10% of the placed molar quantities of oxalic acid. Additionally, the mixed acid composition did not vary significantly during the reaction time because it was in large excess when compared to the organic acid concentration and because no other compound (able to consume nitric or sulfuric acid) was placed in the reaction medium. Consequently, oxalic acid decomposition should not have stopped.

To confirm that oxalic acid was still present in the reaction medium, a small portion of KMnO₄ was added to the reactor, being noticed an increase of CO and CO₂ concentration, more pronounced for CO₂. This finding suggests that even in the absence of Bz, oxalic acid decomposition is not complete. Aiming to relate CO formed amounts with those of CO₂, the graphic from Figure 3.19 was plotted.

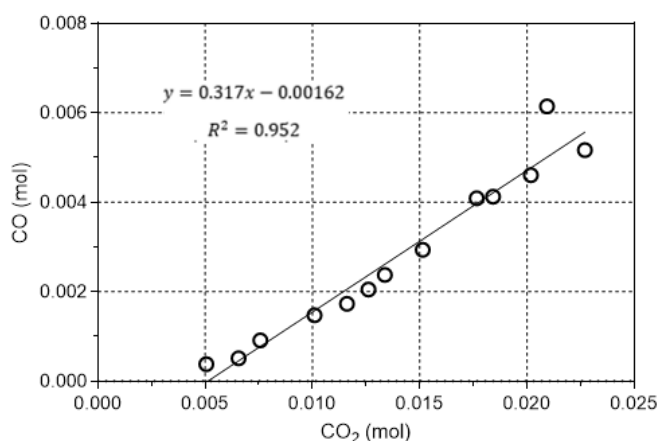


Figure 3.19 – Carbon monoxide vs. carbon dioxide formation in oxalic acid decomposition. Reaction conditions: T = 100 °C; Oxalic acid concentration = 2000 ppm; mixed acid composition: 66% wt. H₂SO₄; 5% wt. HNO₃.

As demonstrated in Figure 3.19, CO and CO₂ formation can be correlated by a linear regression. This was an important finding because it allows to predict the amounts of CO based in the detected amounts of CO₂ and *vice-versa*.

Once CO₂ is formed in higher quantities than those of CO, a set of oxalic acid decomposition tests was conducted in a round-bottom flask, at different temperatures (but within the industrial range), in which only CO₂ was quantified resorting to the barium carbonate formation. The goal of these tests was to relate the reaction temperature with oxalic acid decomposition. The obtained results are depicted in Figure 3.20.

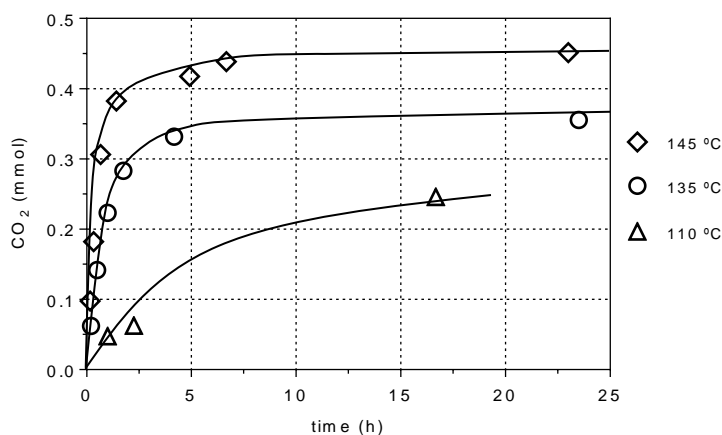


Figure 3.20 – Carbon dioxide formed amounts for different temperatures. Mixed acid composition: 66% wt. H₂SO₄; 5% wt. HNO₃. Lines are added just for better visualization of the trends.

The influence of temperature on oxalic acid decomposition is observable in Figure 3.20; when the temperature increases there is also a rise of CO₂ formation, as well as an increase of its formation rate. A detailed analysis of this figure shows that after almost 24 h of reaction time, 0.45 mmol of CO₂ were formed in the highest temperature run while in the 135 °C run only 0.35 mmol were generated. For the lowest temperature run (110 °C) it is seen that nearly 0.25 mmol of CO₂ were generated 16 h after the test start. Although there are few experimental points in the lowest temperature runs, the reached conclusions are unquestionable. The positive impact of the temperature increase on CO₂ generation was expected because it is known that the temperature rise tends to favour the oxidative decomposition of organic compounds [44, 47-48].

In order to evaluate the oxalic acid decomposition, a carbon balance was performed considering only the CO₂ formation, because only this compound was directly quantified during the reaction time. The carbon balance enabled deducing that not all oxalic acid had been decomposed. Even considering CO generation, using the slope from the linear regression of Figure 3.19, although CO₂ formed amounts were lower than those from Figure 3.19, it was found that these gaseous compounds accounted only for 79% (for the 145 °C run) of the carbon mass balance. These results denote oxalic acid resistance to oxidation at Bz nitration conditions and explain why this compound is detected in plant. In fact, oxalic acid refractory behaviour has already been addressed by Zazo *et al.* [49] when studying phenol oxidation by Fenton's reagent at different conditions, being shown that below 100 °C, this species is quite resistant to Fenton oxidation [47, 49].

It is worth to mention that during the oxalic acid decomposition runs, the only oxidizing agent present in the reaction medium was nitric acid. Therefore, to demonstrate this mineral acid influence on oxalic acid decomposition, a nitric acid-free experiment was conducted employing the same temperature (135 °C) and sulfuric acid concentration of the previous tests. The results achieved are represented in Figure 3.21.

Decomposition Reactions in Aromatic Nitration

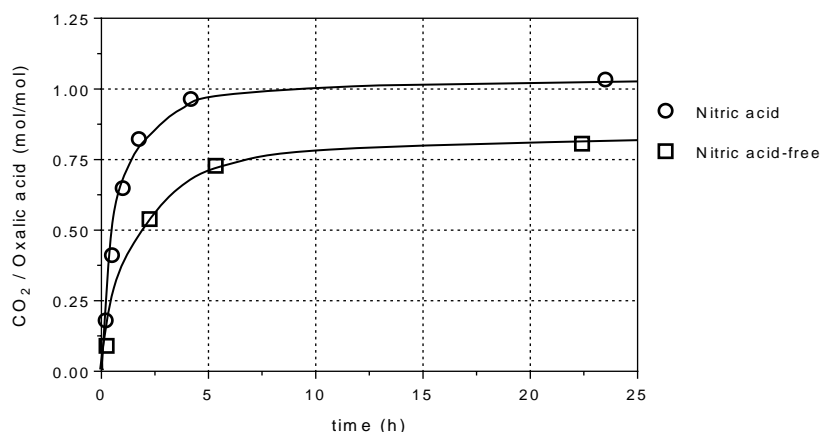


Figure 3.21 – Nitric acid influence on oxalic acid decomposition. Mixed acid composition: 66% wt. H₂SO₄; 5% wt. HNO₃ for nitric acid run; reaction temperature: 135 °C. Lines are added just for better visualization of the trends.

As illustrated in Figure 3.21, the oxalic acid decomposition rate is faster in the reaction beginning for both runs, tending then to slow down as the reaction proceeds, which can be explained by the organic acid disappearance from the medium. Comparing both runs, is visible that oxalic acid decomposition rate and CO₂ formation were higher for the nitric acid run. Based in these results, it can be concluded that the nitric acid presence in the reaction medium favours the oxalic acid decomposition.

Since oxalic acid was found to be decomposed in the range of Bz nitrating conditions (in the absence of Bz), yielding CO and CO₂, it was intended to ascertain if the others identified compounds could also be decomposed. Therefore, mesoxalic, succinic acid, fumaric acid and adipic acid decomposition was checked in synthetic mixed acid at 130-140 °C. The obtained results, depicted in Figure 3.22, were normalized with the initial amounts of each dicarboxylic acid because a C₄ dicarboxylic acid can yield higher CO₂ amounts than a C₂ acid.

Figure 3.22 shows that all the tested carboxylic acids were decomposed in the range of the industrial adiabatic Bz nitration conditions (mixed acid composition and reaction temperature), although at different rates. This supports the occurrence of decomposition reactions during Bz nitration and evidences that these compounds might yield CO₂ in the industrial plant. Although CO formation was only confirmed in oxalic acid decomposition, considering the open literature [33, 44], one can state that the oxidative decomposition of the remaining (tested) dicarboxylic acids leads also to CO formation.

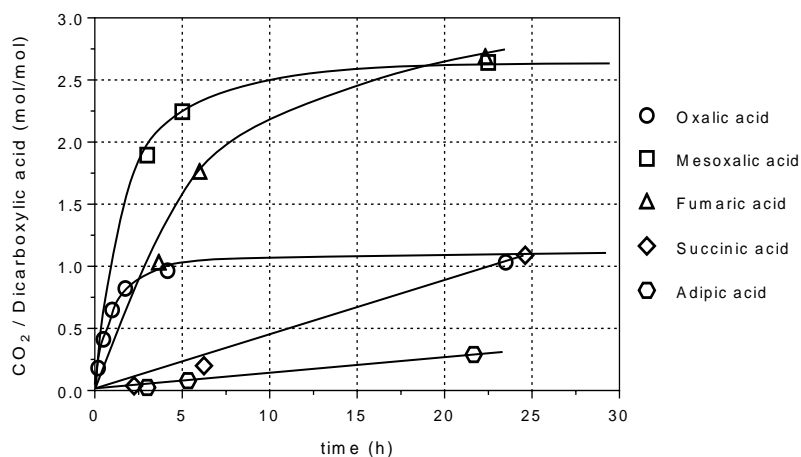


Figure 3.22 – Decomposition of different dicarboxylic acids at adiabatic benzene nitration conditions in the absence of benzene. Mixed acid composition: 66% wt. H_2SO_4 ; 5% wt. HNO_3 . Reaction temperature [130; 140] °C. Lines are added just for better visualization of the trends.

Analysing the CO_2 formed amounts, is visible that succinic acid and adipic acid are the organic acids, among the studied ones, more resistant to oxidation because were the compounds that presented a lower CO_2 formation rate. This was verified because these acids are saturated dicarboxylic acids, a characteristic that confer them higher stability. Comparing succinic acid and adipic acid oxidation, it is seen that the higher chain organic acid is more resistant to decomposition, result which is in accordance with Cornils and Lappe [50] when they state that lower dicarboxylic acids decompose more easily than higher ones.

In what concerns to oxalic and mesoxalic acids, Figure 3.22 shows that these species are those more prone to oxidation since were the ones with the highest CO_2 formation rate. Regarding the fumaric acid decomposition rate, is noticeable that it is higher than that of succinic acid, although both compounds have 4 carbons in their chain. This is consequence of fumaric acid C-C double bond, a less stable bond than C-C single bond from succinic acid. This lower stability is due to the π orbital of the C-C double bond, a weak bond with a high electron density, being thus easily broken.

Concluding, the obtained results evidence that the studied organic acids are decomposed at the typical nitration conditions, by action of the temperature and nitric acid, and are in accordance, although partially, with the proposed oxidation pathway – Figure 3.17. Furthermore, it was revealed that oxalic acid is also a CO precursor, being suspected that the remaining carboxylic acid can also yield this gas. According to Figure 3.17, phenol, which is originated *via* benzene oxidation [4, 9], is the precursor of several dicarboxylic acids. Therefore, one might suspect that CO_2 formation in the nitration plant starts with benzene oxidation to phenol.

3.4. Conclusions

The development of a HPLC-DAD analytical methodology enabled to find that during the adiabatic mixed acid benzene nitration another class of by-products is formed, apart from nitrophenols and dinitrobenzene. Such by-products arise from the oxidation of the organic matter, most likely from the organic raw material (benzene), and were found to be dicarboxylic acids, namely oxalic, mesoxalic, fumaric, maleic, and succinic acid. This was the first time that these dicarboxylic acids were identified in benzene nitration plants and their detection is a further evidence supporting the occurrence of oxidation reactions during benzene nitration.

In order to verify if the identified dicarboxylic acids could be oxidized at the typical nitration conditions, they were individually added to synthetic mixed acid, being found that the performed tests yielded carbon dioxide (and carbon monoxide in oxalic acid decomposition). It was found that succinic acid and adipic acid were the organic acids (among the tested ones) more resistant to oxidation and that higher temperature and higher nitric acid concentration tend to favour the decomposition of the dicarboxylic acids.

Nomenclature

Acronyms

Bz	Benzene
DNB	Dinitrobenzene
GC-ToFMS	Gas Chromatography – Time-of-Flight Mass Spectrometry
HPLC-DAD	High Performance Liquid Chromatography - Diode Array Detector
HS-SPM	Headspace Solid Phase Microextraction
MNB	Mononitrobenzene
MNT	Mononitrotoluene
MS	Mass Spectrometry
NPs	Nitrophenols
TIC	Total Ion Chromatogram
UHPLC-MS	Ultra High Performance-Liquid Chromatography – Mass spectrometry

3.5. References

- [1]. Urbański, T., *Chemistry and Technology of Explosives*. Pwn-Polish Scientific Publishers, Vol. 1, Warszawa, Poland, 1964.
- [2]. Quadros, P. A.; Castro, J. A. A. M.; Baptista, C. M. S. G., Nitrophenols Reduction in the Benzene Adiabatic Nitration Process. *Industrial & Engineering Chemistry Research* **2004**, 43 (15), 4438-4445, 10.1021/ie034263o.
- [3]. Berretta, S.; Louie, B., Effect of Reaction Conditions on the Formation of Byproducts in the Adiabatic Mononitration of Benzene into Mononitrobenzene (MNB). In *Chemistry, Process Design, and Safety for the Nitration Industry*, American Chemical Society, Washington, DC. ACS Symposium Series, 2013; Vol. 1155, pp 13-26, doi:10.1021/bk-2013-1155.ch002
10.1021/bk-2013-1155.ch002.
- [4]. Afonso, D.; Ribeiro, A. F. G.; Araújo, P.; Vital, J.; Madeira, L. M., Phenol in Mixed Acid Benzene Nitration Systems. *Industrial & Engineering Chemistry Research* **2018**, 57 (46), 15942-15953,
- [5]. Guenkel, A. A.; Maloney, T. W., Recent Advances in the Technology of Mononitrobenzene Manufacture. In *Nitration*, American Chemical Society, Washington, DC. ACS Symposium Series, 1996; Vol. 623, pp 223-233, doi:10.1021/bk-1996-0623.ch020
10.1021/bk-1996-0623.ch020.
- [6]. Gattrell, M.; Louie, B., Adiabatic Nitration for Mononitrotoluene (MNT) Production. In *Chemistry, Process Design, and Safety for the Nitration Industry*, American Chemical Society, Washington, DC. ACS Symposium Series, 2013; Vol. 1155, pp 27-48, doi:10.1021/bk-2013-1155.ch003
10.1021/bk-2013-1155.ch003.
- [7]. Ross, D. S.; Kirshen, N. A., Nitration and Oxidative Side Reactions of Dinitrotoluenes. In *Industrial and Laboratory Nitrations*, American Chemical Society, Washington, DC. ACS Symposium Series, 1976; Vol. 22, pp 114-131, doi:10.1021/bk-1976-0022.ch007
10.1021/bk-1976-0022.ch007.
- [8]. Hanson, C.; Kaghazchi, T.; Pratt, M. W. T., Side Reactions During Aromatic Nitration. In *Industrial and Laboratory Nitrations*, American Chemical Society, Washington, DC. ACS Symposium Series, 1976; Vol. 22, pp 132-155, doi:10.1021/bk-1976-0022.ch008
10.1021/bk-1976-0022.ch008.
- [9]. Burns, J. R.; Ramshaw, C., Development of a Microreactor for Chemical Production. *Chemical Engineering Research and Design* **1999**, 77 (3), 206-211, <http://dx.doi.org/10.1205/026387699526106>.
- [10]. Albright, L. F., Nitration. In *Kirk-Othmer Encyclopedia of Chemical Technology*, John Wiley & Sons, Inc., 2000, 10.1002/0471238961.1409201801120218.a01.

- [11]. Odle, R. R.; Guggenheim, T. L.; DeLong, L. M., Solubility, Equilibrium, Behavior, and Analytical Characterization of Tetranitromethane, Trinitromethane, Methyl Amine, and Ammonia in a Nitration Facility. In *Chemistry, Process Design, and Safety for the Nitration Industry*, American Chemical Society, Washington, DC. ACS Symposium Series, 2013; Vol. 1155, pp 203-228, doi:10.1021/bk-2013-1155.ch014
10.1021/bk-2013-1155.ch014.
- [12]. Kramer, G. M., Oxidation of paraffins in sulfuric acid. *The Journal of Organic Chemistry* **1967**, 32 (6), 1916-1918, 10.1021/jo01281a047.
- [13]. Costa, T. J. G.; Nogueira, A. G.; Silva, D. C. M.; Ribeiro, A. F. G.; Baptista, C. M. S. G., Nitrophenolic By-Products Quantification in the Continuous Benzene Nitration Process. In *Chemistry, Process Design, and Safety for the Nitration Industry*, American Chemical Society, Washington, DC. ACS Symposium Series, 2013; Vol. 1155, pp 49-60, doi:10.1021/bk-2013-1155.ch004
10.1021/bk-2013-1155.ch004.
- [14]. Käkölä, J.; Alén, R., A fast method for determining low-molecular-mass aliphatic carboxylic acids by high-performance liquid chromatography–atmospheric pressure chemical ionization mass spectrometry. *Journal of Separation Science* **2006**, 29 (13), 1996-2003, doi:10.1002/jssc.200600106.
- [15]. Niessen, W. M. A., *Liquid Chromatography-Mass Spectrometry*. 3rd edition, CRC Press, New York, 2006.
- [16]. Chen, Z.; Jin, X.; Wang, Q.; Lin, Y.; Gan, L.; Tang, C., Confirmation and determination of carboxylic acids in root exudates using LC–ESI-MS. *Journal of Separation Science* **2007**, 30 (15), 2440-2446, doi:10.1002/jssc.200700234.
- [17]. Käkölä, J.; Alén, R.; Pakkanen, H.; Matilainen, R.; Lahti, K., Quantitative determination of the main aliphatic carboxylic acids in wood kraft black liquors by high-performance liquid chromatography–mass spectrometry. *Journal of Chromatography A* **2007**, 1139 (2), 263-270, <https://doi.org/10.1016/j.chroma.2006.11.033>.
- [18]. Lee, M. S., *Mass Spectrometry Handbook*. 1st edition, Wiley, New Jersey, USA, 2012.
- [19]. McMaster, M. C., *LC/MS: A Practical User's Guide*. John Wiley & Sons, Inc., New Jersey, USA, 2005.
- [20]. Afonso, D.; Ribeiro, A. F. G.; Araújo, P.; Vital, J.; Madeira, L. M., (Nitro)benzenesulfonic acids in nitrobenzene production. *Submitted* **2019**,
- [21]. Diogo Afonso, Bondalti Chemicals, Internal Report. **2018**.
- [22]. Minero, C.; Pelizzetti, E.; Piccinini, P.; Vincenti, M., Photocatalyzed transformation of nitrobenzene on TiO₂ and ZnO. *Chemosphere* **1994**, 28 (6), 1229-1244, [https://doi.org/10.1016/0045-6535\(94\)90340-9](https://doi.org/10.1016/0045-6535(94)90340-9).

- [23]. Shen, J.-m.; Chen, Z.-l.; Xu, Z.-z.; Li, X.-y.; Xu, B.-b.; Qi, F., Kinetics and mechanism of degradation of p-chloronitrobenzene in water by ozonation. *Journal of Hazardous Materials* **2008**, 152 (3), 1325-1331, <https://doi.org/10.1016/j.jhazmat.2007.08.009>.
- [24]. Li, X.; Huang, Y.; Li, C.; Shen, J.; Deng, Y., Degradation of pCNB by Fenton like process using α -FeOOH. *Chemical Engineering Journal* **2015**, 260, 28-36, <https://doi.org/10.1016/j.cej.2014.08.042>.
- [25]. Pulgarin, C.; Adler, N.; Péringer, P.; Comninellis, C., Electrochemical detoxification of a 1,4-benzoquinone solution in wastewater treatment. *Water Research* **1994**, 28 (4), 887-893, [https://doi.org/10.1016/0043-1354\(94\)90095-7](https://doi.org/10.1016/0043-1354(94)90095-7).
- [26]. Frauendorf, H.; Herzschuh, R., Application of High-Performance Liquid Chromatography/Electrospray Mass Spectrometry for Identification of Carboxylic Acids Containing Several Carboxyl Groups from Aqueous Solutions. *European Mass Spectrometry* **1998**, 4 (4), 269-278, 10.1255/ejms.220.
- [27]. PubChem, 5-Nitro-2-furoic acid. <<https://pubchem.ncbi.nlm.nih.gov/compound/12577#section=Top>>, 2005, accessed in 2018.
- [28]. Scheck, C. K.; Frimmel, F. H., Degradation of phenol and salicylic acid by ultraviolet radiation/hydrogen peroxide/oxygen. *Water Research* **1995**, 29 (10), 2346-2352, [https://doi.org/10.1016/0043-1354\(95\)00060-X](https://doi.org/10.1016/0043-1354(95)00060-X).
- [29]. Alnaizy, R.; Akgerman, A., Advanced oxidation of phenolic compounds. *Advances in Environmental Research* **2000**, 4 (3), 233-244, [https://doi.org/10.1016/S1093-0191\(00\)00024-1](https://doi.org/10.1016/S1093-0191(00)00024-1).
- [30]. Chen, Y.; Li, H.; Liu, W.; Tu, Y.; Zhang, Y.; Han, W.; Wang, L., Electrochemical degradation of nitrobenzene by anodic oxidation on the constructed TiO₂-NTs/SnO₂-Sb/PbO₂ electrode. *Chemosphere* **2014**, 113, 48-55, <https://doi.org/10.1016/j.chemosphere.2014.03.122>.
- [31]. Käkölä, J.; Alén, R., A fast method for determining low-molecular-mass aliphatic carboxylic acids by high-performance liquid chromatography–atmospheric pressure chemical ionization mass spectrometry. *Journal of Separation Science* **2006**, 29 (13), 1996-2003, 10.1002/jssc.200600106.
- [32]. Felthouse, T. R.; Burnett, J. C.; Horrell, B.; Mummey, M. J.; Kuo, Y., Maleic Anhydride, Maleic Acid, and Fumaric Acid. In *Kirk-Othmer Encyclopedia of Chemical Technology*, John Wiley & Sons, Inc., 2001, 10.1002/0471238961.1301120506051220.a01.pub2.
- [33]. Devlin, H. R.; Harris, I. J., Mechanism of the oxidation of aqueous phenol with dissolved oxygen. *Industrial & Engineering Chemistry Fundamentals* **1984**, 23 (4), 387-392,
- [34]. Moldoveanu, S. C.; David, V., Derivatization Methods in GC and GC/MS. In *IntechOpen*, 2018,
- [35]. Shrader, S., *Introductory Mass Spectrometry*. Second Edition, CRC Press, New York, 2013.

- [36]. Liu, Y.; Liu, H.; Li, Y., Comparative study of the electrocatalytic oxidation and mechanism of nitrophenols at Bi-doped lead dioxide anodes. *Applied Catalysis B: Environmental* **2008**, 84 (1), 297-302, <https://doi.org/10.1016/j.apcatb.2008.04.011>.
- [37]. Ayoub, K.; van Hullebusch, E. D.; Cassir, M.; Bermond, A., Application of advanced oxidation processes for TNT removal: A review. *Journal of Hazardous Materials* **2010**, 178 (1), 10-28, <https://doi.org/10.1016/j.jhazmat.2010.02.042>.
- [38]. Ortiz-Gomez, A.; Serrano-Rosales, B.; Salas, M.; de Lasa, H., Photocatalytic Oxidation of Phenol: Reaction Network, Kinetic Modeling, and Parameter Estimation. *Industrial & Engineering Chemistry Research* **2007**, 46 (23), 7394-7409, 10.1021/ie0611960.
- [39]. Qiu, C.; Yuan, S.; Li, X.; Wang, H.; Bakheet, B.; Komarneni, S.; Wang, Y., Investigation of the synergistic effects for p-nitrophenol mineralization by a combined process of ozonation and electrolysis using a boron-doped diamond anode. *Journal of Hazardous Materials* **2014**, 280, 644-653, <https://doi.org/10.1016/j.jhazmat.2014.09.001>.
- [40]. Lee, D. G.; Chang, V. S., Oxidation of hydrocarbons. 9. The oxidation of alkynes by potassium permanganate. *The Journal of Organic Chemistry* **1979**, 44 (15), 2726-2730, 10.1021/jo01329a027.
- [41]. Yan, Y. E.; Schwartz, F. W., Kinetics and Mechanisms for TCE Oxidation by Permanganate. *Environmental Science & Technology* **2000**, 34 (12), 2535-2541, 10.1021/es991279q.
- [42]. Matta, R.; Hanna, K.; Chiron, S., Fenton-like oxidation of 2,4,6-trinitrotoluene using different iron minerals. *Science of The Total Environment* **2007**, 385 (1), 242-251, <https://doi.org/10.1016/j.scitotenv.2007.06.030>.
- [43]. Vignoli, J. A.; Bassoli, D. G., Determinação de ácidos carboxílicos e fenólicos em café solúvel utilizando HPLC/DAD. *Revista Analytica* **2007**, 27, 76-79,
- [44]. Carbajo, J.; Quintanilla, A.; Casas, J. A., Assessment of carbon monoxide formation in Fenton oxidation process: The critical role of pollutant nature and operating conditions. *Applied Catalysis B: Environmental* **2018**, 232, 55-59,
- [45]. Rodrigues, C. S. D.; Borges, R. A. C.; Lima, V. N.; Madeira, L. M., p-Nitrophenol degradation by Fenton's oxidation in a bubble column reactor. *Journal of Environmental Management* **2018**, 206, 774-785,
- [46]. Di Somma, I.; Marotta, R.; Andreozzi, R.; Caprio, V., Nitric acid decomposition kinetics in mixed acid and their use in the modeling of aromatic nitration. *Chemical Engineering Journal* **2013**, 228, 366-373, <https://doi.org/10.1016/j.cej.2013.04.100>.
- [47]. Zazo, J. A.; Pliego, G.; Blasco, S.; Casas, J. A.; Rodriguez, J. J., Intensification of the Fenton Process by Increasing the Temperature. *Industrial & Engineering Chemistry Research* **2011**, 50 (2), 866-870, 10.1021/ie101963k.

- [48]. Mason, C.; Brown, T. L.; Buchanan, D.; Maher, C. J.; Morris, D.; Taylor, R. J., The Decomposition of Oxalic Acid in Nitric Acid. *Journal of Solution Chemistry* **2016**, *45* (3), 325-333, 10.1007/s10953-016-0437-2.
- [49]. Zazo, J. A.; Casas, J. A.; Mohedano, A. F.; Gilarranz, M. A.; Rodríguez, J. J., Chemical Pathway and Kinetics of Phenol Oxidation by Fenton's Reagent. *Environmental Science and Technologies* **2005**, *39* (23), 9295-9302,
- [50]. Cornils, B.; Lappe, P., Dicarboxylic Acids, Aliphatic. In *Ullmann's Encyclopedia of Industrial Chemistry*, Wiley-VCH, 2014, 10.1002/14356007.a08_523.pub3.

Chapter 4 – Phenol in mixed acid benzene nitration systems¹

Abstract

Phenol was detected for the first time in the mononitrobenzene production process by benzene adiabatic nitration, supporting the theory which proposes phenol as the precursor of nitrophenols, unwanted by-products. For that, analytical procedures (based in liquid and gas chromatographic techniques) have been developed and improved aiming to detect these chemical species both in the industrial nitration process as well as in laboratory tests at different reaction conditions. The obtained results confirmed the proposed and accepted mechanism for the nitrophenols formation during benzene nitration, showing that phenol is indeed the nitrophenolic by-products precursor. Moreover, it is shown the phenol's high reactivity even at smooth reaction conditions (namely low temperatures and low sulfuric acid concentration), which explains the difficulty of detecting this compound within the reaction medium using the analytical techniques applied for monitoring benzene nitration process. In this study it was also discovered that 4-mononitrophenol had higher affinity into the aqueous acid phase when compared to the other nitrophenolic by-products (2-mononitrophenol; 2,4-dinitrophenol; 2,6-dinitrophenol; and 2,4,6-trinitrophenol) that have more affinity into the organic phase. Phenol distribution between both the reaction phases was found to be similar to the majority of the nitrophenols, i.e., it is present in higher concentration in the organic phase.

Keywords: Phenol, nitrophenols, benzene nitration, mixed acid systems, mononitrobenzene.

¹ This chapter was adapted from: Diogo Afonso, Alejandro F. G. Ribeiro, Paulo Araújo, Joaquim Vital and Luis Miguel Madeira, Phenol in Mixed Acid Benzene Nitration Systems, *Industrial & Engineering Chemistry Research* **2018** 57 (46), 15942-15953. (DOI: 10.1021/acs.iecr.8b04226)

4.1. Introduction

Nitroaromatic compounds play an important role in industry as intermediates or final products. These compounds are obtained by aromatic nitration, which is one of the oldest and most important reactions performed in the chemical industry, being responsible for the production of chemical commodities such as mononitrobenzene (MNB) or mononitrotoluene (MNT) [1-2].

MNB is obtained by benzene (Bz) nitration and is used mainly as feedstock for aniline production [3-4]. Due to the importance of Bz nitration, this process has been subjected to improvements and studies over time [5-7]. Such improvements (namely the change of the nitration technology from the isothermal process to the adiabatic one) allowed a reduction of the process costs. On the other hand, this technology shift enhanced the formation of reaction by-products.[8] The main impurities formed by adiabatic MNB production in continuous stirred tank reactors (CSTRs) are nitrophenols (dinitrophenol – DNP - and trinitrophenol - TNP) and dinitrobenzene [7, 9], being crucial to minimize these by-products due to their negative environmental, safety and economic impacts [10-11].

It is known that nitration reactions are always followed by side reactions that are influenced by different factors like the composition of the nitrating mixture, the nature of the compound to be nitrated and the operating conditions [12]. Studies aiming the reduction of nitrophenols formation during aromatic nitration were already done [7, 13-15], being achieved some interesting conclusions. For instance, several authors stated that reaction temperature, despite contributing positively for the MNB production, enhances also the nitrophenols formation [7, 9, 13]. The mixed acid (a mixture of nitric and sulfuric acid) composition influences also the by-products formation because sulfuric acid, the reaction catalyst, is responsible for the nitric acid dissociation and, consequently, for the nitronium ion formation (NO_2^+), the accepted nitrating agent. Moreover, undissociated nitric acid is suggested as a Bz oxidation agent [16] being responsible for phenol (Ph) formation, the species proposed to be the nitrophenols precursor [17] – Figure 4.1. However, to date Ph was never detected within Bz nitration medium, being this the main goal of the present work.

According to Figure 4.1, by action of undissociated nitric acid present in the organic phase Bz is oxidized to Ph, which then migrates into the acid phase where it is nitrated or poly-nitrated, forming mono-, di-nitrophenols and tri-nitrophenol [17]. Thus, it is important to work within proper concentrations of each acid to guarantee the total nitric acid dissociation [6, 18].

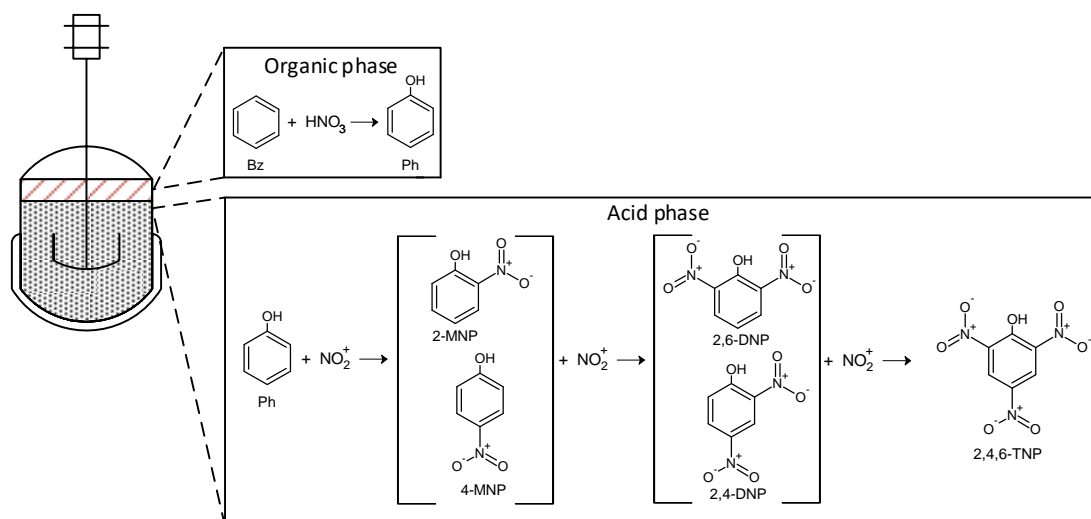


Figure 4.1 – Proposed nitrophenolic by-products formation mechanism. Adapted from [15, 17].

Another important parameter influencing the nitrophenols formation is the Bz to nitric acid ratio. Using an excess of organic substrate (Bz), the produced nitrophenols quantities are reduced due to a lower nitric acid content in the organic phase [9, 15, 19]. By this way, it is expected to reduce Ph formation and, consequently, the nitrophenolic by-products amounts.

Despite the importance of the developed studies, they are mostly focused in the nitrophenols minimization and not in their formation mechanism. Regarding this last subject, Hanson *et al.* [10] compiled some theories for the by-products formation in aromatic nitration which can be summarized as follows: i) the nitrosonium ion (NO⁺) reacts with the aromatic substrate being then, by rearrangement, formed Ph that can be nitrated; and ii) NO₂⁺ reacts with the aromatic compound through nitronium ion's oxygen atom, originating an aryl nitrite which decomposes into Ph, suitable to be nitrated. These theories were abandoned due to the lack of evidences supporting them. Currently, as explained before, it is accepted that nitrophenols formation starts *via* Bz oxidation to Ph, by action of nitric acid – see Figure 4.1.

Regardless of the work done concerning Bz nitration, there is some information lacking, namely, experimental proofs that Ph is present in Bz nitration medium (to our knowledge was never detected) and that it is formed by nitric acid action during nitration with the mixed acid. Some works have already been done regarding the quantification of phenolic compounds by HPLC [20-23]; however, in none of these works is addressed Ph presence and detection in the adiabatic nitration medium.

Therefore, enabling this compound detection in the nitration medium (both in industrial and laboratory samples) was one of the driving forces of this work, since is postulated that it is the nitrophenols precursor without, to date, clear experimental evidence. Moreover, accomplishing this goal will allow the construction of mechanistic models for formation of nitrophenols instead of the statistical ones, which have been already developed [7, 11, 15]. To study the referred subject,

several industrial samples were collected from Bondalti Chemicals industrial nitration plant and a set of laboratory batch tests were performed using a variety of nitrating conditions.

4.2. Experimental section

The chemical reagents used in this study were the following: benzene nitration grade (> 99.99 wt.%) from Vitol S.A., MNB (99.99 wt.%) from Bondalti Chemicals production process, phenol (99.5 wt.%) from Riedel-de-Haën, sulfuric acid (99 wt.%) from Quimitecnica, nitric acid (65 wt.%) from Baker, 2-mononitrophenol (98 wt.%) from Fluka, 4-mononitrophenol (98 wt.%) from Aldrich, 2,4-dinitrophenol (97 wt.%) from Aldrich, 2,6-dinitrophenol (98 wt.%) from TCI and 2,4,6-trinitrophenol (99 wt.%) from BDH. To guarantee the reaction cessation in the retrieved samples and to extract the nitrophenols into the aqueous phase, a sodium hydroxide (Merck) solution (1 M) was used.

The laboratorial nitrations were carried out discontinuously, in a 0.75 L jacketed glass / Teflon reactor equipped with a tantalum air-impeller stirrer and a Teflon coated thermocouple (see the laboratorial reactor section in the Appendix D). This reactor was constructed specifically to carry out nitration reactions and it allows to easily change operational parameters such as the mixed acid composition, the organic substrate composition and the reaction temperature, while being resistant to the aggressive conditions employed.

The reaction conditions (initial reaction temperature, organic substrate nature, acids strengths and stirring speed) were chosen according to each defined test goals. The conditions of the experiments performed in this study are given in Table 4.1.

Table 4.1 – Reaction conditions of the performed nitration tests.

Test	Organic substrate	H ₂ SO ₄ (wt.%)	HNO ₃ (wt.%)	T _{initial} (°C)	X _{HNO₃} (%)*
E1	Bz and Ph (1817 ppm)	52	5	10	n.d.
E2	Bz and Ph (1817 ppm)	39	2	5	n.d.
E3	Bz and Ph (1706 ppm)	39	2	15	n.d.
E4	Bz and Ph (1706 ppm)	39	2	15	n.d.
E5	Bz and Ph (1706 ppm)	39	2	15	n.d.
E6	Bz	60	5	90	99.5
E7	Bz (50%) and MNB (50%)	32	9	89	13.6
E8	Bz (50%) and MNB (50%)	33	9	89	n.d.

* Nitric acid conversion after one hour of reaction time.

The conducted tests, except runs E7 and E8, were performed with benzene / HNO₃ = 1.10 (mol/mol).

n.d. – not determined.

4.3. Analytical methods

To determine the mixed acid composition and to quantify Bz and MNB in the reaction medium, analytical methods previously developed have been used.

Mixed acid composition was verified checking nitric acid and sulfuric acid concentrations in the reaction's aqueous phase. Nitric acid content was determined by manual titration with an iron (II) sulphate solution and the total acidity (used to calculate sulfuric acid concentration) was measured by titrating the aqueous phase with a NaOH solution (1 M) using a 751 GDP Titrino from Metrohm. The analytical procedures are detailed by Santos [14], Nogueira [15].

Bz and MNB present in the retrieved samples were also analysed, although sporadically. These analyses were performed by gas chromatography, in a Perkin-Elmer Clarus 580 gas chromatograph, equipped with a flame ionization detector (FID). Both the injector and detector temperatures were set at 240 °C. It was used an Elite 1 (100% dimethylpolysiloxane 30 m x 0.32 mm x 1 µm) column from Perkin Elmer, and helium as the carrier gas.

An analytical method using high-performance liquid chromatography (HPLC) was already developed, validated and used to quantify nitrophenols produced in Bz nitration; further details can be found elsewhere [23].

4.3.1. Developed methods for phenol detection

During this study, the standard analytical procedures (samples collection and preparation and chromatographic analysis) used to quantify nitrophenols, Bz and MNB were adapted to achieve a specific goal, which was Ph detection in the reaction medium.

The liquid chromatographic analyses for phenol detection were performed in an Elite LaChrom HPLC-DAD apparatus from VWR-Hitachi equipped with a reverse phase column (Purospher® STAR RP-18e LiChroCART®) packed with silica microspheres (5 µm, 250 mm x 4 mm) and a guard column (LiChroCART® - 5 µm, 4mm x 4mm). The temperature of the chromatographic column was maintained at 30 °C by the HPLC's oven and the volume of the injected sample was 10 µL. The HPLC-DAD analytical method (eluent flow rate = 1 mL.min⁻¹, 30% acetonitrile, 70% KH₂PO₄ solution (25mM)) is described with more detail by Costa *et al.* [23].

Regardless the used chromatographic technique (HPLC or GC), the sampling procedure consisted in the sample's collection to a test tube which was then immediately closed and placed in an ice bath (from where it was withdrawn), allowing the phases separation. After the phases separation (< 5 min), the organic one was transferred into a 1.5 mL vial filled beforehand with a determined NaOH (1 M) mass, forming a new two-phase system. The aqueous phase, of basic nature, containing the phenolic by-products (extracted from the organic phase) was separated from the organic one, and its pH was adequately adjusted (with sulfuric acid) to an acidic range aiming to guarantee a well-defined and resolved Ph's chromatographic peak. This procedure of sample

preparation enables the use of the standard HPLC analytical method for Ph detection and quantification.

The reaction's acid phase was also neutralized with NaOH (1 M) to guarantee the reaction cessation. Then, its pH was adjusted with sulfuric acid to an acidic range to improve the Ph's chromatographic peak resolution. Thus, the reaction's acid phase could also be analysed to verify Ph presence.

For detecting Ph by GC-FID, after the pH adjustment procedure described above, the acidified samples were mixed with an organic solvent such as Bz. By this way, the phenolic by-products were extracted into the organic phase, allowing Ph analysis by gas chromatography.

4.4. Results and discussion

Despite the studies done concerning benzene nitration, there is information lacking regarding the formation of nitrophenolic by-products, namely, to experimentally detect Ph in the reaction medium and ascertain that it is formed through benzene oxidation. With that goal in mind, work was developed in order to achieve the right sampling conditions, the proper sample preparation procedure and to optimize the analytical methods.

4.4.1. Developed method for phenol detection in laboratory phenol-added benzene solutions nitration

The standard HPLC method and samples preparation procedure used to quantify the nitrophenolic by-products produced during Bz nitration was found to be unsuitable to be used for detecting Ph. This observation was withdrawn after analysing a sample from a Ph-added laboratory test (run E1 performed in mild conditions – Table 4.1) with the standard HPLC method. Due to the obtained results, the experimental and analytical procedures, which were based on the previously described ones, were tuned for Ph detection. Santos [14] reported a sampling and sample preparation procedure which consisted in the sample collection to a cooled glass flask filled with glass spheres and immersed in an ice bath, aiming at the decrease of the temperature of the samples. Then, a few hours after the sample collection they were prepared for the chromatographic analysis. Based in these procedures, the samples retrieved during the laboratory tests were collected to test tubes, previously immersed in an ice bath and placed back on the bath immediately after sampling. The main difference between both procedures was related with the faster samples analysis which was done shortly after the sampling instead of waiting several hours. For the industrial samples (taken from an industrial nitration reactor at Bondalti Chemicals) the sampling procedure was similar, differing only in the used sample's container which was a glass flask.

A faster samples analysis was achieved by modifying the samples preparation procedure. As Ph is a highly reactive molecule [24], to detect it, an immediate reaction stoppage was needed. Thus, in addition to the temperature decrease and the stirring cessation, a sample's neutralization step was added to the sampling procedure. As detailed in section 4.2.2., the neutralization was done, as soon as possible, by transferring a portion of either the organic or acid phase into a vial previously filled with NaOH. By this way, i.e., by combining all these factors, it was expected to ensure the stopping of the reaction. Using this sampling procedure it was possible to analyse both the organic and acid phases in search of Ph and nitrophenols.

To test these new procedures a Ph-added laboratory nitration was performed in smooth conditions (run E2 – Table 4.1). During this test, it was found that after the basic extraction of the retrieved organic samples, they must be acidified to obtain a well-defined and symmetric Ph's chromatographic peak (Figure 4.2). However, for low concentrated samples, its acidification must be carefully done since extremely acid mediums do not favour the formation of well-defined Ph chromatographic peaks, i.e., the sample's pH should be above or equal to 2. Nevertheless, despite the samples' pH influence on the definition of Ph's chromatographic peak, it is noticeable that its UV-Vis spectrum is independent from the medium pH.

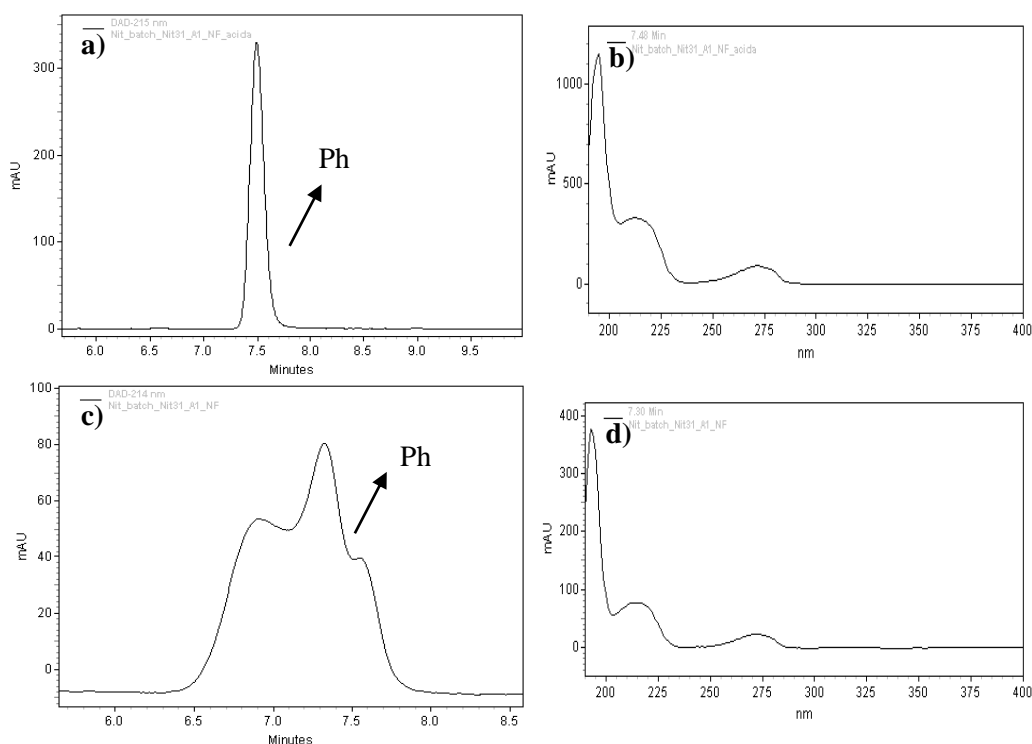


Figure 4.2 – Effect of the sample preparation procedure on the HPLC chromatogram (a) and c)) and on the corresponding Ph UV-Vis spectrum (b) and d)); a) and b) acidified sample (pH < 2); c) and d) alkaline sample (pH > 10). Samples' reaction time = 0.5 min. Reaction conditions: $T_{\text{initial}} = 5\text{ }^{\circ}\text{C}$, $\text{H}_2\text{SO}_4 = 39\text{ wt.}\%$; $\text{HNO}_3 = 2\text{ wt.}\%$.

Additionally, with the proper procedures (section 4.2.2.) this sampling methodology allowed Ph detection also by gas chromatography. This procedure was adopted after a set of nitration tests of Bz with Ph addition be conducted without Ph detection.

The simple discovery, yet important, of the influence of sample pH on Ph detection can explain the reason for the lack of information regarding Ph detection and quantification in Bz nitration medium. Additionally, its high reactivity together with the standard sampling procedure and the non-immediate sample preparation, hindered its detection in mixed acid systems.

To ascertain the developed techniques suitability to follow Ph consumption during a batch reaction, a Ph-added Bz solution was nitrated at low temperatures and smooth mixed acid strengths (15 °C, 2% wt. HNO₃ and 39 % wt. H₂SO₄ – Table 4.1, Runs E3 to E5). At these conditions, it should be possible to check if the developed procedure would enable Ph detection, not being ensured its detection in harsher reaction conditions. Moreover, by employing these smooth conditions it was intended to enable only Ph nitration maintaining Bz nitration in a small extent.

A set of preliminary tests was done to assess the experiment reproducibility and to validate the assembled laboratorial reactor and experimental procedure. The achieved results are depicted in the Supporting Information section (Appendix D, preliminary tests section - Figure D.2) and show concentration profiles with similar behaviour, being almost overlapped for the employed conditions.

By applying the developed techniques, Ph was clearly detected in both reaction phases 3 minutes and even 10 minutes after the reaction start – Figure 4.3. In addition to Ph, mononitrophenols (2-MNP and 4-MNP) were also detected in the reaction medium. DNP and TNP were not detected since the employed conditions did not lead to their formation.

Decomposition Reactions in Aromatic Nitration

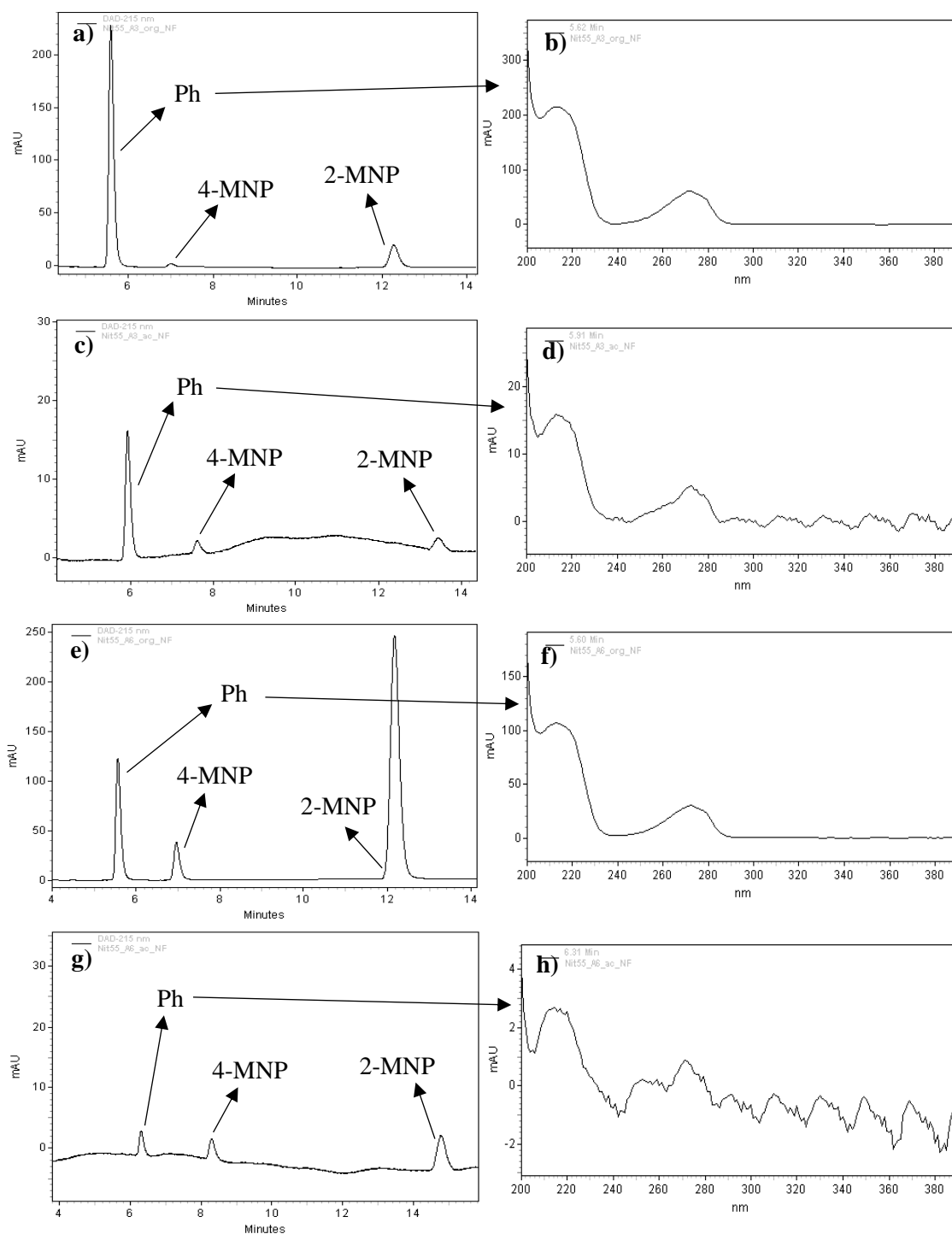


Figure 4.3 – Run E3 – HPLC chromatograms (a, c, e, g) and UV-vis spectra of phenol peak (b, d, f, h). **a)** and **b)** 3 min reaction time, organic phase. **c)** and **d)** 3 min reaction time, acid phase. **e)** and **f)** 10 min reaction time, organic phase. **g)** and **h)** 10 min reaction time, acid phase. Reaction conditions: $T_{\text{initial}} = 15\text{ }^{\circ}\text{C}$, $\text{H}_2\text{SO}_4 = 39\text{ wt.}\%$; $\text{HNO}_3 = 2\text{ wt.}\%$.

Ph was identified in the analysed samples by its relative retention time and by its UV-Vis spectrum. As shown in Figure 4.3, the UV-Vis spectra, except the one presented in Figure 4.3 – h), are similar to the one displayed in Figure 4.2. Comparing the UV-Vis spectra from the organic and

acid phases is perceptible a better spectra definition for the organic phase samples, which can be justified by the much higher Ph concentration in this phase (Fig. 4.4). Still, despite the poor resolution of the spectrum shown in Figure 4.3 h), it is visible a maximum of absorption near 215 nm, typical of Ph (Figure 4.2), which, together with the analyte retention time, allowed its identification as being Ph.

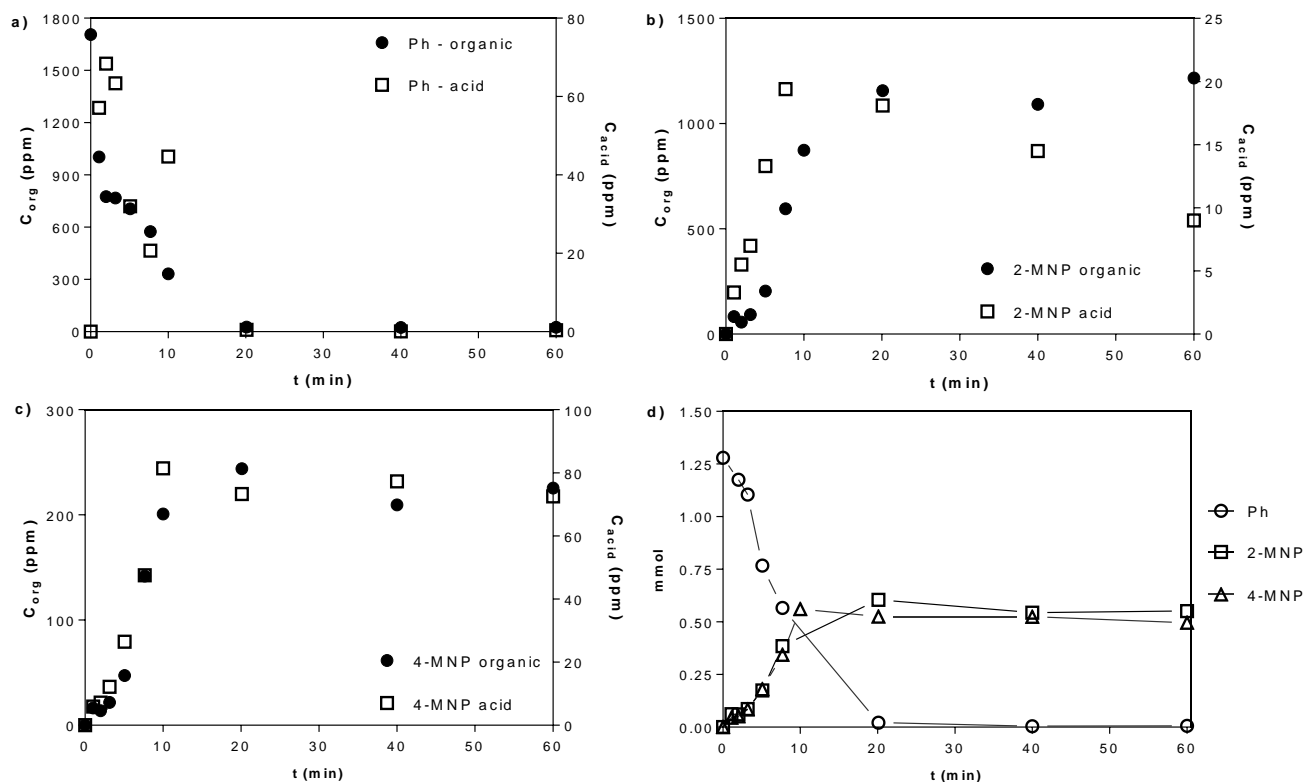


Figure 4.4 – Run E3. Phenol and nitrophenols concentration profiles. a) Ph, b) 2-MNP, and c) 4-MNP concentration profiles in the acid (right axis) and organic (left axis) phases; d) Ph, 2-MNP, and 4-MNP profiles (both phases analysed). Reaction conditions: $T_{initial} = 15\text{ }^{\circ}\text{C}$, $\text{H}_2\text{SO}_4 = 39\text{ wt.}\%$; $\text{HNO}_3 = 2\text{ wt.}\%$.

For reaction times higher than 20 minutes Ph amounts became negligible in both phases as shown in Figure 4.4, which is indicative of the Ph's high reactivity even at smooth reaction conditions.

The obtained results for run E3 – Figures 4.3 and 4.4 – evidenced Ph partition among both reaction phases and allowed to verify that 2-MNP and 4-MNP (formed during the reaction) were also distributed within both reaction phases, being noticeable a higher 4-MNP affinity into the aqueous phase ($\approx 29\%$ in the acid phase and $\approx 71\%$ in the organic one – Figure 4.4 – c)) when compared with 2-MNP ($\approx 5\%$ in the acid phase and $\approx 95\%$ in the organic one – Figure 4.4 – b)). The 2-MNP distribution is in accordance with the typical nitrophenols distribution and was found

to be similar to the Ph distribution ($\approx 5\%$ in the acid phase and $\approx 95\%$ in the organic one – Figure 4.4 – a)).

This higher 4-MNP solubility in the aqueous phase had already been noticed by Sidgwick *et al.* [25] while studying nitrophenols solubility in water. The authors concluded that this contrasting isomers behaviour was related with some difference in their structure. Indeed, the compounds' structure should play a role in their solubility since 4-MNP can form intermolecular hydrogen bonds (between 4-MNP molecules or 4-MNP and water molecules) whereas 2-MNP can form intramolecular hydrogen bonds as illustrated in Figure 4.5.

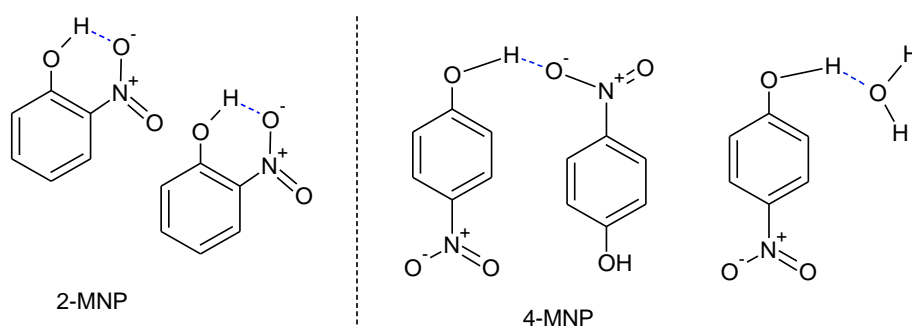


Figure 4.5 – 2-MNP intramolecular and 4-MNP intermolecular hydrogen bonds.

This structural difference can also explain the difference between the MNPs dissociation constant (pK_a), which is lower for 4-MNP (7.15 vs. 7.22) [26].

Additionally, Figure 4.4 – d) shows that 2-MNP and 4-MNP were formed simultaneously with Ph consumption. Under these conditions, in addition to the nitration of Bz, which occurs to a very small extent (ca. 0.5% only, cf. Figure D.3 of the Appendix D), it is unlikely that any other reaction occurs, and therefore it can be concluded that Ph is the nitrophenols precursor.

The evidences of Ph and MNPs distribution in both phases is in agreement with the mechanism proposed by Burns and Ramshaw [17] that considers Ph migration from the organic phase to the acid one, its nitration occurring in the latter. Considering the data of 2-MNP, which is mainly in the organic phase (Figure 4.4 – b)), one can expect that immediately after its formation in the acid phase, this compound turns back to the organic phase.

The achieved results show a satisfactory performance of the developed techniques, enabling their employment for monitoring Ph and nitrophenolic by-products in Bz nitration by mixed acid.

4.4.2. Phenol detection in the industrial plant

Industrial samples were collected from the Bondalti Chemicals' nitration reactor. The sampling procedure and sample preparation were done accordingly with the developed method described above (section 4.3.1.): sampling to a glass flask placed in an ice bath to, as soon as possible (<1

minute for phase separation), transfer a portion of each phase to vials previously filled with a NaOH solution. By this way, i.e., neutralizing both phases shortly after sampling, the chances of detecting Ph were increased since mixed acid was eliminated from the sample's medium, thus preventing Ph consumption. Then, after the pH correction, the prepared samples were analysed by HPLC-DAD. The achieved results are depicted in Figure 4.6.

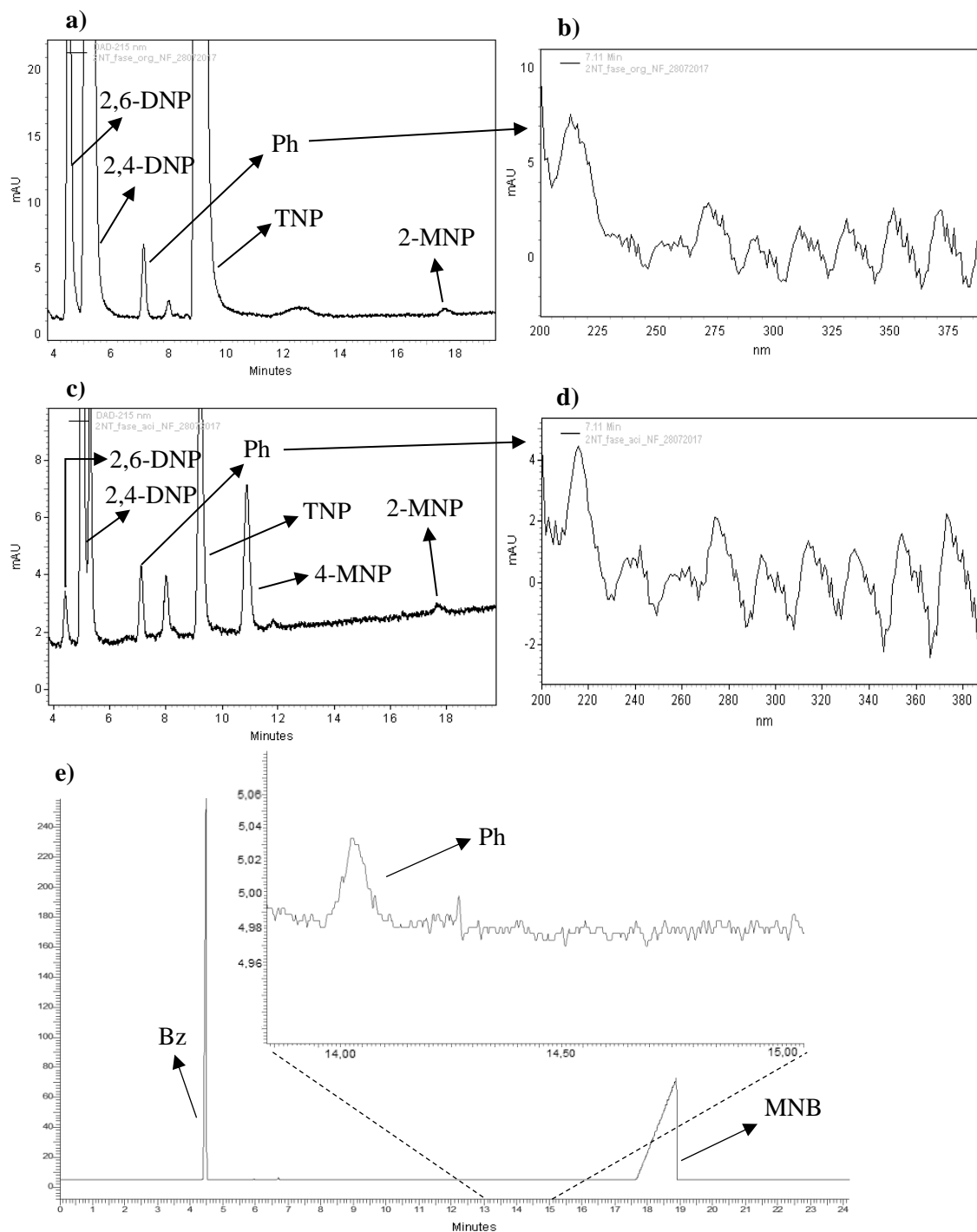


Figure 4.6 – Bz nitration in industrial reactor. **a)** Organic phase HPLC chromatogram. **b)** Corresponding Ph's UV-Vis spectrum. **c)** Acid phase HPLC chromatogram. **d)** Corresponding Ph's UV-Vis spectrum. **e)** GC-FID chromatogram of the organic phase.

Figure 4.6 – a) shows the organic phase chromatogram, at 215 nm, of an industrial sample retrieved from the Bondalti Chemicals reactor. The typically observed nitrophenols, 2,4-DNP and TNP, can be identified in the chromatogram. Furthermore, the analytical method and sample preparation procedures allowed also detecting 2,6-DNP as well as 2-MNP. However, since the selected chromatogram wavelength was 215 nm to maximize Ph's peak (far from nitrophenols absorption maximum), the peaks areas are not comparable with nitrophenols mass proportions. At about 7 minutes retention time, Ph typical retention time, is noticeable the presence of a chromatographic peak, that despite the noise (Figure 4.6 – b)) – due to the low analyte concentration – has a UV-Vis spectrum similar to that of Ph (maximum of absorbance at 215 and 275 nm, Figure 4.2). Both facts lead to the conclusion that it was possible, for the first time (to our knowledge), to identify Ph in industrial reaction medium. Such finding supports the postulated formation path of the dicarboxylic acids and carbon dioxide detected in the nitration plant disclosed in Chapter 3.

In Figure 4.6 – c) is illustrated the obtained chromatogram for the industrial reactor's acid phase. As observed for the organic phase, 2-MNP, 2,4-DNP, 2,6-DNP and TNP were also detected in the industrial acid phase, although in a lower concentration since these compounds have higher affinity to the organic phase. In addition, it is also visible the presence of Ph in the analyzed sample, being evidenced, as referred in section 4.3.1., the compound distribution between both reaction phases. This matches the proposed location of the nitration reaction, which is accepted to take place in the acid phase (near the interface) – see Figure 4.1. As described above, Ph was identified in the chromatogram by its retention time and by its UV-Vis spectrum, which despite the spectrum's noise shows a maximum of absorbance at 215 nm, typical of Ph.

Observing Figure 4.6 – c) is noticeable, contrary to Figure 4.6 – a), the presence of 4-MNP in the analyzed sample. This happened most probably due to two combined reasons: i) higher compound's affinity to the acid phase than the remaining nitrophenolic by-products (which could lead to its faster consumption, and consequently lower concentration in the organic phase); ii) the 4-MNP chromatographic peak is overlapped with that of TNP in the organic phase chromatogram since both compounds have close retention times.

Regarding the nitrophenols detection, the chromatograms depicted in Figure 4.6 display DNPs and TNP in higher concentrations than MNPs. This concentration difference between the phenolic by-products is a consequence of the nitro groups that each compound possesses. Since the nitro group is a ring deactivating one, its presence in the aromatic ring should decrease the molecule's reactivity, reason why DNPs and TNP (which have two and three nitro groups, respectively) are easily detected and Ph and MNPs are difficult to detect (since they are very reactive compounds).

The presence of Ph in the industrial nitration organic phase was also observed by GC-FID. The chromatographic peaks of Bz and MNB, the main constituents of the organic phase, can be clearly seen in Figure 4.6 – e). In addition, a very small chromatographic peak is also visible, which has been found to have the same retention time as Ph. The obtained results are in accordance with the

HPLC-DAD ones, thus allowing to confirm the presence of Ph in the reaction medium by two different analytical techniques.

4.4.3. Phenol detection in phenol-free laboratory nitrations

After Ph detection in industrial samples a set of experiments, aiming Ph detection, was planned at lab scale in conditions similar to the industrial ones and in non-usual nitrating conditions to enhance Ph formation.

A first batch nitration test, E6 run, was performed at reaction conditions (Table 4.1) in the range of the industrial ones. The performed test (run E6) allowed to detect clearly all the reaction by-products, from Ph to TNP, as it can be seen in Figure 4.7, which refers to a sample taken at $t = 5$ min (chromatograms of other samples, taken at higher reaction times, are presented in Figure D.4 of the Appendix D). The sampling and sample preparation procedures were done as described above, the identification of the chemical species being done by their relative retention times together with their UV-Vis spectra – Figure 4.7.

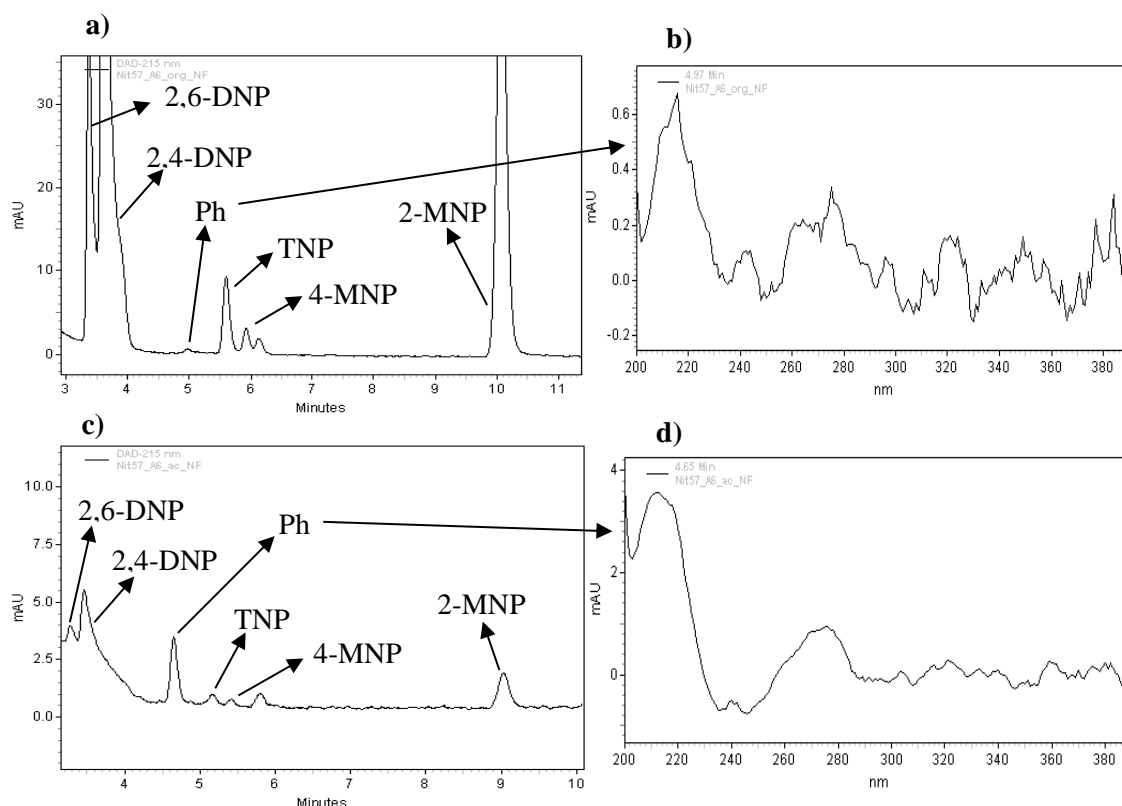


Figure 4.7 – Run E6. **a)** Organic phase HPLC chromatogram. **b)** Corresponding Ph's UV-Vis spectrum. **c)** Acid phase HPLC chromatogram. **d)** Corresponding Ph's UV-Vis spectrum. Sample collected 5 minutes after the reaction start. Reaction conditions: $T_{\text{initial}} = 90\text{ }^{\circ}\text{C}$, $\text{H}_2\text{SO}_4 = 60\text{ wt.}\%$; $\text{HNO}_3 = 5\text{ wt.}\%$.

As it can be seen (Figure 4.7 – a) and c)) Ph was detected in both reaction phases, which is in agreement with the results previously shown. In the organic phase, Ph's UV-Vis spectrum (Figure 4.7 – b)) was poorly defined; however, despite the spectrum noise (due to the analyte low concentration), is visible the Ph's typical maximum of absorbance (215 nm). Contrarily, in the acid phase Ph's UV-Vis spectrum (Figure 4.7 – d)) was well-defined and similar to the one shown in Figure 4.2.

The obtained chromatograms allowed to plot the concentration profiles along time of all the phenolic by-products – Figure 4.8.

The achieved concentration profiles for the organic phase, shown in Figure 4.8 – a), are in accordance with the expected results, i.e., it was expected to have 2,4-DNP (right axis) and TNP as the most abundant reaction by-products, particularly for longer reaction times. Additionally, as expected, nitrophenols total concentration obtained in this lab test was lower than the typical industrial values since the reaction conditions were not so harsh as the industrial ones.

It is also visible that during the reaction time, 2-MNP, 2,4-DNP and 2,6-DNP reached a maximum concentration value which then starts decreasing. The 2-MNP decrease was followed by the concentration increase of 2,4-DNP, 2,6-DNP and TNP, and the reduction of the DNPs concentration was accompanied by the TNP concentration raise. This is indicative of the sequential nitrophenols nitration, meaning that the MNPs are the DNPs precursors which in turn are the TNP precursors. Regarding Ph concentration in the organic phase, Figure 4.8 – a) shows that, despite being successfully detected (Figure 4.7 – a)), its amounts were low during all the reaction time.

Observing Figure 4.8 – b), where are depicted the concentration profiles of the reaction's by-products in the acid phase, it is noticeable Ph formation along the reaction time. After being formed in the organic phase, Ph is transferred into the acid phase where it should be nitrated to MNPs. However, despite the expected Ph depletion from the reaction medium, this was not observed most probably due to a variety of situations: i) low nitric acid content (< 900 ppm 30 minutes after the reaction beginning and < 260 ppm at the reaction end), reason that could explain the low extent of Ph nitration; ii) Bz oxidation to Ph by nitrogen oxides (NO_x) known to be formed by nitric acid decomposition (which yields potential oxidants [27-28]) during Bz nitration; iii) Bz oxidation to Ph by NO_x formed by nitrous acid (HNO_2) decomposition, originated during Ph formation *via* Bz oxidation by nitric acid.

Typically, in Bz nitration studies only the di- and trinitrated phenolic by-products are accounted for because as Ph and MNPs have less nitro groups ($-\text{NO}_2$), which is a powerful deactivating group, they are more reactive than DNPs and TNP, reason why it is difficult to detect them in the reaction medium. However, the obtained results show clearly that the developed procedures enabled Ph detection in the reaction medium, as well as the remaining nitrophenolic by-products. Furthermore, the fact of being detected Ph in the acid phase (as in run E3) is in agreement with the proposed

mechanism by Burns and Ramshaw [17] regarding Ph migration from the organic phase to the acid one, and its nitration in the latter (cf. Figure 4.1).

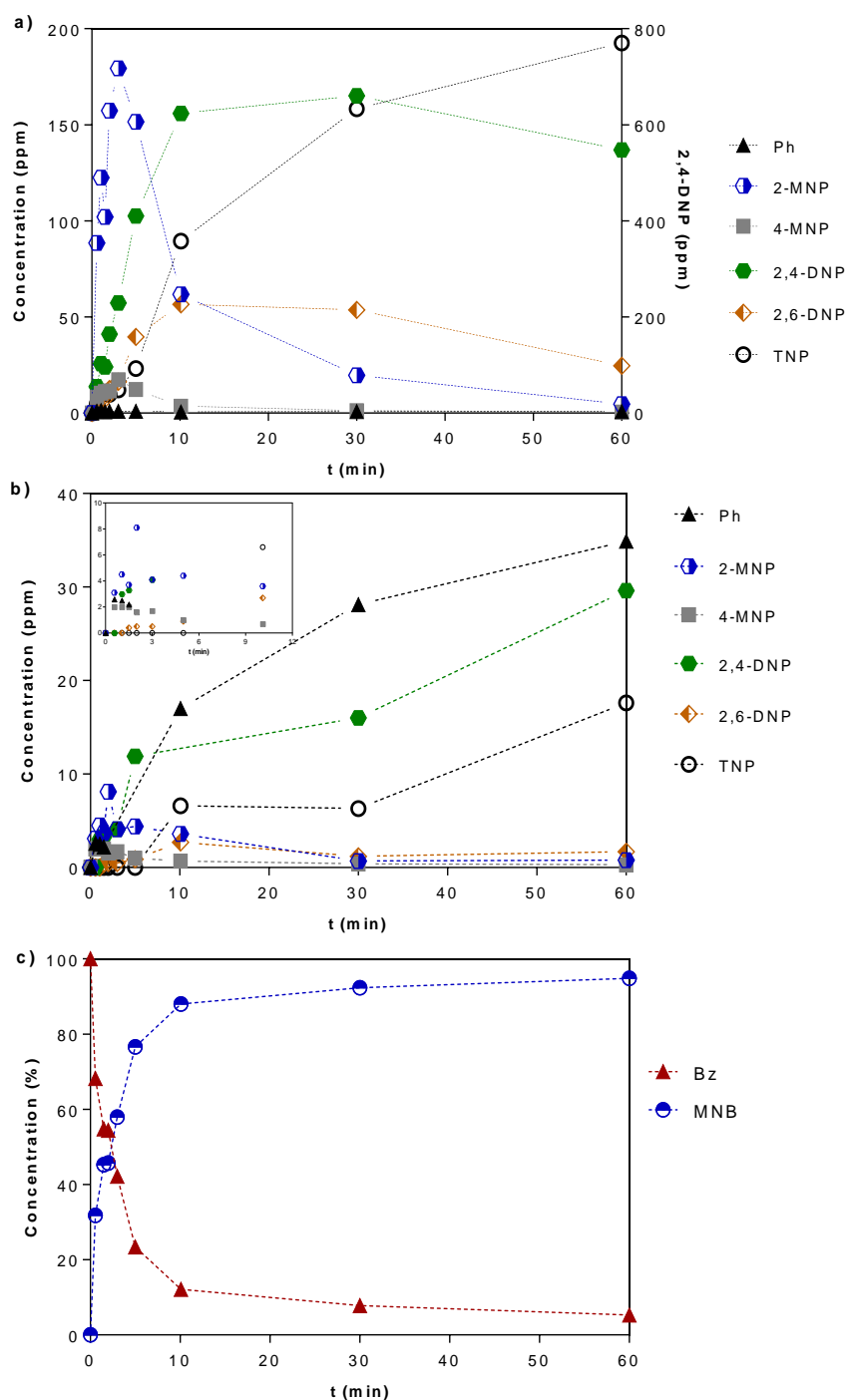


Figure 4.8 – E6 concentration profiles obtained from: **a)** the HPLC analysis of the organic phase samples; **b)** the HPLC analysis of the acid phase samples; **c)** the GC analysis of the organic phase samples. Reaction conditions: $T_{\text{initial}} = 90\text{ }^{\circ}\text{C}$, $\text{H}_2\text{SO}_4 = 60\text{ wt.}\%$; $\text{HNO}_3 = 5\text{ wt.}\%$.

Regarding Bz and MNB concentration profiles, it is visible (Figure 4.8 – c)) that in spite of the smoother reaction conditions (as compared to the industrial ones), five minutes after the reaction

start over half of Bz initial amount has already been nitrated to MNB, and ten minutes after the reaction start the MNB concentration was close to its maximum value. It is also noteworthy the high Bz nitration selectivity towards MNB. Nevertheless, nitrophenols are always formed during Bz nitration, which, even in low amounts, represent an industrial problem due to their toxicity.

After the successful Ph detection in harsh reaction conditions (industrial samples and run E6), additional tests were performed in non-usual nitrating conditions to enhance Ph formation. Accordingly to the chosen conditions, the acid phase was composed by nitric acid and sulfuric acid with strengths (run E7 – Table 4.1 - $\text{HNO}_3 = 9 \text{ wt.}\%$; $\text{H}_2\text{SO}_4 = 32 \text{ wt.}\%$) higher and lower, respectively, than those usually used in industrial plants; the goals behind were to slow down the reaction rate (by using a lower sulfuric acid concentration, which acts as the reaction catalyst) and to force the presence of undissociated nitric acid within the reaction medium (by combining high nitric acid concentration and low sulfuric acid concentration, once sulfuric acid is responsible for nitric acid dissociation). The selected organic substrate to be nitrated was a mixture of Bz ($\approx 50 \text{ wt.}\%$) and MNB ($\approx 50 \text{ wt.}\%$) because the presence of higher MNB amounts favours nitric acid dissolution in the organic phase [19]. The initial reaction temperature was in the range of the employed industrial values.

Under these reaction conditions and employing the developed procedures Ph was successfully detected once again – Figure 4.9. As before, Ph was identified throughout the obtained chromatograms by its relative retention time and UV-Vis spectrum. For this run, Ph's UV-Vis spectrum, illustrated in Figure 4.9 – b), was notoriously better defined than the previously shown spectra (Figures 4.6 and 4.7), a fact that can be explained by the compound's higher concentration. The chromatograms obtained from the retrieved samples enabled tracing Ph concentration profile during the reaction time – Figure 4.10.

The Ph's concentration profile in the organic phase (Figure 4.10) indicates that it is formed and consumed during the reaction time, being such results another experimental evidence that validates Burns and Ramshaw [17] theory. Ph detection implies that it is indeed formed through Bz oxidation, by action of nitric acid, since MNB is expected to be inert under this low sulfuric acid concentration [29]. Additionally, sulfuric acid action in nitrophenols formation is to be excluded as reported by Nogueira [15].

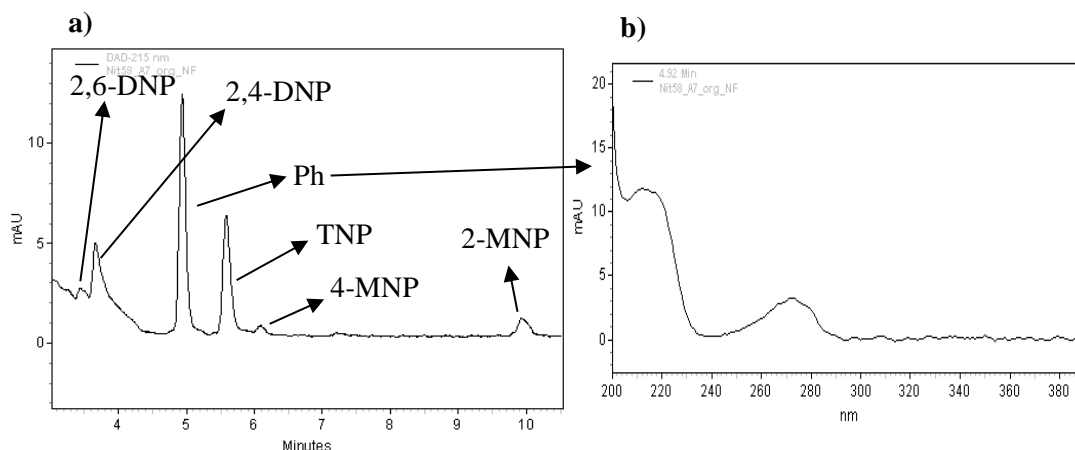


Figure 4.9 – Run E7. **a)** Organic phase HPLC chromatogram. **b)** Corresponding Ph's UV-Vis spectrum. Sample's reaction time = 10 min. Reaction conditions: $T_{\text{initial}} = 89\text{ }^{\circ}\text{C}$, $\text{H}_2\text{SO}_4 = 32\text{ wt.}\%$; $\text{HNO}_3 = 9\text{ wt.}\%$, $\text{Bz} \approx 50\text{ wt.}\%$; $\text{MNB} \approx 50\text{ wt.}\%$.

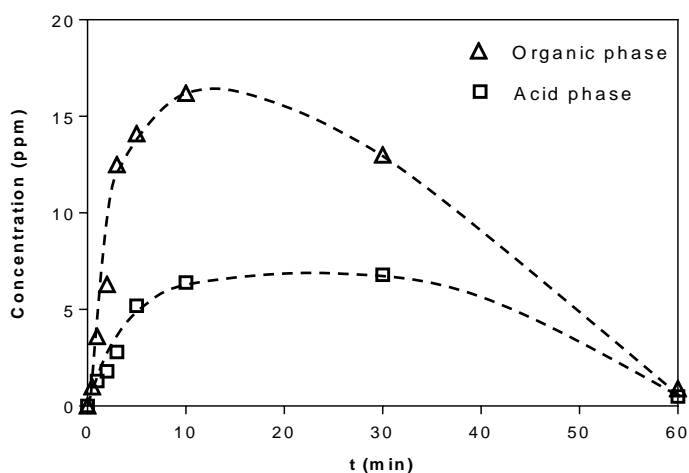


Figure 4.10 – Ph concentration profile for run E7. Organic phase analysis. Reaction conditions: $T_{\text{initial}} = 89\text{ }^{\circ}\text{C}$, $\text{H}_2\text{SO}_4 = 32\text{ wt.}\%$; $\text{HNO}_3 = 9\text{ wt.}\%$; $\text{Bz} \approx 50\text{ wt.}\%$; $\text{MNB} \approx 50\text{ wt.}\%$.

Ph presence in the aqueous phase of the reaction mixture was also assessed. It was found that Ph's concentration profile in the aqueous phase was similar to the organic phase one, being noticed, as previously in Figure 4.8, a higher affinity into the organic phase.

To confirm that Ph was indeed formed under these unusual nitrating conditions, the experimental test E7 was repeated (run E8 – Table 4.1 – Figure 4.11) being Ph detected once again. As usual, Ph was identified in the reaction medium through HPLC analysis by its retention time and by its UV-Visible spectrum – Figure 4.11 a) and b). The Ph presence in the reaction medium was also confirmed resorting to GC-FID analysis. The results are given in Figure 4.11 c) and the compound's identification was done by comparing Ph's retention time in a Ph added solution with the retention time of the chromatographic peak identified as Ph.

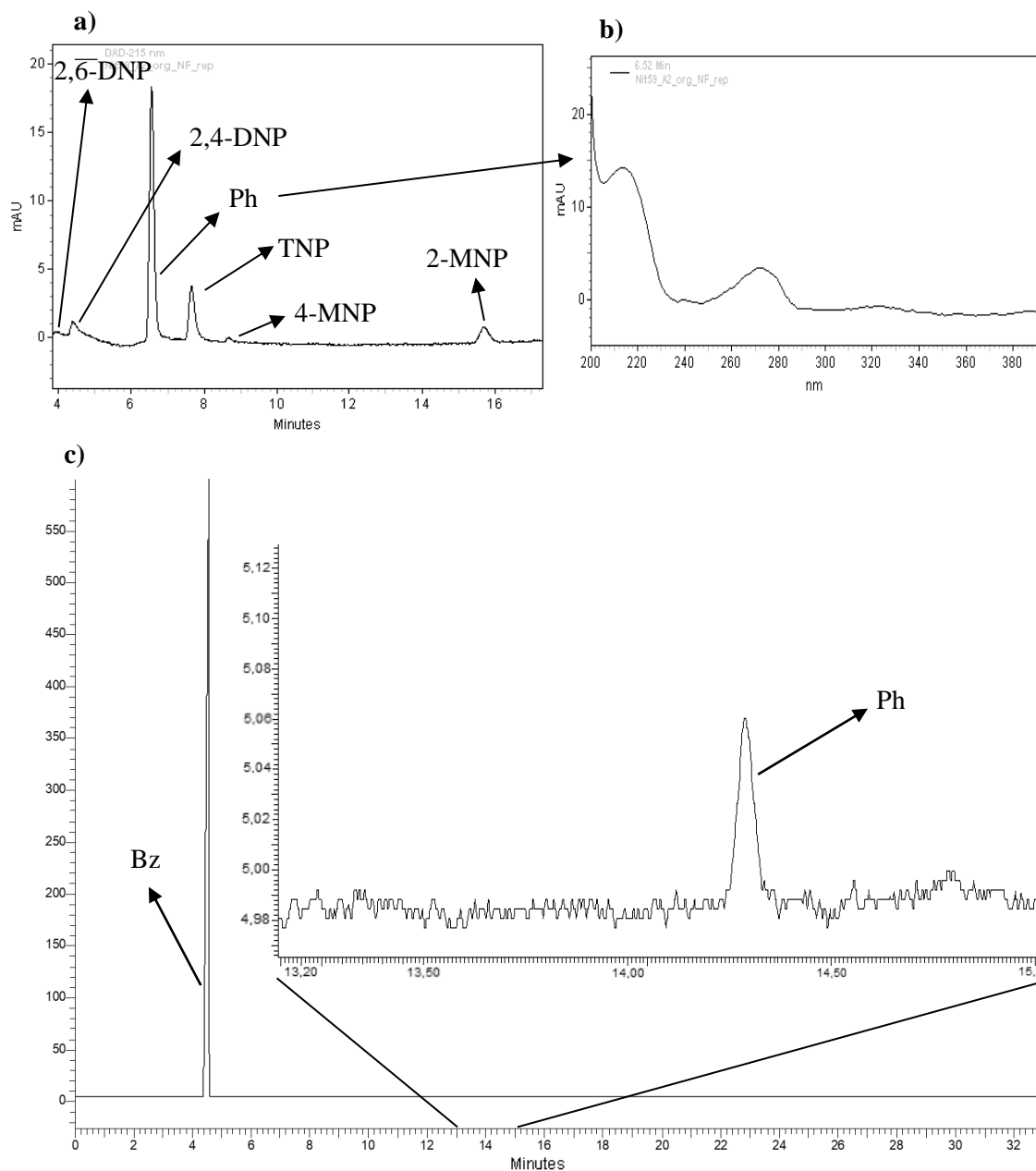


Figure 4.11 – Run E8. a) Organic phase HPLC chromatogram. b) Corresponding Ph's UV-Vis spectrum. c) GC-FID chromatogram from the retrieved sample. Sample's reaction time = 1 min. Reaction conditions: $T_{\text{initial}} = 89\text{ }^{\circ}\text{C}$, $\text{H}_2\text{SO}_4 = 33\text{ wt.}\%$; $\text{HNO}_3 = 9\text{ wt.}\%$, $\text{Bz} \approx 50\text{ wt.}\%$; $\text{MNB} \approx 50\text{ wt.}\%$.

4.5. Conclusions

Ph was detected for the first time in mixed acid benzene nitration media, both in the industrial process and in laboratory nitrations. Such achievement was accomplished by adapting and improving the conventional analytical methods used for nitrophenols quantification.

Ph formation in laboratory nitrations was evidenced experimentally by nitric acid action over Bz. Furthermore, it was shown that Ph is the nitrophenolic by-products precursor by nitrating Ph-added solutions at soft reaction conditions; it was also demonstrated the Ph's high reactivity.

This study allowed to verify that 4-MNP has a higher affinity into the aqueous phase than the other nitrophenols (2-MNP; 2,4-DNP; 2,6-DNP and TNP), which have higher affinity into the organic phase. This can be justified by 4-MNP structure that allows the formation of intermolecular hydrogen bonds with the aqueous phase.

It was also found that Ph is distributed among both reaction phases, being its distribution similar to that of most nitrophenols, with predominance in the organic one.

The evidence of the Ph presence in the benzene nitration medium, obtained in the present study, is a contribution that supports the proposed and accepted by-products nitration theory which states that Ph is the nitrophenols precursor and that the reactions occur in the acid phase or near the interphase.

Nomenclature

Abbreviations

Bz	Benzene
CSTR	Continuous stirred tank reactor
DNP	Dinitrophenol
GC-FID	Gas Chromatography – Flame Ionizer Detector
HPLC-DAD	High Performance Liquid Chromatography - Diode Detector
MNB	Mononitrobenzene
MNT	Mononitrotoluene
MNP	Mononitrophenol
Ph	Phenol
TNP	Trinitrophenol

4.6. References

- [1]. Albright, L. F.; Carr, R. V. C.; Schmitt, R. J., Nitration: An Overview of Recent Developments and Processes. In *Nitration*, American Chemical Society, Washington, DC. ACS Symposium Series, 1996; Vol. 623, pp 1-9, doi:10.1021/bk-1996-0623.ch001
10.1021/bk-1996-0623.ch001.
- [2]. Koskin, A. P.; Kenzhin, R. V.; Vedyagin, A. A.; Mishakov, I. V., Sulfated perfluoropolymer–CNF composite as a gas-phase benzene nitration catalyst. *Catalysis Communications* **2014**, 53, 83-86, <http://dx.doi.org/10.1016/j.catcom.2014.04.026>.
- [3]. Dugal, M., Nitrobenzene and Nitrotoluenes. In *Kirk-Othmer Encyclopedia of Chemical Technology*, John Wiley & Sons, Inc., 2000, 10.1002/0471238961.1409201801041109.a01.pub2.
- [4]. Maxwell, G. R., Aniline and Nitrobenzene. In *Synthetic Nitrogen Products: A Practical Guide to the Products and Processes*, Springer US, Boston, MA, 2004; pp pp. 361-371, 10.1007/0-306-48639-3_20.
- [5]. Alexanderson, V.; Trecek, J. B.; Vanderwaart, C. M., Continuous adiabatic process for the mononitration of benzene. US Patent 4,091,042, May 23, 1978.
- [6]. Guenkel, A. A.; Rae, J. M.; Hauptmann, E. G. Nitration process. US Patent 5,313,009, May 17, 1994.
- [7]. Berretta, S.; Louie, B., Effect of Reaction Conditions on the Formation of Byproducts in the Adiabatic Mononitration of Benzene into Mononitrobenzene (MNB). In *Chemistry, Process Design, and Safety for the Nitration Industry*, American Chemical Society, Washington, DC. ACS Symposium Series, 2013; Vol. 1155, pp 13-26, doi:10.1021/bk-2013-1155.ch002
10.1021/bk-2013-1155.ch002.
- [8]. Guenkel, A., The Adiabatic Mononitrobenzene Process from the Bench Scale in 1974 to a Total World Capacity Approaching 10 Million MTPY in 2012. In *Chemistry, Process Design, and Safety for the Nitration Industry*, American Chemical Society, Washington, DC. ACS Symposium Series, 2013; Vol. 1155, pp 1-11, doi:10.1021/bk-2013-1155.ch001
10.1021/bk-2013-1155.ch001.
- [9]. Quadros, P. A.; Castro, J. A. A. M.; Baptista, C. M. S. G., Nitrophenols Reduction in the Benzene Adiabatic Nitration Process. *Industrial & Engineering Chemistry Research* **2004**, 43 (15), 4438-4445, 10.1021/ie034263o.
- [10]. Hanson, C.; Kaghazchi, T.; Pratt, M. W. T., Side Reactions During Aromatic Nitration. In *Industrial and Laboratory Nitrations*, American Chemical Society, Washington, DC. ACS Symposium Series, 1976; Vol. 22, pp 132-155, doi:10.1021/bk-1976-0022.ch008
10.1021/bk-1976-0022.ch008.

- [11]. Nogueira, A. G.; Silva, D. C. M.; Reis, M. S.; Baptista, C. M. S. G., Prediction of the By-products Formation in the Adiabatic Industrial Benzene Nitration Process. *Chemical Engineering Transactions* **2013**, 32, 1249-1254,
- [12]. Urbański, T., *Chemistry and Technology of Explosives*. Pwn-Polish Scientific Publishers, Vol. 1, Warszawa, Poland, 1964.
- [13]. Burns, J. R.; Ramshaw, C., A Microreactor for the Nitration of Benzene and Toluene. *Chemical Engineering Communications* **2002**, 189 (12), 1611-1628, 10.1080/00986440214585.
- [14]. Santos, P. A. Q. d. O. Nitração de Compostos Aromáticos: Transferência de Massa e Reação Química. PhD Thesis, Universidade de Coimbra, Portugal, 2004.
- [15]. Nogueira, A. Optimização da Nitração de Aromáticos. PhD thesis, Universidade de Coimbra, Portugal, 2014.
- [16]. Albright, L. F.; Schiefferle, D. F.; Hanson, C., Reactions occurring in the organic phase during aromatic nitrations. *Journal of Applied Chemistry and Biotechnology* **1976**, 26, 522-525, 10.1002/jctb.5020260174.
- [17]. Burns, J. R.; Ramshaw, C., Development of a Microreactor for Chemical Production. *Chemical Engineering Research and Design* **1999**, 77 (3), 206-211, <http://dx.doi.org/10.1205/026387699526106>.
- [18]. Edwards, H. G. M.; Fawcett, V., Quantitative Raman spectroscopic studies of nitronium ion concentrations in mixtures of sulphuric and nitric acids. *Journal of Molecular Structure* **1994**, 326, 131-143, [http://dx.doi.org/10.1016/0022-2860\(94\)85013-5](http://dx.doi.org/10.1016/0022-2860(94)85013-5).
- [19]. Schiefferle, D. F.; Hanson, C.; Albright, L. F., Heterogeneous Nitration of Benzene. In *Industrial and Laboratory Nitrations*, American Chemical Society, Washington, DC. ACS Symposium Series, 1976; Vol. 22, pp 176-189, doi:10.1021/bk-1976-0022.ch011 10.1021/bk-1976-0022.ch011.
- [20]. Belloli, R.; Barletta, B.; Bolzacchini, E.; Meinardi, S.; Orlandi, M.; Rindone, B., Determination of toxic nitrophenols in the atmosphere by high-performance liquid chromatography. *Journal of Chromatography A* **1999**, 846 (1), 277-281, [https://doi.org/10.1016/S0021-9673\(99\)00030-8](https://doi.org/10.1016/S0021-9673(99)00030-8).
- [21]. Hofmann, D.; Hartmann, F.; Herrmann, H., Analysis of nitrophenols in cloud water with a miniaturized light-phase rotary perforator and HPLC-MS. *Analytical and Bioanalytical Chemistry* **2008**, 391 (1), 161-169, 10.1007/s00216-008-1939-6.
- [22]. Spínola, V.; Pinto, J.; Castilho, P. C., Identification and quantification of phenolic compounds of selected fruits from Madeira Island by HPLC-DAD–ESI-MSⁿ and screening for their antioxidant activity. *Food Chemistry* **2015**, 173 (Supplement C), 14-30, <https://doi.org/10.1016/j.foodchem.2014.09.163>.

- [23]. Costa, T. J. G.; Nogueira, A. G.; Silva, D. C. M.; Ribeiro, A. F. G.; Baptista, C. M. S. G., Nitrophenolic By-Products Quantification in the Continuous Benzene Nitration Process. In *Chemistry, Process Design, and Safety for the Nitration Industry*, American Chemical Society, Washington, DC. ACS Symposium Series, 2013; Vol. 1155, pp 49-60, doi:10.1021/bk-2013-1155.ch004
10.1021/bk-2013-1155.ch004.
- [24]. Carey, F., *Organic Chemistry*. 4th edition, McGraw-Hill, New York, 2000.
- [25]. Sidgwick, N. V.; Spurrell, W. J.; Davies, T. E., CXXXII.-The solubility of the nitrophenols and other isomeric disubstitution products of benzene. *Journal of the Chemical Society, Transactions* **1915**, 107 (0), 1202-1213, 10.1039/CT9150701202.
- [26]. Dean, J. A.; Lange, N. A., *Lange's Handbook of Chemistry*. McGraw-Hill, 1999.
- [27]. Ross, D. S.; Kirshen, N. A., Nitration and Oxidative Side Reactions of Dinitrotoluenes. In *Industrial and Laboratory Nitrations*, American Chemical Society, Washington, DC. ACS Symposium Series, 1976; Vol. 22, pp 114-131, doi:10.1021/bk-1976-0022.ch007
10.1021/bk-1976-0022.ch007.
- [28]. Di Somma, I.; Marotta, R.; Andreozzi, R.; Caprio, V., Nitric acid decomposition kinetics in mixed acid and their use in the modeling of aromatic nitration. *Chemical Engineering Journal* **2013**, 228, 366-373, <https://doi.org/10.1016/j.cej.2013.04.100>.
- [29]. Modak, S. Y.; Juvekar, V. A., Role of Interfacial Reaction in Heterogeneous Aromatic Nitration. *Industrial & Engineering Chemistry Research* **1995**, 34 (12), 4297-4309, 10.1021/ie00039a021.

Chapter 5 – (Nitro)Phenols reactivity in mixed acid benzene nitration systems²

Abstract

Phenol was nitrated in mixed acid systems (a mixture of nitric and sulphuric acid) incorporated in a benzene matrix, employing smooth conditions for enabling its detection in the reaction medium. The performed tests allowed the construction of a kinetic model for this species nitration evidencing its high reactivity while supporting a reaction mechanism assuming phenol as the nitrophenols precursor.

Phenol-free benzene nitrations were also carried out, in reaction conditions similar to those employed in the industrial production of mononitrobenzene, aiming the detection of all reaction by-products formed by benzene nitration (2-mononitrophenol; 4-mononitrophenol; 2,4-dinitrophenol; 2,6-dinitrophenol; and 2,4,6-trinitrophenol). This methodology is an unusual aspect in benzene nitration studies which are typically only focused in 2,4-dinitrophenol and trinitrophenol, the nitrophenolic species formed in higher amounts. The effect of some operating conditions, namely the reaction temperature, sulfuric acid and nitric acid concentration was evaluated, which allowed verifying that upon phenol formation, nitrophenols are formed by consecutive reactions, i.e., mononitrophenols are nitrated into dinitrophenols that are the trinitrophenol precursors. A kinetic model assuming nitrophenols formation by consecutive reactions was constructed (for the first time to our knowledge), showing a good agreement with the experimental results.

Keywords: Phenol, Nitrophenols, Mixed acid, Benzene nitration, Mononitrobenzene

² Diogo Afonso, Alejandro F. G. Ribeiro, Paulo Araújo, Joaquim Vital and Luis Miguel Madeira, (Nitro)Phenols reactivity in mixed acid benzene nitration, *submitted*.

5.1. Introduction

Nitration can be defined as the irreversible reaction between an organic compound and a nitrating agent [1-2]. This reaction, one of the earliest to be operated in the chemical industry [3], can be used to produce mononitrobenzene (MNB), a precursor of several compounds such as aniline, paracetamol or pesticides.

MNB production results from a highly exothermic reaction between benzene (Bz) and nitric acid [1]. In industrial nitrations, sulfuric acid is used as a catalyst due to its relatively low price and catalytic efficiency [1, 4], originating the so-called mixed acid, a mixture of sulfuric and nitric acid. The sulfuric acid role is to donate a proton to nitric acid [5], which will be protonated and dissociated forming, by this way, the nitrating agent: the nitronium ion (NO_2^+) [2, 6] – equation 6.1. The reaction mechanism for the MNB ($\text{C}_6\text{H}_5\text{NO}_2$) formation from benzene (C_6H_6) can be represented by equations 6.2 and 6.3 [7-9].



The benzene nitration with mixed acid is a heterogeneous liquid-liquid reaction, being accepted that MNB formation occurs in the acid phase. Accordingly to Giles *et al.* [10], the Bz nitration mechanism can be disclosed by the following steps: i) Bz diffusion from the organic phase to the interface and then to the aqueous phase; ii) on the interface or in the aqueous phase, Bz reacts with the nitronium ion to form MNB; iii) MNB diffuses from the aqueous phase to the interface, and then to the organic phase.

Industrially, Bz nitration was improved over time [11-12], allowing a gain in the reaction rate and a reduction in the production costs. Despite the achieved process improvements and the high reaction selectivity towards MNB formation, Bz nitration is always accompanied by side reactions. In the MNB production process, the main reaction by-products are dinitrobenzene - DNB - and nitrophenols - NPs - particularly 2,4-dinitrophenol (2,4-DNP) and trinitrophenol (TNP) [13-14].

The formation of reaction by-products, namely the NPs, demands the installation of removal/treatment sections within the industrial plants. Additionally, NPs are thought to form tar-like deposits on hydrogenation catalysts used in aniline production from MNB. Therefore, it is essential the minimization of the reaction by-products.

Efforts have already been made to reduce the NPs formation [13-15]. Nonetheless, and despite the achieved results, which allowed to relate the reaction parameters with NPs formation, their formation mechanism is still uncertain, not being reported any kinetic studies for these species formation. It is postulated that NPs formation starts *via* Bz oxidation to phenol (Ph) in the organic

phase by the action of nitric acid or nitric acid derivatives such as nitrous acid or NO_2 [16-18]. Then, it diffuses to the aqueous phase, and by sequential nitrations, Ph can originate mono-, di- or tri-nitrophenols – Figure 5.1. Only very recently, in a work of the authors, [19] Ph was detected for the first time both in industrial and laboratory Bz nitration media. Additionally, Ph-added Bz nitrations in mixed acid systems, performed in smooth reaction conditions, allowed to verify that as Ph was being consumed, 2-mononitrophenol (2-MNP) and 4-mononitrophenol (4-MNP) were being formed [19]. These results are the first experimental evidence supporting the postulated Ph formation in the reaction medium and the role of Ph as the NPs precursor.

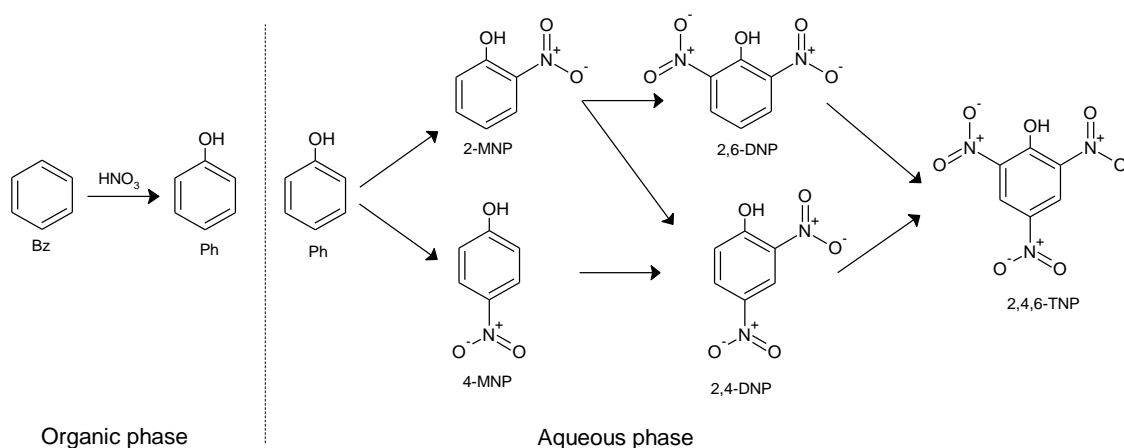


Figure 5.1 – Nitrophenols interconversion scheme. Adapted from refs [15, 19].

There are a few studies dealing with Ph nitration [20-23], however, in none of these studies is referred Ph nitration in mixed acid systems or during Bz nitration. This evidences that Ph detection and nitration during mixed acid Bz nitration is an almost unexplored subject.

Regarding the effect of the operating conditions on NPs formation, it is known that a higher reaction temperature enhances NPs formation [13-14]. The mixed acid composition is also an important parameter; because nitric acid or nitric acid derivatives may oxidize Bz [16-18, 24], because sulfuric acid concentration is known to affect nitric acid dissociation [25], which in turn yields the accepted nitrating agent (NO_2^+), the mixed acid composition needs to be chosen to ensure the maximum dissociation of HNO_3 . The ratio between Bz and nitric acid was also found to be an important operational parameter affecting NPs formation because higher Bz amounts lead to a lower nitric acid content in the organic phase [13, 15, 26].

Despite the studies done concerning Bz nitration, there is a lack of information in the literature regarding the formation of the nitrophenolic by-products, namely evidencing the NPs interconversion, i.e., MNPs being converted into DNPs and DNPs originating TNP – Figure 5.1 – data typically not presented in Bz nitration studies. For instance, Berretta and Louie [14], when studying the effect of the reaction conditions in the Bz nitration by-products formation, revealed

only the total amounts of NPs formed. On the other hand, Quadros *et al.* [13] considered only the 2,4-DNP and TNP formed amounts. Burns and Ramshaw [27] refer MNPs, DNPs and TNP concentration for tests conducted in a microreactor (not employed at industrial level), but the individual isomer concentrations are not presented. In none of these works are depicted nitrophenols interconversion profiles, only the NPs quantities at the end of the reaction.

At the industrial level, it is important to know the NPs concentration profiles in order to choose the suitable alkaline agent to be used for extracting these organic acids from the produced MNB, thus ensuring that MNB is complying with the final product specifications. The effluent treatment technology is also dependent on the chosen extraction agent [28]. For instance, if MNPs are mainly formed during Bz nitration, sodium hydroxide is employed for extracting the nitrophenolic by-products, but in this case, incineration/thermal oxidation processes are not suitable for treating the effluent stream [28]. On the other hand, if DNPs and TNP are the main reaction by-products, ammonia might be used, as well as incineration/thermal oxidation technologies, for the effluent treatment. Consequently, an objective of the present study was to display all the NPs concentration profiles, to show how the reaction conditions can affect the NPs formation and their subsequent removal from the produced MNB.

Once Ph is formed during mixed acid Bz nitration, the present work aimed also the construction of a simple kinetic model to evidence Ph's high reactivity towards nitration (based on the determined kinetic constants), even in smooth reaction conditions, while supporting its role as the NPs precursor. Additionally, a more complex mechanistic model, although somewhat simplified, was intended to be constructed to demonstrate NPs interconversion while revealing their loss of reactivity as they are nitrated. A mechanistic model for predicting the adiabatic nitration of Bz with mixed acid has already been developed [29], and kinetic studies addressing the nitration of other aromatic compounds have also been performed [17, 30-33]. However, to the best of our knowledge, any mechanistic model has been developed for representing the NPs concentration profiles during mixed acid Bz nitration. The already performed studies are based on statistical models [14, 34].

To achieve the enumerated objectives, a set of laboratory batch tests was performed using a variety of nitrating conditions.

5.2. Material and methods

The chemical reagents used in this study were: benzene nitration grade (> 99.99 wt.%) from Vitol S.A., phenol (99.5 wt.%) from Riedel-de-Haën, sulfuric acid (99 wt.%) from Quimitécnica, nitric acid (65 wt.%) from Baker, 2-mononitrophenol (98 wt.%) from Fluka, 4-mononitrophenol (98 wt.%) from Aldrich, 2,4-dinitrophenol (97 wt.%) from Aldrich, 2,6-dinitrophenol (98 wt.%) from TCI, 2,4,6-trinitrophenol (99 wt.%) from BDH and sodium hydroxide (1 M) from Merck.

The reaction conditions employed in the conducted tests (initial reaction temperature, organic substrate nature, acids strengths and stirring speed) were chosen aiming to enable the observation of Ph consumption (Ph-added benzene nitrations) and the visualization of the NPs concentration profiles. The conditions of the experiments performed in this study are given in Table 5.1.

Table 5.1 – Reaction conditions of the performed nitration tests.

Test	Organic substrate	H ₂ SO ₄ (wt.%)	HNO ₃ (wt.%)	T _{initial} (°C)	Aqueous phase / Benzene (wt./wt.)	Stirring speed (r.p.m.)
E1	Bz and Ph (1817 ppm)			7		1200
E2	Bz and Ph (1817 ppm)	40	2	15	13	1200
E3	Bz and Ph (1817 ppm)			25		1200
E4	Bz and Ph (2841 ppm)	40	2	15	13	1200
E5	Bz and Ph (2841 ppm)			15		1400
E6	Bz					1300
E7	Bz	66	5	70	15	1300
E8	Bz					1300
E9	Bz	61	5	70	15	1300
E10	Bz		5	90		1300
E11	Bz	51	5	90	15	1300
E12	Bz		9	90		1300

The parameters changed between the conducted tests are highlighted in bold.

The laboratory nitrations were carried out discontinuously, in a jacketed reactor equipped with a tantalum air-impelled stirrer and a Teflon coated thermocouple (Figure 5.2 – sketch of the jacketed laboratory batch reactor used). The experimental procedure used for the performed tests is summarized as follows: before the start of each reaction, sulfuric acid was added to the reactor by its top (valve V-5) and the thermostatic bath (MPC-K6) from Huber (E-2) was turned on, being the intended initial temperature set up. Water was the thermal fluid used in the reactor's jacket. Then, demineralized water was carefully added to sulfuric acid and when the temperature of the reaction medium was the intended one, nitric acid was added, again by the reactor's top (valve V-5). During the aqueous phase heating or cooling, the stirrer was working to promote the acids mixture and the homogenization of the composition and temperature of the reaction medium. When the intended reaction temperature was reached, the stirring speed was adjusted to the defined value and the organic substrate was added, through the reactor's bottom (valve V-3). The injection time was about 5 seconds and after half of the organic substrate has been injected, the reaction time started to be counted ($t = 0$ in the reaction runs).

Along the reaction time samples were collected from the reactor's bottom by means of valve V-4. Valve V-6 was kept closed to avoid both the pressure loss of the system and the contact with the atmosphere during the tests. The temperature of the system was recorded using a Therna 1 thermometer from ETI Ltd.

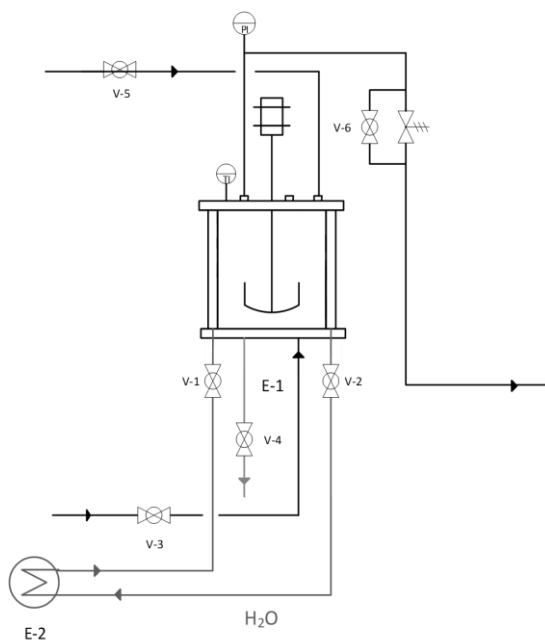


Figure 5.2 – Scheme of the laboratory reactor used in the batch reactions.

5.2.1. Organic phase analysis

The employed sampling procedure and sample preparation is described in detail in a previous work [19]. For quantifying phenolic by-products in the organic phase, after each sample collection, a portion of the organic phase was collected into a 1.5 mL vial previously filled with NaOH (1 M) to enable stopping the reaction immediately. Then, the resulting aqueous phase, to where the phenolic by-products were extracted, was separated from the organic one, and its pH corrected with sulfuric acid to improve the chromatographic peaks' resolution, allowing thus its analysis by High-Performance Liquid Chromatography-Diode Array Detector (HPLC-DAD), as described by Afonso *et al.* [19]. The liquid chromatographic analyses were performed in an Elite LaChrom HPLC-DAD apparatus from VWR-Hitachi equipped with a reverse phase column (Purospher® STAR RP-18e LiChroCART®) packed with silica microspheres (5 µm, 250 mm x 4 mm) and a guard column (LiChroCART® - 5 µm, 4mm x 4mm). The chromatographic column temperature was maintained at 30 °C by the HPLC's oven and the injected sample volume was 10 µL.

Bz and MNB were analyzed by gas chromatography (GC), in a Perkin-Elmer Clarus 580 gas chromatograph, equipped with a flame ionization detector (FID). Both the injector and detector

temperatures were set at 240 °C. It was used an Elite 1 (100% dimethylpolysiloxane 30 m x 0.32 mm x 1 µm) column from Perkin Elmer, and helium as the carrier gas.

5.2.2. Acid phase characterization

Nitric acid content was measured by manual titration with an iron (II) sulfate solution while the sulfuric acid concentration was determined by titrating the aqueous phase with a NaOH solution (1 M) using a 751 GDP Titrino apparatus from Metrohm [15, 35].

For quantifying phenolic by-products in the reaction's acid phase, the collected samples (a portion of the aqueous phase) were neutralized with NaOH (1 M) shortly after collection. Then, after the proper sample dilution, the pH of the neutralized sample was corrected with sulfuric acid for subsequent analysis by HPLC-DAD, as described in section 5.2.1.

5.3. Results and discussion

In the next sections, the obtained results from Ph-added Bz and Ph-free Bz nitrations will be presented. For Ph-added Bz nitrations the reaction conditions (soft when compared to the industrial ones) were chosen aiming to monitor Ph consumption (which is a highly reactive molecule) and MNPs formation during the reaction time. Regarding Ph-free Bz nitration, the selected reaction conditions were closer to the industrial ones to enable recording all the NPs interconversion profiles.

5.3.1. Phenol-added benzene nitrations in soft conditions

Ph-added Bz solutions were nitrated at very soft conditions (Table 5.1, runs E1 to E5) because in reaction conditions similar to the industrial ones, Ph detection is very challenging [19]. The results for runs E1 to E3 are shown in Figure 5.3 in which Ph consumption during the reaction time is displayed at different reaction temperatures. Due to the employed soft conditions and to the reactor's jacket, the reaction temperature was constant during the reaction time.

Figure 5.3 allows observing a drastic reduction in Ph concentration at the reaction start, which is then attenuated along the reaction time. A further analysis of the figure enables to visualize that at 7 °C, 20 minutes after the reaction start, Ph concentration in the organic phase was still about 150 ppm while at 25 °C less than 10 minutes were needed to Ph amounts became vestigial, being recognizable a positive influence of the reaction temperature on Ph consumption. This shows that even in soft mixed acid systems and at quite low temperatures, Ph is very reactive, reason why it is very difficult to be detected in the usual nitrating reaction mediums in which, typically, the initial reaction temperature is higher than 50 °C [2, 36]. Additionally, it was observed that, after 60 minutes, under these conditions, Bz nitration to MNB was minimal ($X_{\text{Benzene}} < 1\%$), and that nitric

acid conversion was below 2%, being again evidenced Ph's high reactivity. In these conditions, Ph sulfonation was not observed, as expected, because both the sulfuric acid concentration and the operation temperature were lower than required for the mentioned reaction [37-38].

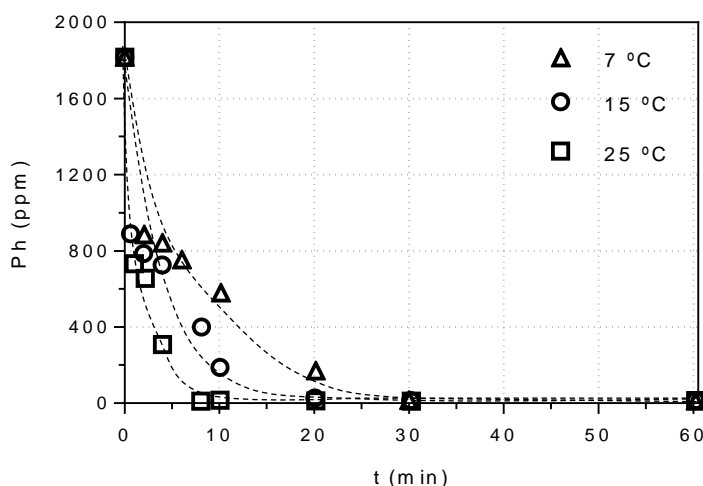


Figure 5.3 – Phenol concentration profiles at different reaction temperatures. Analysis of the organic phase. Mixed acid composition: % wt. $\text{H}_2\text{SO}_4 = 40$; % wt. $\text{HNO}_3 = 2$. $X_{\text{HNO}_3} < 2\%$, $X_{\text{Bz}} < 1\%$, at the reaction end. Lines are added just for better visualization of the trends.

The decrease of Ph concentration in the organic phase is explained by its nitration into MNPs and by Ph's transfer from the organic phase into the aqueous one, which is known to occur given the results previously presented by the authors [19]. To corroborate the presented justification, another Ph-added Bz nitration test was conducted, in which both reaction phases were analysed, whose results are illustrated in Figure 5.4. In this figure is displayed the Ph, 2-MNP and 4-MNP partition among both reaction phases; it is well evidenced MNPs formation simultaneous to Ph consumption. Under the employed conditions (run E4 – Table 5.1) only MNPs were formed, i.e., the typical nitrophenolic by-products from industrial mixed acid adiabatic Bz nitration, DNP and TNP, were not detected.

Scrutinizing 2-MNP concentration profiles is noticeable, particularly in the acid phase, a scattering of the experimental points. This is due to the vestigial concentrations of this species in the acid phase, which increases drastically the analytical uncertainty.

These results corroborate our previous work [19] supporting Burns and Ramshaw [16] theory regarding the NPs formation mechanism (Figure 5.1). Consequently, the observed initial Ph concentration decrease in the organic phase is indeed due to both its consumption and migration into the acid phase (where it is also consumed over time). Regarding MNPs distribution, it was verified a higher affinity of 4-MNP for the aqueous acid phase when compared with the one of 2-

MNP, which is in agreement with our previous findings [19]. As for 2-MNP, its affinity towards the aqueous phase is alike the one of 2,4-DNP and TNP [39].

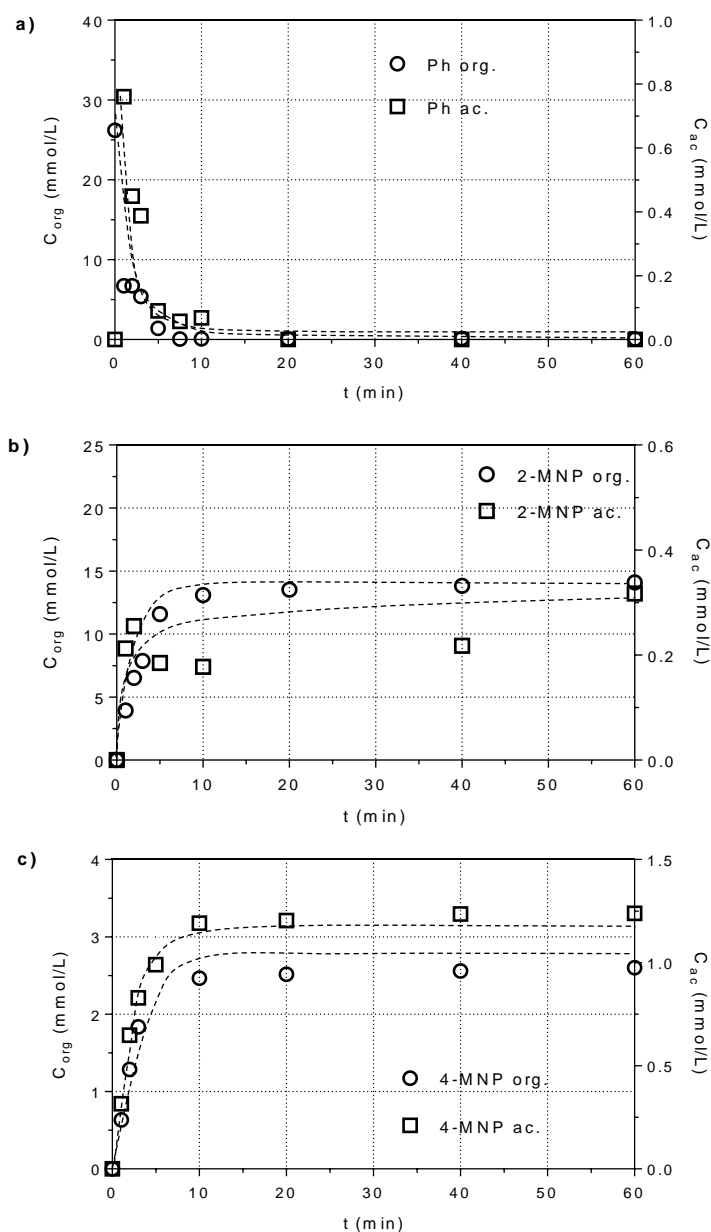


Figure 5.4 – a) Phenol, b) 2-MNP, and c) 4-MNP profiles in the acid and organic phase from run E4. Reaction conditions: $T = 15\text{ }^{\circ}\text{C}$, % wt. $\text{H}_2\text{SO}_4 = 40$; % wt. $\text{HNO}_3 = 2$. $X_{\text{HNO}_3} < 2\%$ at the reaction end. Lines are added just for better visualization of the trends.

Based on the Ph and MNPs concentration profiles, obtained from an isothermal nitration (run E4), a simple kinetic model was constructed assuming a parallel reaction network, represented in Figure 5.5, and described by equations (5.4), (5.9) and (5.10). Due to the used soft reaction conditions, low temperature and low sulfuric acid concentration compared to the industrial

conditions, DNPs and TNP were not formed, thus these compounds were not accounted for in the construction of the kinetic model.

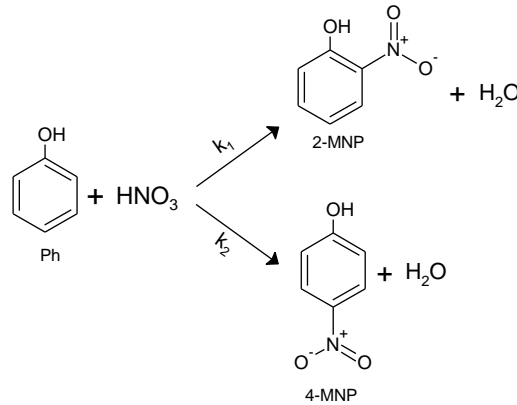


Figure 5.5 – Postulated Ph nitration scheme in mixed acid phenol-added benzene nitration.

$$(-r_{Phenol}) = -\frac{dC_{Phenol}}{dt} = k_1 C_{Phenol} C_{HNO_3} + k_2 C_{Phenol} C_{HNO_3} \quad (5.4)$$

In equation (5.4), which results from the mass balance to the batch reactor, assuming perfectly stirring conditions and the existence of a single (pseudo-homogenous) liquid phase (thus neglecting mass transfer limitations), k_1 represents the kinetic constant for 2-MNP formation and k_2 the constant for 4-MNP formation; C_i stands for the concentration of species i , (r_{Phenol}) for the reaction rate relative to Ph and t for the reaction time. The constructed kinetic model was intended to be a simple initial modelling approach. As nitric acid was in much higher concentration than Ph (*vide* Table 5.1), its concentration is assumed to remain nearly constant over time (actually, nitric acid conversion for Ph nitration was $< 2\%$), and inherently Ph nitration was considered to be a pseudo-first order reaction. Consequently, equation 5.4 can be simplified as follows,

$$(-r_{Phenol}) = -\frac{dC_{Phenol}}{dt} = k'' C_{Phenol} \quad (5.5)$$

being:

$$k'' = k_1' + k_2' \quad (5.6)$$

$$k_1' = k_1 C_{HNO_3} \quad (5.7)$$

$$k_2' = k_2 C_{HNO_3} \quad (5.8)$$

The MNPs concentration profiles can be described by the following equations:

$$(r_{2MNP}) = \frac{dC_{2MNP}}{dt} = k_1' C_{Phenol} \quad (5.9)$$

$$(r_{4MNP}) = \frac{dC_{4MNP}}{dt} = k_2' C_{Phenol} \quad (5.10)$$

To check whether the simplifications made for the kinetic model, namely, the absence of mass transfer resistances could be assumed, the stirring speed was changed being the remaining operational parameters (temperature, mixed acid composition, organic substrate fed) kept constant. The stirring speed was increased in about 200 revolutions per minute (r.p.m), from 1200 r.p.m (run E4) to 1400 r.p.m (run E5) – Figure 5.6. Lower stirring speeds were also used, however, as they did not allow good phases mixture, the results were discarded.

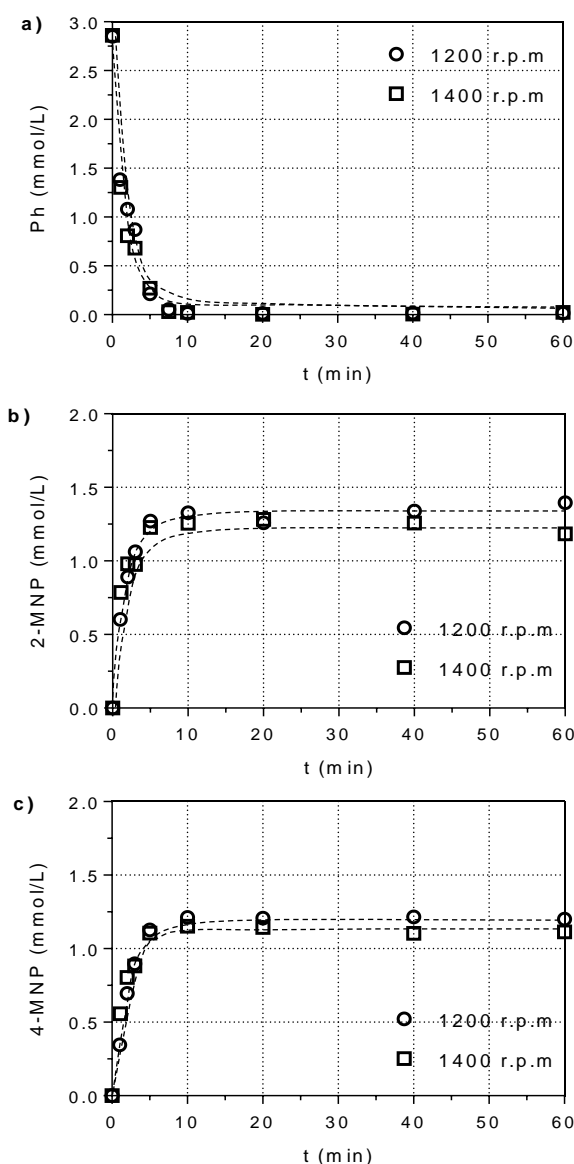


Figure 5.6 – a) Phenol, b) 2-MNP, and c) 4-MNP total concentration profiles for runs E4 (1204 r.p.m) and E5 (1422 r.p.m). Reaction conditions: $T = 15\text{ }^{\circ}\text{C}$, % wt. $\text{H}_2\text{SO}_4 = 40$; % wt. $\text{HNO}_3 = 2$. Lines are added just for a better visualization of the trends.

The results obtained for the outlined concentration profiles, shown in Figure 5.6, revealed that the stirring speed increase hadn't favored Ph consumption rate neither NPs formation. This means that even for the lower stirring speed test (E4), mass transfer limitations were not observed for this mixed acid Ph-added Bz nitration.

The kinetic parameters k'' , k_1' and k_2' , were determined by solving simultaneously equations 5.5, 5.9 and 5.10, using a regression tool to fit the kinetic constants (minimizing the mean square error between the experimental concentration data and the model results). The obtained values were the following: $k'' = 0.45 \text{ min}^{-1}$, $k_1' = 0.21 \text{ min}^{-1}$ and $k_2' = 0.19 \text{ min}^{-1}$. For determining these values, the restriction described by equation 6 was relaxed, which implied a deviation of about 10% between k'' and $k_1' + k_2'$ values. From these apparent kinetic constants and the nitric acid concentration, it was possible to calculate k_1 ($0.53 \text{ L}\cdot\text{mol}^{-1}\cdot\text{min}^{-1}$) and k_2 ($0.46 \text{ L}\cdot\text{mol}^{-1}\cdot\text{min}^{-1}$) at 15°C .

Quadros *et al.* [29] determined, based on other studies [4, 40], the kinetic constant value for Bz nitration in mixed acid systems at different temperatures and sulfuric acid concentrations. Using the developed correlations for the present reaction conditions, it was obtained a value of $2.91 \times 10^{-6} \text{ L}\cdot\text{mol}^{-1}\cdot\text{min}^{-1}$ for the Bz nitration kinetic constant, which is much lower (by several orders of magnitude) than that of the Ph nitration found in this work ($k_1 + k_2$). This is in accordance with what was previously stated, i.e., that Ph is a highly reactive compound and that Ph nitration is indeed an extremely fast reaction when compared with Bz nitration, justifying the difficulty in detecting Ph in the reaction medium under conditions close to those employed industrially [19].

Figure 5.7 shows the fitting of the proposed model to the experimental data (total concentrations). Despite the small deviation between the fitted model and the MNPs experimental data, the proposed model expresses the Ph, 2-MNP and 4-MNP concentration profiles very satisfactorily. In addition to the evaluation of the Ph's kinetic constant consumption, which shows the compound high reactivity towards the nitration reaction, the constructed kinetic model allowed verifying also that the assumed parallel reaction network (Figure 5.5) is verified and that Ph is indeed the NPs precursor.

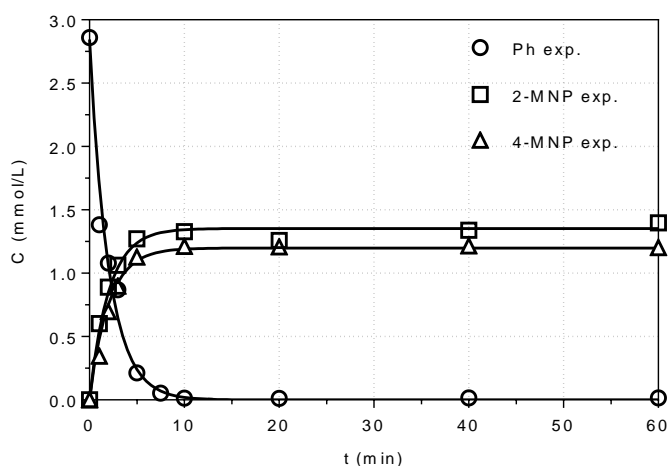


Figure 5.7 – Total concentration profiles and fitting of the proposed model to experimental data. Reaction conditions (run E4): $T = 15\text{ }^{\circ}\text{C}$, % wt. $\text{H}_2\text{SO}_4 = 40$; % wt. $\text{HNO}_3 = 2$. $X_{\text{HNO}_3} < 2\%$ at the reaction end.

5.3.2. Phenol-free benzene nitrations

It is worth mentioning that these tests were not performed aiming to minimize NPs formation during Bz nitration, but instead, it was intended to evidence MNPs presence in the reaction medium and to show their concentration profiles at different reaction conditions. This is of great importance since depending on the reaction conditions, MNPs may not be converted in DNPs, which at industrial level influences the choice of the proper alkaline agent used for NPs extraction from the produced MNB, and on the effluents treatment technologies.

Additionally, based on the obtained results for the influence of different parameters on the formation of the reaction by-products, a mechanistic model was constructed aiming to demonstrate NPs interconversion while showing their loss of reactivity as they are nitrated.

To verify the viability of detecting all the nitrophenolic by-products within the reaction medium at conditions close to the industrial ones, and to check the tests and analytical methodology repeatability, a set of experiments was performed under identical conditions (runs E6 to E8 – Table 5.1); the mixed acid composition used is within the industrial range, but a lower reaction temperature was employed.

The obtained results show an excellent repeatability (low variability, noticeable by the imperceptible standard deviation bars) both for the temperature and nitric acid consumption profiles, Figure 5.8 – a) and b), respectively. Regarding NPs concentration profiles, reasonably good repeatability is evidenced for 2-MNP and DNPs, being noticed slightly higher deviations (higher standard deviation bars) in 4-MNP profiles. For this species (Figure 5.8 – d)), deviations can be related to the very low analyte concentration, which tends to amplify the errors associated with the experimental analytical procedures.

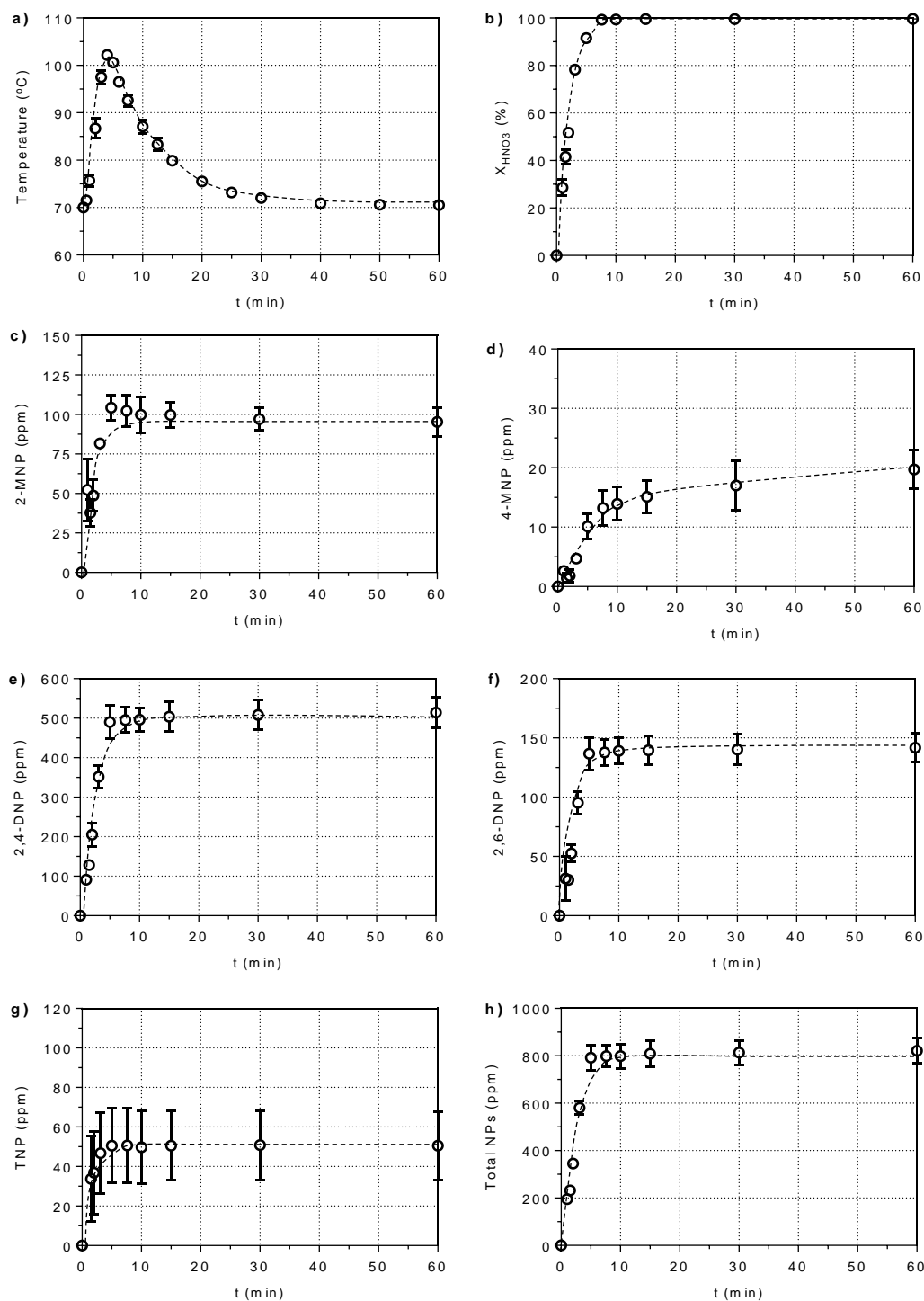


Figure 5.8 – a) Temperature evolution; and b) nitric acid; c) 2-MNP; d) 4-MNP; e) 2,4-DNP; f) 2,6-DNP; g) TNP; and h) total NPs concentration profiles for different runs. $T_{\text{initial}} = 70$ °C; % wt. $\text{H}_2\text{SO}_4 = 66$; % wt. $\text{HNO}_3 = 5$. The data points represent the average values for the different runs (E6, E7 and E8) while the vertical lines are related with the population standard deviation between the data (determined with a confidence interval of 95%). Lines are added just for better visualization of the trends.

Among the analysed nitrophenolic by-products, TNP was the one who displayed higher deviations between the conducted runs. This can be explained by the low initial reaction temperature, which hindered TNP formation resulting in higher analytical errors associated with the analyte quantification. At these reaction conditions and TNP concentration levels, the detection of this compound can be difficult [13, 27].

Analysing the temperature history, it is noticeable an increase of about 35 °C in the first 5 minutes of reaction time. This temperature rise is due to the strong exothermicity of Bz nitration. Then, the temperature starts decreasing because the reaction rate slows down. Concerning nitric acid conversion, the achieved overall conversions were quite similar, being obtained conversions higher than 99.5% for runs E6, E7 and E8.

The performed tests revealed that 10 minutes after the reaction start nitric acid conversion is nearly complete, being NPs formed until this instant. In fact, after this moment, NPs concentration values remain constant since in the absence of nitric acid MNPs are not formed either nitrated, thus hindering the consequent DNPs and TNPs concentration increase. This is seen for all nitrophenolic by-products, except for 4-MNP, which can be attributed to the low compound's concentration (< 25 ppm).

Under these reaction conditions, the total NPs amounts were about 800 ppm (Figure 5.8 – h)) and 2,4-DNP is the most representative by-product, as usually occurs industrially. Together with 2,4-DNP, TNP is the most abundant by-product in industrial CTSRs mixed acid Bz nitrations; however, the results obtained herein exhibit TNP concentrations lower than those of 2-MNP and 2,6-DNP, due to the low reaction temperature (when compared to the industrial one). Notwithstanding, it is important to refer that even in these harsh reaction conditions, in the range of the industrial ones except for the initial reaction temperature, all the nitrophenolic by-products were detected and quantified.

5.3.2.1. Modelling

For describing NPs concentration profiles under different reaction conditions, a kinetic model was constructed based on the reaction network illustrated in Figure 5.9.

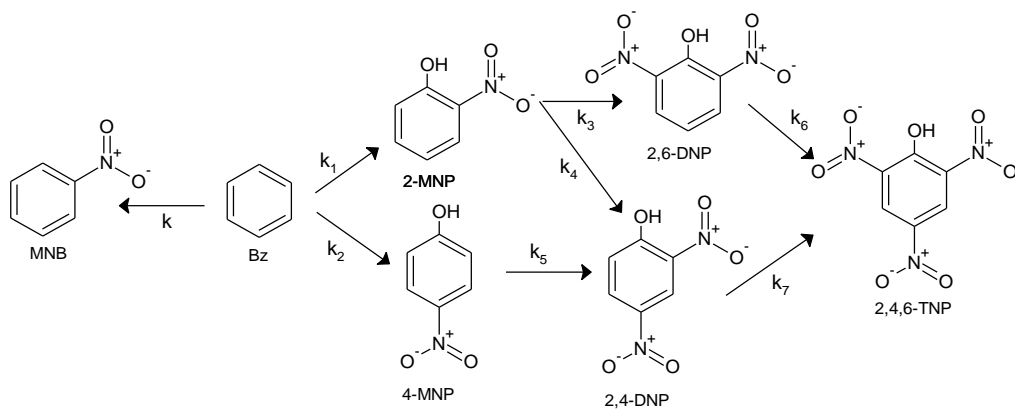


Figure 5.9 – Scheme of Bz nitration and NPs formation. Ph was intentionally not considered as the NPs precursor.

In this reaction network Ph, although being the NPs precursor, was not considered because of its high reactivity in such harsh conditions, hindering thus its accurate detection. Therefore, it was assumed that NPs are formed through Bz. It was also considered the existence of a single liquid phase (pseudo-homogeneous reaction), consequently, the inexistence of mass transfer limitations and that the nitrating agent was HNO_3 instead the NO_2^+ ion [29]. Additionally, while determining nitric acid and Bz concentration profiles, these compounds consumption on NPs formation was neglected because of the low NPs formed amounts ($m_{\text{Bz}}/m_{\text{NPs}} > 600$). Therefore, the kinetic model can be described by equations (5.11), (5.12) and (5.13).

$$(-r_{\text{HNO}_3}) = -\frac{dC_{\text{HNO}_3}}{dt} = kC_{\text{HNO}_3}C_{\text{Benzene}} \quad (5.11)$$

$$(-r_{\text{Benzene}}) = -\frac{dC_{\text{Benzene}}}{dt} = kC_{\text{HNO}_3}C_{\text{Benzene}} \quad (5.12)$$

In equations (5.11) and (5.12), that have arisen from the mass balance to the batch reactor, k represents the kinetic constant for Bz nitration.

As the runs were not conducted isothermally, to account with the temperature evolution, an energy balance to the batch reactor was performed – equation (5.13) [41].

$$\frac{dT}{dt} = \frac{Q + (-\Delta H_{rx}) \times (-r_{\text{HNO}_3} \times V)}{(\sum_i^n N_i c_{p_i} + N_{\text{HNO}_3} \Delta c_p X)} \quad (5.13)$$

In equation (5.13), T corresponds to the temperature of the reaction medium, Q to the heat removed by the reactor's jacket, $(-\Delta H_{rx})$ stands for the reaction enthalpy, V for the reaction

volume, N_i for the molar amount of species i , Δc_p the overall change in heat capacity per mole of HNO_3 reacted and X represents the conversion. In the energy balance, NPs formation was not accounted for due to their low amounts.

The heat removed from the reactor was determined using equation (5.14), assuming that the thermal fluid in the jacket is perfectly mixed [42].

$$Q = UA(T_{fluid} - T) \quad (5.14)$$

In equation (5.14), U corresponds to the overall heat transfer coefficient considering only the heat transfer by conduction through the reactor walls ($k_{thermal} / x_p = 129 \text{ W} \cdot \text{m}^{-2} \cdot \text{K}^{-1}$) [43-44], A to the heat transfer area (0.047 m^2), T_{fluid} to the temperature of the thermal fluid (70 or 90 °C, depending on the initial reaction temperature) and T to the temperature of the reaction medium.

The reaction enthalpy was determined according to equation (5.15),

$$\Delta H_{rx} = \Delta H^0 + \Delta c_p(T - T_R) \quad (5.15)$$

in which ΔH^0 is the standard enthalpy of formation for Bz nitration, determined using the Aspen software ($-143.9 \text{ kJ} \cdot \text{mol}^{-1}$), and where T_R corresponds to 298 K.

The following equations can describe the NPs concentration profiles:

$$(r_{2MNP}) = \frac{dC_{2MNP}}{dt} = (k_1 C_{Benzene} - k_3 C_{2MNP} - k_4 C_{2MNP}) \times C_{HNO_3} \quad (5.16)$$

$$(r_{4MNP}) = \frac{dC_{4MNP}}{dt} = (k_2 C_{Benzene} - k_5 C_{4MNP}) \times C_{HNO_3} \quad (5.17)$$

$$(r_{2,4DNP}) = \frac{dC_{2,4DNP}}{dt} = (k_4 C_{2MNP} + k_5 C_{4MNP} - k_7 C_{2,4DNP}) \times C_{HNO_3} \quad (5.18)$$

$$(r_{2,6DNP}) = \frac{dC_{2,6DNP}}{dt} = (k_3 C_{2MNP} - k_6 C_{2,6DNP}) \times C_{HNO_3} \quad (5.19)$$

$$(r_{TNP}) = \frac{dC_{TNP}}{dt} = (k_6 C_{2,6DNP} + k_7 C_{2,4DNP}) \times C_{HNO_3} \quad (5.20)$$

being the kinetic constants determined by the Arrhenius law:

$$k_i = k_{0i} \left(\frac{-E_{ai}}{RT} \right) \quad (5.21)$$

in which k_{0i} stands for the pre-exponential constant of reaction i , E_{a_i} stands for the activation energy of reaction i and R corresponds to the ideal gas constant.

Because of the simplifications made the set of ordinary differential and algebraic equations was solved in a two-step procedure. Initially, equations (5.11) to (5.15) were solved using the 4th order Runge-Kutta method and estimating both the pre-exponential factor and activation energy for Bz nitration. These kinetic parameters were estimated by minimizing the relative error between the experimental data points and the predicted ones (temperature and concentration profiles – Figures 5.10, 5.11 and 5.12 a) and b)). The initial estimates for the pre-exponential factor and activation energy were based on the correlations presented by Quadros *et al.* [29].

Having both nitric acid and Bz concentration profiles, as well as the temperature history, NPs concentration profiles were obtained solving equations (5.16) to (5.21), once again using the 4th order Runge-Kutta method and estimating the kinetic parameters. The kinetic parameters were estimated by minimizing the relative error between the experimental NPs concentrations and the model results (Figures 5.10, 5.11 and 5.12 c), d), e), f), g) and h)). The estimated kinetic parameters are presented in Table 5.2.

Table 5.2 – Kinetic parameters estimated for the reaction network presented in Figure 5.9.

Reaction	70 °C; 66 % wt. H ₂ SO ₄		70 °C/90 °C; 61 % wt. H ₂ SO ₄		90 °C; 51 % wt. H ₂ SO ₄	
	k_0	E_a	k_0	E_a	k_0	E_a
	(m ³ ·mol ⁻¹ ·s ⁻¹)	(J·mol ⁻¹)	(m ³ ·mol ⁻¹ ·s ⁻¹)	(J·mol ⁻¹)	(m ³ ·mol ⁻¹ ·s ⁻¹)	(J·mol ⁻¹)
(k) Bz→MNB	2.1×10^{-3}	1.6×10^4	1.9×10^{-2}	2.5×10^4	3.8×10^{-2}	3.4×10^4
(k ₁) Bz→2-MNP	1.2×10^{-2}	4.6×10^4	1.3	6.2×10^4	10.2	7.5×10^4
(k ₂) Bz→4-MNP	2.6×10^{-3}	4.3×10^4	2.9×10^{-1}	6.0×10^4	8.4×10^{-1}	7.2×10^4
(k ₃) 2-MNP→2,6-DNP	3.2×10^4	6.8×10^4	6.0×10^6	8.4×10^4	2.9×10^7	9.2×10^4
(k ₄) 2-MNP→2,4-DNP	3.9×10^3	6.1×10^4	8.1×10^5	7.6×10^4	6.6×10^6	8.5×10^4
(k ₅) 4-MNP→2,4-DNP	2.4×10^4	6.4×10^4	4.1×10^6	7.9×10^4	1.0×10^7	8.7×10^4
(k ₆) 2,6-DNP→TNP	1.1×10^6	8.1×10^4	3.4×10^7	9.1×10^4	2.6×10^8	1.0×10^5
(k ₇) 2,4-DNP→TNP	6.3×10^5	8.6×10^4	7.1×10^5	9.6×10^4	4.1×10^7	1.1×10^5

Observing Table 5.2, one can see that increasing sulfuric acid concentration led to the decrease of the activation energies of all the addressed reactions, as expected because sulfuric acid is the reaction catalyst. Additionally, comparing the activation energies for the formation of the reaction by-products it is noticeable that the higher number of nitro groups (-NO₂) the aromatic molecule has, the higher the activation energy; thus the less reactive it is. This is because the nitro group is a highly deactivating group [7].

In what concerns to the pre-exponential factor, the displayed estimates show that this parameter depends on the sulfuric acid concentration because the acid strength increase leads to a k_0 decrease.

This tendency is in accordance with the correlation presented by Quadros *et al.* [29] for this parameter calculation.

5.3.2.2. Effect of the sulfuric acid strength

Runs E6 to E8 enabled the visualization of all NPs profiles (cf. Figure 5.8), but their interconversion was not very explicit due to the high reaction rate, consequence of the harsh reaction conditions. Thus, sulfuric acid concentration was decreased, aiming to slow down the reaction rate and to check the catalyst impact on NPs concentration profiles. The achieved results are illustrated in Figure 5.10.

As expected, the decrease of sulfuric acid concentration has slowed down Bz nitration, fact noticed by the analysis of nitric acid conversion (Figure 5.10 – b)). For the highest sulfuric acid strength run (E7) nitric acid conversion has reached its maximum value (99.7%) 10 minutes after the reaction start while in the lowest sulfuric acid concentration run (E9) nitric acid conversion increased until the reaction end (97.4 %). The reaction rate decrease is also noticeable by analysing the temperature history, which shows that for run E7 the maximum of temperature (102 °C) is reached 4 minutes after the reaction start while in run E9 the temperature maximum (88 °C) is reached 7 minutes after the reaction start (Figure 5.10 – a)). The attenuation of the temperature rise for decreasing sulfuric acids concentration culminated in a reduction of NPs formation (Figure 5.10 – h)), an expected outcome since it is known the temperature's positive effect on these compounds generation [13].

As seen before, for the test with a higher sulfuric acid concentration (66% - run E7), all the nitrophenolic reaction by-products were detected and 10 minutes after the reaction start their concentrations remained nearly constant (because nitric acid was depleted from the reaction medium). Considering the run with the lowest sulfuric acid content (61% - E9), from the MNPs concentration profiles (Figure 5.10 – c) and d)) is observable a slightly different behavior. It is visible that both MNPs concentration profiles reach a maximum value (5 to 8 minutes after the reaction start), which then starts decreasing as a result of a MNPs nitration rate higher than the rates of Ph formation and its nitration. These concentration profiles were obtained due to the lower catalyst concentration, which delayed the nitric acid depletion from the reaction medium (Figure 5.10 – b)), enabling, therefore, visualizing the MNPs concentration decrease and the consequent rise of DNPs concentration.

As the reaction proceeds the DNPs formation rate is slowed down (run E9, $t > 20$ minutes; Figure 5.10 – e) and f)) due to the decrease of the nitric acid and MNPs content in the reaction medium, proving that DNPs are formed through MNPs nitration. These results allow confirming that the nitrophenolic by-products are formed by consecutive nitrations – Figure 5.1.

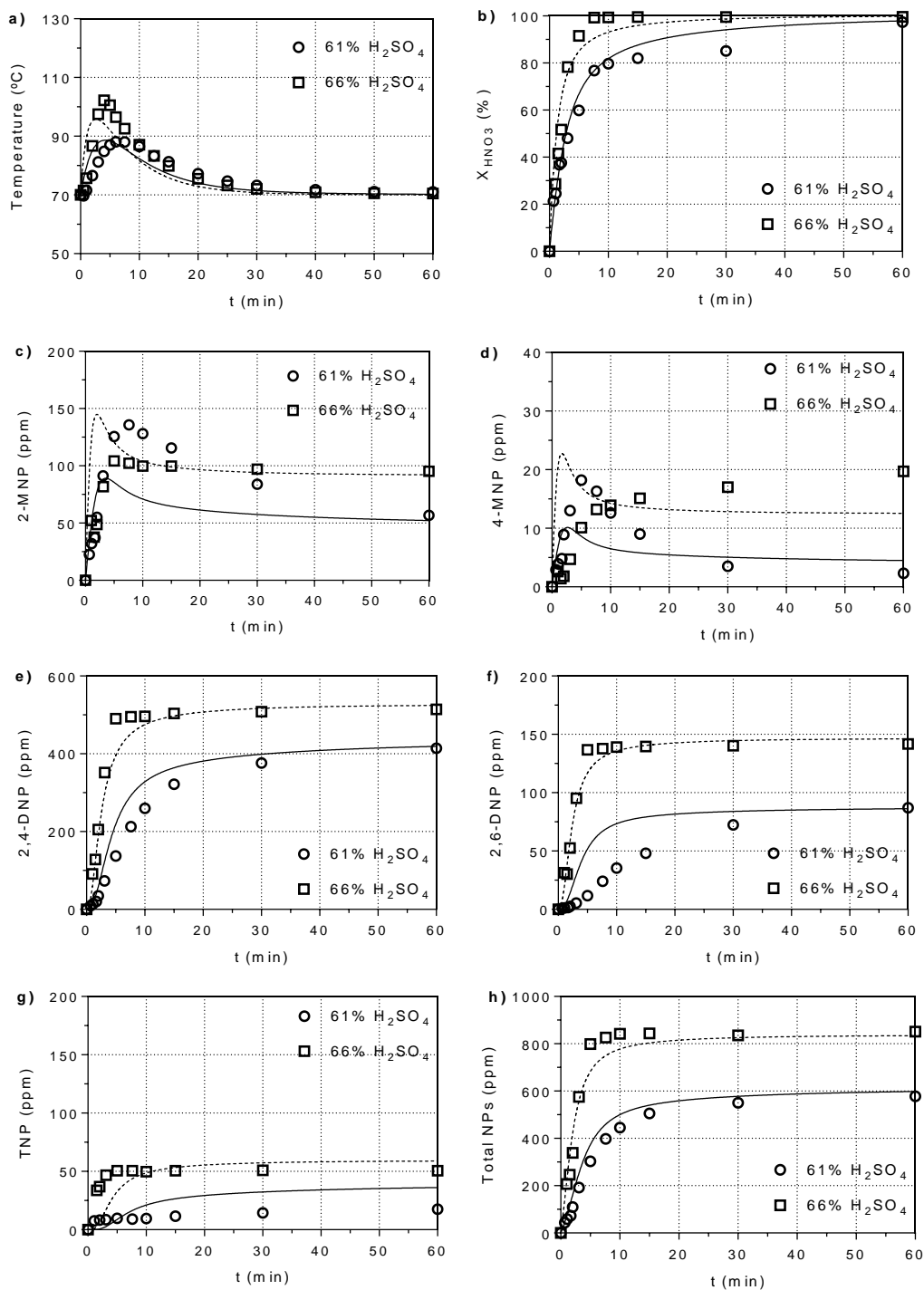


Figure 5.10 – Effect of sulfuric acid concentration and fitting of the proposed model to experimental data on the: **a)** Temperature history; **b)** Nitric acid conversion; and **c)** 2-MNP; **d)** 4-MNP; **e)** 2,4-DNP; **f)** 2,6-DNP; **g)** TNP; and **h)** total NPs concentration profiles for the average values of runs E6, E7, E8 (66 wt.% H_2SO_4) and E9 (61 wt.% H_2SO_4); $T_{\text{initial}} = 70^{\circ}\text{C}$, wt.% $\text{HNO}_3 = 5$. The solid lines represent the adjusted values for run E9 while the dashed lines refer to the adjusted values for the average of the runs E6, E7 and E8.

Regarding DNPs and TNP concentration profiles, displayed in Figure 5.10 – e), f) and g) is visible that for the highest sulfuric acid strength run (E7), when the DNPs concentration tends to be constant, the TNP quantities remain constant as well, while in the lowest sulfuric acid concentration run (E9) is noticeable that TNP concentration increases with increasing DNPs amounts. Such evidence indicates that DNPs are the TNP precursors.

The analysis of the presented concentration profiles shows clearly that a higher catalyst concentration leads to higher NPs concentrations in the reaction medium. This is a consequence of the faster Bz nitration, which caused a higher temperature increase, thus promoting NPs formation [13-14, 27].

For the test with the lowest sulfuric acid concentration it would be expected to have higher NPs amounts since the nitric acid dissociation into NO_2^+ wouldn't be so effective and, therefore, undissociated nitric acid would be present in higher amounts in the reaction medium (thus being able to oxidize Bz to Ph). However, the same tendency observed by us, of lower NPs formation for lower H_2SO_4 concentrations, was found by Burns and Ramshaw [27], although these authors have studied Bz nitration in microreactors, and by Berretta and Louie [14]. This indicates that Bz oxidation is favoured by the combined action of high reaction temperature and undissociated nitric acid.

As for the fitting of the proposed model, a good agreement between the experimental values and the kinetic model was obtained, particularly for the temperature profiles, nitric acid conversion and for the 2,4 DNP and total NPs concentration profiles (sum of all NPs concentration values obtained by the model), being notorious higher deviations in the MNPs profiles. This is due to the model assumptions and particularly to the different concentration levels of the nitrophenolic by-products, which have diffculted the estimation of the kinetic parameters.

Nevertheless, the developed model, although having some simplifications in its genesis, allows evidencing that nitrophenols are formed by consecutive reactions, i.e., mononitrophenols are nitrated into dinitrophenols that are the trinitrophenol precursors, and that these compounds' reactivity decreases with increasing number of nitro groups in the molecule. Additionally, comparing the NPs (determined) kinetic constants (e.g. 2,6-DNP formation: $4.7 \times 10^{-6} \cdot \text{m}^3 \cdot \text{mol}^{-1} \cdot \text{s}^{-1}$ at 70 °C and 66% wt. H_2SO_4) with that of Ph's nitration (e.g. 2-MNP formation: $8.7 \times 10^{-6} \cdot \text{m}^3 \cdot \text{mol}^{-1} \cdot \text{s}^{-1}$ at 15 °C and 40% wt. H_2SO_4), it can be concluded that 2-MNP is less reactive than Ph, because even in much softer conditions Ph's kinetic constant is of the same order of magnitude of 2-MNP's one. This is the reason why NPs are more easily detected in the reaction medium than Ph.

5.3.2.3. Effect of the temperature

In Figure 5.11 – a) it is shown that a higher initial reaction temperature leads to a higher temperature increase. This can be explained by the positive effect of the reaction temperature on

the reaction rate. After 1 hour of reaction time nitric acid conversion was 99.7% for the run at 90 °C (E10) whereas for the run at 70 °C (E9) it was 97.4%; however, bigger differences are noticed at smaller times. The higher reaction rate causes a higher energy release (due to Bz nitration exothermicity) in a shorter time interval, explaining thus the greater temperature rise for the highest temperature run. The increase of the reaction temperature led to a rise in the total NPs concentration (Figure 5.11 – h)), as expected from previous works [13-14].

Analysing the MNPs concentration profiles (Figure 5.11 – c) and d)), it is visible that the reaction temperature did not affected significantly their behaviour, i.e., it is noticeable for both tests that these compounds' concentration reaches a maximum value starting then to decrease. However, such maximum is reached sooner at the highest temperature and their final quantities in the reaction mixture are lower. These observations evidence the high reactivity of MNPs and explain the reason why these compounds are not typically accounted for (or even detected) in Bz nitration studies. As found before, 2-MNP formed amounts were higher in both runs than 4-MNP ones.

For the 90 °C run (E10) it is noticeable that 10 minutes after the reaction start both MNPs amounts are vestigial, that 2,4-DNP concentration reached a nearly constant value, but 2,6-DNP concentration was already decreasing. This is indicative that both 2-MNP and 4-MNP have contributed for 2,4-DNP formation while only 2-MNP could have been in the 2,6-DNP origin (Figure 5.1), and that 2,6-DNP consumption rate was higher than its formation rate. Regarding the 2,4-DNP concentration profiles (Figure 5.11 – e)), it is clearly noticeable the positive impact of the reaction temperature in this compound formation. Regarding 2,6-DNP, after achieving its maximum value, 2,6-DNP concentration starts decreasing and TNP concentration increases while 2,4-DNP amounts increased till reaching a nearly constant value. Relating both 2,6-DNP and TNP concentration profiles for run E10, it can be concluded the existence of a dependence between these species, because when 2,6-DNP consumption rate decreases ($t > 20$ minutes), TNP formation rate decreases as well.

TNP concentration profiles (Figure 5.11 – g)) evidence also that its formation is enhanced for higher reaction temperatures, increasing from 25 ppm to 325 ppm with the increase of the reaction temperature from 70° C to 90° C. It is noticeable that in both runs the TNP formed amounts are lower than those of DNPs. This can be explained by the powerful deactivating effect of the nitro groups (-NO₂) present in the nitrophenolic reaction by-products [7], noticeable by the increase of the activation energy (Table 5.2). The more nitro groups the aromatic ring of the nitrophenol molecule has, the more deactivated it is and therefore the more stable (less reactive).

Decomposition Reactions in Aromatic Nitration

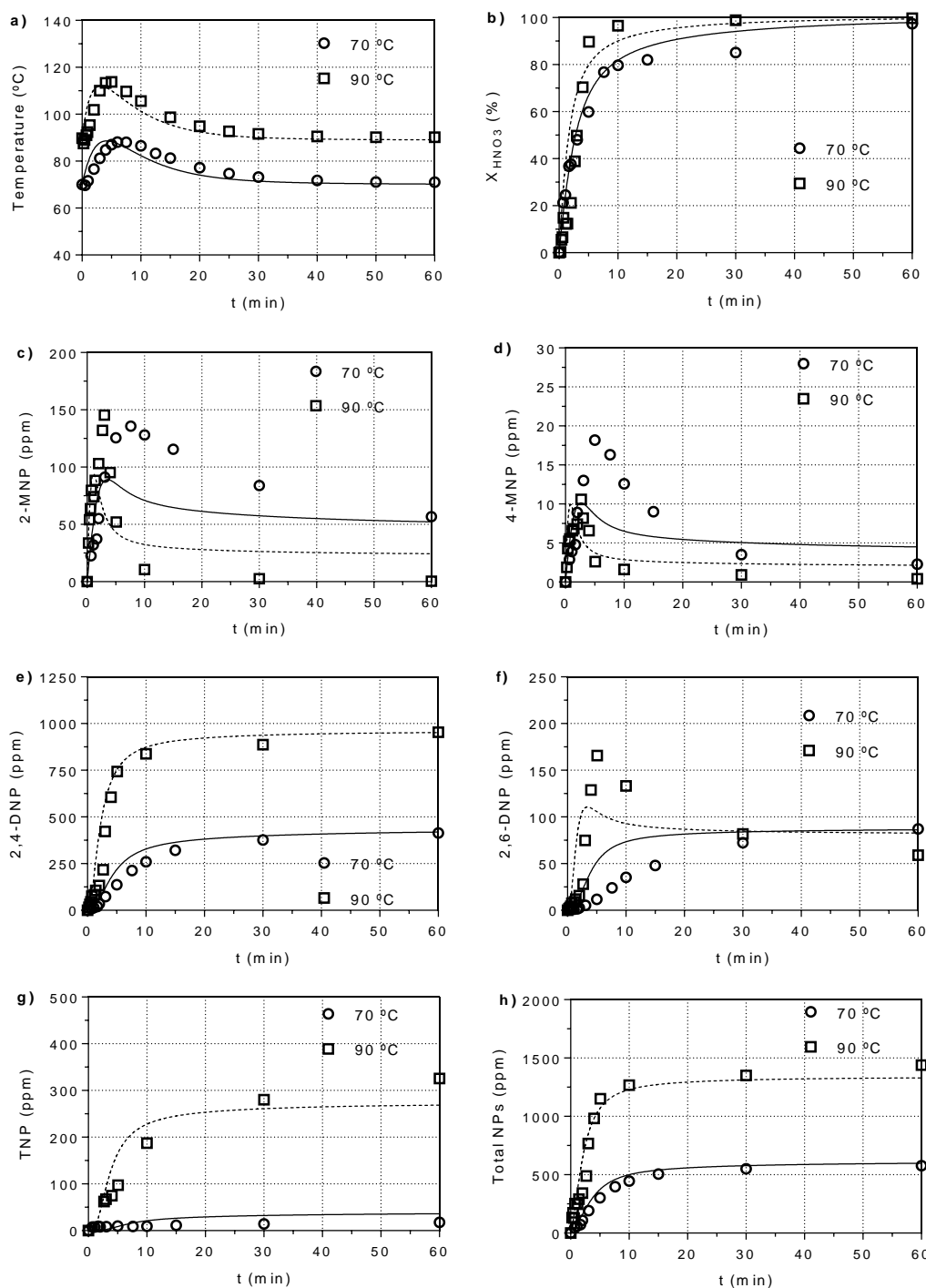


Figure 5.11 – Effect of initial the reaction temperature and fitting of the proposed model to experimental data on: **a)** Temperature history; **b)** Nitric acid conversion; and **c)** 2-MNP; **d)** 4-MNP; **e)** 2,4-DNP; **f)** 2,6-DNP; **g)** TNP; and **h)** total NPs concentration profiles for runs E9 (70 °C) and E10 (90 °C); % wt. H₂SO₄ = 61. % wt. HNO₃ = 5. The dashed lines represent the adjusted values for run E10 while the solid lines refer to the adjusted values for run E9.

The obtained results are in general in accordance with some published works [13-14, 27, 45] regarding the positive reaction temperature effect on the NPs, namely 2,4-DNP and TNP formation and with the mechanism shown in Figure 5.1.

Regarding the fitting of the proposed model, as verified previously, a satisfactory agreement between the experimental values and the kinetic model was obtained for the temperature evolution, nitric acid conversion and for the 2,4 DNP and total NPs concentration profiles. Once again, the higher deviations are associated with the MNPs concentration profiles, being the analytes low concentration and the model simplifications the reason for these higher discrepancies.

When analyzing 2,6-DNP and TNP experimental concentration profiles, a dependence between these species was detected. This dependence is also evidenced by the estimated activation energies for DNPs nitration, which were found to be lower for 2,6-DNP nitration (Table 5.2), indicating that 2,6-DNP is more reactive than 2,4-DNP, thus more prone to be nitrated into TNP.

As previously verified (section 5.3.2.2), the developed model supports nitrophenols interconversion and their reactivity decreases with the increase of the number of nitro groups in the aromatic ring.

5.3.2.4. Effect of the nitric acid concentration

The effect of nitric acid in NPs formation – Figure 5.12 – was also evaluated by comparing the obtained results from two nitrations performed with different concentrations of the referred acid (run E11 and run E12 – Table 5.1).

The nitric acid conversion in the highest acid concentration run (E12) reached a maximum value of 55 % in less than 1 h, which remained constant afterwards due to nearly complete consumption of Bz (determined by mass balance as a function of nitric acid consumption). For the lowest acid strength run (E11), nitric acid conversion was smoothly increasing and was not complete (< 80 %) after 1 h due to the low sulfuric acid concentration – Figure 5.12 – b).

The obtained results show that higher nitric acid concentration increased the reaction rate and the total concentration of NPs (Figure 5.12 – h)). Moreover, and as observed previously, the reaction rate increase led to a higher temperature rise (Figure 5.12 – a)). However, the temperature rise in these runs was not so abrupt as in the previous tests due to the lower sulfuric acid concentration.

Decomposition Reactions in Aromatic Nitration

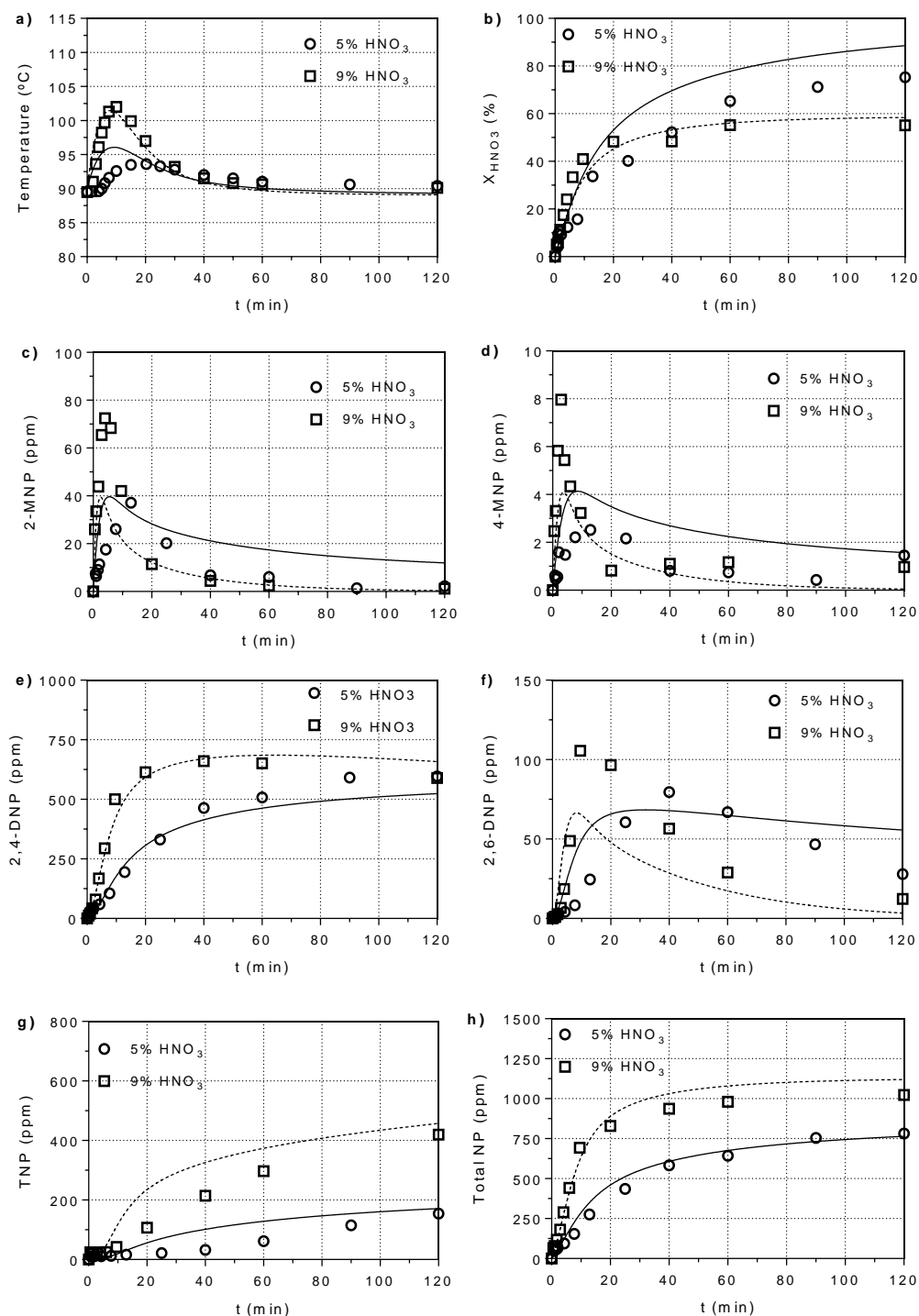


Figure 5.12 – Effect of nitric acid concentration and fitting of the proposed model to experimental data on: **a)** Temperature history; **b)** Nitric acid conversion; and **c)** 2-MNP; **d)** 4-MNP; **e)** 2,4-DNP; **f)** 2,6-DNP; **g)** TNP; and **h)** total NPs concentration profiles for runs E11 (5 % wt. HNO₃) and E12 (9 % wt. HNO₃); T_{initial} = 90 °C; wt.% H₂SO₄ = 51. The dashed lines represent the adjusted values for run E12 while the solid lines refer to the adjusted values for run E11.

The MNPs concentration profiles (Figure 5.12 – c) and d)) revealed that both species reached a maximum of concentration 5 minutes and 15 minutes after the reaction start in runs E12 and E11,

respectively, which then starts decreasing. Even at these low sulfuric acid concentration tests MNPs amounts became vestigial in the reaction medium, evidencing once again the compounds high reactivity.

The results obtained also show that higher nitric acid concentration favors MNPs formation. For higher nitric acid concentration in the reaction medium, its dissociation into the nitronium ion (NO_2^+) is not so effective. Therefore, undissociated nitric acid amounts are higher in the reaction medium, able to oxidize Bz into Ph (in the organic phase), the MNPs precursor. It is also visible that MNPs formation and consumption rates are higher for the highest nitric acid concentration.

As for the DNPs profiles, in run E12 it is noticeable that 2,4-DNP reaches a maximum concentration value of 660 ppm, which then starts (slightly) decreasing until the reaction end. In run E11, this compound concentration profile is different, increasing till the reaction end. In both runs 2,4-DNP amounts at the reaction end are similar, being noticeable a higher formation rate for the higher nitric acid concentration (because of the faster MNPs consumption). For 2,6-DNP it is noticeable a similar behavior in both runs, i.e., a maximum concentration value is reached, which then starts decreasing until the reaction end. It is also perceptible a faster formation and consumption rate of 2,6-DNP and for higher nitric acid concentration.

As verified in section 5.3.2.3., it is observed that the MNPs concentration decrease leads to the decrease of DNPs formation rate, proving once again that MNPs are at the genesis of DNPs. Analyzing 2,4-DNP concentration profiles, it is noticeable that its amounts tend to be constant when MNPs concentration reaches vestigial values, which is indicative that both 2-MNP and 4-MNP are responsible for this compound formation. The small 2,4-DNP concentration decrease (run E12) noticed at the reaction end can only be explained by its nitration, in a small extent, to TNP. The decrease of 2,6-DNP amounts (in both runs) can be justified by the nitration of this compound into TNP. Indeed, comparing the depicted 2,6-DNP and TNP concentration profiles for run E12, it is seen that when 2,6-DNP consumption rate decreases (ca. 40-60 minutes after the reaction start) the TNP formation rate decreases as well. This proves that 2,6-DNP is nitrated to TNP.

Regarding TNP profiles, it is clearly visible the positive effect of the higher nitric acid concentrations in the compound's formed amounts. The most plausible justification to explain the total NPs concentration increase (mostly due to the increase of TNP amounts) with the increasing nitric acid concentration is the conjunction of two factors: i) higher nitric acid concentration led to a higher temperature rise, which is known, and was verified (section 5.3.2.3.) to affect positively NPs formation; ii) higher nitric acid concentration tends to increase the presence of undissociated nitric acid in the reaction medium, lowering the Bz / nitric acid ratio [13], and thus enhancing Bz oxidation to Ph and Ph's subsequent nitration.

Comparing the values predicted by the model and the experimental data, an acceptable agreement can be found, especially for the highest nitric acid concentration run. Nevertheless,

despite the visible deviations, the proposed model predicts quite well 2,4-DNP concentration profiles, the most abundant reaction by-product, independently of the nitric acid concentration.

5.4. Conclusions

The present study allowed to evidence Ph's and mononitrophenol's high reactivity, being thus justified the difficulty of detecting these compounds in Bz mixed acid nitrating systems, particularly under the conditions employed industrially. Moreover, Ph-added Bz nitrations enabled the construction of a simple kinetic model that expressed satisfactorily Ph, 2-MNP and 4-MNP concentration profiles. This kinetic model evidenced Ph's high reactivity, helping to support our previous findings and providing further evidence for Ph as the NPs precursor in mixed acid systems.

Ph-free Bz nitrations were studied at different reaction conditions aiming to analyze all the nitrophenolic by-products (2-MNP; 4-MNP; 2,4-DNP; 2,6-DNP; and TNP) concentration profiles; this represents an added-value in this thematic, since it is unusual in Bz nitration studies. It was noticed that DNPs reach a maximum concentration after MNPs concentration starts decreasing, which evidences that MNPs are the DNPs precursors. It was also seen a dependency between DNP and TNP concentration profiles, indicating that the DNPs are in the genesis of TNP.

Regarding the impact of the tested parameters, it was found that the nitrophenolic by-products formation increases with the temperature, sulphuric acid and nitric acid concentrations; the same occurs in terms of Bz nitration rate.

Using the collected data from the reactions performed under different conditions, a kinetic model was constructed which exhibited a quite good fitting to the experimental values, considering the simplifications made. The developed model allowed to corroborate nitrophenols interconversion and to verify that Ph is more reactive than NPs and that the higher number of nitro groups the molecule has, the less reactive it is (higher activation energy).

The NPs concentration profiles enabled to determine which reaction conditions lead to MNPs depletion from the reaction medium, a valuable industrial information since the MNPs formed amounts have a direct impact on the NPs extracting agent and the effluent treatment technology.

Nomenclature

A	Heat transfer area (m^2)
Bz	Benzene
C_{i_0}	Molar concentration of the compound i at the reaction start ($\text{mol}\cdot\text{m}^{-3}$)
C_i	Molar concentration of the compound i ($\text{mol}\cdot\text{m}^{-3}$)
c_{p_i}	Heat capacity of the compound i ($\text{J}\cdot\text{mol}^{-1}\cdot\text{K}$)
CSTR	Continuous stirred tank reactor
DNB	Dinitrobenzene
DNP	Dinitrophenol
GC-FID	Gas Chromatography – Flame Ionizer Detector
H_{rx}	Reaction enthalpy ($\text{J}\cdot\text{mol}^{-1}$)
HPLC-DAD	High Performance Liquid Chromatography - Diode Array Detector
k_i	Kinetic constant of the reaction i ($\text{volume}\cdot\text{mol}^{-1}\cdot\text{time}^{-1}$)
k'_i	Apparent kinetic constant of the reaction i (time^{-1})
$k_{thermal}$	Thermal conductivity of the reactor's wall ($\text{W}\cdot\text{m}^{-1}\cdot\text{K}^{-1}$)
MNB	Mononitrobenzene
MNP	Mononitrophenol
N_i	Moles of the compound i (mol)
NP	Nitrophenol
Ph	Phenol
Q	Heat removed from the reaction ($\text{J}\cdot\text{s}^{-1}$)
R	Universal gas constant ($\text{J}\cdot\text{mol}^{-1}\cdot\text{K}^{-1}$)
r_i	Reaction rate relative to compound i ($\text{mol}\cdot\text{volume}^{-1}\cdot\text{time}^{-1}$)
T	Reaction temperature (K)
$T_{thermal}$	Temperature of the thermal fluid (K)
t	Reaction time (s)
TNP	Trinitrophenol
V	Reaction volume (m^3)
X	Conversion
x_p	Thickness of the reactor's wall (m)

5.5. References

- [1]. Albright, L. F., Nitration. In *Kirk-Othmer Encyclopedia of Chemical Technology*, John Wiley & Sons, Inc., 2000, 10.1002/0471238961.1409201801120218.a01.
- [2]. Booth, G., Nitro Compounds, Aromatic. In *Ullmann's Encyclopedia of Industrial Chemistry*, Wiley-VCH, Weinheim, 2000, doi:10.1002/14356007.a17_411.
- [3]. Urbański, T., *Chemistry and Technology of Explosives*. Pwn-Polish Scientific Publishers, Vol. 1, Warszawa, Poland, 1964.
- [4]. Marziano, N. C.; Tomasin, A.; Tortato, C.; Zaldivar, J. M., Thermodynamic nitration rates of aromatic compounds. Part 4. Temperature dependence in sulfuric acid of $\text{HNO}_3 \rightarrow \text{NO}_2^+$ equilibrium, nitration rates and acidic properties of the solvent. *J. Chem. Soc., Perkin Trans. 2* **1998**, (9), 1973-1982, 10.1039/A802521E.
- [5]. Halder, R.; Lawal, A.; Damavarapu, R., Nitration of toluene in a microreactor. *Catalysis Today* **2007**, 125 (1–2), 74-80, <http://dx.doi.org/10.1016/j.cattod.2007.04.002>.
- [6]. Carey, F. A.; Sundberg, R. J., *Advanced Organic Chemistry Part B: Reactions and Synthesis*. 5th edition, Springer US, 2007.
- [7]. Carey, F., *Organic Chemistry*. 4th edition, McGraw-Hill, New York, 2000.
- [8]. Olah, G. A.; Malhotra, R.; Narang, S. C., *Nitration: Methods and Mechanisms*. Wiley-VCH, 1989.
- [9]. Kulkarni, A. A., Continuous flow nitration in miniaturized devices. *Beilstein Journal of Organic Chemistry* **2014**, 10, 405-424, 10.3762/bjoc.10.38.
- [10]. Giles, J.; Hanson, C.; Ismail, H. A. M., A Model for Rate of Nitration of Toluene Under Heterogeneous Conditions. In *Industrial and Laboratory Nitrations*, American Chemical Society, Washington, DC. ACS Symposium Series, 1976; Vol. 22, pp 190-209, doi:10.1021/bk-1976-0022.ch012
10.1021/bk-1976-0022.ch012.
- [11]. Alexanderson, V.; Trecek, J. B.; Vanderwaart, C. M., Continuous adiabatic process for the mononitration of benzene. US Patent 4,091,042, May 23, 1978.
- [12]. Guenkel, A. A.; Rae, J. M.; Hauptmann, E. G. Nitration process. US Patent 5,313,009, May 17, 1994.
- [13]. Quadros, P. A.; Castro, J. A. A. M.; Baptista, C. M. S. G., Nitrophenols Reduction in the Benzene Adiabatic Nitration Process. *Industrial & Engineering Chemistry Research* **2004**, 43 (15), 4438-4445, 10.1021/ie034263o.
- [14]. Berretta, S.; Louie, B., Effect of Reaction Conditions on the Formation of Byproducts in the Adiabatic Mononitration of Benzene into Mononitrobenzene (MNB). In *Chemistry, Process Design, and Safety for the Nitration Industry*, American Chemical Society, Washington, DC. ACS Symposium Series, 2013; Vol. 1155, pp 13-26, doi:10.1021/bk-2013-1155.ch002

10.1021/bk-2013-1155.ch002.

- [15]. Nogueira, A. G. Optimização da Nitração de Aromáticos. PhD Thesis, Universidade de Coimbra, Portugal, 2014.
- [16]. Burns, J. R.; Ramshaw, C., Development of a Microreactor for Chemical Production. *Chemical Engineering Research and Design* **1999**, 77 (3), 206-211, <http://dx.doi.org/10.1205/026387699526106>.
- [17]. Di Somma, I.; Russo, D.; Andreozzi, R.; Marotta, R.; Guido, S., Kinetic modelling of benzyl alcohol selective oxidation in aqueous mixtures of nitric and sulfuric acids. *Chemical Engineering Journal* **2017**, 308, 738-744, <https://doi.org/10.1016/j.cej.2016.09.113>.
- [18]. Ross, D. S.; Kirshen, N. A., Nitration and Oxidative Side Reactions of Dinitrotoluenes. In *Industrial and Laboratory Nitrations*, American Chemical Society, Washington, DC. ACS Symposium Series, 1976; Vol. 22, pp 114-131, doi:10.1021/bk-1976-0022.ch007
10.1021/bk-1976-0022.ch007.
- [19]. Afonso, D.; Ribeiro, A. F. G.; Araújo, P.; Vital, J.; Madeira, L. M., Phenol in Mixed Acid Benzene Nitration Systems. *Industrial & Engineering Chemistry Research* **2018**, 57 (46), 15942-15953,
- [20]. Yang, G.-s.; Shi, J.-h.; Li, J., Selective nitration of phenol to ortho-nitrophenol using dilute nitric acid by microemulsion of cetyltrimethylammonium bromide (CTAB) in isooctane. *Korean J. Chem. Eng.* **2003**, 20 (5), 886-888, 10.1007/bf02697293.
- [21]. Khabarov, Y. G.; Lakhmanov, D. E.; Kosyakov, D. S.; Ul'yanovskii, N. V.; Veshnyakov, V. A.; Nekrasova, O. A., Nitration of phenol in 1,4-dioxane. *Russian Journal of Applied Chemistry* **2015**, 88 (11), 1783-1787, 10.1134/s10704272150110075.
- [22]. Ducry, L.; Roberge, D. M., Controlled Autocatalytic Nitration of Phenol in a Microreactor. *Angew. Chem., Int. Ed.* **2005**, 44 (48), 7972-7975, 10.1002/anie.200502387.
- [23]. Vione, D.; Belmondo, S.; Carnino, L., A kinetic study of phenol nitration and nitrosation with nitrous acid in the dark. *Environmental Chemistry Letters* **2004**, 2 (3), 135-139, 10.1007/s10311-004-0088-1.
- [24]. Albright, L. F.; Schiefferle, D. F.; Hanson, C., Reactions occurring in the organic phase during aromatic nitrations. *Journal of Applied Chemistry and Biotechnology* **1976**, 26, 522-525, 10.1002/jctb.5020260174.
- [25]. Russo, D.; Marotta, R.; Commoco, M.; Andreozzi, R.; Somma, I. D., Ternary HNO₃-H₂SO₄-H₂O Mixtures: A Simplified Approach for the Calculation of the Equilibrium Composition. *Industrial & Engineering Chemistry Research* **2018**, 57 (5), 1696-1704,
- [26]. Schiefferle, D. F.; Hanson, C.; Albright, L. F., Heterogeneous Nitration of Benzene. In *Industrial and Laboratory Nitrations*, American Chemical Society, Washington, DC. ACS Symposium Series, 1976; Vol. 22, pp 176-189, doi:10.1021/bk-1976-0022.ch011
10.1021/bk-1976-0022.ch011.

- [27]. Burns, J. R.; Ramshaw, C., A Microreactor for the Nitration of Benzene and Toluene. *Chemical Engineering Communications* **2002**, 189 (12), 1611-1628, 10.1080/00986440214585.
- [28]. Buchi, S. D.; Guenkel, A. A. Method of purifying nitrated aromatic compounds from a nitration process. WO2016198921A1, December 15, 2016.
- [29]. Quadros, P. A.; Oliveira, N. M. C.; Baptista, C. M. S. G., Continuous adiabatic industrial benzene nitration with mixed acid at a pilot plant scale. *Chemical Engineering Journal* **2005**, 108 (1), 1-11, <http://dx.doi.org/10.1016/j.cej.2004.12.022>.
- [30]. Andreozzi, R.; Canterino, M.; Caprio, V.; Somma, I. D.; Sanchirico, R., Batch salicylic acid nitration by nitric/acetic acid mixture under isothermal, isoperibolic and adiabatic conditions *Journal of Hazardous Materials* **2006**, 138 (3), 452-458,
- [31]. Russo, D.; Somma, I. D.; Marotta, R.; Tomaiuolo, G.; Andreozzi, R.; Guido, S.; Lapkin, A. A., Intensification of Nitrobenzaldehydes Synthesis from Benzyl Alcohol in a Microreactor. *Org. Process Res. Dev.* **2017**, 21 (3), 357-364,
- [32]. Russo, D.; Tomaiuolo, G.; Andreozzi, R.; Guido, S.; Lapkin, A. A., Heterogeneous benzaldehyde nitration in batch and continuous flow microreactor. *Chemical Engineering Journal* **2018**,
- [33]. Russo, D.; Onotri, L.; Marotta, R.; Andreozzi, R.; Somma, I. D., Benzaldehyde nitration by mixed acid under homogeneous condition: A kinetic modeling. *Chemical Engineering Journal* **2017**, 307, 1076-1083,
- [34]. Nogueira, A. G.; Silva, D. C. M.; Reis, M. S.; Baptista, C. M. S. G., Prediction of the By-products Formation in the Adiabatic Industrial Benzene Nitration Process. *Chemical Engineering Transactions* **2013**, 32, 1249-1254,
- [35]. Santos, P. A. Q. d. O. Nitração de Compostos Aromáticos: Transferência de Massa e Reação Química. PhD Thesis, Universidade de Coimbra, Portugal, 2004.
- [36]. Denissen, L.; Stroofer, E.; Arndt, J.-D.; Mattke, T.; Heinen, K.; Leschinski, J. Process for Preparing Mononitrated Organic Compounds. US Patent 8,592,637 B2, November 26, 2013.
- [37]. Olsen, F.; Goldstein, J. C., The Preparation of Picric Acid from Phenol. *Ind. Eng. Chem.* **1924**, 16 (1), 66-71, 10.1021/ie50169a027.
- [38]. Lindner, O.; Rodefeld, L., Benzenesulfonic Acids and Their Derivatives. In *Ullmann's Encyclopedia of Industrial Chemistry*, Wiley-VCH, 2000, doi:10.1002/14356007.a03_507.
- [39]. Lopes, A. L. C. V.; Ribeiro, A. F. G.; Reis, M. P. S.; Silva, D. C. M.; Portugal, I.; Baptista, C. M. S. G., Distribution models for nitrophenols in a liquid-liquid system. *Chemical Engineering Science* **2018**, 189, 266-276,
- [40]. Deno, N. C.; Stein, R., Carbonium Ions. III. Aromatic Nitration and the C0 Acidity Function. *J. Am. Chem. Soc.* **1956**, 78 (3), 578-581, 10.1021/ja01584a018.

- [41]. Fogler, H. S., Elements of Chemical Reaction Engineering. Prentice Hall, New Jersey, USA, 2006,
- [42]. Krämer, S.; Gesthuisen, R., Simultaneous estimation of the heat of reaction and the heat transfer coefficient by calorimetry: estimation problems due to model simplification and high jacket flow rates—theoretical development. *Chemical Engineering Science* **2005**, *60* (15), 4233-4248, <https://doi.org/10.1016/j.ces.2005.02.060>.
- [43]. Carwile, L. C. K.; Hoge, H. J. *Thermal Conductivity of Pyrex Glass: Selected Values*; United States Army Natick Laboratories: Massachusetts, 1966.
- [44]. Ashby, M. F., Chapter 15 - Material profiles. In *Materials and the Environment*, 2nd edition, Butterworth-Heinemann, Boston, 2013; pp 459-595, <https://doi.org/10.1016/B978-0-12-385971-6.00015-4>.
- [45]. Dumann, G.; Quittmann, U.; Gröschel, L.; Agar, D. W.; Wörz, O.; Morgenschweis, K., The capillary-microreactor: a new reactor concept for the intensification of heat and mass transfer in liquid–liquid reactions. *Catalysis Today* **2003**, *79–80*, 433-439, [http://dx.doi.org/10.1016/S0920-5861\(03\)00056-7](http://dx.doi.org/10.1016/S0920-5861(03)00056-7).

Chapter 6 – (Nitro)benzenesulfonic acids in nitrobenzene production³

Abstract

An analytical methodology was developed which allowed identifying, for the first time, the presence of sulfonated aromatic species such as benzenesulfonic acid, 2-mononitrobenzenesulfonic acid, 3-mononitrobenzenesulfonic acid and 4-mononitrobenzenesulfonic acid in an industrial mixed acid benzene nitration plant. The compounds identification was accomplished by analysing their molecular ion and fragmentation pattern, data obtained from a mass spectrometry analysis, and their UV-Vis spectra.

The effect of some operating conditions in the formation of the identified species during lab scale nitration experiments such as the reaction temperature, sulfuric acid concentration and the composition of the nitrated organic substrate was analysed. It was found that higher reaction temperature and sulfuric acid concentration enhances sulfonic acids formation and that benzene nitration tends to form higher sulfonic acids amounts than mononitrobenzene nitration. It was also found that benzenesulfonic acid partition coefficient ($C_{\text{Organic phase}}/C_{\text{Aqueous phase}}$) in the liquid-liquid reaction system was comprehended between 0.11 and 0.45, meaning higher affinity for the acid phase. For the mononitrobenzenesulfonic acids the determined partition coefficients were between 0.04 and 0.13 in benzene nitration and between 0.19 and 0.35 in mononitrobenzene nitration (again with higher affinity for the acid phase). The performed nitration tests allowed to prove unequivocally, for the first time, that sulfonic acids are formed during benzene nitration at the typical range of industrial mixed acid benzene nitrating conditions.

Keywords: Benzene nitration, sulfonation, benzenesulfonic acid, mononitrobenzenesulfonic acid.

³ Diogo Afonso, Alejandro F. G. Ribeiro, Paulo Araújo, Joaquim Vital and Luis Miguel Madeira, (Nitro)benzene sulfonic acids in nitrobenzene production, *submitted*.

6.1. Introduction

Aromatic nitration is a known chemical reaction that has been subject to continuous improvements and studies due to its importance for the chemical industry. Still, despite the performed studies, there are some matters concerning aromatic nitration which remain not fully understood, namely the parallel reactions that can occur.

Usually, in studies addressing mixed acid benzene (Bz) nitration, a reaction between Bz and nitric acid catalysed by sulfuric acid, the considered side reactions are related with nitrophenols or dinitrobenzene formation, the typical reaction by-products. Regarding nitrophenols formation, it is postulated that these compounds are initially formed by benzene oxidation to phenol [1]. Recently, it was experimentally proved that phenol is the nitrophenols precursor and that nitrophenols are formed by sequential nitrations, i.e., phenol forms mononitrophenols, mononitrophenols originate dinitrophenols which in turn are nitrated to trinitrophenol [2-3]. As for dinitrobenzene formation, it is known to occur by mononitrobenzene (MNB) nitration [4] – Figure 6.1.

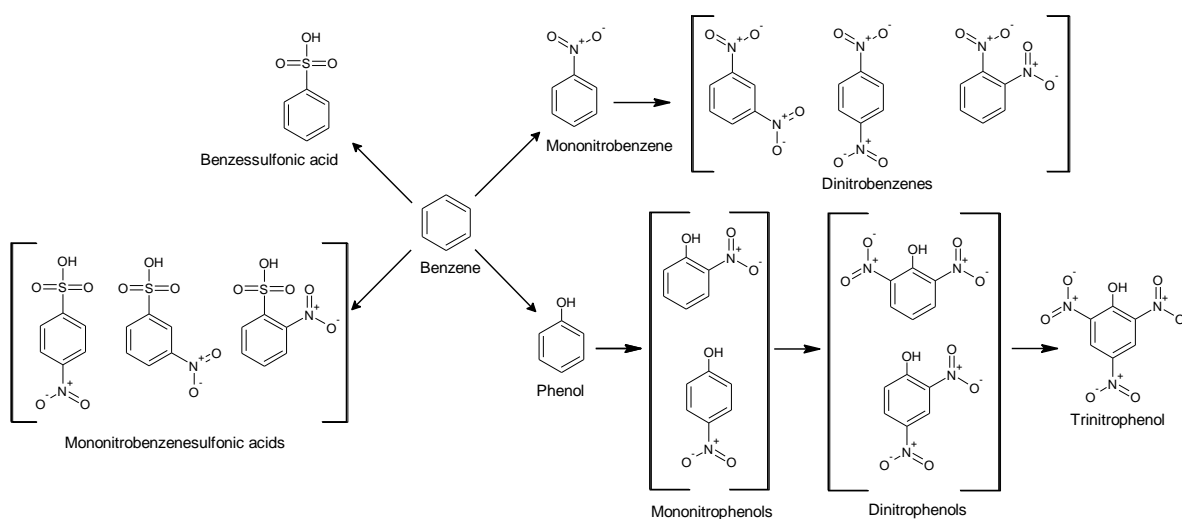


Figure 6.1 – Possible by-products of the mixed acid ($\text{HNO}_3 + \text{H}_2\text{SO}_4$) benzene nitration reaction.

However, in industrial mixed acid Bz nitration, other reaction by-products such as benzenesulfonic acid (BSA) and mononitrobenzenesulfonic acids (MNBSA) are also formed – Figure 6.1. To our knowledge, these reaction by-products were never addressed in industrial mixed acid Bz nitration studies.

Although Rahaman *et al.* [5] have anticipated 3-MNBSA formation at 298 K, through MNB sulfonation, when studying MNB nitration at high sulfuric acid concentrations, the authors were not able to detect this compound. The authors justified 3-MNBSA absence by the presence of the nitro group (-NO₂) in the Bz ring, which hinders MNB sulfonation turning it in a slow reaction. Later, Rahaman *et al.* [6] found that at high sulfuric acid concentrations and temperatures above 323 K, 3-MNBSA formation was significant.

Additionally, while studying Bz nitration at high sulfuric acid concentration, Sarkar *et al.* [7] found that Bz could be converted into BSA in the absence of nitric acid, and that Bz sulfonation is directly proportional to sulfuric acid concentration.

Notwithstanding, it is important to emphasize that none of the mentioned works [5-7] had as objective the study of the sulfonic acids derivatives (BSA and MNBSA) formation. Beyond that, the employed reaction conditions, namely the sulfuric acid concentration, were harsher than the typical industrial values used for Bz nitration and these studies did not contemplate industrial data.

Sulfonation reactions can be used together with nitration, in a two-step system, when nitration is intended to be moderated and the side reactions minimized [8-9]. This is a common strategy for nitrating phenolic substrates. Despite that, studies regarding sulfonic acids formation during Bz nitration are inexistent. This is most likely due to Bz nitration conditions, which do not favour neither BSA nor MNBSA formation. For instance, in Bz sulfonation aqueous sulfuric acid (76 – 100% wt.) or oleum (mixture of sulfuric trioxide and sulfuric acid) are usually used as the sulfonation agent [10-11], while in mixed acid Bz nitration sulfuric acid concentration is lower than 70% wt. [12-13]. For producing MNBSA, the starting organic raw material can be either BSA, MNB or nitrochlorobenzene, and the reaction conditions depend on the isomer to be produced [12]. Neither one of these production processes involve a two-step system in which the first step is Bz nitration. Additionally, in MNB production by mixed acid Bz nitration only the typical reaction by-products, nitrophenols and dinitrobenzene, are controlled [14-15] to ensure that the produced MNB complies with the final product specifications. Therefore, the formation and presence of the sulfonic acid derivatives (BSA and MNBSA) in the reaction medium is an unexplored subject in Bz nitration papers.

In this study, an analytical methodology was developed aiming to determine BSA and MNBSA presence in the reaction medium of both industrial and lab scale mixed acid Bz nitrations. Detecting these compounds in an industrial Bz nitration plant was a goal of the present work because it allows to verify if they are building-up in the plant and because sulfonic acids can form viscous gels with water [16] leading to the formation of emulsions that may jeopardize the nitration plant operation. At lab scale, a preliminary parametric study was performed in which sulfonic acids formation was related with the following parameters: temperature, sulfuric acid concentration and organic substrate composition.

6.2. Material and methods

The chemical reagents used in the present study were: benzene nitration grade (> 99.99 %) from Vitol S.A., mononitrobenzene (99.99 %) from Bondalti production process, benzenesulfonic acid (>97%) from Merck, 2-nitrobenzenesulfonic acid hydrate (>98%) from TCI, 3-

nitrobenzenesulfonic acid hydrate (>97%) from TCI, 4-nitrobenzenesulfonic acid hydrate (> 98%) from TCI, sulfuric acid (99 wt.%) from Quimitecnica, and nitric acid (65 wt.%) from Baker.

6.2.1. Laboratorial tests

Batch reactions were performed to verify sulfonic acids formation during mixed acid Bz nitration. These tests were conducted in a jacketed laboratory reactor equipped with a tantalum air-impelled stirrer and a Teflon coated thermocouple (Figure 6.2).

The experimental procedures used for the performed tests are summarized as follows: before the start of each reaction, sulfuric acid was added to the reactor by its top (valve V-5) and the thermostatic bath (MPC-K6) from Huber (E-2) was turned on. Then, when the temperature of the reaction medium was the intended one, nitric acid was added, again by the reactor's top (valve V-5). Throughout the aqueous phase heating or cooling, the stirrer was working to promote the acids mixture and the homogenization of the reaction medium composition and temperature. When the intended reaction temperature was reached, the stirring speed was adjusted to the defined value and the organic substrate was added (quickly, < 5 seconds), through the reactor's bottom (valve V-3). During the reaction time samples were collected from the reactor's bottom (valve V-4) at predefined times. At the reaction end the stirrer was turned off and the reactional mixture was decanted for 10 minutes. Then the distinct phases of the reaction mixture were collected, separately, from the reactor's bottom by means of valve V-4. The temperature of the system was recorded using a Therna 1 thermometer from ETI Ltd.

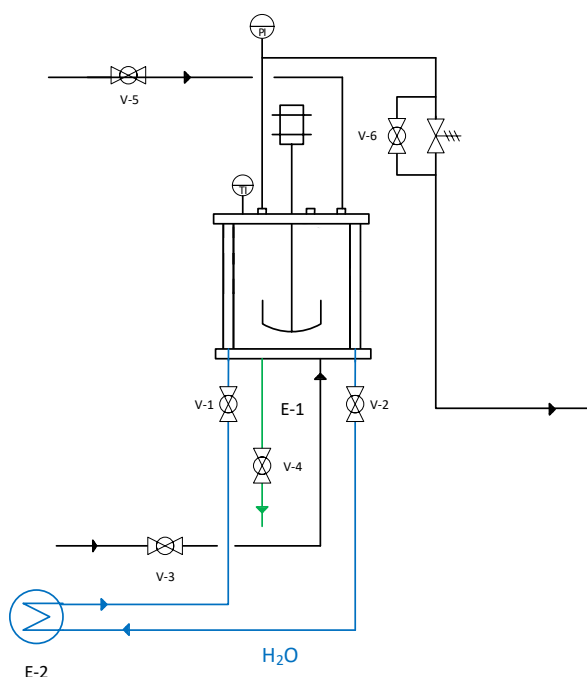


Figure 6.2 – Scheme of the laboratorial reactor used in the batch reactions.

The conditions of the experiments performed in this study (given in Table 6.1) were similar to industrial Bz nitration ones once it was proposed to ascertain if (nitro)sulfonic acids were being formed in the industrial reactor.

Table 6.1 – Reaction conditions of the performed nitration tests. Reaction time: 30 minutes; stirring speed: 1200 r.p.m; HNO₃ = 5% wt..

Run	Organic substrate	H ₂ SO ₄ (% wt.)	T _{initial} (°C)
E1	Bz	66	90
E2	Bz	66	70
E3	Bz	60	90
E4	MNB	66	90
E5	MNB+BSA (150 ppm)	66	90
E6	MNB+BSA (150 ppm)	66	90

The parameters changed between the conducted tests are highlighted in bold.

6.2.2. Samples preparation

The organic samples needed to be extracted to an aqueous phase to be injected in the HPLC-DAD equipment. The extraction was done by adding a determined demineralized water amount to the organic phase being then the mixture vigorously shaken. The final step was the mixture phase separation which was done resorting to a centrifuge from Hettich (Rotanta 460). The resulting aqueous phase was the one analysed by HPLC. The extraction yield was found to be higher than 90%. If the organic sample was basic, the extracted aqueous phase was acidified with sulfuric acid to prevent acid base reactions since the eluent was acid. The same pH adjustment was done for alkaline aqueous samples.

As for the acidic aqueous samples, they were simply diluted with demineralized water to decrease the acid strength and, consequently, protect the chromatographic column.

6.2.3. HPLC-DAD analytical method

The liquid chromatographic analyses were performed in an Elite LaChrom HPLC-DAD apparatus from VWR-Hitachi equipped with a reverse phase column (Purospher® STAR RP-18e LiChroCART®) packed with silica microspheres (5 µm, 250 mm x 4 mm) and a guard column (LiChroCART® - 5 µm, 4mm x 4mm). The temperature of the chromatographic column was maintained at 30 °C by the HPLC's oven and the volume of the injected sample was 10 µL. The eluent feed was in gradient mode with a KH₂PO₄ solution (2.5 mM, pH ≈ 2.4) and acetonitrile as follows:

- 0 – 5 minutes: 0.4 mL/min, 88% KH_2PO_4 , 12% acetonitrile;
- 5 – 11 minutes: 1.0 mL/min, 88% KH_2PO_4 , 12% acetonitrile;
- 11 – 23 minutes: 1.0 mL/min: 50% KH_2PO_4 , 50% acetonitrile;
- 23 – 26 minutes: 1.0 mL/min, 88% KH_2PO_4 , 12% acetonitrile;
- 26 – 30 minutes: 0.4 mL/min, 88% KH_2PO_4 , 12% acetonitrile.

6.2.4. UHPLC-MS analytical method

In order to perform mass spectroscopy (MS) analysis, the developed HPLC-DAD analytical method had to be adapted to comply with some restrictions since the use of H_2SO_4 (the eluent's acidifying agent) and of non-volatile buffers is not recommended in MS analysis [17-18]. The mobile phase was replaced by a simple 0.15% (V/V) aqueous acid solution, since formic acid can be used both as the acidifying agent and as the KH_2PO_4 salt substitute [19-20].

To separate the different analytes, an Ultimate 3000RSLC HPLC from Thermo Scientific equipped with a Thermo Fisher Hypersil GOLD column (100 x 2.1mm; particle size 1.9 μm) and a Dionex Ultimate 300 RS diode array detector was used. The UHPLC was coupled to a LTQ XL Lianar Ion Trap 2D mass spectrometer (Thermofisher Scientific), equipped with an orthogonal electrospray ionization source operating in the negative ion mode. The spray voltage was 5 kV and the capillary voltage temperature was 275 °C.

6.3. Results and discussion

6.3.1. Identification of (nitro)benzenesulfonic acids in mixed acid industrial benzene nitration medium

A new analytical methodology was developed for detecting nitration by-products. This analytical methodology allowed to detect some chromatographic peaks, not detected to date, that show high intensities and well-defined UV-Vis spectra as it is visible in the HPLC-DAD chromatogram of a crude MNB (non-purified MNB) sample – Figure 6.3, namely peaks 1, 2, 3 and 4.

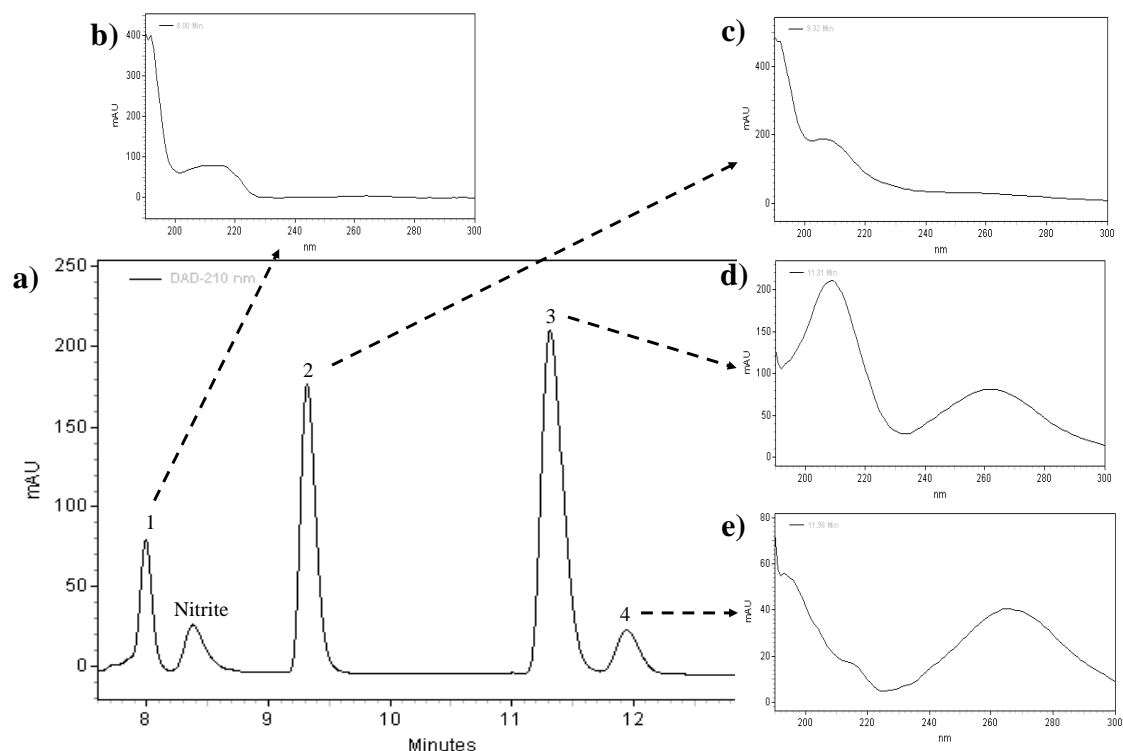


Figure 6.3 – a) Crude MNB HPLC-DAD chromatogram. b), c), d) and e) UV-Vis spectra of different detected chemical species.

The presented UV-Vis spectra (Figure 6.3 – b), c) and d)) show that three of the four compounds have a maximum of absorption near 210 nm, having the other compound (Figure 6.3 – e)) a maximum of absorption at 265 nm. However, in addition to the chemical species UV-Vis spectra, no more indications were known aiming their identification. A literature survey was done aiming identifying these chemical species by comparing the obtained UV-Vis spectra, a “fingerprint” of each compound, with internet databases and scientific papers without positive results. Thus, MS analysis were performed. Assessing the analyte’s MS information, their structure could be enlightened since when ionized the analytes’ molecular ion and mass fragments are formed. These fragments represent building blocks and can describe the original structure of the analyte while the molecular ion enables determining the analyte’s molecular weight [21].

The obtained results are depicted in Figure 6.4. In this figure is presented a total ion chromatogram (Figure 6.4 – a)), that evidences the presence of several chemical species in the crude MNB sample, and mass and UV-Vis spectra of different compounds (Figure 6.4 – b), c), d) and e)). The conducted analysis allowed also to obtain the molecular ion and the fragmentation pattern of the detected analytes (Table 6.2).

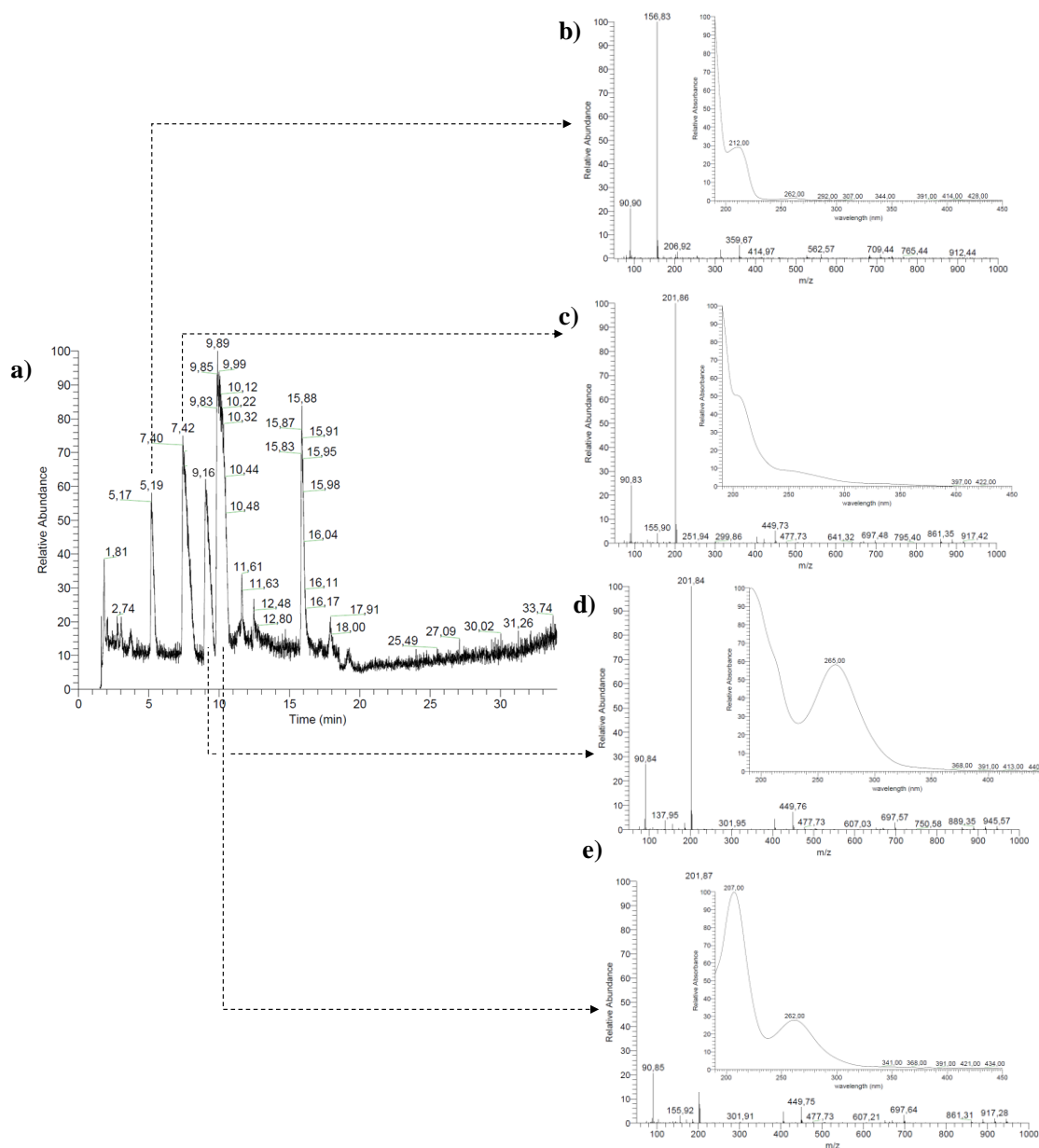


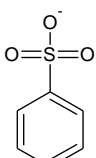
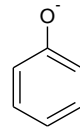
Figure 6.4 – Crude MNB **a)** Total Ion Chromatogram. **b), c), d)** and **e)** mass and UV-Vis spectra of different analytes.

From the achieved analytical data, is noteworthy the resemblance between the analytes UV-Vis spectra (Figure 6.3) with the ones present in Figure 6.4. This is indicative that the detected unknown compounds (1, 2, 3 and 4, Figure 6.3) were during the mass spectroscopy analyses.

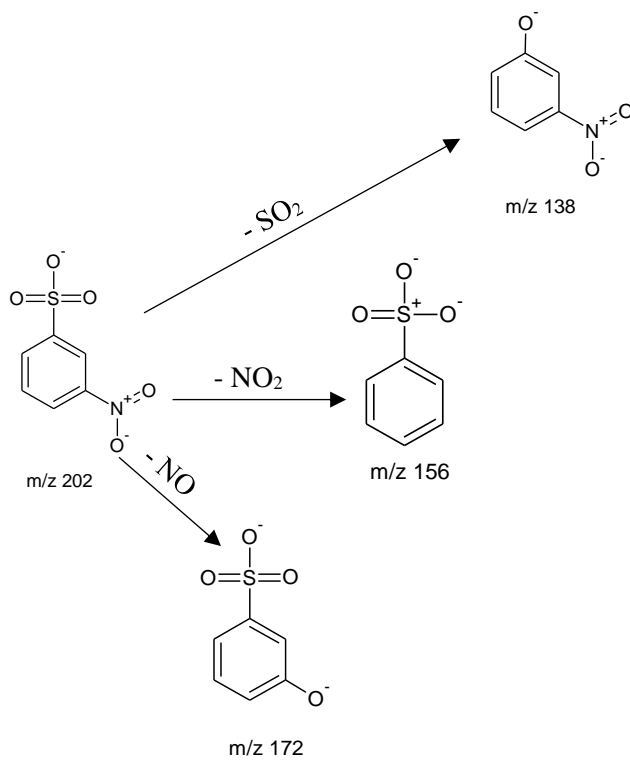
Scrutinizing the total ion chromatogram is visible the presence of three analytes with large and intense chromatographic peaks (retention times: 7.42, 9.16 and 9.89 minutes) and two others with large but less intense peaks (retention times: 5.19 and 15.88). A quick analysis to each analyte's mass spectrum enabled to identify one of the analytes (retention time: 15.88 minutes) as trinitrophenol, a typical benzene nitration by-product. The remaining analytes mass spectra were studied in detail since they didn't correspond to the other usual Bz nitration by-products.

In Figure 6.4 – c), d), e) and in Table 6.2 is shown that the compounds with retention times of 7.42, 9.16 and 9.89 minutes have the same molecular ion and the same fragmentation pattern, which means that they are isomers.

Table 6.2 – Mass fragmentation pattern of some of the detected species.

Retention time (min)	m/z [M-H] ⁻	MS/MS			
	157	129	113	93	
5.19	 m/z 157	$\xrightarrow{-\text{SO}_2}$		 m/z 93	
7.42	202	172	156	138	
9.16	202	172	156	138	
9.89	202	172	156	138	

7.42; 9.16; 9.89



The isomers' molecular weight was related with their molecular ion value (202) once the molecular ion is formed by the removal of positive ions (H^+) from the molecule. Therefore, it was determined that the compounds' molecular weight was 203. The fragmentation pattern enabled to figure out which functional groups were present in the analytes' structure, being found that the detected isomers exhibits mass fragments which allowed deducing the loss of 30 u (202-172), 46 u

(202-156) and 64 u (202-138) from the molecular ion – Table 6.2 - indicating the loss of NO, NO₂ and SO₂, respectively. Additionally, the high intensity signal detected for these three species reinforces the suspicion of sulfur presence in the analysed molecules since this atom is responsible for the production of intense peaks [22]. The detection of NO and NO₂ indicates that these compounds are nitrated and the SO₂ fragment points that they are sulfonated as well. Compiling the obtained data referent to the molecular ion and the mass fragments, these analytes were identified as MNBSA (203.16 g·mol⁻¹) isomers (2-MNBSA, 3-MNBSA and 4-MNBSA).

Regarding the analyte with the retention time of 5.19 minutes (Figure 6.4 – a)), it is noticeable that its molecular ion has a m/z value of 157 (Figure 6.4 – b); Table 6.2). As for this analyte mass fragmentation pattern, the gotten results show indicate the loss of 64 u (157 - 93), 44 u (157 - 113) and 28 u (157 - 129), corresponding, respectively, to SO₂, CO₂ and CO, N₂ or C₂H₄. Relating this data, the analyte could be identified as BSA since this acid molar mass is 158.117 g·mol⁻¹ and contains SO₂ in its structure. Nevertheless, the remaining determined mass fragments (44 u and 28 u) shouldn't be present in the BSA fragmentation pattern. This suggests that at 5.19 minutes retention time two chromatographic peaks should be overlapped.

To confirm BSA identification, a crude MNB sample and a BSA-added crude MNB sample were analysed by HPLC-MS. These analyses allowed to confirm BSA presence in crude MNB since the addition of the sulfonic acid led to a chromatographic peak area rise for the analyte identified as BSA (with the retention time of 5.9 minutes, see Appendix E, Figure E.1). Moreover, it was verified in both the analysed samples the same molecular ion value for the analyte in question.

The identification of sulfonic acids (BSA and MNBSA) reveals that sulfonation reactions are occurring in a Bz nitration plant, most likely in the reaction section because this is the location where higher temperatures are reached in the presence of sulfuric acid. This means that in addition to the typical benzene nitration by-products (nitrophenols and dinitrobenzene) there is another by-products class, the sulfonic one.

To confirm unequivocally that the detected compounds, i.e. (nitro)benzenesulfonic acids, are present in the a Bz nitration plant, standards of such species were added individually to a crude MNB sample, being the sample then analysed by the developed HPLC-DAD method – Figure 6.5. The goal of these analyses was to determine the standard sulfonic acids retention times, to check if the standards retention times corresponded to any of the detected chromatographic peaks and to compare the obtained UV-Vis spectra (Figure 6.3) with those of the standards ones.

Decomposition Reactions in Aromatic Nitration

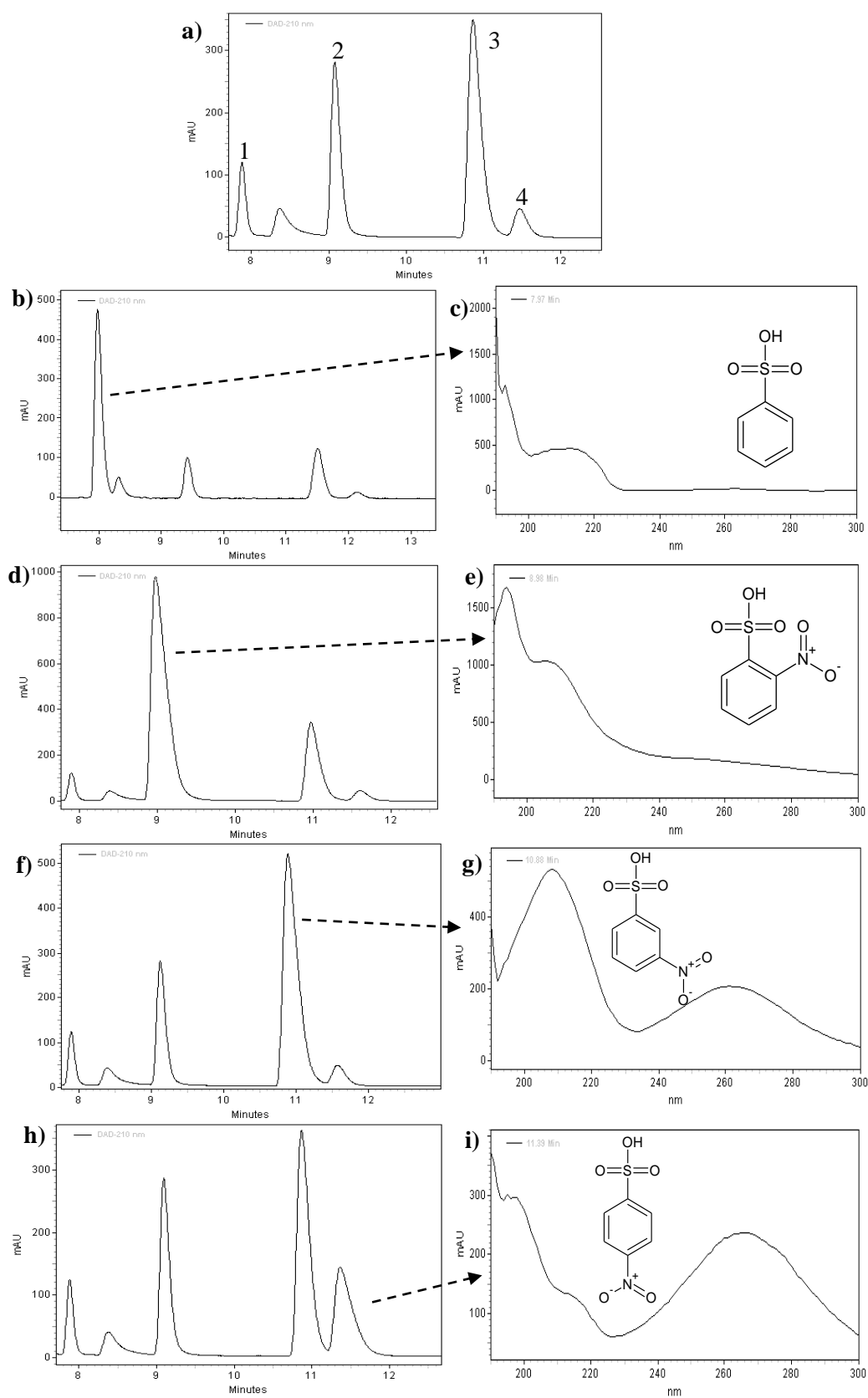


Figure 6.5 – HPLC chromatograms of **a)** crude MNB, and crude MNB added with **b)** BSA, **d)** 2-MNBSA, **f)** 3-MNBSA or **h)** 4-MNBSA. UV-Vis spectra of **c)** BSA, **e)** 2-MNBSA, **g)** 3-MNBSA and **i)** 4-MNBSA.

In Figure 6.5 – a) is presented a crude MNB chromatogram which was used as reference. Figure 6.5 – b), d), f) and h) represent the HPLC chromatograms for the crude MNB sample to which the different sulfonic acids standards were added, while Figure 6.5 – c), e), g) and i) illustrate the sulfonic acids UV-Vis spectra.

When BSA was added to the crude MNB sample it was noticed that the chromatographic peak (1) increased its area – comparison of Figure 6.5 – a) and b). Additionally, the standard UV-Vis spectrum (Figure 6.5 – c)) is very similar to the one displayed in Figure 6.3 – b), showing an absorption maximum near 210 nm. These facts allow to confirm BSA presence in the benzene nitration plant and are in accordance with the results from the MS analysis.

The results obtained for the 2-MNBSA addition to the crude MNB sample show an area increase of the chromatographic peak (2) – Figure 6.5 – d). Comparing both the reference test UV-Vis spectrum (Figure 6.3 – c)) and the standard 2-MNBSA UV-Vis spectrum (Figure 6.5 – e)) is noticeable their resemblance, thus being possible to confirm the 2-MNBSA presence in a nitration plant. The same procedure was followed to determine the 3-MNBSA and 4-MNBSA presence, chromatographic peaks (3) and (4), respectively, being once again noticeable the resemblance between the UV-Vis spectra of the standard acids and of the reference test.

The detection of BSA and MNBSA isomers in a benzene nitration plant was an important discovery since their presence is not addressed in benzene nitration studies. These compounds were found to be present in different plant locations of the nitration plant [23].

6.3.2. Laboratorial tests

To prove that (nitro)benzenesulfonic acids were being formed in the reaction section of a nitration plant, a set of Bz nitrations was conducted at lab scale. These tests aimed also to understand how the effect of several operating conditions such as temperature, sulfuric acid concentration and the organic substrate composition could be related with sulfonic acids formation.

The influence of the reaction temperature, an important parameter in Bz nitration because affects both the reaction rate and the nitrophenols formation [24-25], was checked by varying its initial values between 90 °C and 70 °C (runs E1 and E2, respectively, Table 6.1), which are within the industrial range of temperatures. The achieved results for these runs are depicted in Figure 6.6.

According to the depicted temperature profiles (Figure 6.6 – a)) it is noticeable their resemblance, i.e., 2 minutes after the reaction start is reached a temperature maximum in both tests, which then starts decreasing. This temperature rise is explained by Bz nitration exothermicity.

Decomposition Reactions in Aromatic Nitration

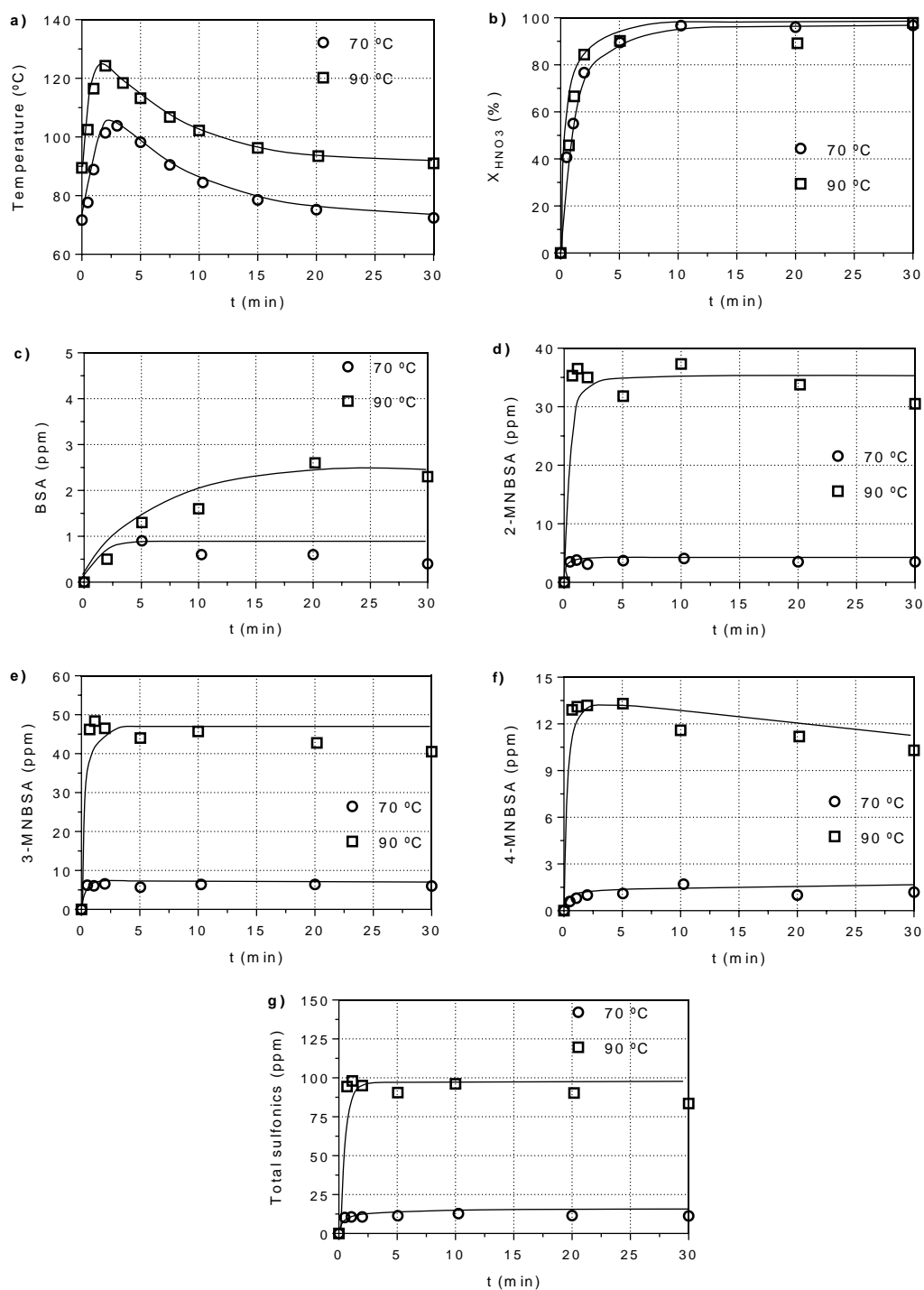


Figure 6.6 – a) Temperature evolution; b) Nitric acid conversion; and c) BSA; d) 2-MNBSA; e) 3-MNBSA; f) 4-MNBSA and g) total sulfonic acids concentration profiles for runs E1 (90 °C) and E2 (70 °C) in both reaction phases. % wt. H_2SO_4 = 66; % wt. HNO_3 = 5. Lines are added just for a better visualization of the trends.

Regarding nitric acid conversion during the reaction time (Figure 6.6 – b)), it is observable a slightly higher consumption rate for the highest temperature run. This can be justified by the known

positive effect of the (higher) temperature on nitration rate. Nevertheless, the acid conversion at the reaction end was similar in both tests (98% - run E1; 97% run E2).

The conducted runs allowed also to observe that the sulfonic acids previously detected (in industrial samples) are indeed formed during Bz nitration – Figure 6.7. In fact, in this figure is visible the resemblance between the detected sulfonic acid's UV-Vis spectra with those of the standard chemicals (Figure 6.5). Only the BSA UV-Vis spectrum evidences some differences when compared to the standard one, which can be explained by the effect of the large chromatographic peak in which BSA is overlapped. The 4-MNBSA UV-Vis spectrum is not well defined as the remaining ones due to the analyte low concentration.

Moreover, these tests enabled plotting, individually, each sulfonic acid total concentration profiles, i.e., in both reaction phases, as illustrated in Figure 6.6 – c), d), e) and f), and the total sulfonic acids amounts (also in both reaction phases) – Figure 6.6 – g). Analysing the sulfonic acids concentration history, it is concluded that higher reaction temperatures enhances these compounds formation. It is also visible, for the highest temperature run that BSA amounts are increased till 20 minutes after the reaction start while in run E2 BSA reaches a maximum concentration value shortly after the reaction start (5 minutes).

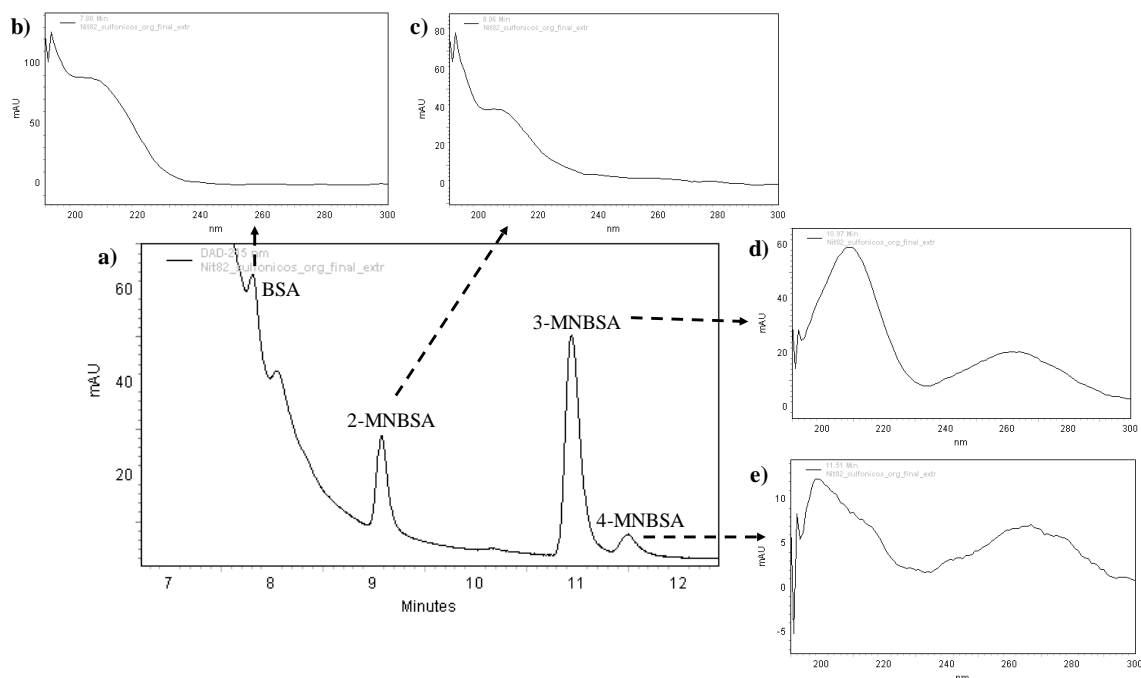


Figure 6.7 – a) HPLC-DAD chromatogram for run E1 (at the reaction end). b) BSA; c) 2-MNBSA; d) 3-MNBSA; e) 4-MNBSA UV-Vis spectra.

The presence of BSA in the reaction medium can be attributed to Bz sulfonation. Accordingly to Sarkar *et al.* [7], Bz sulfonation occurs when nitric acid disappears from the reaction medium; however, our results evidence that BSA formation occurs in the presence of unreacted nitric acid,

most likely because the temperature rise has a higher influence in sulfonation than the presence (or absence) of nitric acid in the nitration medium.

In the case of 2-MNBSA, the represented concentration profiles show that 0.5 minutes after the reaction start its maximum concentration is reached, tending, afterwards, to remain constant.

Scrutinizing the presented results for 3-MNBSA, one can find a similarity to the 2-MNBSA concentration profile, i.e., higher temperature enhances 3-MNBSA formation; 3-MNBSA amounts reach a maximum of concentration (at $t = 0.5$ minutes), that then tends to remain constant towards the reaction end. The data obtained from these tests reveals that this is the isomer formed in higher amounts, independently of the reaction temperature (for the employed mineral acids concentrations). This fact can be explained by the deactivating groups present in the molecule since both the nitro group and the sulfonic one are *meta* directors [26]. On the other hand, 4-MNBSA is the isomer formed in lower amounts in both the conducted tests.

As for the 4-MNBSA, the exhibited results reflect, once again, the positive effect of the reaction temperature in the sulfonic acids formation. Analysing 4-MNBSA concentration profiles, it is clearly seen that its maximum amount is reached 0.5 minutes after the reaction start for the highest temperature run, while in the lowest temperature run the reaction time needed for achieving the maximum concentration value is higher (5 to 10 minutes). Then, 4-MNBSA concentration remains nearly constant until the reaction end, decreasing marginally in the highest temperature run.

The plateau behaviour of MNBSA isomers is explained by the nitric acid depletion from the reaction medium ($t > 5$ minutes, $X_{\text{HNO}_3} > 90\%$), rendering unfeasible BSA nitration into MNBSA. Since BSA was detected in the reaction medium, it might be assumed that MNBSAs can be formed either by BSA acid nitration or by MNB sulfonation.

Summarizing, the comparison between the performed tests clearly confirms that the sulfonic acids formation is favoured by increasing the reaction temperature, which is in accordance with Rahaman *et al.* [6] and Kaandorp *et al.* [27] studies. This temperature dependence can be explained by the exponential temperature effect in the kinetics (according to the Arrhenius law) and by the solubility increase of benzene in the aqueous phase with increasing temperature [28]. However, despite the achieved conclusions, these tests do not reveal which compound (Bz or / and MNB) is the MNBSA isomers precursor. This issue will be addressed below.

Another important parameter in Bz nitration is the sulfuric acid concentration. Therefore, the influence of this parameter in the sulfonic acids formation was tested by comparing the results of two nitrations with different acid concentrations (runs E1 and E3 – Table 1). The gotten results are displayed in Figure 6.8.

The decrease of sulfuric acid concentration led to a lower temperature rise as it can be seen in Figure 6.8 – a). In the lowest sulfuric acid concentration run (E3) the reaction temperature reached a maximum value of 114 °C while in the highest acid concentration run (E1) the maximum value was of 124 °C. Lowering sulfuric acid concentration has also lowered nitric acid consumption rate,

resulting in a decrease of nitration rate, explaining thus the softer temperature rise verified in run E3. Nevertheless, nitric acid conversion at the reaction end was high in both runs (98% in run E1 and 95% in run E3).

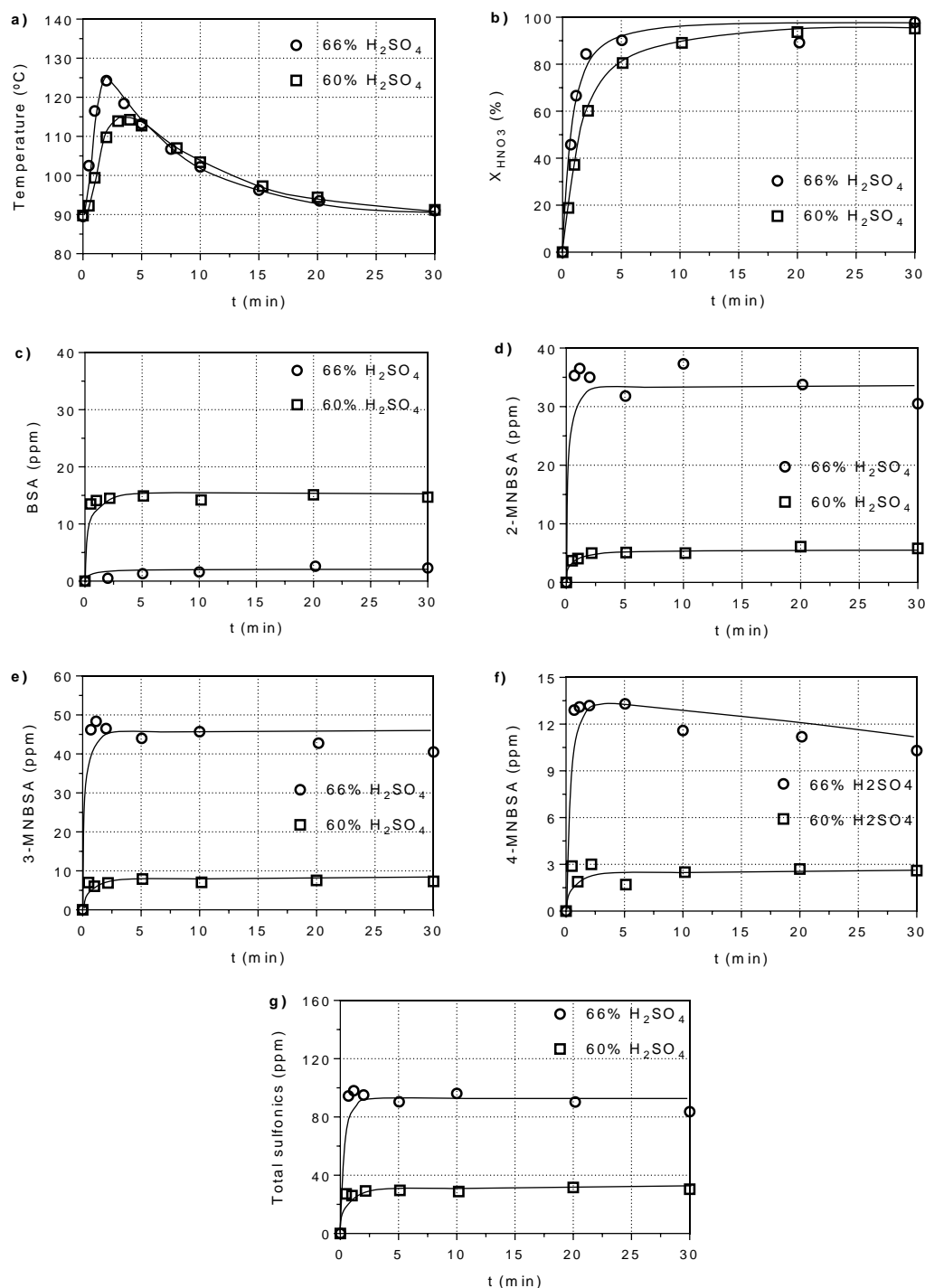


Figure 6.8 – a) Temperature evolution; b) Nitric acid conversion; and c) BSA; d) 2-MNBSA; e) 3-MNBSA; f) 4-MNBSA; and g) total sulfonic acids concentration profiles for runs E1 (66% wt. H_2SO_4) and E3 (60% wt. H_2SO_4) in both reaction phases. $T_{\text{initial}} = 90\text{ }^{\circ}\text{C}$; % wt. $\text{HNO}_3 = 5$. Lines are added just for a better visualization of the trends.

Examining the featured results for BSA in the lowest sulfuric acid concentration test, it is seen that this species concentration increases till 2 minutes after the reaction start, reaching a value of about 16 ppm, moment from where its amounts remained constant till the reaction end. Comparing the BSA concentration profiles for both runs, it is noticeable that the decrease of sulfuric acid concentration enabled increasing BSA amounts in the reaction medium. This fact, when analysed taking in consideration the depicted MNBSA concentration profiles, enables stating that BSA concentration is higher for the lowest sulfuric acid concentration run because its nitration into MNBSA was lower in this test. Additionally, as Bz sulfonation is directly proportional to the concentration of sulfuric acid [27], BSA nitration into MNBSA arises as the only logical explanation for the achieved results.

In the 2-MNBSA concentration history plot is visible that the increase of sulfuric acid concentration favours the formation rate of this sulfonic acid because the reaction time needed for reaching its maximum concentration rises from 0.5 in the highest sulfuric acid run to 2 minutes in the lowest mineral acid concentration test. Then, 2-MNBSA amounts remained nearly constant until the reaction end.

Comparing 3-MNBSA concentration profiles depicted in Figure 6.8 – e) it is seen that independently of the sulfuric acid concentration they are similar, i.e., a concentration maximum is achieved, and then the compound's amounts tend to remain constant. However, the concentration values for the lowest sulfuric acid run are 5 times lower than in run E1. Even so, as noticed before, 3-MNBSA is the isomer formed in higher amounts. Once again, this can be justified by the substituents groups present in the molecule, which are *meta* directors.

The results obtained for the 4-MNBSA show, once more, that this species concentration profile is represented by a plateau, although is visible a slight concentration decrease towards the reaction end in the highest sulfuric acid run. Additionally, as notice before, this isomer is the one formed in lesser amounts and its formation is influenced by sulfuric acid concentration.

The total sulfonic acids concentration depicted in Figure 6.8 – g) shows much larger amounts of sulfonic acids for the highest sulfuric acid run, evidencing thus the dependence between sulfonic acids formation and the sulfuric acid concentration.

In conclusion, the variation of sulfuric acid concentration allowed observing its impact on sulfonic acids origin, being concluded that higher sulfuric acid concentration enhance sulfonic acids formation. These results are in accordance with those of Cerfontain [29] addressed in Olah and Molnár [30] work and of Kaandorp *et al.* [27].

As the performed tests enabled suggesting that MNBSA isomers are formed by BSA nitration, the organic substrate was changed (from Bz to MNB) maintaining constant the remaining operation conditions (mixed acid composition, initial temperature and stirring speed – runs E1 and E4). The achieved results are illustrated in Figure 6.9.

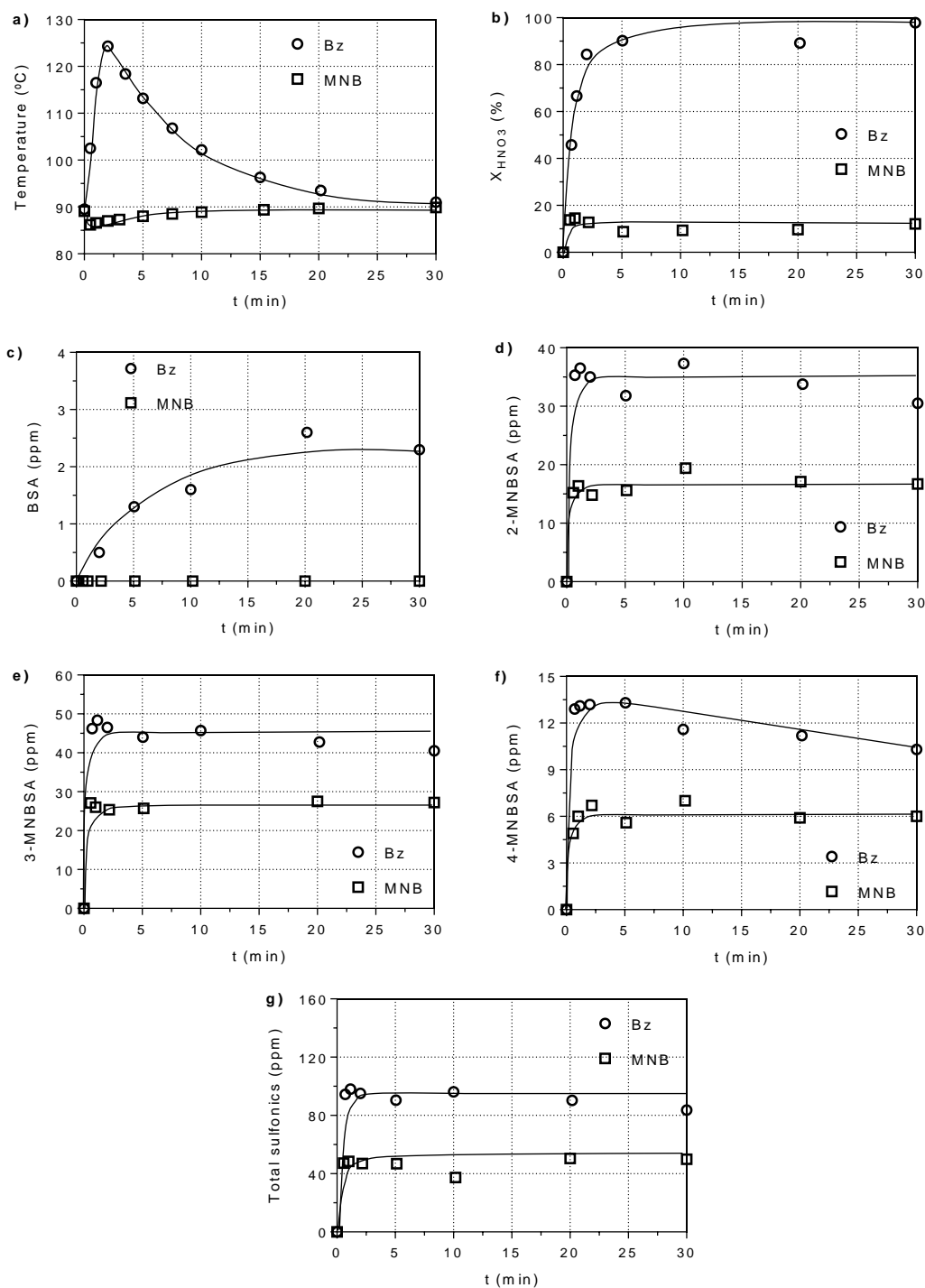


Figure 6.9 – a) Temperature evolution; b) Nitric acid conversion; and c) BSA; d) 2-MNBSA; e) 3-MNBSA; f) 4-MNBSA; and g) total sulfonic acids concentration profiles for runs E1 (organic substrate: Bz) and E4 (organic substrate: MNB) in both reaction phases. $T_{\text{initial}} = 90^\circ\text{C}$; % wt. $\text{H}_2\text{SO}_4 = 66$; % wt. $\text{HNO}_3 = 5$. Lines are added just for a better visualization of the trends.

The analysis of the temperature history for MNB nitration (run E4) reveals that initially the temperature diminishes slightly and then starts to increase until the reaction end. This initial

temperature drop can be justified by the temperature difference between the injected MNB (room temperature) and the mixed acid (90 °C). The following temperature increase is explained by the heat transferred from the reactor's jacket to the reaction medium.

Concerning nitric acid conversion, the results displayed in Figure 6.9 – b) show that the acid conversion was low (about 10%) for MNB nitration, an expected outcome since MNB nitration conditions are harsher than the ones employed in Bz nitration. The low nitric acid conversion led to a low extent of nitration and, consequently, to the release of low heat amounts, explaining thus the absence of a temperature peak in MNB nitration.

Regarding the sulfonic acid concentration profiles, when the used organic substrate was MNB, BSA was not detected in the reaction medium. This evidences, as expected, that BSA is formed by Bz sulfonation. On the other hand, MNBSA isomers were detected, being these compounds concentration about half of the detected values for Bz nitration run (E1). As noticed before, the MNBSA isomers reach a maximum concentration value which then remains constant until the reaction end. Once again, the isomer formed in higher amounts is the 3-MNBSA.

Analysing the total sulfonic acids quantities for both runs, it is visible that they are more than twice for Bz nitration when compared to MNB nitration. This fact is related with the absence of BSA in MNB nitration reaction medium and with the absence of a temperature peak, which was verified only in Bz nitration run and was found to affect positively the sulfonic acids formation.

The obtained results for MNB nitration clearly reveal that MNBSA can be formed by MNB sulfonation. Therefore, in order to confirm if BSA could be a MNBSA precursor other tests were performed in which the organic substrate (MNB) was enriched in BSA (run E5 and E6 – Table 6.1). MNB was the chosen organic substrate since it was verified that it is not a BSA precursor. The employed nitration conditions were similar to those of MNB nitration (run E4), being the obtained results disclosed in Figure 6.10.

The temperature and nitric acid conversion profiles were similar in both runs. As explained before, the temperature decreases slightly after the reaction start once the organic substrate temperature was lower than the one of the mixed acid, tending then to increase along the reaction time due to the heat transferred by the reactor's jacket. As for nitric acid conversion, it was low in both runs (about 10%) because the employed conditions do not favour MNB nitration. The similarity between both runs was an expected outcome since BSA added amounts were low (150 ppm in the organic phase).

Regarding BSA concentration profile (Figure 6.10 – c)) it is seen that its initial value is 13 ppm (considering both reaction phases, 150 ppm considering only the organic phase) which then, as the reaction proceeds, decreases until becoming undetected (5 minutes). BSA depletion from the reaction medium was expected once it was seen that MNB is not a BSA precursor.

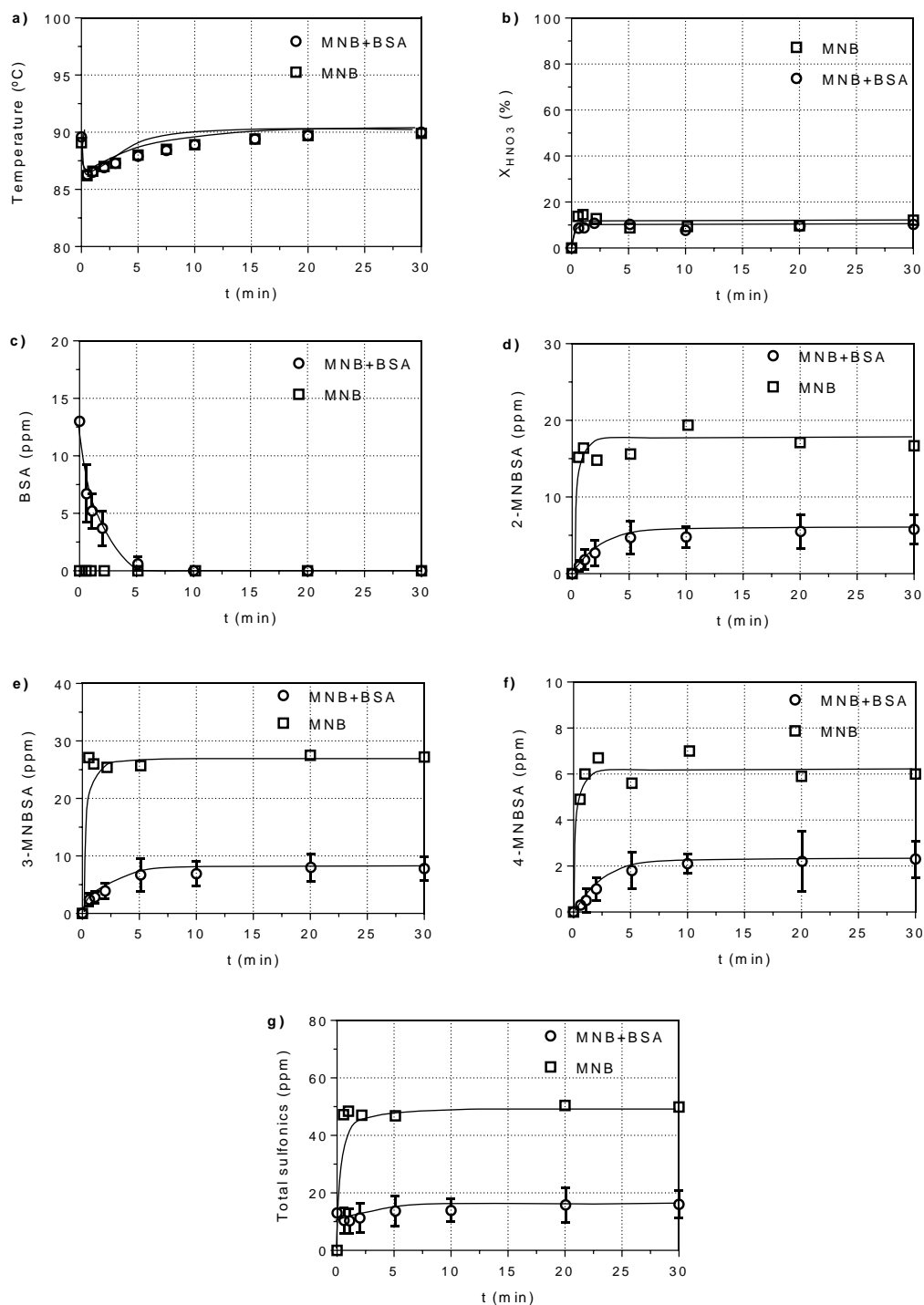


Figure 6.10 – a) Temperature evolution; b) Nitric acid conversion; and c) BSA; d) 2-MNBSA; e) 3-MNBSA; f) 4-MNBSA; and g) total sulfonic acids concentration profiles for runs E4 (organic substrate: MNB) and E5 and E6 (organic substrate: MNB+BSA (150 ppm in the organic phase)) in both reaction phases. For runs E5 and E6 the data points represent the average values for the performed runs while the vertical lines are related with the population standard deviation between the data. $T_{initial} = 90\text{ }^{\circ}\text{C}$; % wt. $\text{H}_2\text{SO}_4 = 66$; % wt. $\text{HNO}_3 = 5$. Lines are adjusted for a better visualization of the trends.

In Figure 6.10 – d) is depicted the 2-MNBSA amounts variation during the reaction time. In this figure is visible that 2-MNBSA concentration profile is described by a plateau, being the maximum concentration value reached 5 minutes after the reaction start (for the BSA-added MNB nitration), the moment in which BSA amounts became negligible, while in MNB nitration the maximum concentration value is reached 1 minute after the reaction start. This is indicative that this isomer was also formed by BSA nitration.

The analysis of 3-MNBSA and 4-MNBSA concentration profiles allow to infer the same behaviour noticed for 2-MNBSA, i.e., a maximum value of concentration is attained, which tends to remain constant after BSA disappearance from the reaction medium.

An interesting result is seen when analysing the sulfonic acids concentration profiles (individually or the total amounts), namely the fact that these compounds quantities were lower when the nitrated organic substrate was enriched in BSA. This was not expected since it was thought that the produced MNBSA amounts in the BSA-added MNB nitration would be similar to those of MNB nitration plus the amounts formed by (the added) BSA nitration. This is indicative that the initial BSA presence in the reaction medium, together with nitric acid, may have an inhibitory effect on MNBSA formation by MNB sulfonation. Nevertheless, the results point out that MNBSA isomers may be formed either by BSA nitration or by MNB sulfonation, as illustrated in Figure 6.11.

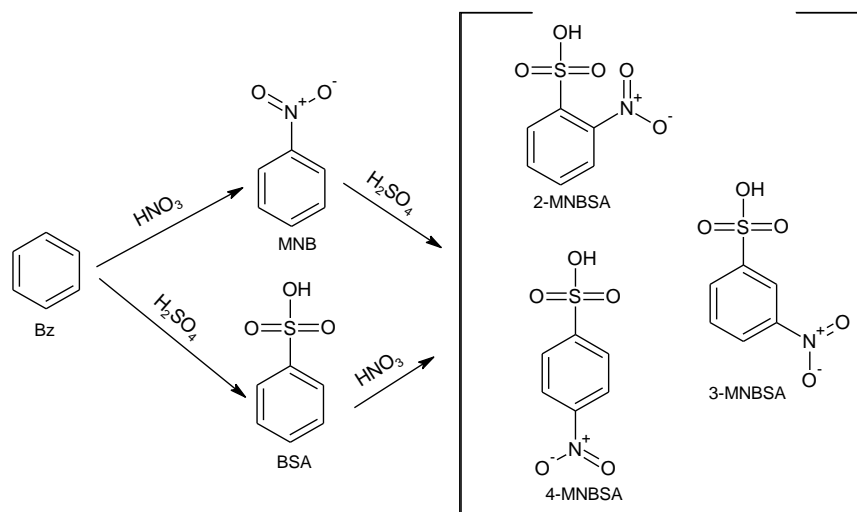


Figure 6.11 – Possible MNBSAs formation routes.

The achieved results for all the conducted runs have an aspect in common, namely the higher affinity of the sulfonic acids to the aqueous phase (distribution coefficients < 1 – Table 6.3), which is conferred by the presence of the sulfonic group $-\text{SO}_3\text{H}$ in the aromatic molecules. This hydrophilic characteristic of the sulfonic group is well known, being used industrially for conferring water solubility in dye intermediates [31].

Table 6.3 – Distribution coefficients determined at the reaction end.^{a)}

	Compound	Run					
		E1	E2	E3	E4	E5	E6
	BSA	0.34	0.45	0.11	n.dt.	n.dt.	n.dt.
Distribution coefficient	2-MNBSA	0.07	0.10	0.04	0.20	0.19	0.21
	3-MNBSA	0.12	0.12	0.07	0.34	0.35	0.31
	4-MNBSA	0.11	0.13	0.06	0.30	0.31	0.26

n.dt. – not determined; ^{a)} Distribution coefficient: $C_j^{organic\ phase} / C_j^{acid\ phase}$.

Table 6.3 reveals that sulfonic acids distribution coefficient is only slightly affected by the reaction temperature variation since the displayed results for runs E1 and E2 show similar distribution coefficient values for the analysed species. The same is not noticed when the effect of sulfuric acid concentration was studied (runs E1 and E3). The analysis of the determined distribution coefficients demonstrates that the increase of sulfuric acid concentrations (run E1) tend to increase sulfonic acids affinity to the organic phase. This fact can be explained by sulfuric acid acidity, which is higher than sulfonic acids ones, decreasing thus the organic acids solubility in the aqueous phase.

Regarding the change of the organic substrate (run E1 – Bz; run E4 – MNB), it is seen that the MNBSA affinity to the organic phase was higher in the MNB nitration run. As explained for the effect of sulfuric acid concentration, the higher affinity of sulfonic acids towards the organic phase can be enlightened by the presence of two strong mineral acids (sulfuric and nitric acid) in the aqueous phase during all the reaction time, which hinders the organic acids solubility in the latter. When Bz was the nitrated organic substrate, nitric acid conversion was nearly complete, lowering thus the aqueous phase acidity which had favoured the sulfonic acids solubility in the aqueous phase. Additionally, the composition of the organic phase may have also played a role on the sulfonic acids distribution between both reaction phases because despite the nearly complete nitric acid conversion in Bz nitration, at the reaction end the organic phase was mainly composed by MNB and unreacted Bz (feed in excess as usual in Bz nitration) while in MNB nitration Bz was never present in the reaction medium. This is indicative that Bz may hinder the solubility of sulfonic acids in the organic phase.

Finally, the presented results show that the presence of BSA in the fed organic substrate in low amounts does not affect MNBSA distribution coefficient (comparison between runs E4 and E5 and E6).

6.4. Conclusions

In the present work benzenesulfonic acid and 2-mononitrobenzene, 3-mononitrobenzene and 4-mononitrobenzene sulfonic acid isomers presence was detected for the first time in an industrial mixed acid benzene nitration plant.

A parametric study was performed in which it was intended to relate operational parameters during lab scale nitration experiments (such as reaction temperature, sulfuric acid and organic substrate composition) with sulfonic acids origin. It was found that these species formation is favoured using higher reaction temperature, higher sulfuric acid concentration and using benzene as the organic substrate. It was also found that these sulfonic acids derivatives affinity towards the reaction aqueous phase is higher than to the organic one.

The performed lab scale tests proved that (nitro)benzenesulfonic acids are originated during benzene nitration. This finding evidences that during benzene nitration are occurring sulfonation reactions, leading to the formation of other reaction by-products in addition to the typically detected ones, nitrophenols and dinitrobenzene.

Nomenclature

Acronyms

BSA	Benzenesulfonic acid
Bz	Benzene
HPLC-DAD	High Performance Liquid Chromatography - Diode Array Detector
MNB	Mononitrobenzene
2-MNBSA	2-mononitrobenzenesulfonic acid
3-MNBSA	3-mononitrobenzenesulfonic acid
4-MNBSA	4-mononitrobenzenesulfonic acid
MS	Mass Spectrometry
UHPLC-MS	Ultra-High Performance Liquid Chromatography – Mass Spectrometry

6.5. References

- [1]. Burns, J. R.; Ramshaw, C., Development of a Microreactor for Chemical Production. *Chemical Engineering Research and Design* **1999**, 77 (3), 206-211, <http://dx.doi.org/10.1205/026387699526106>.
- [2]. Afonso, D.; Ribeiro, A. F. G.; Araújo, P.; Vital, J.; Madeira, L. M., Phenol in Mixed Acid Benzene Nitration Systems. *Industrial & Engineering Chemistry Research* **2018**, 57 (46), 15942-15953,
- [3]. Afonso, D.; Ribeiro, A. F. G.; Araújo, P.; Vital, J.; Madeira, L. M., (Nitro)Phenols reactivity in mixed acid benzene nitration. *Submitted* **2019**,
- [4]. Dumann, G.; Quittmann, U.; Gröschel, L.; Agar, D. W.; Wörz, O.; Morgenschweis, K., The capillary-microreactor: a new reactor concept for the intensification of heat and mass transfer in liquid–liquid reactions. *Catalysis Today* **2003**, 79–80, 433-439, [http://dx.doi.org/10.1016/S0920-5861\(03\)00056-7](http://dx.doi.org/10.1016/S0920-5861(03)00056-7).
- [5]. Rahaman, M.; Mandal, B. P.; Ghosh, P., Nitration of nitrobenzene at high-concentrations of sulfuric acid. *AIChE Journal* **2007**, 53 (9), 2476-2480, doi:10.1002/aic.11222.
- [6]. Rahaman, M.; Mandal, B.; Ghosh, P., Nitration of nitrobenzene at high-concentrations of sulfuric acid: Mass transfer and kinetic aspects. *AIChE Journal* **2010**, 56 (3), 737-748, doi:10.1002/aic.11989.
- [7]. Sarkar, S.; Ghosh, S. K.; Ghosh, P., Nitration of Benzene at High-Concentrations of Sulfuric Acid. *Asian Journal of Chemistry* **2009**, 21 (6), 4533-4542,
- [8]. Agrawal, J. P.; Hodgson, R., *Organic Chemistry of Explosives*. Wiley, 2007.
- [9]. Urbański, T., *Chemistry and Technology of Explosives*. Pwn-Polish Scientific Publishers, Vol. 1, Warszawa, Poland, 1964.
- [10]. Lindner, O.; Rodefeld, L., Benzenesulfonic Acids and Their Derivatives. In *Ullmann's Encyclopedia of Industrial Chemistry*, Wiley-VCH, 2000, doi:10.1002/14356007.a03_507.
- [11]. Dado, G.; Bernhardt, R., Sulfonation and Sulfation. In *Kirk-Othmer Encyclopedia of Chemical Technology*, John Wiley & Sons, 2017, doi:10.1002/0471238961.1921120611140107.a01.pub3.
- [12]. Booth, G., Nitro Compounds, Aromatic. In *Ullmann's Encyclopedia of Industrial Chemistry*, Wiley-VCH, Weinheim, 2000, doi:10.1002/14356007.a17_411.
- [13]. Dugal, M., Nitrobenzene and Nitrotoluenes. In *Kirk-Othmer Encyclopedia of Chemical Technology*, John Wiley & Sons, 2005, doi:10.1002/0471238961.1409201801041109.a01.pub2.
- [14]. Costa, T. J. G.; Nogueira, A. G.; Silva, D. C. M.; Ribeiro, A. F. G.; Baptista, C. M. S. G., Nitrophenolic By-Products Quantification in the Continuous Benzene Nitration Process. In *Chemistry, Process Design, and Safety for the Nitration Industry*, American Chemical

- Society, Washington, DC. ACS Symposium Series, 2013; Vol. 1155, pp 49-60, doi:10.1021/bk-2013-1155.ch004
- 10.1021/bk-2013-1155.ch004.
- [15]. Nogueira, A. G. Optimização da Nitração de Aromáticos. PhD thesis, Universidade de Coimbra, Portugal, 2015.
- [16]. Franck, H.-G.; Stadelhofer, J. W., Production and uses of benzene derivatives. in: *Industrial Aromatic Chemistry: raw materials processes products*. Springer Berlin Heidelberg, Berlin, 1988; pp 132-235, 10.1007/978-3-642-73432-8_5.
- [17]. Käkölä, J.; Alén, R., A fast method for determining low-molecular-mass aliphatic carboxylic acids by high-performance liquid chromatography–atmospheric pressure chemical ionization mass spectrometry. *Journal of Separation Science* **2006**, 29 (13), 1996-2003, doi:10.1002/jssc.200600106.
- [18]. Niessen, W. M. A., *Liquid Chromatography-Mass Spectrometry*. 3rd edition, CRC Press, New York, 2006.
- [19]. Chen, Z.; Jin, X.; Wang, Q.; Lin, Y.; Gan, L.; Tang, C., Confirmation and determination of carboxylic acids in root exudates using LC–ESI-MS. *Journal of Separation Science* **2007**, 30 (15), 2440-2446, doi:10.1002/jssc.200700234.
- [20]. Käkölä, J.; Alén, R.; Pakkanen, H.; Matilainen, R.; Lahti, K., Quantitative determination of the main aliphatic carboxylic acids in wood kraft black liquors by high-performance liquid chromatography–mass spectrometry. *Journal of Chromatography A* **2007**, 1139 (2), 263-270, <https://doi.org/10.1016/j.chroma.2006.11.033>.
- [21]. Shrader, S., *Introductory Mass Spectrometry*. Second Edition, CRC Press, New York, 2013.
- [22]. Lee, M. S., *Mass Spectrometry Handbook*. 1st edition, Wiley, New Jersey, USA, 2012.
- [23]. Diogo Afonso, Bondalti Chemicals, Internal Report. **2018**,
- [24]. Quadros, P. A.; Oliveira, N. M. C.; Baptista, C. M. S. G., Continuous adiabatic industrial benzene nitration with mixed acid at a pilot plant scale. *Chemical Engineering Journal* **2005**, 108 (1), 1-11, <http://dx.doi.org/10.1016/j.cej.2004.12.022>.
- [25]. Quadros, P. A.; Castro, J. A. A. M.; Baptista, C. M. S. G., Nitrophenols Reduction in the Benzene Adiabatic Nitration Process. *Industrial & Engineering Chemistry Research* **2004**, 43 (15), 4438-4445, 10.1021/ie034263o.
- [26]. Carey, F., *Organic Chemistry*. 4th edition, McGraw-Hill, New York, 2000.
- [27]. Kaandorp, A. W.; Cerfontain, H.; Sixma, F. L. J., Aromatic sulphonation IV Kinetics and mechanism of the sulphonation of benzene in aqueous sulphuric acid. *Recueil des Travaux Chimiques des Pays-Bas* **1962**, 81 (11), 969-992, doi:10.1002/recl.19620811108.
- [28]. Cerfontain, H.; Telder, A., The solubility of toluene and benzene in concentrated aqueous sulfuric acid; implications to the kinetics of aromatic sulfonation. *Recueil des Travaux Chimiques des Pays-Bas* **1965**, 84, 545-550,

- [29]. Cerfontain, H., *Mechanistic aspects in aromatic sulfonation and desulfonation*. Interscience Publishers, New York, 1968.
- [30]. Olah, G. A.; Molnár, Á., *Hydrocarbon Chemistry*. 2nd edition, John Wiley & Sons, New Jersey, 2003.
- [31]. Kent, J. A., *Kent and Riegel's Handbook of Industrial Chemistry and Biotechnology*. 11th edition, Springer, New York, USA, 2007; Vol. 1.

Chapter 7 – Benzene deep oxidation in mixed acid nitration

Abstract

Laboratory scale nitrations of pure benzene and benzene enriched in impurities and by-products from the mononitrobenzene production process were carried out employing reaction conditions in the range of the industrial ones. These tests revealed that benzene is the substrate oxidized to the dicarboxylic acids intermediates and carbon monoxide and dioxide found in benzene nitration. This finding is contrary to what is stated in the literature, which is that in benzene nitration, aliphatic impurities typically present in the benzene feed, are those responsible for the formation of the oxidized compounds and carbon dioxide. Furthermore, CO generation was detected for the first time during benzene nitration, being evidenced a directly proportional relationship between CO₂ and CO formation ($\text{CO}_2 \approx 2 \times \text{CO}$), which is indicative that these gases have the same origin.

The performed study allowed verifying that, similarity to what happens in nitrophenols formation, that the decrease of benzene / nitric acid ratio favours CO₂ formation. It was also found that the increase of the reaction temperature, of sulfuric acid and nitric acid concentrations enhanced the formation of CO₂ and nitrophenols while the formation of oxalic acid was mainly affected by the concentration of these mineral acids. Furthermore, a directly proportional relation between the formation of nitrophenols and CO₂ and between the generation of oxalic acid and nitrophenols was noticed, indicating that upon benzene oxidation to phenol, this last species is not only nitrated, being also further oxidized short chain acids which are decomposed to CO and CO₂.

Keywords: Carbon dioxide; carbon monoxide; benzene; oxidation; phenol; nitration; nitrophenols; dicarboxylic acids.

7.1. Introduction

Mononitrobenzene (MNB) is an important chemical commodity, being produced by mixed acid (a mixture of sulfuric acid, the reaction catalyst, and nitric acid) benzene (Bz) nitration and used as a chemical intermediate for several applications [1]. Despite the importance of Bz nitration, which leveraged the reaction study and improvement over time [2-4], due to the complexity of the reaction system (heterogeneous liquid-liquid reaction), some issues remain poorly explored, namely those related with reaction by-products.

It is known that the main secondary products from Bz nitration are dinitrobenzene (DNB), 2,4-dinitrophenol (2,4-DNP) and 2,4,6-trinitrophenol (TNP) [4-6]. However, only recently the postulated presence of phenol (Ph) in the nitration medium was experimentally evidenced for the first time [7], being evidenced that it is the mononitrophenols (MNPs) precursor and that these compounds are formed by consecutive reactions, i.e., MNPs are nitrated into DNPs which in turn origin TNP [8]. During the course of this work, it was found that a different type of by-products is also formed in Bz nitration, the sulfonic acids, specifically benzenesulfonic acid (BSA) and mononitrobenzenesulfonic acid isomers (2-MNBSA, 3-MNBSA and 4-MNBSA) [9]. Furthermore, during this work, new oxidized intermediate species, namely, fumaric acid, mesoxalic acid, succinic acid, were detected for the first time in the MNB production process (Chapter 3). These compounds are suspected of being formed due to the oxidation of organic matter by action of nitric acid, because this mineral acid is a powerful oxidizing agent [10] and the responsible for Bz oxidation to Ph [7, 11]. In fact, under the Bz nitration conditions, nitric acid promotes the decomposition of oxalic acid (Chapter 3). Moreover, Odle *et al.* [12] reported that at 50 °C (a temperature lower than that employed in benzene nitration) concentrated nitric acid can completely oxidize phenolic compounds, yielding oxalic acid, CO₂ and CO, among other organic acids, evidencing thus its oxidant capacity.

Urbański [13] states that during nitration, oxidation reactions can occur if the aromatic ring is liable for such. For instance, Ph can be oxidized to oxalic acid or naphthalene can lead to phthalic acid formation [13]. According to Seyewetz and Poizat [14], by action of nitric acid 2,4-DNP and TNP can yield hydrogen cyanide and CO₂. However, the authors are not explicit about the reaction conditions. Once formed, hydrogen cyanide can be hydrolysed to formic acid which in turn can be decomposed into CO and H₂O [13].

In toluene nitration, nitric acid can promote ring oxidations or decomposition leading to the formation of gaseous by-products [15]. Within the nitration temperature range (>70 °C), nitric acid can be decomposed yielding potential oxidants [16] that may contribute to the organic matter oxidation during nitration reactions. Additionally, the sulfuric acid action as a potential oxidant should not be excluded since it is suggested that it can play a role in the organic matter oxidation, although in a smaller extent [16-17].

The formation of all the detected Bz nitration by-products, namely Ph [7] and nitrophenols (NPs) [4], sulfonic acids [9] and dicarboxylic acids (Chapter 3) was already addressed, being known that their appearance is dependent on the reaction conditions [13]. However, to the authors knowledge, studies assessing CO and CO₂ formation during Bz nitration are inexistent. Therefore, to overcome this gap, in this work CO and CO₂ generation during this reaction will be addressed and related with the organic substrate composition and with some important reaction parameters such as the reaction temperature and the mixed acid composition. Additionally, oxalic acid and NPs formation at different reaction conditions will also be considered. Such knowledge can be used both to clarify the origin of oxalic acid, CO and CO₂ in Bz nitration and to minimize the formation of these species, enabling thus the decrease of oxidation reactions during Bz nitration.

7.2. Material and methods

The chemical reagents used in this study were: oxalic acid dihydrate (99.5%) from Panreac, barium hydroxide octahydrate (> 99%) from Fischer Chemical, sulfuric acid (99%) from Quimitecnica and (97%) from Merck, nitric acid (65%) from Baker, *n*-hexane (>98%) from Merck, methylcyclohexane (>98%) from Fluka, benzenesulfonic acid (>97%) from Merck, 2-mononitrobenzenesulfonic acid hydrate (>98%) from TCI, benzene from Honeywell (Chromasolv Plus, >99.9%), mononitrobenzene (99.99%) from Bondalti Chemicals production process, toluene (99.85%) from Acros Organics, 2-mononitrophenol (98%) from Fluka, 4-mononitrophenol (98%) from Aldrich, 2,4-dinitrophenol (97%) from Aldrich, 2,6-dinitrophenol (98%) from TCI, 2,4,6-trinitrophenol (99%) from BDH, 1,3-dinitrobenzene (>99%) from TCI, phenol (99.5%) from Riedel-de-Haen, acetonitrile (HPLC grade) from Fischer Scientific, and potassium dihydrogen phosphate from Merck.

7.2.1. Laboratorial reactor

The laboratory nitrations were carried out discontinuously (1 h of reaction time), in a jacketed glass / Teflon reactor equipped with a tantalum air-impeller stirrer and a Teflon coated thermocouple. In Figure 7.1 is shown the sketch of the jacketed laboratory batch reactor used.

Before the start of each reaction, sulfuric acid was added to the reactor by its top (valve V-5) and the thermostatic bath (MPC-K6) from Huber (E-2) was turned on. Then, demineralized water was carefully added to sulfuric acid and when the temperature of the reaction medium was the intended one, nitric acid was added, again by the reactor's top (valve V-5). The added amounts of sulfuric acid, demineralized water and nitric acid were such that the mixed acid composition was in the range of the industrial values (H₂SO₄ = [60-70] %wt.; HNO₃ = [2-6] %wt.). Throughout the aqueous phase heating or cooling, the stirrer was working to promote the acids mixture and the

homogenization of the reaction medium composition and temperature. When the predetermined reaction temperature was reached, and after flowing a nitrogen stream (rendering inert the reactor atmosphere), the stirring speed was adjusted to the defined value (1200 r.p.m) and the organic substrate was added through the reactor's bottom (valve V-3). At the reactor's top was placed a condenser to ensure that, when working at atmospheric pressure, Bz wasn't escaping from the reaction medium. The temperature of the system was recorded using a Therna 1 thermometer from ETI Ltd.

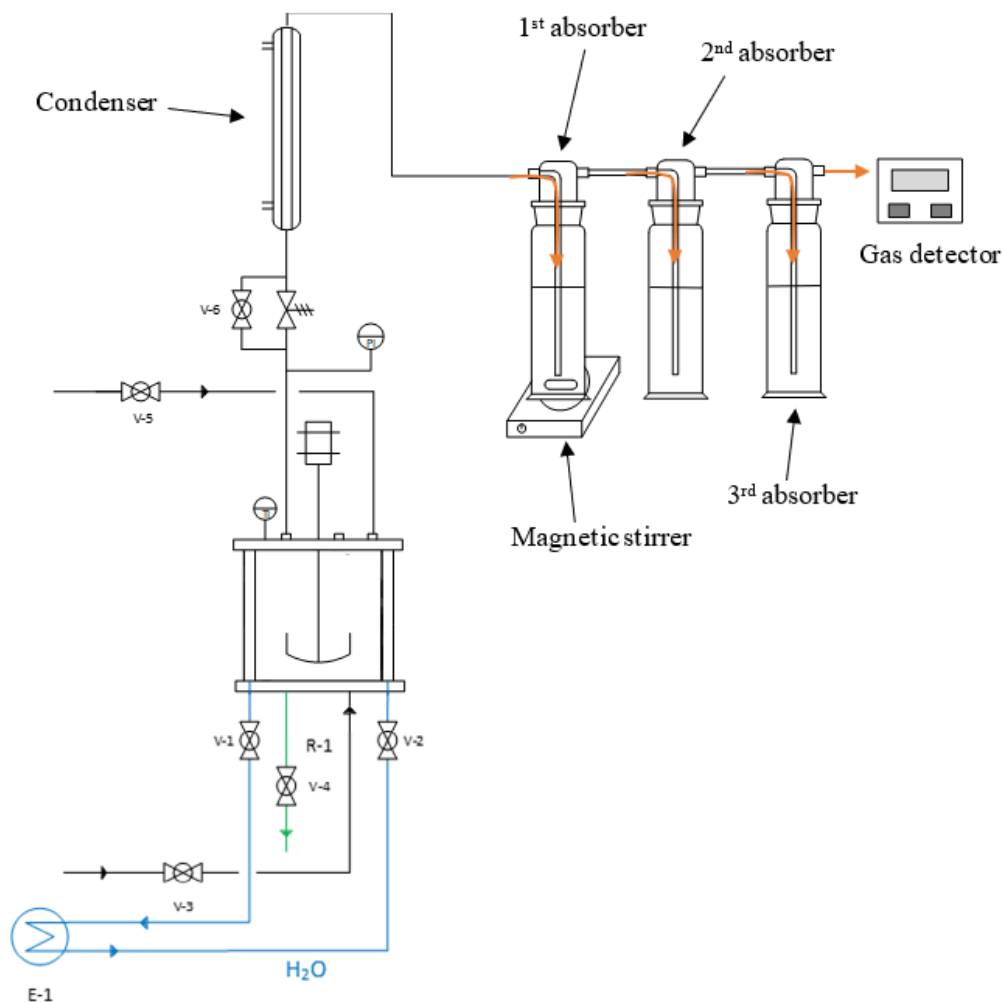


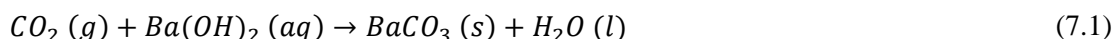
Figure 7.1 – Sketch of the laboratorial unit.

During the reaction time, a nitrogen stream was fed to the reactor to maintain the system pressure (in the pressurized tests) and to remove the formed gaseous products (CO and CO₂) to the gas absorbers, connected in series after the condenser. The gas absorbers were filled with a barium hydroxide solution aiming to capture the CO₂ formed in the reaction. After the gas absorbers a gas detector from Crowcon was placed in order detect CO formation. For quantifying simultaneously

the formed amounts of CO and CO₂ the gas detector was connected after the condenser, without the presence of the gas absorbers.

7.2.2. Gaseous phase analysis

To quantify the formed amounts of CO₂, a gravimetric method was employed in which BaCO₃, formed by the contact between CO₂ and a Ba(OH)₂ solution (cf. equation 7.1) was recovered from the Ba(OH)₂ solution by a solid-liquid filtration, accomplished using vacuum.



Then, the retentate was placed in a hot (> 100 °C) heating plate until reaching a constant mass. By this way, it was assured that moisture was eliminated from BaCO₃ and that only the formed precipitate was being accounted for determining the formed CO₂.

For quantifying simultaneously carbon monoxide and carbon dioxide a Gas-Pro detector from Crowcon was used, placed after the condenser (Figure 7.1).

7.2.3. Organic phase analysis

For quantifying phenolic by-products in the organic phase, after the reaction end, a portion of the organic phase (≈ 0.5 g) was retrieved to a 1.5 mL vial being then, immediately, diluted with NaOH (1M; ≈ 0.5 g). The resulting aqueous phase, to where the phenolic by-products were extracted (extraction efficiency > 90% [18]), was separated from the organic one, diluted with demineralized water and its pH corrected with sulfuric acid. The liquid chromatographic analyses were performed in an Elite LaChrom High-Performance Liquid Chromatography – Diode Array Detector (HPLC-DAD) apparatus from VWR-Hitachi equipped with a reverse phase column (Purospher® STAR RP-18e LiChroCART®) packed with silica microspheres (5 μm, 250 mm x 4 mm) and a guard column (LiChroCART® - 5 μm, 4mm x 4mm). The temperature of the chromatographic column was maintained at 30 °C by the HPLC's oven, and the injected sample volume was 10 μL.

Benzene impurities were analysed by gas chromatography (GC), in a Perkin-Elmer Clarus 580 gas chromatograph, equipped with a flame ionization detector (FID). Both the injector and detector temperatures were set at 240 °C. It was used an Elite 1 (100% dimethylpolysiloxane 30 m x 0.32 mm x 1 μm) column from Perkin Elmer, and helium as the carrier gas.

7.2.4. Acid phase characterization

The nitric acid content was measured by manual titration with an iron (II) sulphate solution while the sulfuric acid concentration was determined by titrating the aqueous phase with a NaOH solution (1 M) using a 751 GDP Titrino apparatus from Metrohm.

For quantifying dicarboxylic acids, the collected samples were diluted with demineralized water and analysed by HPLC-DAD. The chromatographic apparatus was the same as described in section 7.2.3. The temperature of the chromatographic column was maintained at 30 °C by the HPLC's oven and the volume of the injected sample was 10 µL. The eluent feed was in gradient mode with a KH₂PO₄ solution (2.5 mM, pH ≈ 2.4) and acetonitrile as follows:

- 0 – 5 minutes: 0.4 mL/min, 88% KH₂PO₄, 12% acetonitrile;
- 5 – 11 minutes: 1.0 mL/min, 88% KH₂PO₄, 12% acetonitrile;
- 11 – 23 minutes: 1.0 mL/min: 50% KH₂PO₄, 50% acetonitrile;
- 23 – 26 minutes: 1.0 mL/min, 88% KH₂PO₄, 12% acetonitrile;
- 26 – 30 minutes: 0.4 mL/min, 88% KH₂PO₄, 12% acetonitrile.

7.3. Results and discussion

In the following sections are shown the performed studies for determining the CO₂ origin (7.3.1) and how the reaction conditions influence this gas and other species formation (7.3.2).

7.3.1. Impurities and by-products added-benzene nitration

In the medium of Bz nitration, there are several organic compounds of different nature such as MNB, DNB, Ph, NPs, (nitro)benzene sulfonic acids, species resulting from oxidation of organic matter such as oxalic, fumaric and succinic acids, or typical impurities present in Bz nitration grade such as toluene, cyclohexane, n-hexane, methylcyclohexane (MCH) and cyclopentane – Figure 7.2. Since these compounds are constituents of the Bz nitration medium, it was verified if they could yield CO₂ during Bz nitration.

Decomposition Reactions in Aromatic Nitration

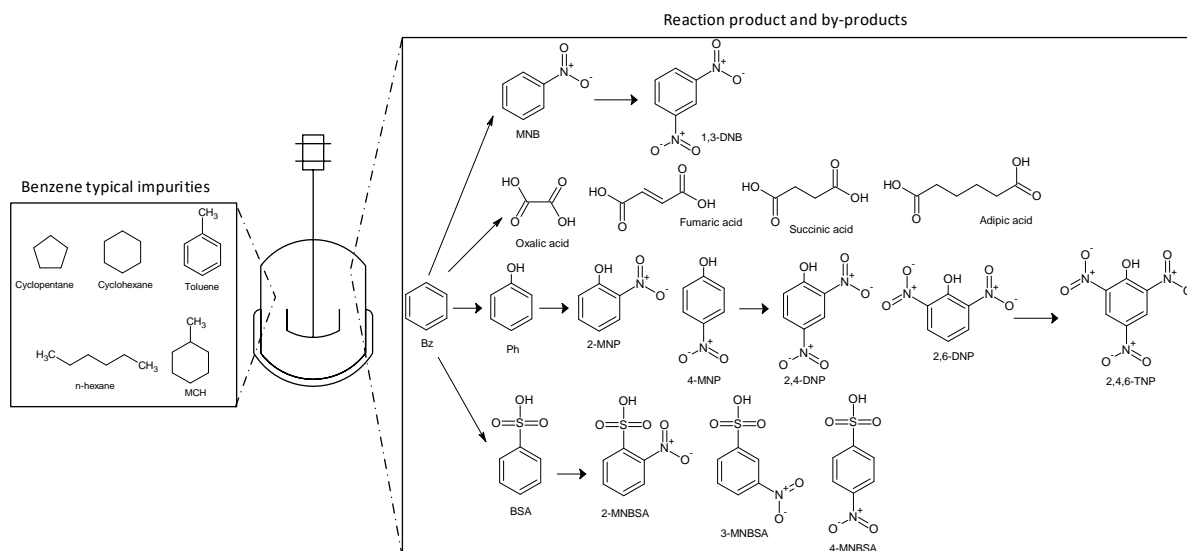


Figure 7.2 – Organic compounds present in the benzene nitration medium.

When conducting Bz nitrations, it was verified that in addition to NPs, sulfonic acids [9], dicarboxylic acids (Chapter 3), CO₂ and CO were also being formed. During the course of this work, CO₂ was also detected in the industrial MNB production process (Chapter 2). Even though Guenkel and Maloney [19] refer that CO₂ is formed through the oxidation of aliphatic compounds, present as Bz impurities, they haven't quantified this gas formation or mentioned CO formation. Although CO formation is addressed in Urbański [13] and Odle *et al.* [12] work, it is not in the specific context of Bz nitration. Therefore, the detection of both CO and CO₂ during Bz nitration is a significant finding, suggesting the occurrence of oxidation reactions in parallel to nitration.

In order to determine if some of the compounds illustrated in Figure 7.2 were precursors of CO₂ (and CO) in the typical Bz nitration conditions, each species was incorporated (individually) in a Bz matrix, being the achieved results compared with those of pure Bz nitrations at the same conditions. The incorporation of these organic compounds was such that their concentration was similar to that of NPs found in a typical Bz nitration. The obtained results are summarized in Figure 7.3.

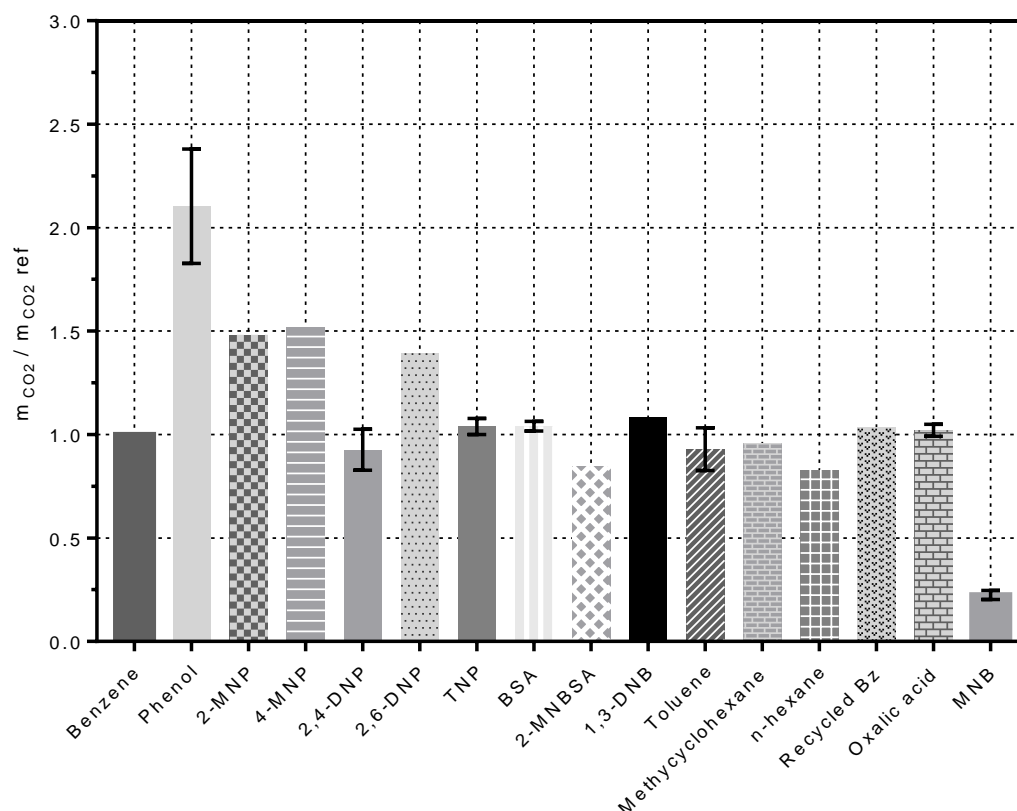


Figure 7.3 – CO₂ formation in nitration as function of the different compounds incorporated in benzene (except for MNB). $m_{CO_2, ref}$ refers to the CO₂ formed amounts in the nitration of pure benzene. Reaction conditions: $T_{initial} = 90\text{ }^{\circ}\text{C}$; % wt. H₂SO₄ = 66; % wt. HNO₃ = 5; reaction time = 1 h; concentration of the organic species in benzene = 2500 ppm. Aliphatics concentration in recycled benzene = 3% wt..

Analysing Figure 7.3 is clearly noticeable that the incorporation of Ph in the Bz matrix have favoured CO₂ formation because the generated gas amounts increased over 2 times when compared to a pure Bz nitration. This indicates that Ph is a carbon dioxide precursor, a major finding since it was demonstrated that it is converted into NPs [8], not being evidenced, to date, that it could also lead to CO₂ formation in MNB production. As Ph is a highly reactive molecule, because of the hydroxyl group (-OH), a strong activator [7, 20], once formed it can be further oxidized originating hydroquinone which then, by ring opening reactions and decarboxylation, lead to CO₂ and CO (also detected during these tests). Given that Ph is formed by Bz oxidation, Figure 7.3 data allows inferring that Bz is indeed a CO₂ precursor.

Regarding the obtained results from the NPs-added Bz nitrations, the following pattern was noticed for CO₂ formation:

$$CO_2 (4-MNP) \approx CO_2 (2-MNP) > CO_2 (2,6-DNP) > CO_2 (TNP) \approx CO_2 (2,4-DNP) \approx CO_2 (Bz)$$

This behaviour shows that, tendentially, the higher the number of nitro groups ($-\text{NO}_2$) the aromatic molecule has, the lower amounts of CO_2 are generated, which is because the nitro group is a powerful deactivating, stabilizing thus the aromatic molecule. However, when comparing 2,6-DNP results with those of 2,4-DNP nitration, it is evident that the generated CO_2 content was higher in the 2,6-DNP nitration. This indicates that 2,6-DNP is a more easily oxidized than 2,4-DNP. Since the hydroxyl group ($-\text{OH}$) is an *ortho* and *para* activator [18], 2,6-DNP can be further oxidized in the unsubstituted *para* position, leading to an increase of CO_2 formation.

The results displayed in Figure 7.3 show that among the phenolic by-products resulting from Bz nitration Ph, 2-MNP, 4-MNP, and 2,6-DNP have increased CO_2 generation. Because NPs have their origin in Ph, which in turn is formed by Bz oxidation, these results reinforce Bz role as the responsible for CO_2 formation.

A further analysis of Figure 7.3 reveals that addition of sulfonic acids (BSA and 2-MNBSA), typically generated during nitration [9], to Bz had no effect on CO_2 formation, as expected because the sulfonic group ($-\text{SO}_3\text{H}$), similarly to the nitro group, is a powerful deactivating group [20], hindering thus oxidation reactions and the consequent carbon oxides formation within the typical range of Bz nitration conditions.

In terms of CO_2 generation by 1,3-DNB nitration, Figure 7.3 indicates that it was similar to the nitration of pure Bz. As explained for the sulfonic acids runs, the deactivation of the aromatic ring, conferred by the presence of two nitro groups, tends to decrease 1,3-DNB susceptibility to be oxidized.

Regarding the effect of toluene (typical impurity from Bz nitration) presence in the Bz matrix, according to Figure 7.3, it does not influence the CO_2 formation. Since this compound is more easily oxidized than Bz [1, 21], due to the presence of the methyl group ($-\text{CH}_3$) in the aromatic ring, it was suspected that it could be oxidized during Bz nitration. However, facing the presented generated gas amounts, having in mind the low concentration of toluene and knowing beforehand that the methyl group enhances nitration besides oxidation [1, 22], one can deduce that toluene was mainly mono- or poly-nitrated, being CO_2 formation controlled by Bz oxidation because of its high concentration in the nitration media.

Regarding n-hexane and methylcyclohexane runs, aliphatics typically present in nitration grade Bz [19], it is visible that their effect in CO_2 formation is negligible despite the slight variation compared to the reference values (pure Bz nitration). This reinforces that CO_2 is formed by Bz oxidation during MNB production, instead of being generated by aliphatic oxidation as suggested by Guenkel and Maloney [19].

To confirm that aliphatics oxidation during Bz nitration is negligible, a recycled benzene sample from the nitration plant was nitrated, yielding similar CO_2 amounts to those produced in pure Bz nitration (Figure 7.3). Recycled benzene is a typical stream from the MNB production process, composed by unreacted benzene from the nitration section and enriched in other impurities (present

in nitration grade Bz besides those already addressed) such as cyclopentane, methylcyclopentane or n-heptane. Furthermore, different mixtures of pure Bz and recycled Bz were made and posteriorly nitrated – Figure 7.4. The exhibited results are indicative that the variation of the aliphatics concentration almost does not affect CO₂ generation. This corroborates both the achieved results for n-hexane, methylcyclohexane, and recycled Bz, and the role of Bz, instead of the aliphatic compounds, as the precursor of the gaseous by-products.

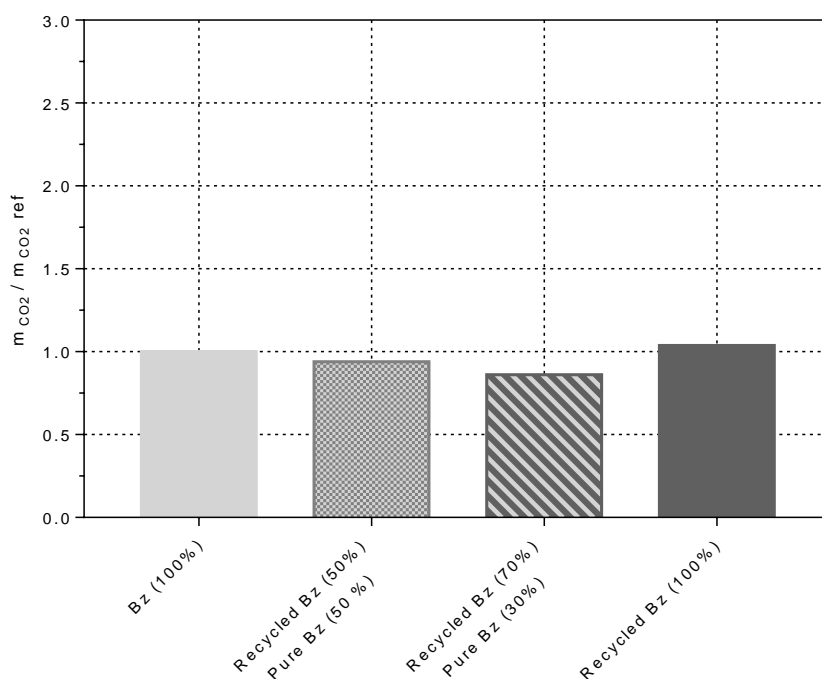


Figure 7.4 – Amounts of CO₂ formed in the nitration of mixtures of recycled benzene and pure benzene. $m_{CO_2 \text{ ref}}$ is referent to CO₂ amounts formed in the nitration of pure Bz. Reaction conditions: $T_{\text{initial}} = 90 \text{ }^{\circ}\text{C}$; % wt. H₂SO₄ = 66; % wt. HNO₃ = 5; Reaction time = 1 h. Aliphatics concentration in recycled benzene = 3% wt..

Aiming to further reinforce that the aliphatic compounds are not being oxidized during Bz nitration, industrial samples from the inlet and outlet streams of the industrial reactor were analysed in different periods – Table 7.1.

Table 7.1 – Aliphatic compounds at the inlet and outlet of the industrial nitration section.

Sample	Aliphatics in / Aliphatics out
1	0.99
2	1.05
3	1.05
4	1.02

As can be seen, the aliphatic compounds present in the Bz nitration plant are not being oxidized because their amounts are similar at the inlet and outlet of the reaction section. Once again, this data is in accordance with the performed batch nitration tests, pointing that is Bz the CO₂ precursor.

Oxalic acid was also incorporated in Bz and nitrated being evidenced that it had no impact on the formed CO₂ quantities (Figure 7.3). This is due to the competition for nitric acid consumption between Bz nitration and oxalic acid decomposition, being favoured Bz nitration. The resistance of oxalic acid to decomposition, demonstrated in the Chapter 3 and in the open literature [23-24], the relatively short reaction time (1 h) and the short contact time with nitric acid (< 15 minutes) are factors that have contributed for the non-variation of CO₂ amounts. Oxalic acid was incorporated in Bz nitration tests because this compound is known to be present in the nitration plant and because when decomposed it might be a CO and CO₂ precursor (Chapter 3).

To check if the Bz nitration reaction product could be a carbon oxide precursor, pure MNB was nitrated. As expected, Figure 7.3 shows that CO₂ formed amounts were much lower in MNB nitration than in Bz nitration. This result was anticipated because the nitrating conditions for MNB are harsher than those of Bz [22, 25], due to its higher stability. This higher compound's stability is reinforced when comparing nitric acid consumption, which was complete for Bz nitration (>99.5%) while in MNB nitration was negligible, meaning that MNB was in contact with a higher acid concentration for a longer period of time. Even so, the CO₂ formed amounts were about 4 times lower than those obtained in Bz nitration.

In the industrial MNB production process these reaction conditions are not verified, i.e., when MNB concentration in the reaction medium is high, nitric acid amounts are low due Bz and HNO₃ conversion into MNB, thus CO₂ formed amounts by MNB decomposition during Bz nitration are certainly lower than the experimentally obtained values, if not negligible. This statement is corroborated by the outcome of an experiment in which a mixture of Bz and MNB (50 / 50 % wt.) was nitrated under the conditions of temperature and mixed acid composition mentioned in Figure 7.3, being obtained higher mass of CO₂ than that determined in MNB nitration, but lower than that gotten from Bz nitration ($m_{\text{CO}_2} / m_{\text{CO}_2 \text{ ref}} = 0.8$).

As previously stated, while nitrating pure Bz, it was found that in addition to CO₂, CO was also being formed. This same result was obtained in all the tests presented in Figure 7.3. However, due to the gas detector quantification limits, CO formed amounts were not followed during the entire reaction time. An example of a gotten CO concentration profile in Bz nitration is illustrated in Figure 7.5. Although it was not possible to record the CO concentration profile entirely, the results depicted demonstrate, for the first time to the best of our knowledge, this gas generation during Bz nitration.

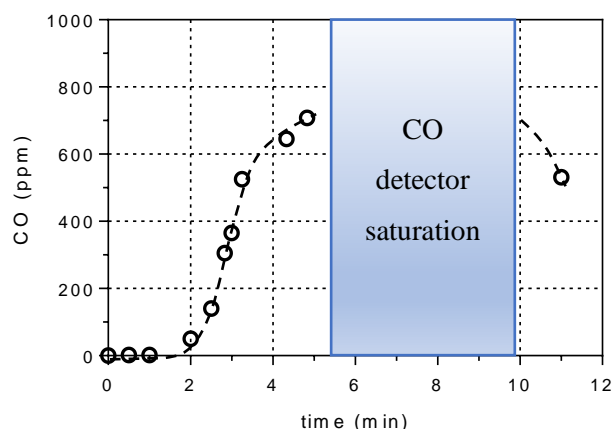


Figure 7.5 – Carbon monoxide concentration profile in pure benzene nitration. Reaction conditions: $T_{\text{initial}} = 90\text{ }^{\circ}\text{C}$; % wt. $\text{H}_2\text{SO}_4 = 66$; % wt. $\text{HNO}_3 = 5$. The line is added just for better visualization of the trend.

The concentration profile of CO shows that the species amounts begin to increase 1-2 minutes after the reaction start, reaching a maximum of concentration between 6 to 10 minutes after the reaction start, decreasing then till the reaction end. According to the results disclosed by Afonso *et al.* [8], under the employed reaction conditions nitric acid depletion occurs before 10 minutes of reaction time being reached. Because nitric acid (or nitric acid derivatives) is the most likely oxidizing agent, this fact explains the CO concentration decrease for reaction times higher than 10 minutes.

Aiming to correlate CO and CO_2 formation during Bz nitration, sulfuric acid concentration was drastically reduced, for levels lower than those typically employed, to slow down and decrease the reaction by-products formation, enabling thus a proper record of the CO concentration profile. The obtained results are depicted in Figure 7.6.

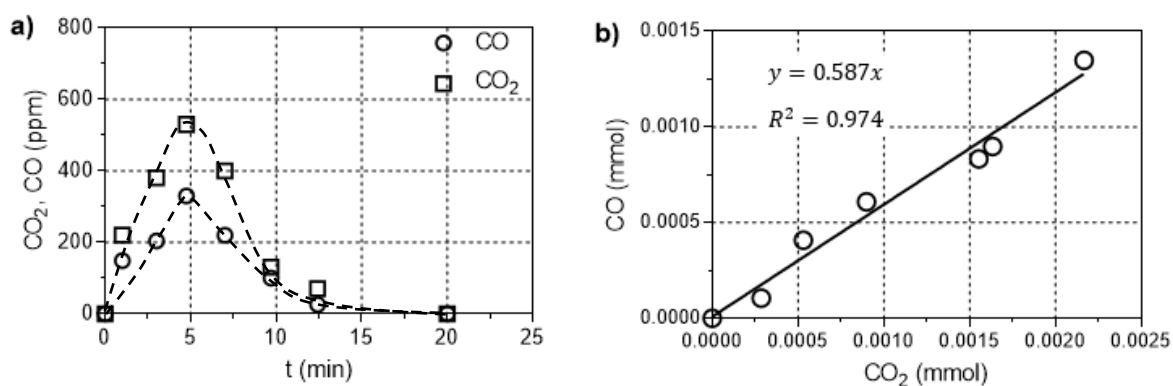


Figure 7.6 – **a)** Carbon dioxide and carbon monoxide concentration profile; **b)** carbon monoxide vs. carbon dioxide formation in a pure benzene nitration. Reaction conditions: $T_{\text{initial}} = 90\text{ }^{\circ}\text{C}$; % wt. $\text{H}_2\text{SO}_4 = 61$; % wt. $\text{HNO}_3 = 5$. Dashed lines are added just for a better visualization of the trends.

In Figure 7.6-a) are presented the concentration profiles for both carbon oxides as a function of the reaction time. It is noticed that CO and CO₂ concentration profiles are similar, although CO₂ was formed in higher amounts. This evidences a relation between the generation of CO and that of CO₂, which were correlated using a linear regression – Figure 7.6-b). Although the experimental data are only a few, the obtained linear regression enables a remarkable prediction of CO concentration based on CO₂ amounts, being noticed that by each mol of CO are formed about 1.7 mol of CO₂.

Comparing the determined CO and CO₂ concentrations in Bz nitration with those of oxalic acid decomposition (reported in the Chapter 3), one can see that the CO to CO₂ ratio is higher in Bz nitration (higher slope, 0.587 vs. 0.317). This finding is in accordance with the Carbajo *et al.* [26] work, which states that CO is mainly formed by the aromatic ring opening, in this specific case, by the possible ring cleavage of Bz or Bz derivatives such as phenol, catechol or hydroquinone.

7.3.2. Effect of the operation conditions

Aiming to identify which reaction parameters affect more significantly the formation of CO₂, the influence of the reaction pressure and of the Bz / nitric acid ratio was firstly studied (Figure 7.7), being then assessed the impact of the reaction temperature and mixed acid composition.

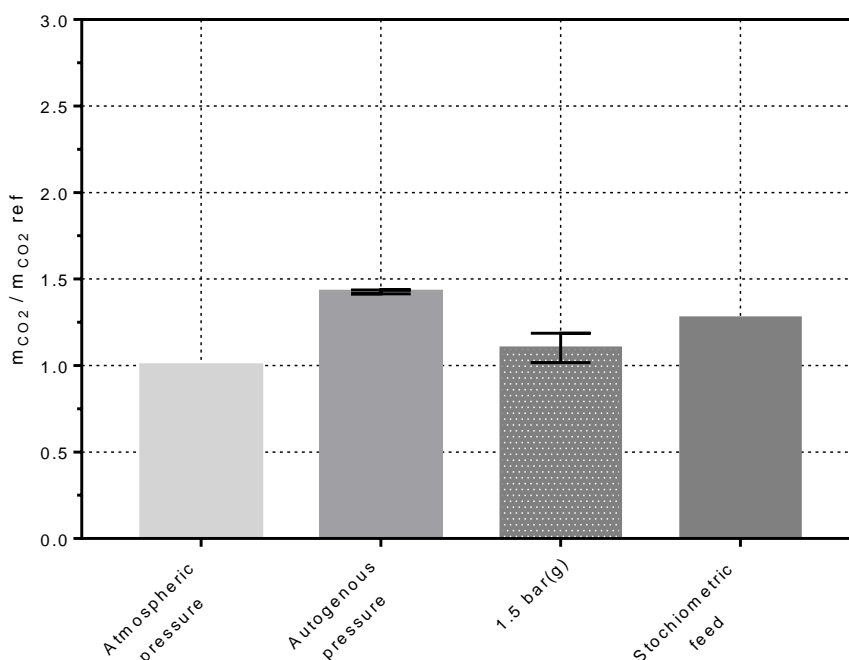


Figure 7.7 – CO₂ formed amounts in Bz nitration at the following reaction conditions: $T_{\text{initial}} = 90\text{ }^{\circ}\text{C}$; % wt. H₂SO₄ = 66; % wt. HNO₃ = 5; reaction time = 1 h. Bz was fed in excess (11% mol) except for the stoichiometric feed run in which Bz / nitric acid = 1, $P = P_{\text{atm}}$. The reference test was conducted at atmospheric pressure, maintaining the remaining reaction conditions unchanged.

The generated CO₂ quantities in Bz nitration at atmospheric pressure ($m_{\text{CO}_2 \text{ ref}}$) were compared with those retrieved from tests conducted with the reactor closed (autogenous pressure). It was found that at atmospheric pressure, the formed amounts of CO₂ were lower than those of the closed reactor tests. This was due to Bz reflux, which didn't allow a so pronounced temperature increase to occur in the atmospheric pressure test (113 °C vs. 122 °C), a parameter likely to affect CO₂ formation since it has an impact on NPs formation [4]. Additionally, in the closed reactor test, the nitrogen stream used to direct the formed gaseous products to the alkaline absorbers (section 7.2.1) was only connected to the reactor after the nitric acid depletion from the reaction medium. This means that some potential oxidants formed during Bz nitration [16, 27] were not (immediately) removed from the reaction medium, being able to oxidize the organic compounds (Bz), yielding thus CO₂.

When the experimental runs were conducted at 1.5 bar(g), the formed gas content was somewhat higher than the results obtained for the atmospheric pressure tests. This is explained by the higher temperature achieved during this test, which was similar to that of the closed reactor run. However, the connection of the N₂ stream to the reactor shortly after the reaction start allowed the removal of some of the formed oxidizing species such as NO₂, formed by nitric acid decomposition [16, 27], explaining thus the lower amounts of CO₂ in the run conducted at 1.5 bar(g).

Finally, Bz which is typically fed in excess to minimize NPs formation [4], was fed stoichiometrically to nitric acid – atmospheric pressure run. The displayed results evidence that the excess of Bz contributes also to decrease the CO₂ generation. Because the increase of Bz concentration in the organic phase reduces nitric acid solubility in the latter [4], leading to the decrease of Ph formation, the reduction of Bz fed amounts caused the increase of Ph generation, which in turn promoted CO₂ production. This result points out that nitric acid, besides being responsible for Bz oxidation to Ph, also plays a role in CO₂ formation.

The remaining reaction parameters, namely the initial reaction temperature and mixed acid composition, typically studied in Bz nitration, were also related with carbon dioxide, NPs and oxalic acid formation. The obtained results are disclosed in Table 7.2.

The first parameter targeted was the reaction temperature because it is known to affect positively both the reaction rate as well as the NPs formation. Regarding the temperature influence on CO₂ formation, one can see that the temperature rise favoured this species generation because the CO₂ amounts have increased from 43 (run 1, 90 °C) to 74 (run 2, 114 °C) mg/kg MNB in MNB nitration and from 59 (run 3, 70 °C) to 149 (run 5, 90 °C) mg/kg Bz in Bz nitration. These results evidence that the increase of the reaction temperature favours the occurrence of decomposition reactions, a conclusion that is in accordance with our results (Chapter 3) and with those of Carbajo *et al.* [26] and Zazo *et al.* [24].

Table 7.2 – Formation of benzene (and mononitrobenzene) nitration by-products at different reaction conditions. Reaction time = 1 h; Operation pressure = 1.8 bar(g)

Run #	Organic substrate	T _{initial} (°C)	% wt. H ₂ SO ₄	% wt. HNO ₃	NPs (ppm)	Oxalic acid (ppm)	CO ₂ (mg/kg Bz)
1	MNB	90	65	5	n.d.	n.d.	43*
2		114					74*
3	Bz	70	65	5	664	2042	59
4		90	60		1059	2139	125
5			65		1161	2117	149
6			70		1651	2401	271
7			65	3	806	1854	99

n.d. – not detected;

* In these runs the organic substrate was MNB, therefore CO₂ amounts are presented in mg/kg MNB.

In MNB nitration, the formed amounts of CO₂ were lower than those in Bz nitration because MNB is a more stable compound than Bz and because during MNB nitration no temperature rise was verified. The same was not observed in Bz nitration due to the reaction exothermicity [11]. Both these facts explain the increment of CO₂ generation in Bz nitration.

In what concerns to Bz nitration, Table 7.2 shows, as expected, that the temperature rise has enhanced NPs formation [4].

Concerning the effect of sulfuric acid concentration on NPs and CO₂ generation, it is noticeable that the rise of this mineral acid concentration led to the increase of NPs amounts from 1059 ppm (run 4, 60% wt. H₂SO₄) to 1651 ppm (run 6, 70% wt. H₂SO₄) and to the increment of CO₂ quantities from 125 mg/kg Bz (run 4) to 271 mg/kg Bz (run 6). This behaviour represents a proportionality relation between sulfuric acid concentration and the formed amounts of both NPs and CO₂. The increase of NPs quantities for higher sulfuric acid concentration had already been noticed in a previous study of ours [8]. However, no information was known addressing CO₂ formation for different sulfuric acid concentrations in Bz nitration. The observed behaviour can be justified by the increase of the nitration rate, consequence of the higher sulfuric acid concentration (process catalyst), which caused a higher temperature rise, known to affect NPs formation [4-5] as well as CO₂ generation by the decomposition of organic compounds [26]. The increase of oxalic acid (detected in Bz nitration medium) generation with increasing sulfuric acid concentration [28] can also explain the rise of CO₂ quantities because oxalic acid might be formed by the decarboxylation, and subsequent oxidation, of higher chain compounds, as happens in advanced oxidation processes [29], leading to the consequent increase of CO₂ release.

As regards to nitric acid effect on NPs and CO₂ genesis (run 5 and 7), the disclosed results show that the variation of the acid concentration had a significant impact on the by-products formation.

This finding, although being expected both in NPs [8] and CO₂ generation (by dicarboxylic acids decomposition, Chapter 3), is a novelty because it allows demonstrating that nitric acid influences Bz oxidation during nitration.

The ratio between nitric acid and Bz was similar in both reactions, therefore this parameter cannot be used to justify the increase of NPs and CO₂ with the rise of nitric acid concentration. On the other hand, in run 5 (higher HNO₃ concentration) was expected a lower nitric acid dissociation than in run 7. This can explain the increment of NPs and CO₂ generation because nitric acid (or nitric acid derivatives) is known to be a powerful oxidizing agent [10, 16, 30] and the responsible for Ph formation [7, 11]. Therefore, as phenol is the NPs precursor, the increase of these compounds' concentration implies the rise of Ph formation, which according to section 7.3.1 is known to enhance CO₂ generation.

The analysis of Table 7.2 evidences that independently of the studied parameter, when NPs formation increased, CO₂ generation increased as well. Consequently, aiming to predict CO₂ formation as a function of NPs concentration in Bz nitration, the results disclosed in Table 7.2 and of other Bz nitration runs were represented graphically – Figure 7.8. In this figure is perceptible the existence of an almost linear relationship between the generation of these compounds, enabling predicting the CO₂ formed amounts based on NPs formation.

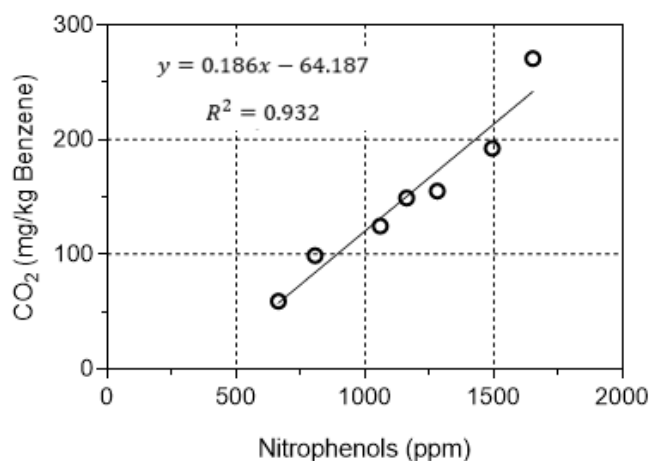


Figure 7.8 – Nitrophenols vs. carbon dioxide formation in Bz nitration. Reaction conditions: T = [70; 90] °C; % wt. H₂SO₄ = [60; 70]; % wt. HNO₃ = [3; 5].

Since NPs formation starts with Bz oxidation to Ph and because a directly proportional relationship between CO₂ and NPs generation was noticed, one can deduce that Bz is indeed the precursor of this gaseous species. This statement is also supported by the results disclosed in section 7.3.1.

The studied parameters, specifically, the initial reaction temperature, the sulfuric acid and nitric acid concentration were also correlated with CO_2 generation in order to develop an empirical equation able to predict the gas production as function of the reaction conditions – equation (7.2).

$$\text{CO}_2(\text{ppm}) = -1528.3 + 14.5 \times \text{H}_2\text{SO}_4(\% \text{ wt.}) + 41.6 \times \text{HNO}_3(\% \text{ wt.}) + 6.2 \times T(^{\circ}\text{C}) \quad (7.2)$$

This multivariable regression has a significance F value lower than 0.05 and a R squared value equal to 0.91, which is a good fit considering the reduced number of observations (7) used in the correlation – Figure 7.9. As Figure 7.9 shows, the estimated CO_2 concentration tends to have an associated error lower than 15%.

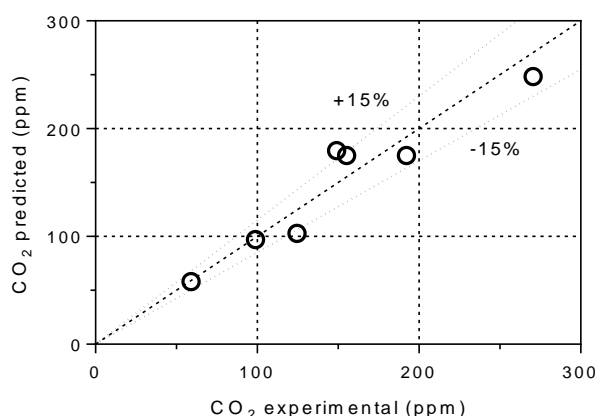


Figure 7.9 – Experimental vs. predicted values for CO_2 formation as function of the reaction conditions.

Analysing oxalic acid amounts for the different Bz nitration runs is noticeable an insignificant variation of this dicarboxylic acid concentration, except for the runs with the lowest nitric acid (run 7) and the highest sulfuric acid (run 6) concentrations. The consistency of oxalic acid concentration for different reactions conditions is explained by the species' resistance to oxidation [23-24, 26].

The low oxalic acid concentration for the lowest nitric acid strength run (run 7) support this mineral acid role as the oxidizing agent during Bz nitration. On the other hand, the results of oxalic acid for the highest sulfuric acid concentration (run 6) are explained by the temperature rise during Bz nitration (the highest), consequence of the high catalyst concentration, which led to the increase of Bz decomposition.

The comparison of oxalic acid concentration for different reactions temperatures (70°C – run 3 vs. 90°C – run 5) shows that it was slightly higher in run 5. However, when analysing the CO_2 formed amounts a significant variation is perceived (59 vs. 149 mg/kg Bz). Since the variation of the formed CO_2 amounts was higher than that of oxalic acid concentration, one can suggest that this

organic acid should have no contribution in CO₂ formation at the employed reaction conditions, which is in accordance with the results depicted in Figure 7.3.

In order to relate oxalic acid and NPs formation for the runs conducted at the same temperature (90 °C, runs 4 to 7), the results from Table 7.2 were plotted – Figure 7.10 – revealing a relationship between these species close to direct proportionality.

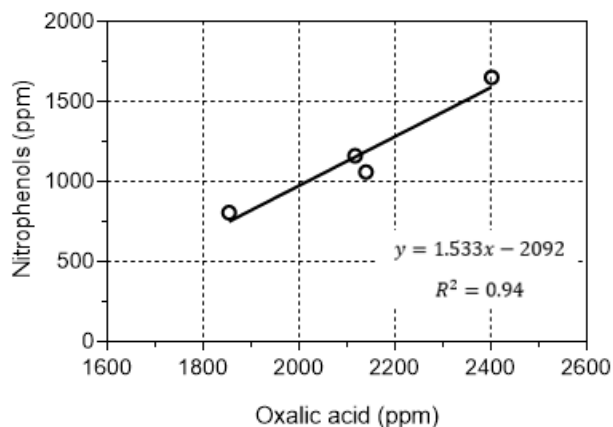


Figure 7.10 – Oxalic acid vs. NPs formation in Bz nitration. Reaction conditions: T = 90 °C; % wt. H₂SO₄ = [60; 70]; % wt. HNO₃ = [3; 5].

This behaviour had already been detected when relating NPs and CO₂ formation (Figure 7.8), allowing thus to conclude that Ph, formed *via* Bz oxidation, can either be nitrated yielding NPs, or it can be further oxidized leading to oxalic acid and CO₂ formation. This is in accordance with our proposed pathway for Bz decomposition (Chapter 3), and is a substantial finding because evidences that after Bz oxidation, phenol is not only nitrated, being also decomposed to short chain acids, CO (detected in Bz nitration although not addressed in this section) and CO₂.

In order to minimize the formation of all the addressed species, the reaction conditions, namely the initial temperature and mixed acid composition, should be softened. However, the smoothing of these reaction parameters would decrease Bz nitration rate. Therefore, a compromise is needed between the Bz nitration rate and these species minimization. A possible solution, already implemented in the nitration plant is the distributed feed of nitric acid [31]. Another solution is the reduction of the reaction temperature, although in a small extent to don't compromise MNB production.

Summarizing, the conducted runs allowed to demonstrate that during Bz nitration, the source of CO, CO₂ and of the oxidized intermediates is the reaction's raw material itself and not the aliphatic impurities as suggested in the literature [19]. Bearing in mind this conclusion and considering all the side reactions from benzene nitration (dinitrobenzene, nitrophenols and sulfonic acids formation) [4, 7-9], Figure 7.11 was created.

Decomposition Reactions in Aromatic Nitration

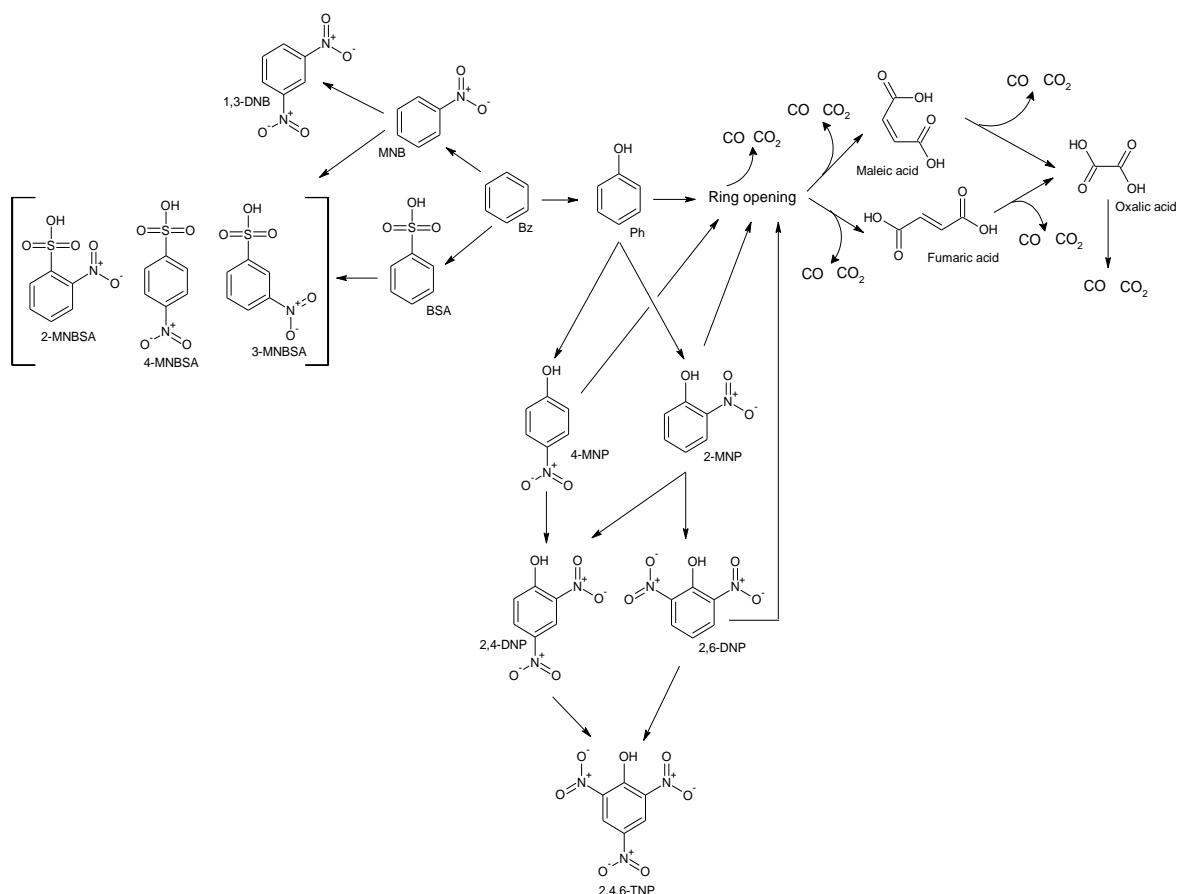


Figure 7.11 – Reaction (by-)products from benzene nitration. Elaborated based on info taken from refs [7-9, 26, 29, 32] and in the Chapters 3.

According to the figure Bz is nitrated to MNB, which in turn can be further nitrated to DNB or sulfonated to MNBSA. Additionally, Bz can either be sulfonated to BSA, being this species then nitrated to MNBSA, or oxidized to Ph yielding thus mononitrophenols that are nitrated to dinitrophenols which in turn are in trinitrophenol origin. These phenolic by-products (whose source is Bz), namely, Ph, 2-MNP, 4-MNP and 2,6-DNP may also be further oxidized, which would lead to the compounds' aromatic ring cleavage, promoting the formation of short chain dicarboxylic acids, carbon dioxide and carbon monoxide.

7.4. Conclusions

During this study, it was experimentally demonstrated, for the first time at lab scale tests that CO_2 is formed during mixed acid benzene nitration. Such finding corroborates the CO_2 detection in the industrial mononitrobenzene production process (disclosed in the Chapter 2). Additionally, it was also evidenced that oxalic acid is generated during this reaction. These facts are indicative of the occurrence of oxidation reactions during benzene nitration.

It was found that in addition to CO₂, CO is also generated during benzene nitration, being evidenced the existence of a linear relation between CO and CO₂ formation. It was also demonstrated that in benzene nitration CO₂ amounts are higher than those of CO by a factor of ca. 1.7. Furthermore, this study allowed concluding that benzene is the source of the detected oxidation products (oxalic acid, CO and CO₂), a finding opposite to what is stated in the literature which is that during benzene nitration CO₂ is formed due to the oxidation of aliphatic species.

The conducted tests allowed to evidence that upon benzene oxidation to phenol, phenol is not only nitrated being also oxidized into dicarboxylic acids which are decomposed to CO and CO₂.

A parametric study was carried out which have shown that the decrease of benzene / nitric acid ratio favours CO₂ formation is favoured, that the reaction temperature increase led to the rise of NPs and CO₂ generation and that the increase of sulfuric acid or nitric acid concentration in mixed acid have amplified NPs, oxalic acid and CO₂ formed amounts.

Nomenclature

Acronyms

BSA	Benzenesulfonic acid
Bz	Benzene
DNB	Dinitrobenzene
2,4-DNP	2,4-dinitrophenol
2,6-DNP	2,6-dinitrophenol
FID	Flame Ionization Detector
GC	Gas Chromatography
HPLC-DAD	High-Performance Liquid Chromatography - Diode Array Detector
MCH	Methylcyclohexane
MNB	Mononitrobenzene
2-MNBSA	2-mononitrobenzenesulfonic acid
3-MNBSA	3-mononitrobenzenesulfonic acid
4-MNBSA	4-mononitrobenzenesulfonic acid
2-MNP	2-mononitrophenol
4-MNP	4-mononitrophenol
NPs	Nitrophenols
Ph	Phenol
TNP	2,4,6-trinitrophenol

7.5. References

- [1]. Dugal, M., Nitrobenzene and Nitrotoluenes. In *Kirk-Othmer Encyclopedia of Chemical Technology*, John Wiley & Sons, Inc., 2000, 10.1002/0471238961.1409201801041109.a01.pub2.
- [2]. Alexanderson, V.; Trecek, J. B.; Vanderwaart, C. M., Continuous adiabatic process for the mononitration of benzene. US Patent 4,091,042, May 23, 1978.
- [3]. Guenkel, A. A.; Rae, J. M.; Hauptmann, E. G. Nitration process. US Patent 5,313,009, May 17, 1994.
- [4]. Quadros, P. A.; Castro, J. A. A. M.; Baptista, C. M. S. G., Nitrophenols Reduction in the Benzene Adiabatic Nitration Process. *Industrial & Engineering Chemistry Research* **2004**, 43 (15), 4438-4445, 10.1021/ie034263o.
- [5]. Berretta, S.; Louie, B., Effect of Reaction Conditions on the Formation of Byproducts in the Adiabatic Mononitration of Benzene into Mononitrobenzene (MNB). In *Chemistry, Process Design, and Safety for the Nitration Industry*, American Chemical Society, Washington, DC. ACS Symposium Series, 2013; Vol. 1155, pp 13-26, doi:10.1021/bk-2013-1155.ch002 10.1021/bk-2013-1155.ch002.
- [6]. Lopes, A. L. C. V.; Ribeiro, A. F. G.; Reis, M. P. S.; Silva, D. C. M.; Portugal, I.; Baptista, C. M. S. G., Distribution models for nitrophenols in a liquid-liquid system. *Chemical Engineering Science* **2018**, 189, 266-276,
- [7]. Afonso, D.; Ribeiro, A. F. G.; Araújo, P.; Vital, J.; Madeira, L. M., Phenol in Mixed Acid Benzene Nitration Systems. *Industrial & Engineering Chemistry Research* **2018**, 57 (46), 15942-15953,
- [8]. Afonso, D.; Ribeiro, A. F. G.; Araújo, P.; Vital, J.; Madeira, L. M., (Nitro)Phenols reactivity in mixed acid benzene nitration. *Submitted* **2019**,
- [9]. Afonso, D.; Ribeiro, A. F. G.; Araújo, P.; Vital, J.; Madeira, L. M., (Nitro)benzenesulfonic acids in nitrobenzene production. *Submitted* **2019**,
- [10]. Albright, L. F.; Schiefferle, D. F.; Hanson, C., Reactions occurring in the organic phase during aromatic nitrations. *Journal of Applied Chemistry and Biotechnology* **1976**, 26, 522-525, 10.1002/jctb.5020260174.
- [11]. Burns, J. R.; Ramshaw, C., Development of a Microreactor for Chemical Production. *Chemical Engineering Research and Design* **1999**, 77 (3), 206-211, <http://dx.doi.org/10.1205/026387699526106>.
- [12]. Odle, R. R.; Guggenheim, T. L.; DeLong, L. M., Solubility, Equilibrium, Behavior, and Analytical Characterization of Tetranitromethane, Trinitromethane, Methyl Amine, and Ammonia in a Nitration Facility. In *Chemistry, Process Design, and Safety for the Nitration*

- Industry*, American Chemical Society, Washington, DC. ACS Symposium Series, 2013; Vol. 1155, pp 203-228, doi:10.1021/bk-2013-1155.ch014
10.1021/bk-2013-1155.ch014.
- [13]. Urbański, T., *Chemistry and Technology of Explosives*. Pwn-Polish Scientific Publishers, Vol. 1, Warszawa, Poland, 1964.
- [14]. Seyewetz, A.; Poizat, L., Sur l'oxidation des dérivés nitrés et nitrosés aromatiques par le persulfate d'ammoniaque. *Comptes Rendus Hebdomadaires des Séances de l'Académie des Sciences* **1909**, 148, 1110-1113,
- [15]. Albright, L. F., Nitration. In *Kirk-Othmer Encyclopedia of Chemical Technology*, John Wiley & Sons, Inc., 2000, 10.1002/0471238961.1409201801120218.a01.
- [16]. Ross, D. S.; Kirshen, N. A., Nitration and Oxidative Side Reactions of Dinitrotoluenes. In *Industrial and Laboratory Nitrations*, American Chemical Society, Washington, DC. ACS Symposium Series, 1976; Vol. 22, pp 114-131, doi:10.1021/bk-1976-0022.ch007
10.1021/bk-1976-0022.ch007.
- [17]. Kramer, G. M., Oxidation of paraffins in sulfuric acid. *The Journal of Organic Chemistry* **1967**, 32 (6), 1916-1918, 10.1021/jo01281a047.
- [18]. Costa, T. J. G.; Nogueira, A. G.; Silva, D. C. M.; Ribeiro, A. F. G.; Baptista, C. M. S. G., Nitrophenolic By-Products Quantification in the Continuous Benzene Nitration Process. In *Chemistry, Process Design, and Safety for the Nitration Industry*, American Chemical Society, Washington, DC. ACS Symposium Series, 2013; Vol. 1155, pp 49-60, doi:10.1021/bk-2013-1155.ch004
10.1021/bk-2013-1155.ch004.
- [19]. Guenkel, A. A.; Maloney, T. W., Recent Advances in the Technology of Mononitrobenzene Manufacture. In *Nitration*, American Chemical Society, Washington, DC. ACS Symposium Series, 1996; Vol. 623, pp 223-233, doi:10.1021/bk-1996-0623.ch020
10.1021/bk-1996-0623.ch020.
- [20]. Carey, F., *Organic Chemistry*. 4th edition, McGraw-Hill, New York, 2000.
- [21]. Gattrell, M.; Louie, B., Adiabatic Nitration for Mononitrotoluene (MNT) Production. In *Chemistry, Process Design, and Safety for the Nitration Industry*, American Chemical Society, Washington, DC. ACS Symposium Series, 2013; Vol. 1155, pp 27-48, doi:10.1021/bk-2013-1155.ch003
10.1021/bk-2013-1155.ch003.
- [22]. Booth, G., Nitro Compounds, Aromatic. In *Ullmann's Encyclopedia of Industrial Chemistry*, Wiley-VCH, Weinheim, 2000, doi:10.1002/14356007.a17_411.
- [23]. Zazo, J. A.; Casas, J. A.; Mohedano, A. F.; Gilarranz, M. A.; Rodríguez, J. J., Chemical Pathway and Kinetics of Phenol Oxidation by Fenton's Reagent. *Environmental Science and Technologies* **2005**, 39 (23), 9295-9302,

- [24]. Zazo, J. A.; Pliego, G.; Blasco, S.; Casas, J. A.; Rodriguez, J. J., Intensification of the Fenton Process by Increasing the Temperature. *Industrial & Engineering Chemistry Research* **2011**, 50 (2), 866-870, 10.1021/ie101963k.
- [25]. Rahaman, M.; Mandal, B. P.; Ghosh, P., Nitration of nitrobenzene at high-concentrations of sulfuric acid. *AIChE Journal* **2007**, 53 (9), 2476-2480, doi:10.1002/aic.11222.
- [26]. Carbajo, J.; Quintanilla, A.; Casas, J. A., Assessment of carbon monoxide formation in Fenton oxidation process: The critical role of pollutant nature and operating conditions. *Applied Catalysis B: Environmental* **2018**, 232, 55-59,
- [27]. Di Somma, I.; Marotta, R.; Andreozzi, R.; Caprio, V., Nitric acid decomposition kinetics in mixed acid and their use in the modeling of aromatic nitration. *Chemical Engineering Journal* **2013**, 228, 366-373, <https://doi.org/10.1016/j.cej.2013.04.100>.
- [28]. Lichty, D. M., The Chemical Kinetics of the Decomposition of Oxalic Acid in Concentrated Sulphuric Acid. *Journal of Physical Chemistry* **1907**, 11 (3), 225-272,
- [29]. Devlin, H. R.; Harris, I. J., Mechanism of the oxidation of aqueous phenol with dissolved oxygen. *Industrial & Engineering Chemistry Fundamentals* **1984**, 23 (4), 387-392,
- [30]. Hanson, C.; Kaghazchi, T.; Pratt, M. W. T., Side Reactions During Aromatic Nitration. In *Industrial and Laboratory Nitrations*, American Chemical Society, Washington, DC. ACS Symposium Series, 1976; Vol. 22, pp 132-155, doi:10.1021/bk-1976-0022.ch008
10.1021/bk-1976-0022.ch008.
- [31]. Nogueira, A. G. Optimização da Nitração de Aromáticos. PhD Thesis, Universidade de Coimbra, Portugal, 2014.
- [32]. Rodrigues, C. S. D.; Borges, R. A. C.; Lima, V. N.; Madeira, L. M., *p*-Nitrophenol degradation by Fenton's oxidation in a bubble column reactor. *Journal of Environmental Management* **2018**, 206, 774-785,

Chapter 8 – Conclusions and future work

8.1. Conclusions

Benzene nitration is a well-known reaction, having been developed over the years, aiming the increase of the reaction productivity with the consequent decrease of by-products formation. However, despite all the achieved improvements, there are some subjects still poorly studied, namely those related to the formation mechanism of the reaction by-products. In this section, a general overview of the main conclusions arising from the PhD work done and presented along this thesis are given.

The main objective of this thesis was determining the CO₂ origin, formation path and understanding how the reaction conditions affect this compound generation. This was an important study because carbon dioxide can originate operation issues in some industrial equipment.

This thesis was carried out in an industrial environment, an aspect that brought several advantages to the work since it enabled the analysis of various industrial streams. The analysis of these streams allowed determining that carbon dioxide is generated in the reaction section of the nitration plant. Such finding helped to justify ammonium carbonate formation in nitration plants and have allowed inferring the occurrence of oxidative degradation reactions during benzene nitration, although without any enlightenment regarding the compound(s) that was (were) being oxidized.

The occurrence of oxidation reactions during benzene nitration is also supported by the detection of dicarboxylic acids in the nitration plant, namely oxalic acid, mesoxalic acid, fumaric acid, maleic acid, succinic acid, and adipic acid. It was found that in the presence of mixed acid (mixture of nitric and sulphuric acid), in the absence of benzene and at temperatures within the industrial nitration range, the detected dicarboxylic acids yield carbon dioxide, revealing their potential role as precursors of the detected gas in the nitration plant. Therefore, based on the detection of these dicarboxylic acids, on advanced oxidation processes studies and in experiments carried out with the chemical species that are typically present in the nitration media it was possible to postulate a CO₂ formation path which involved phenol formation and oxidation.

Once the oxidative degradation of aromatic compounds such as phenol by advanced oxidation processes yields some of the detected dicarboxylic acids, and because phenol is postulated to be the nitrophenols precursor, efforts were made for detecting this compound both in the industrial nitration medium as well as in the lab scale nitrations. The detection of phenol in the nitration medium was a major and novel finding because: i) it has contributed for supporting the proposed and accepted by-products nitration theory, which states that phenol is the nitrophenols precursor

and that the reactions occur in the acid phase or near the interphase, and ii) for supporting the postulated CO₂ formation path.

Phenol's role as the nitrophenols precursors was supported by a kinetic model (with good adherence to the experimental data) which also evidenced its high reactivity. Nitrophenols interconversion was also studied at different reaction conditions, aiming to evidence these compounds reactivity and to evaluate the impact of the reaction parameters on these compounds' formation. The performed parametric study has shown that the increase of either temperature, sulphuric acid or nitric acid concentrations favour nitrophenols formation. Using the data from the conducted nitrations, another kinetic model was constructed which also exhibited a quite good adherence to the experimental values, considering the simplifications made. The developed model allowed to corroborate nitrophenols interconversion and is the first mechanistic-based approach for describing these compounds formation in mixed acid benzene nitrating systems.

When studying CO₂ origin and formation path it was revealed the presence of dicarboxylic acids in the reaction medium. However, in addition to these compounds other chemical species were detected, revealing the existence of a new class of reaction by-products, the sulfonic acids, not mentioned in benzene nitration studies. The detected sulfonic acids were benzenesulfonic acid, 2-mononitrobenzenesulfonic acid, 3-mononitrobenzenesulfonic acid and 4-mononitrobenzenesulfonic acid. A parametric study was performed in which it was concluded that their formation is favoured using higher reaction temperatures and higher sulfuric acid concentrations. It was also found that these sulfonic acids' affinity towards the reaction's aqueous phase is higher than to the organic one.

Additionally, the performed lab scale tests proved that (nitro)benzenesulfonic acids are originated during benzene nitration either by benzene sulfonation followed by benzenesulfonic acid nitration or by benzene nitration followed by mononitrobenzene sulfonation. This finding evidences the occurrence of sulfonation reactions during benzene nitration.

As previously referred, the main objective of this thesis was determining the CO₂ source and formation path and understanding how the reaction conditions affect its generation. Therefore, the impact of several compounds such as the presence of impurities from the industrial nitration process (aliphatics and toluene) and of reaction by-products, known or detected during this work, on CO₂ formation was evaluated. This was accomplished by incorporating them, individually, in benzene and nitrating the mixture in the range of industrial conditions. The obtained results have helped to conclude that benzene, the raw material of the studied nitration, was the CO₂ precursor and that this gaseous species is formed *via* benzene oxidation to phenol followed by phenol oxidation to dicarboxylic acids and their decomposition to CO and CO₂. These findings are contrary to those reported in the open literature which state that CO₂ formation arises from the oxidation of aliphatic species present in the benzene nitration medium.

Additionally, it was found that in addition to CO_2 , CO is also generated during lab scale pure benzene nitrations, being evidenced the existence of a linear relation between CO and CO_2 formation. It was also demonstrated that in benzene nitration CO_2 amounts are higher than those of CO by a factor of ca. 1.7. Furthermore, it was found that the benzene / nitric acid ratio decrease favours CO_2 formation and it was observed that the increase of the reaction temperature leads to the rise of nitrophenols and CO_2 generation; still, the increase of sulfuric acid and nitric acid concentration amplified nitrophenols, oxalic acid and CO_2 formed amounts. The obtained results demonstrate the role of nitric acid on the genesis of the studied compounds.

The conducted tests allowed to evidence that upon benzene oxidation to phenol, phenol is not only nitrated being also oxidized into dicarboxylic acids which are decomposed to CO and CO_2 .

Once in addition to the known reaction by-products (nitrophenols and dinitrobenzene), phenol and new reaction by-products (dicarboxylic acids and sulfonic acids) were detected in the nitration media during this work, the reaction scheme proposed for the origin and formation of the decomposition products (CO and CO_2) during nitration is disclosed in Figure 8.1.

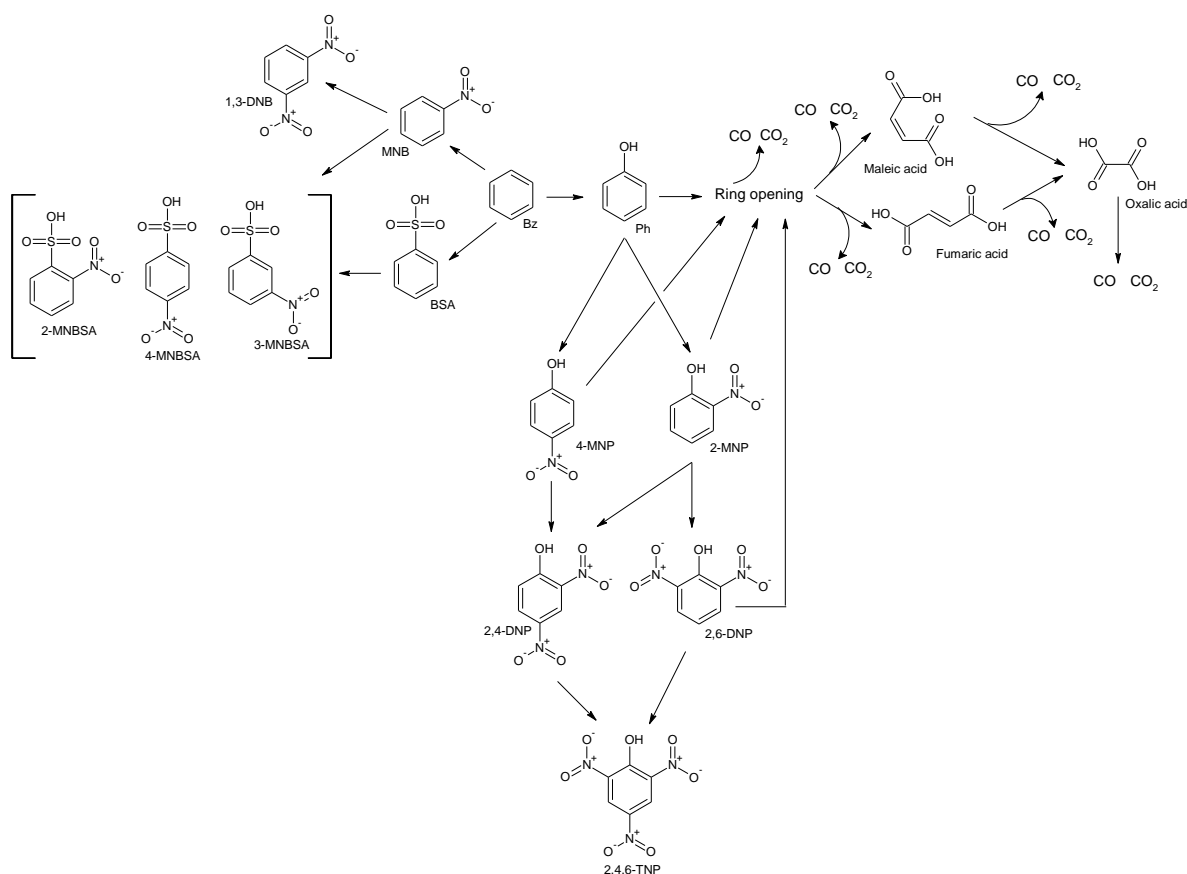


Figure 8.1 – Reaction product and by-products from the benzene nitration.

8.2. Future work

Despite all the findings achieved during this work, there are still some questions that should be analysed and further explored. The suggestions for future work are related to the different topics addressed in the scope of the present work.

During this study, it was detected the presence of dicarboxylic acids and sulfonic acids in different plant locations, a fact unknown to date. Consequently, any action was taken regarding the removal of these compounds from the nitration plant. Therefore, studies for minimizing these compounds formation should be performed and strategies for their removal should be thought.

Further mass spectrometry analyses should be performed to check the presence of other compounds in the nitration plant and to clarify the nature of the unidentified but detected chromatographic peaks in the performed analyses.

The constructed kinetic model for describing nitrophenols interconversion at different reaction conditions was developed taking into account some simplifications, such as considering a single liquid phase (pseudo-homogeneous system) instead of a heterogeneous liquid-liquid reaction mixture. Thus, in order to improve the kinetic model, the mass transfer coefficients for the different species (benzene and nitrophenols) diffusion between the organic phase and the aqueous one should be considered. Moreover, dinitrobenzene formation should also be accounted for in the kinetic model.

The development of a kinetic model for describing the formation of the sulfonic acids during benzene nitration should also be considered since it would allow to more easily optimize the operating conditions aiming to minimize these compounds formation.

It was seen that softening the reaction conditions, having as reference the industrial ones, allows decreasing CO₂ and nitrophenols formation. Therefore, the industrial operation conditions should be slightly softened and the techno-economic impact on nitrophenols, carbon dioxide and benzene conversion assessed. If benzene conversion is not significantly affected by the variation of the reaction conditions, this simple change might allow decreasing the production cost of benzene nitration.

The benzene nitrations performed during this work were all carried out discontinuously, in a stirred batch reactor. Conducting these reactions in a continuously stirred tank reactor would be an added value because it could better simulate the industrial nitration process. Additionally, the use of another type of reactor such as a tubular one would be an interesting possibility because the interfacial area between the organic phase and mixed acid would differ, which most likely would affect the mass transfer between both reaction phases, influencing thus nitrophenols, sulfonic acids, dicarboxylic acids and carbon dioxide and monoxide formation.

Appendix A – Laboratorial unit

A.1. Introduction

One of the goals for the present work was the construction of a laboratory unit capable of working within the industrial range of nitration conditions. By this way, it is possible to easily change some operational parameters such as the mixed acid composition, the reaction temperature or the organic substrate composition evaluating their influence on the by-products formation and on the reaction rate without compromising the industrial production process.

The laboratorial unit assembly wasn't made from scratch, having its construction began in the sequence of a previous internal project that focused on the study of 2,4-dinitrophenol and trinitrophenol oxidation [1]. This nitration unit is similar to the one developed by Santos [2] – Figure A.1.



Figure A.1 – Nitration reactor developed by Santos [2]. Adapted from [2].

The reactor's parts in contact with the reaction medium were composed by glass and *Teflon* because these materials are resistant to highly corrosive mixtures such as mixed acid, to high temperatures (up to 140 °C) and to mononitrobenzene. However, even using a *Teflon* coating technique, some components of Santos [2] reactor were corroded – Figure A.2.



Figure A.2 – Corroded reactor components. Adapted from [2].

A.2. Bondalti's lab scale nitration reactor

Bondalti's laboratorial reactor was constructed resorting to two borosilicate glass cylinders, being the top and bottom extremities (in contact with the reaction medium) made by *Teflon*, similarly to the reactor used by Santos [2]. The glass cylinders had the same thickness (1 cm) but different diameters. Therefore, the smaller glass cylinder was placed inside the larger one (Figure A.3-a)) to provide the reactor with a heating / cooling jacket. The cylinders thickness is considerable, enabling thus a secure reactor pressurization, necessary for replicating the employed industrial pressure. The reactor's dimensions are displayed in Figure A.3-b) and in Table A.1.

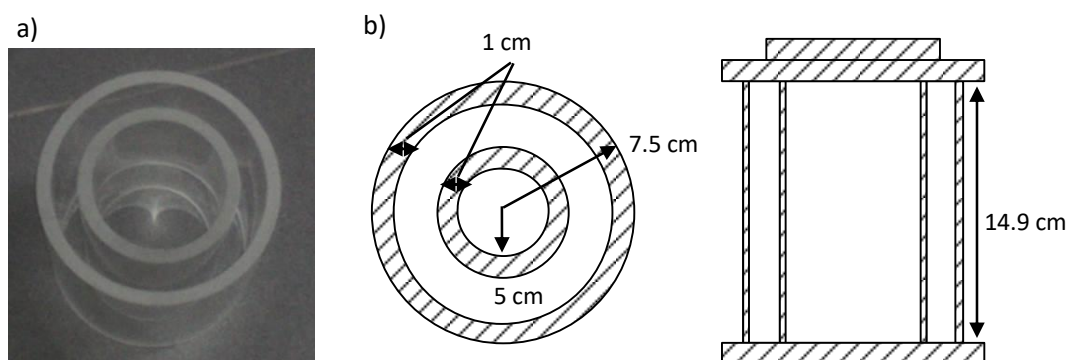


Figure A.3 – a) Reactor glass cylinders before being assembled. b) Reactor diameters, thickness and height.

Table A.1 – Reactor dimensions.

External diameter (cm)	15
Internal diameter (cm)	10
Thickness (cm)	1
Height (cm)	14.9

The reactor is sealed at its top and bottom by a *Teflon* layer, being each extremity covered with a stainless-steel flange – Figure A.4. The stainless-steel material is not directly in contact with the reaction medium since it would be corroded, having these flanges the function supporting the *Teflon* layers.

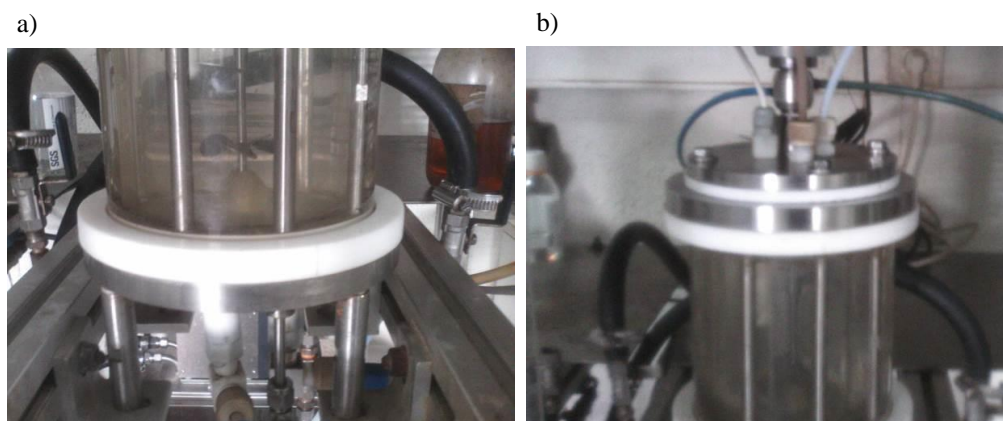


Figure A.4 – a) Reactor's bottom. b) Reactor's top.

A stirrer is used to enhance the reagents mixture inside the reactor. This component is controlled by a pneumatic motor, being the stirring speed directly proportional to the applied air pressure. As it is well known, the nitrating conditions are severe; thus, the stirrer material could not be of stainless-steel. Consequently, a tantalum stirrer, a chemical inertness material, was used in this work – Figure A.5.



Figure A.5 – Steel and tantalum stirrers.

To evaluate the unit's sealing, both the reactor and the installation tubing were subject to leak tests using water and compressed air. Initially, the system was pressurized at 2 bar(g) having been detected leaks in the tube connectors at the reactor top (Figure A.6).

Aiming to verify if either the connector threads or the internal threads of the *Teflon* layer could be the reason for the detected leakage problems, new connectors were constructed, and the *Teflon* layer threads were rebuilt. Nevertheless, the leakage problems subsisted. Therefore, to avoid the construction of a new *Teflon* layer for the reactor top, new connectors were built in PVDF, a harder

material than *Teflon* and compatible with both nitric and sulfuric acids. With this modification, the leakage issues were mitigated.

Regarding the unit piping, it was all made from PFA, as all the tube-tube connections.

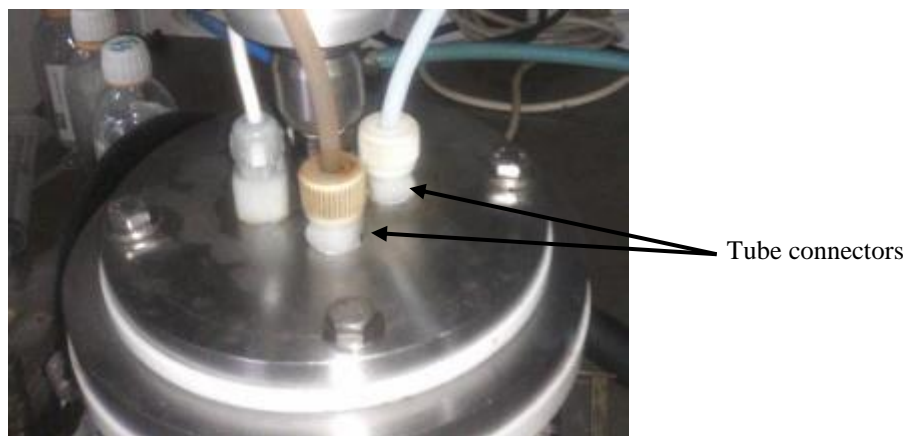


Figure A.6 – Reactor's top connections.

For recording the temperature, initially was used a temperature sensor PT100 inside a thermowell. However, it was verified that the thermowell induced a delay in the sensor response. Consequently, the reactor temperature monitoring started to be done with a *Teflon* coated thermocouple and Therma 1 thermometer from ETI Ltd.

A.3. Experimental procedure

The reagents used in the nitrations were mainly benzene from Bondalti's raw material tank, although HPLC grade benzene has also been used, sulfuric acid (99% wt.) from Quimitecnica, stored in a tank at Bondalti's installations, and nitric acid (65% wt.) from Baker. For achieving the intended mixed acid composition, demineralized water was used. In order to accurately replicate the industrial feed conditions, the reagents were fed separately.

The acid reagents were fed at the reactor's top while the organic substrate was fed at the reactor's bottom. By this way, it was guaranteed that nitration occurred only inside the reactor. As shown in Figure A.7, the mixed acid components (H_2SO_4 , HNO_3 and H_2O) were fed by gravity at the reactor's top.

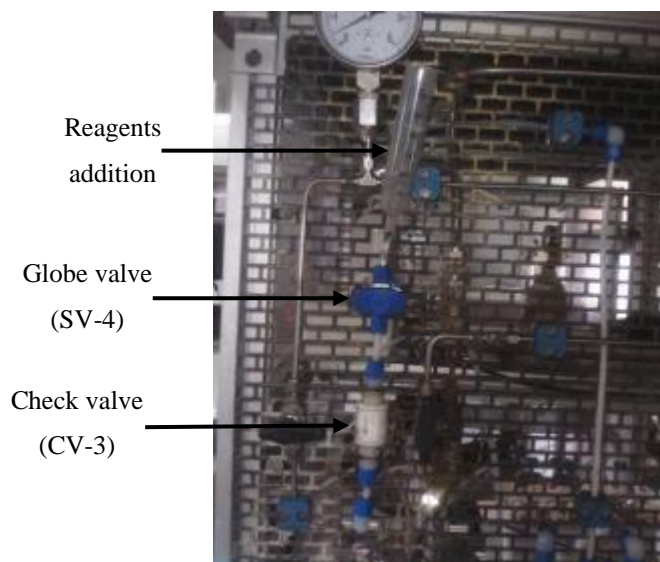


Figure A.7 – Aqueous phase reagents feed.

On the other hand, the organic substrate was fed at the reactor bottom using a syringe – Figure A.8.

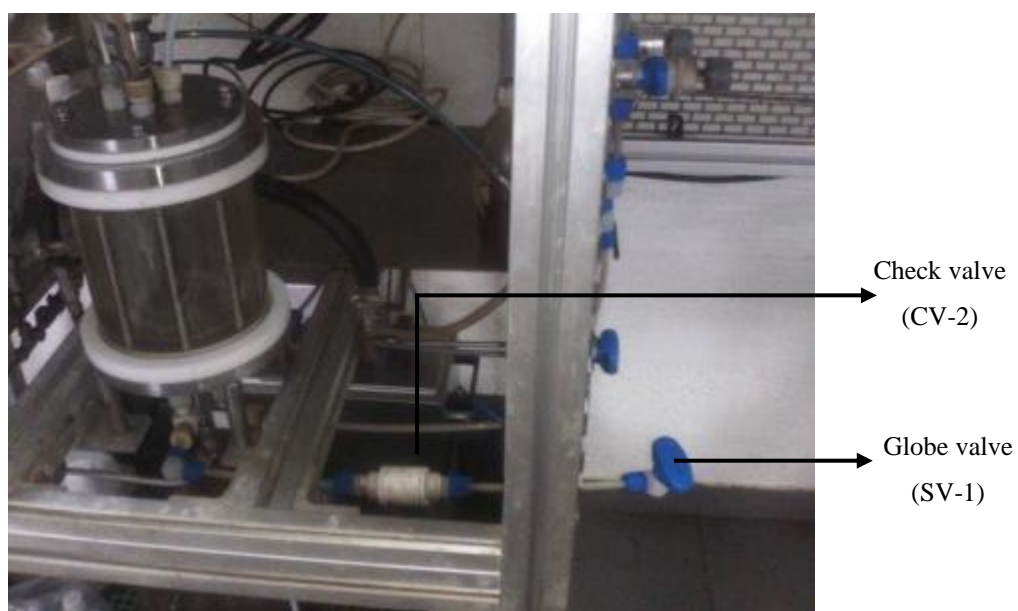


Figure A.8 – Organic substrate feed.

When conducting benzene nitrations, several samples could be taken from the reactor bottom by opening the valve SV-2 – Figure A.9.



Figure A.9 – Sampling point of liquid samples.

In Figure A.10 is represented a scheme of the assembled laboratorial nitration unit.

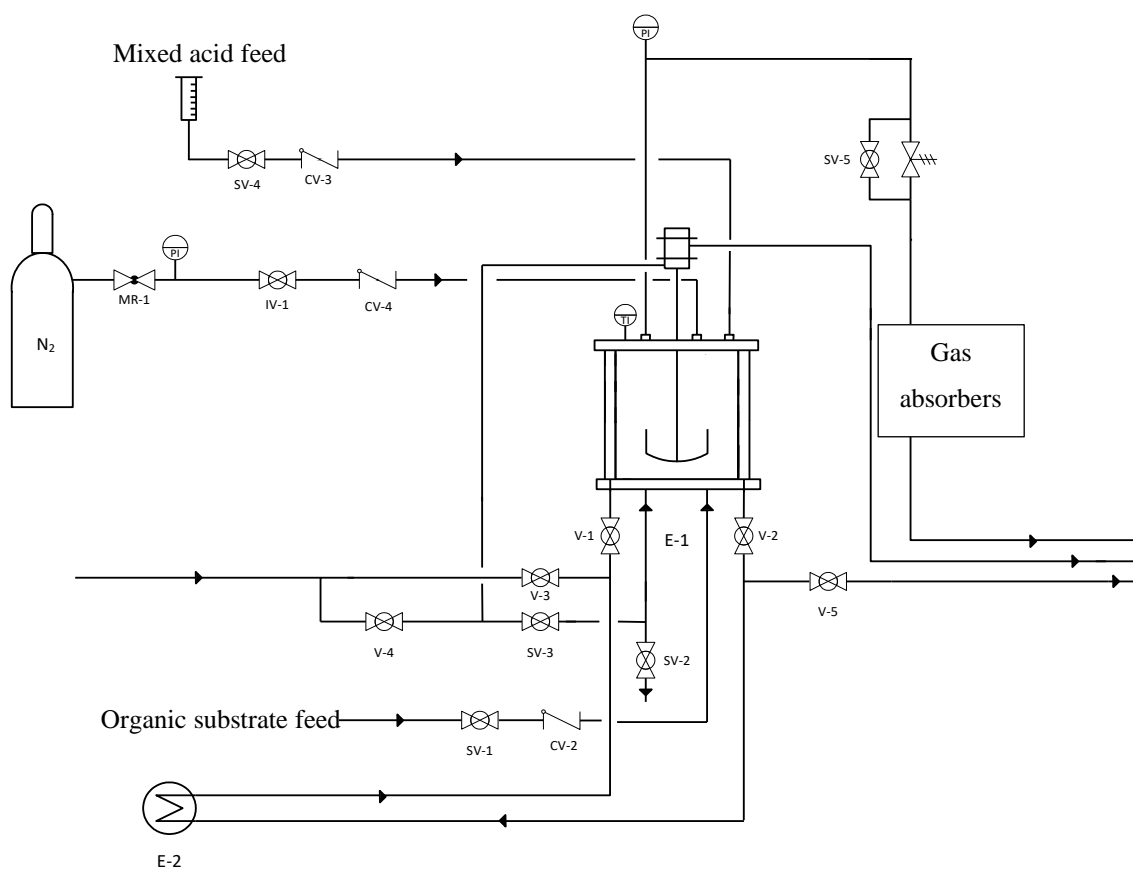


Figure A.10 – Scheme of the laboratorial nitration unit.

Decomposition Reactions in Aromatics Nitration

For performing the lab scale nitrations, an experimental procedure was developed and improved, being the final version described below:

1. Turn on the thermostatic bath and select a slightly higher temperature than the desired one;
2. Open the heating/cooling circuit valves;
3. While waiting for the bath to reach the desired temperature, weight the necessary sulfuric acid and water amounts;
4. Add the weighted sulfuric acid to the reactor through valve SV-4 and turn on the temperature monitor;
5. Turn on the stirrer at a low/medium speed and close the valve SV-4;
6. Open the valve SV-4 and add slowly and partially the water weighted to avoid an abrupt temperature increase due to the acid dilution;
7. After the water addition, if CO₂ formation is intended to be followed, connect the N₂ gas line to the reactor to remove traces of CO₂ present within the reactor;
8. Disconnect the N₂ gas line, add the weighted nitric acid (valve SV-4) and select the intended initial reaction temperature in the thermostatic bath;
9. If CO₂ formation is intended to be followed, connect the N₂ gas line to the reactor and the gas absorbers at the reactor outlet, flowing N₂ for a few seconds;
10. When the reaction medium temperature is the intended one, adjust the stirring speed to the desired value and add the organic substrate by the valve SV-1 using a syringe;
11. If CO₂ formation is intended to be followed, immediately after the organic substrate addition connect the N₂ line to the reactor, setting the gas flow to 0.5 scfh (standard cubic feet per hour);
12. If it is intended to follow nitrophenols or other reaction by-products concentration profiles collect liquid samples opening valve SV-2;
13. After the reaction finish, disconnect the N₂ gas line if it has been previously connected and remove the gas absorbers from the unit, and turn off the stirrer;
14. Allow the phase separation waiting about 5 minutes before collecting the reaction mixture;
15. Collect the acid phase opening the valve SV-2 to a clean glass flask;
16. When almost all the acid phase has been collected, use a separatory funnel to gather the remaining reaction mixture (organic and aqueous phase);
17. Add the acid phase to the acid phase flask and place the organic phase in another glass flask;
18. Afterwards the reaction mixture removal from the reactor, turn off the thermostatic bath, fill the reactor with demineralized water (opening valves V-4 and SV-3) and turn on the stirrer at medium stirring speed;
19. While the reactor is being filled with demineralized water, fill a clean syringe with demineralized water, and add it through valve SV-1 to clean the organic feed line;

20. Close valves V-4 and SV-3 and open valve SV-2, collecting the cleaning water to a waste flask;
21. During the wastewater collection, use compressed air to speed up the process;
22. Repeat the cleaning procedure (points 18 to 21) two more times;
23. Turn off the stirrer and use compressed air (through valve SV-1) to remove water traces from the reactor by opening valve SV-2;

A.4. References

- [1]. Martins, S. D. V. Remoção de Nitrofenóis de uma Corrente de Efluente Rico. Msc Thesis, Faculdade de Engenharia da Universidade do Porto, Porto, 2008.
- [2]. Santos, P. A. Q. d. O. Nitração de Compostos Aromáticos: Transferência de Massa e Reação Química. PhD Thesis, Universidade de Coimbra, Portugal, 2004.

Appendix B – Carbon dioxide generation in nitrobenzene production

B.1. Method validation

The developed method (N_2 bubbling) was validated by adding a determined solid CO_2 mass into the round bottom flask previously filled with a CO_2 -free mononitrobenzene matrix (final product). After adding solid CO_2 , the round bottom flask was immediately closed, and the experimental procedure was started as if an industrial sample was to be analysed. The obtained results are presented in Figure B.1, showing that the collected CO_2 mass was slightly lower than the inserted ones. This is indicative that some CO_2 passed through the barium hydroxide solution without being sequestered. Nevertheless, the deviation between the inserted and collected CO_2 masses is acceptable ($\approx 10\%$).

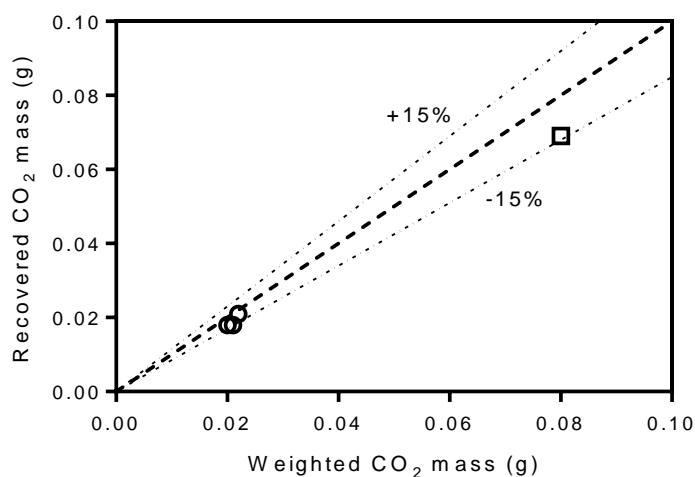


Figure B.1 – CO_2 quantification method validation.

Appendix C – Oxidation by-products in nitrobenzene production

C.1. HPLC-DAD analytical method development

For detecting and quantifying chemical compounds besides nitrophenols in nitration plants, an analytical method was developed that initially consisted on the isocratic feed of a low pH eluent (KH_2PO_4 , ≈ 2 mM, $\text{pH} \approx 2.4$; pH adjusted with H_2SO_4). This initial approach was based on the HPLC-DAD analytical method described by Vignoli and Bassoli [1] for detecting carboxylic acids, and the work of Costa *et al.* [2] that describes nitrophenols quantification. For the analytical method development, the sampling locations chosen were produced MNB (organic phase from the production process) and acid water (stream from the acid washer) because these were the safest sampling points closer to the reaction section.

To quantify nitrophenols an HPLC-DAD method has already been developed [2], which comprises a sample's extraction and dilution step with an alkaline solution, crucial for enabling the analysis of these chemical species by HPLC. Thus, considering Costa *et al.* [2] work, the use of an alkaline solution (NH_3OH) to dilute an acid water sample was assessed. The obtained results are disclosed in Figure C.1 and show that the use of an ammonium solution led to the disappearance of some chromatographic peaks from the chromatogram (until 10 minutes of analysis) which are suspected to correspond to organic acids.

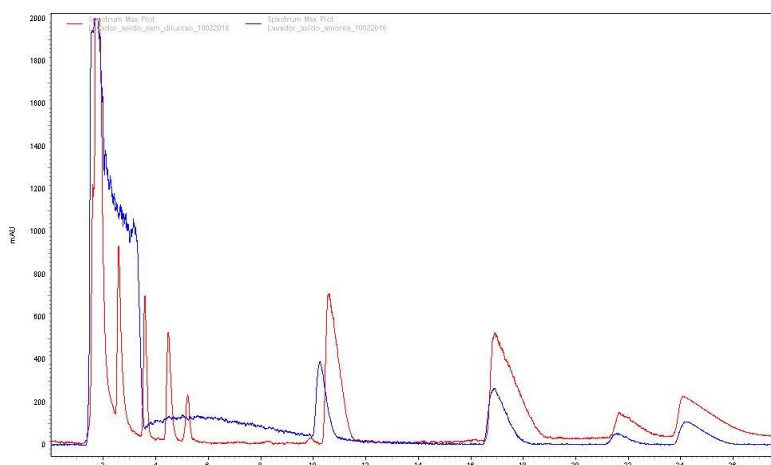


Figure C.1 – Ammonia effect on an acid water sample. Red line – sample without dilution; Blue line – Sample diluted with an ammonia solution.

Consequently, the use of alkaline solutions was avoided to ensure the obtention of representative chromatograms for each analysed sample. The noticed chromatographic peaks disappearance is the most likely reason for the non-detection and, consequently, the non-identification of several compounds in industrial benzene nitration plants.

In order to obtain representative chromatograms from the analysed samples, a neutral extraction procedure was developed for the organic samples, which consisted of mixing a determined amount of demineralized water with the organic phase. Then, the mixture was vigorously shaken, being later used a centrifuge for separating the different sample's phases (Figure C.2).

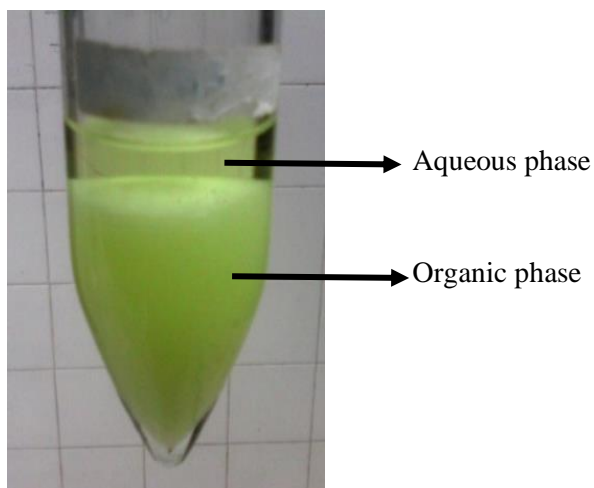


Figure C.2 – Organic phase (produced MNB) / aqueous phase separation.

The resulting aqueous phase, enriched in the unknown compounds, was then able to be injected in the HPLC-DAD apparatus. For the samples of aqueous nature, the only procedure performed consisted of the sample's dilution with demineralized water.

During the analytical method development, different eluent flow rates and feeds (isocratic feed and gradient feed) were tested, being the UV detector set to 210 nm to detect organic acids [1, 3]. After developing the neutral extraction procedure for organic samples, the isocratic feed of the KH_2PO_4 eluent ($0.7 \text{ mL} \cdot \text{min}^{-1}$) has been tested again – Figure C.3.

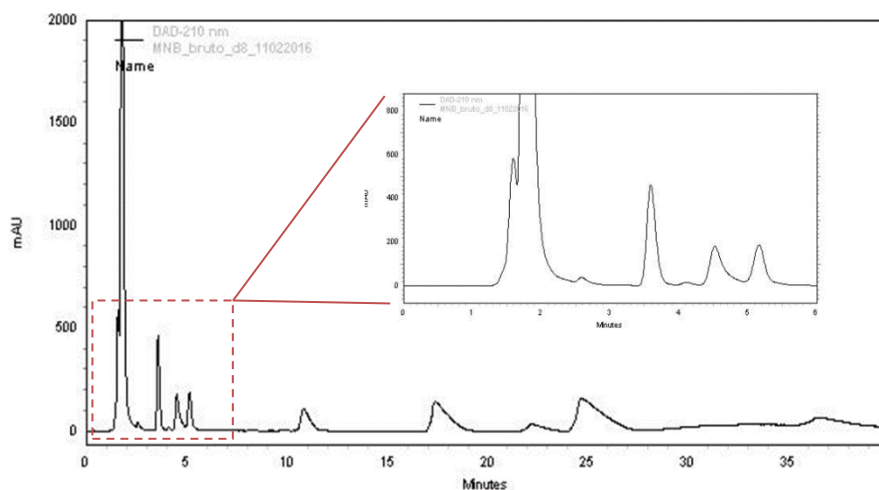


Figure C.3 – Produced MNB chromatogram at 210 nm. Mobile phase (KH_2PO_4) flow = $0.7 \text{ mL} \cdot \text{min}^{-1}$.

Figure C.3 shows that the neutral extraction enabled the transference of the unknown compounds from the organic phase to the analysed aqueous one. Furthermore, comparing Figure C.1 (sample without dilution) with Figure C.3 is visible that the number of chromatographic peaks is very similar, reinforcing the neutral extraction utility for analysing organic samples. Nevertheless, it should be noticed that the compared chromatograms are referent to distinct samples, despite their proximity in the industrial plant and their dependence (crude MNB feeds the acid washer where acid water is present).

When using the isocratic feed (KH_2PO_4 flowrate = $0.7 \text{ mL} \cdot \text{min}^{-1}$) it was seen that the first chromatographic peaks from Figure C.3 chromatogram were well spaced and resolved. However, the same is not verified for the compounds with retention times higher than 15 minutes because they have large width peaks, explained by the interaction between these analytes and the column packing. To improve the resolution of the chromatographic peaks with higher retention times the mobile phase flow was increased to $1 \text{ mL} \cdot \text{min}^{-1}$ – Figure C.4.

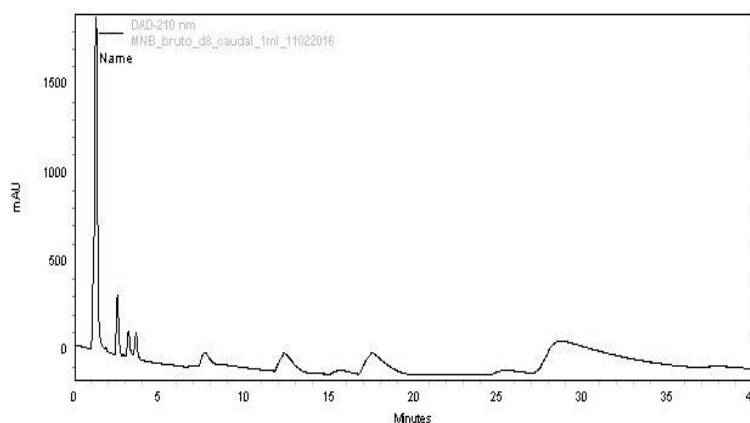


Figure C.4 – Produced MNB chromatogram at 210 nm. Mobile phase (KH_2PO_4) flow = $1 \text{ mL} \cdot \text{min}^{-1}$.

The increase of the mobile phase flow rate hadn't brought any beneficial effect regarding the large width peaks as it can be seen in Figure C.4. Consequently, the eluent feed was changed to a gradient feed with acetonitrile. Different acetonitrile and KH_2PO_4 flow rates were tested, as well as diverse starting times for the gradient feed and different acetonitrile feed rates, being satisfactorily achieved the following conditions (Table C.1).

Employing the eluent feed conditions described in Table C.1, the following chromatogram was achieved – Figure C.5.

Table C.1 – Eluent feed composition.

Time (min)	KH_2PO_4 (%)	Acetonitrile (%)	Flow rate ($\text{mL}\cdot\text{min}^{-1}$)
0 – 4	100	0	1.0
4 – 7	72.5	27.5	1.0
7 – 24	72.5	27.5	1.0
24 – 26	100	0	1.0
26 – 30	100	0	1.0

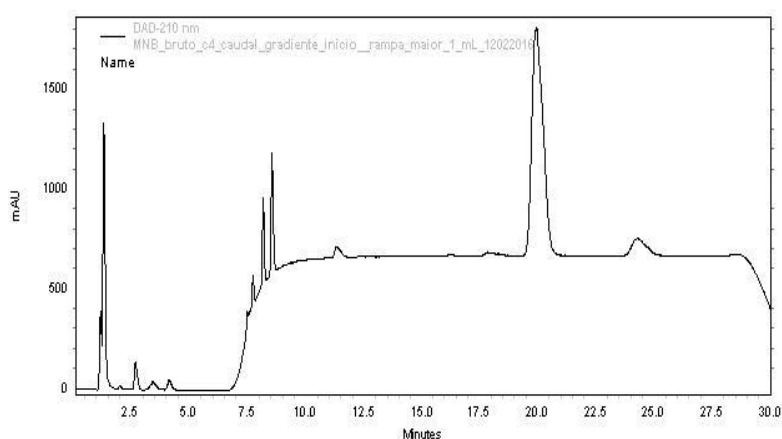


Figure C.5 – Produced MNB HPLC chromatogram at 210 nm (using Table C.1 conditions).

Scrutinizing Figure C.5 is noticeable a better peak resolution for the more retained compounds (the large width chromatographic peaks were turned into sharp peaks), a consequence of the acetonitrile gradient feed. It is also visible a baseline increase that can be justified with the use of demineralized water when preparing the KH_2PO_4 eluent. When purified water was used in the eluent's preparation, the baseline remained constant during the analytical time.

The developed method enabled obtaining well-spaced chromatographic peaks with a satisfactory resolution, reason why there weren't tested different conditions, like using methanol instead acetonitrile, varying the eluent pH or the KH_2PO_4 concentration.

C.2. HPLC-DAD method adaptation to mass spectrometry analysis

The developed HPLC analytical method allowed detecting several chromatographic peaks in the analysed samples but didn't enabled assigning the peaks to chemical compounds. Therefore, mass spectrometry (MS) analysis were conducted since it is widely used in the identification of unknown substances [4]. Notwithstanding, during the method development, some important conclusions were withdrawn, which were:

- The unknown compounds should be organic acids, probably carboxylic acids since they were neutralized with ammonia forming ammonium salts (Figure C.1);
- At wavelengths of 210 nm, the typical absorbance maximum for carboxylic acids, the analytes are clearly visible, suggesting that the detected species are indeed carboxylic acids.

To confirm that the detected chromatographic peaks correspond to carboxylic acids, the developed HPLC-DAD needed to be transposed to an HPLC-MS apparatus. In order to accomplish that, the HPLC-DAD method was adapted to comply with some HPLC-MS restrictions. The acidifying agent used (H_2SO_4) to acidify the mobile phase had to be replaced since sulfuric acid is not suitable to be used in MS analysis [5]. In addition to this limitation, the use of non-volatile buffers (like KH_2PO_4) is not recommended in HPLC-MS since they may lead to the appearance of background noise and the formation of adduct ions [6].

Both formic and acetic acid could be used to acidify the mobile phase once they are suitable to be used in MS due to their volatility [7] and to their potential to separate carboxylic acids [8]. Based on Gamoh *et al.* [8] work, formic acid was selected as the mobile phase acidifier due to its ion current enhancement capacity, feature not verified for acetic acid. Another change implemented on the HPLC-DAD developed method was the elimination of the KH_2PO_4 salt due to its non-volatility. The search for a replacement buffer wasn't necessary because several works [5, 7-10] display satisfactorily resolved peaks and good carboxylic acids separation resorting simply to an aqueous formic acid solution. Therefore, the eluent consisted of an aqueous formic acid solution (1.5% (V/V)). The eluent pH wasn't measured.

Before being transposed to the HPLC-MS equipment, the adapted method was tested in the HPLC-DAD. The performed tests involved the replacement of acetonitrile by methanol in the gradient feed (Figure C.6), different starting times for the gradient feed, and isocratic feed test (Figure C.7). These tests aimed at the optimization of the analytical method.

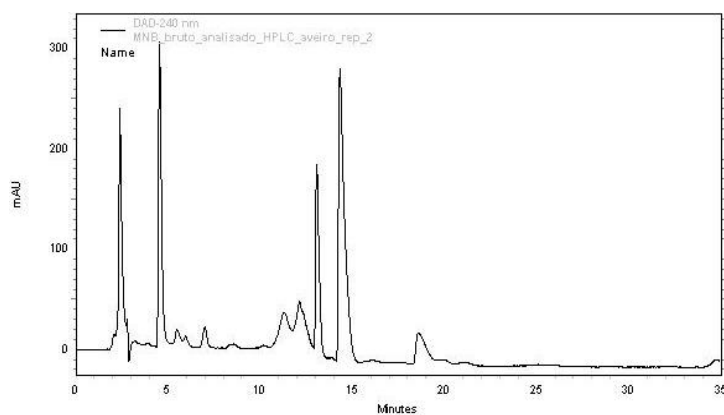


Figure C.6 – Produced MNB HPLC chromatogram. Eluent: formic acid. Gradient feed of methanol.

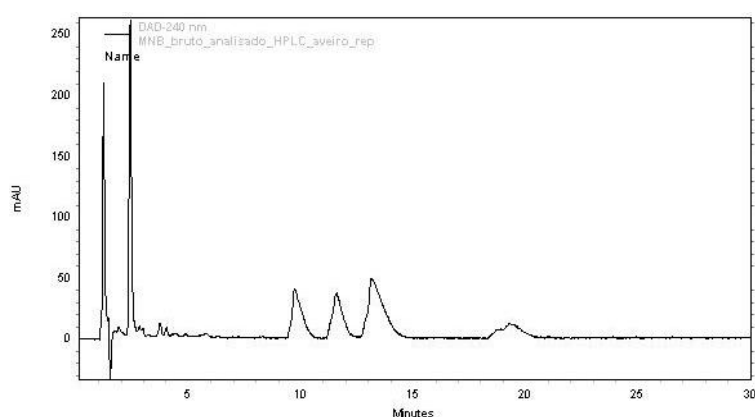


Figure C.7 – Produced MNB HPLC chromatogram. Isocratic feed. Eluent: formic acid.

Despite the optimization efforts, the adapted method was very similar to the one developed for HPLC-DAD. The only promoted change was the eluent replacement to fulfil the MS analysis restrictions. The eluent feed conditions are displayed in Table C.2 and the respective chromatogram is depicted in Figure C.8.

Table C.2 – Eluent feed composition for the HPLC-MS method.

Time (min)	Formic acid solution (%)	Acetonitrile (%)	Flow rate (mL.min ⁻¹)
0 – 4	100	0	1.0
4 – 7	72.5	27.5	1.0
7 – 24	72.5	27.5	1.0
24 – 26	100	0	1.0
26 – 30	100	0	1.0

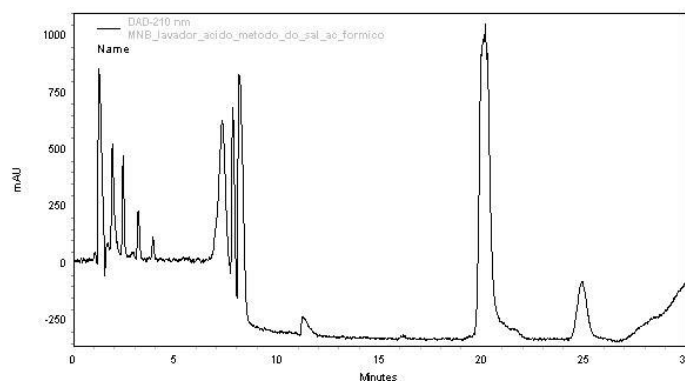


Figure C.8 – Acid water HPLC chromatogram using Table C.2 conditions.

As it is visible in Figure C.8, the obtained chromatographic peaks are well spaced and resolved, which attest the possibility of using this method in HPLC-MS for identifying the unknown compounds.

C.3. Identification of the detected by-products

The performed MS analysis enabled the obtention of the mass spectra of the different detected chromatographic peaks. In the Figure C.9 are revealed all the peaks mass spectra except those with the following retention times: 5.19 minutes; 7.42 minutes; 9.16 minutes and 9.89 minutes (peaks K2 to K5 according to Table 3.1 nomenclature) since they are addressed in Chapter 6.

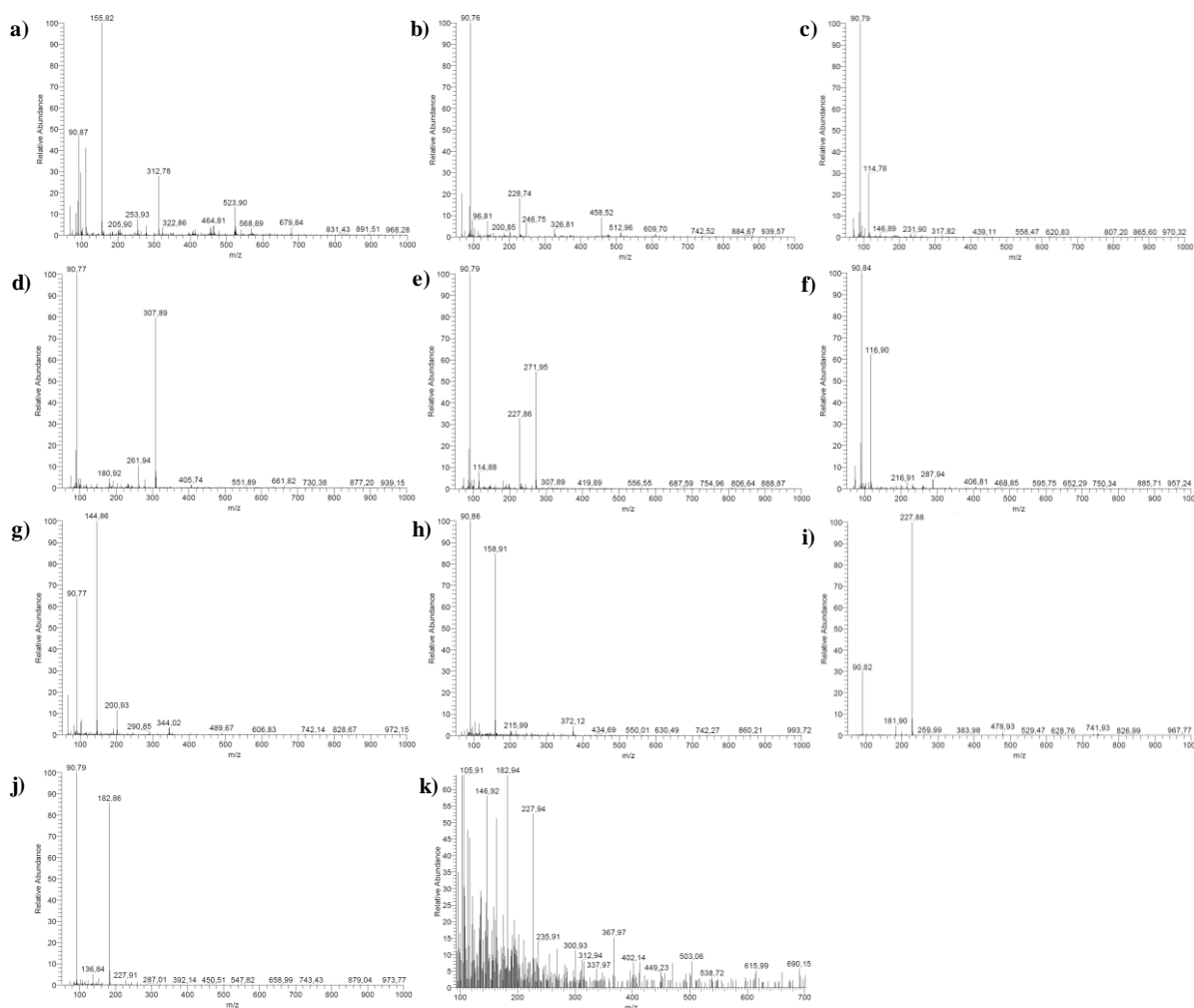


Figure C. 9 – MS spectra of analyte: **a)** U2; **b)** U3; **c)** U4; **d)** U5; **e)** U6; **f)** U7; **g)** U8; **h)** U9; **i)** K6; **j)** K7 and **k)** K8. See Table's 3.1 nomenclature.

To confirm the identification of some of the chromatographic peaks industrial samples were collected and analysed by HPLC-DAD, being then enriched in the standard of the proposed chemical species (for identifying the peak), and finally analysed. After this process, the obtained chromatograms were compared in order to check the standard retention time and UV-Vis spectrum, aiming to link these characteristics with those of the peak detected in the industrial sample.

To verify if the chromatographic peak U2 (Figure 3.1; Table 3.1) could be identified as 5-nitro-2-furoic acid, a standard of this compound was added to an industrial sample – Figure C.10. The gotten results show that the retention time of 5-nitro-2-furoic acid differs from the those of all the detected peaks, implying that neither the peak U2 nor any of the detected compounds are 5-nitro-2-furoic acid.

Decomposition Reactions in Aromatic Nitration

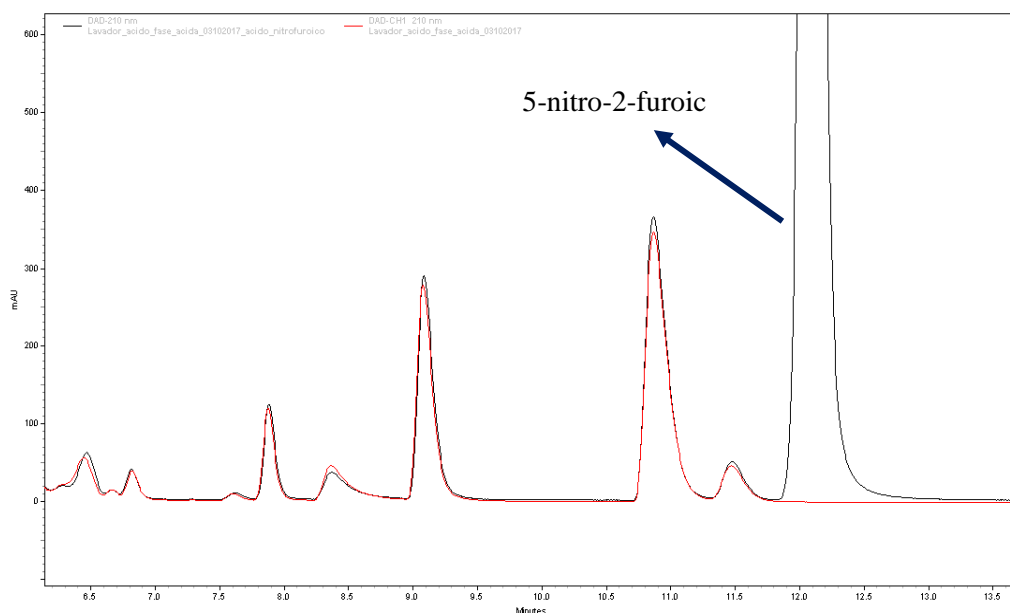


Figure C.10 – Acid water HPLC chromatogram. Red line – industrial sample; black line – 5-nitro-2-furoic acid-added industrial sample.

In order to ascertain the nature of the detected but unidentified chemical species, a test was done, which consisted of adding KMnO_4 to an industrial sample. By this way, it was expected to visualize an area decay of the organic (dicarboxylic acids) chromatographic peaks. The gotten chromatogram is illustrated in Figure C.11.

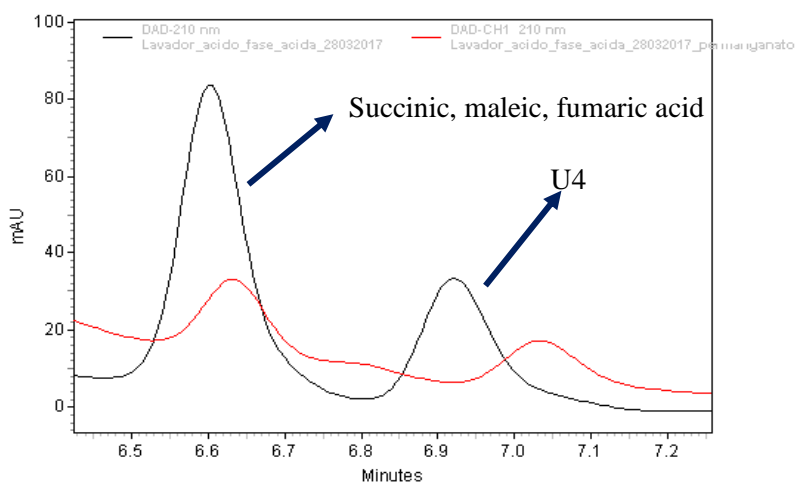


Figure C.11 – Acid water HPLC chromatogram. Black line – industrial sample; Red line – industrial sample + KMnO_4 .

Analysing the figure above it is clearly seen an area decay of the chromatographic peaks after adding KMnO_4 to the industrial sample. The area decrease is more evident than what is noticed

in the chromatogram because the industrial sample was diluted 10 times while the industrial sample to which KMnO_4 was added was only diluted two times. Nevertheless, a conclusion can be withdrawn from this test, which is that some of the unidentified peaks correspond to dicarboxylic acids.

C.4. Repeatability of the analytical method

A preliminary repeatability study was done to assess the viability of employing the developed analytical methodology for quantifying the oxidation intermediates in different plant locations. In this study, three replicates of different plant locations were analysed, although ten (or more) are advised. The achieved results are presented in Table C.3 and Table C.4.

For quantifying the detected unidentified chemical species, fumaric acid calibration curve was used (Figure C.12).

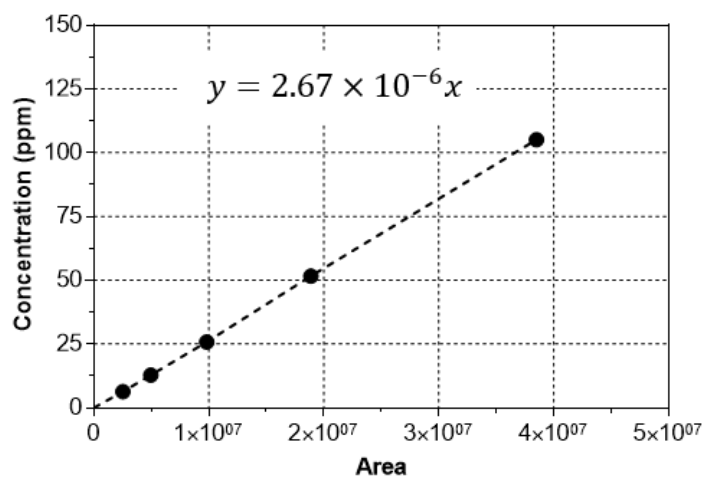


Figure C.12 – Fumaric acid standard curve.

The analysis of both Table C.3 and Table C.4 allows to state that the p -value for the different analytes and sampling locations is higher than 0.05. This is indicative that no significant differences exist between the gotten values [11], indicating the validity of the method for analysing these chemical species.

Decomposition Reactions in Aromatic Nitration

Table C.3 – *p*-value of the analysed samples from different plant locations. Samples collected in March 17th.

Sampling point	Compound	p-value
Mixed acid	Oxalic acid	0.628
	Fumaric acid	0.121
	U2	0.113
	U4	0.191
	U5	0.101
	U6	0.122
Reactor's acid phase	Oxalic acid	0.225
	Fumaric acid	0.613
	U2	0.284
	U4	0.280
	U5	0.170
	U6	0.613
Reactor's organic phase	Oxalic acid	0.333
	Fumaric acid	0.504
	U2	0.534
	U4	0.249
	U5	0.162
	U6	0.505
Crude MNB	Oxalic acid	0.401
	Fumaric acid	0.292
	U2	0.736
	U4	0.320
	U5	0.466
	U6	0.297
Acid water	Oxalic acid	0.567
	Fumaric acid	0.587
	U2	0.166
	U4	0.618
	U5	0.499
	U6	0.587

Table C.4 – *p*-value of the analysed crude MNB samples collected in March 9th.

Sampling point	Compound	p-value
Crude MNB	Oxalic acid	0.065
	Fumaric acid	0.381
	U2	0.605
	U4	0.535
	U5	0.537
	U6	0.381

C.4. References

- [1]. Vignoli, J. A.; Bassoli, D. G., Determinação de ácidos carboxílicos e fenólicos em café solúvel utilizando HPLC/DAD. *Revista Analytica* **2007**, 27, 76-79,
- [2]. Costa, T. J. G.; Nogueira, A. G.; Silva, D. C. M.; Ribeiro, A. F. G.; Baptista, C. M. S. G., Nitrophenolic By-Products Quantification in the Continuous Benzene Nitration Process. In *Chemistry, Process Design, and Safety for the Nitration Industry*, American Chemical Society, Washington, DC. ACS Symposium Series, 2013; Vol. 1155, pp 49-60, doi:10.1021/bk-2013-1155.ch004
10.1021/bk-2013-1155.ch004.
- [3]. Alnaizy, R.; Akgerman, A., Advanced oxidation of phenolic compounds. *Advances in Environmental Research* **2000**, 4 (3), 233-244, [https://doi.org/10.1016/S1093-0191\(00\)00024-1](https://doi.org/10.1016/S1093-0191(00)00024-1).
- [4]. Silverstein, R. M.; Webster, F. X.; Kiemle, D. J., *Spectrometric Identification of Organic Compounds*. 7th Edition, John Wiley & Sons, Inc., New York, USA, 2005.
- [5]. Käkölä, J.; Alén, R., A fast method for determining low-molecular-mass aliphatic carboxylic acids by high-performance liquid chromatography–atmospheric pressure chemical ionization mass spectrometry. *Journal of Separation Science* **2006**, 29 (13), 1996-2003, 10.1002/jssc.200600106.
- [6]. Niessen, W. M. A., *Liquid Chromatography-Mass Spectrometry*. 3rd edition, CRC Press, New York, 2006.
- [7]. Chen, Z.; Jin, X.; Wang, Q.; Lin, Y.; Gan, L.; Tang, C., Confirmation and determination of carboxylic acids in root exudates using LC–ESI-MS. *Journal of Separation Science* **2007**, 30 (15), 2440-2446, 10.1002/jssc.200700234.
- [8]. Gamoh, K.; Saitoh, H.; Wada, H., Improved liquid chromatography/mass spectrometric analysis of low molecular weight carboxylic acids by ion exclusion separation with

electrospray ionization. *Rapid Communications in Mass Spectrometry* **2003**, 17 (7), 685-689, 10.1002/rcm.971.

- [9]. Frauendorf, H.; Herzsuh, R., Application of High-Performance Liquid Chromatography/Electrospray Mass Spectrometry for Identification of Carboxylic Acids Containing Several Carboxyl Groups from Aqueous Solutions. *European Mass Spectrometry* **1998**, 4 (4), 269-278, 10.1255/ejms.220.
- [10]. Käkölä, J.; Alén, R.; Pakkanen, H.; Matilainen, R.; Lahti, K., Quantitative determination of the main aliphatic carboxylic acids in wood kraft black liquors by high-performance liquid chromatography–mass spectrometry. *Journal of Chromatography A* **2007**, 1139 (2), 263-270, <https://doi.org/10.1016/j.chroma.2006.11.033>.
- [11]. Minitab, Example of getting and interpreting a p-value. 2018.

Appendix D – Phenol in mixed acid benzene nitration systems

D.1. Introduction

Figure D.1 shows a sketch of the jacketed laboratorial batch reactor used. Before the start of each reaction, sulfuric acid was added to the reactor by its top (valve V-5) and the thermostatic bath (MPCK6) from Huber (E-2) was turned on. Then, when the temperature of the reaction medium was the intended one, nitric acid was added, again by the reactor's top (valve V-5). Throughout the aqueous phase heating or cooling, the stirrer was working to promote the acids mixture and the homogenization of the reaction medium composition and temperature. When the intended reaction temperature was reached, the stirring speed was adjusted to the defined value and the organic substrate was added, through the reactor's bottom (valve V-3), by means of a 100 mL syringe. The injection time was about 5 seconds and after half of the organic substrate has been injected, the reaction time started to be counted.

During the reaction time samples were collected from the reactor's bottom by means of valve V-4. Valve V-6 was kept closed to avoid both the pressure loss of the system and the contact with the atmosphere during the tests. The temperature of the system was recorded using a Therna 1 thermometer from ETI Ltd.

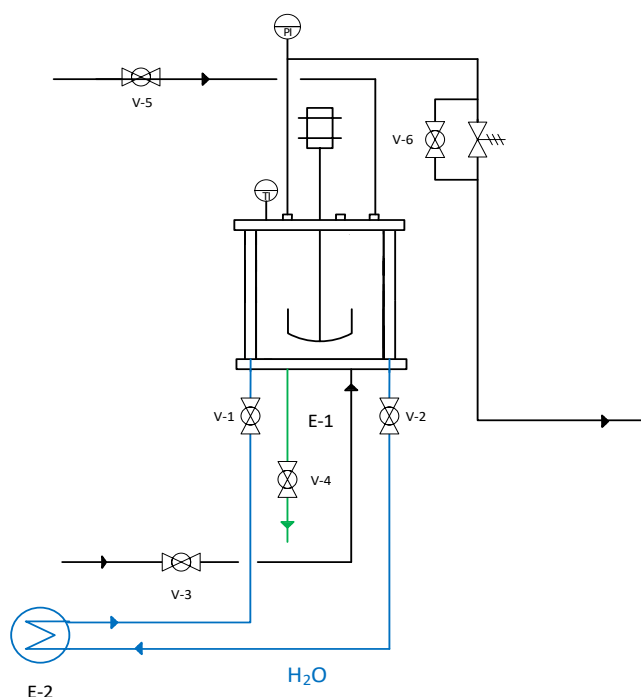


Figure D.1 – Scheme of the laboratorial reactor used in the batch reactions.

D.2. Results and Discussion

Preliminary tests

For the Ph-added Bz solutions, Ph's consumption profiles were subjected to a preliminary repeatability study. Due to the reaction conditions employed, neither the temperature profile is shown (isothermal conditions) nor the nitric acid consumption (smooth conditions wouldn't favour Bz nitration). The tests conditions were the following (cf. Table 4.1): initial temperature = 15 °C, 39 wt.% H₂SO₄, 2 wt.% HNO₃, and 1204 r.p.m.

The achieved results are given in Figure D.2 and show concentration profiles with similar behaviour, being almost overlapped for the employed conditions.

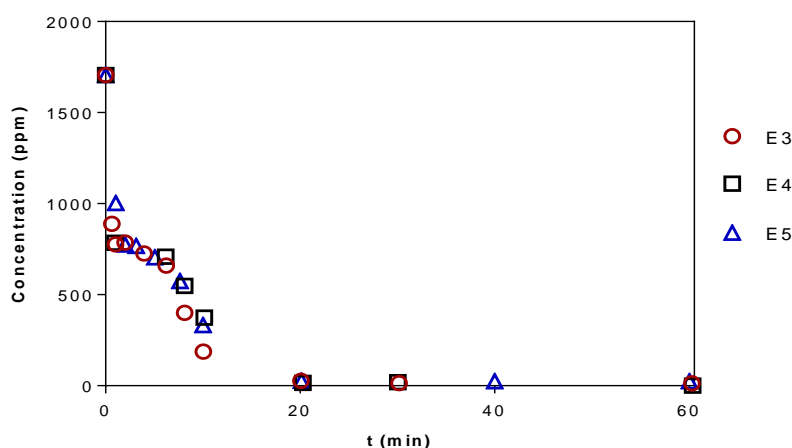


Figure D.2 – Phenol concentration profiles for the runs E3, E4 and E5 ($T_{\text{initial}} = 15\text{ °C}$; H₂SO₄ = 39 wt.%; HNO₃ = 2 wt.%). Analysis of the organic phase.

Phenol-added benzene solution nitration in soft reaction conditions

For the Ph-added Bz solutions nitration at low temperature, nitric acid consumption (for Bz nitration) is not expected to occur in high extent. To confirm this hypothesis, Bz and MNB concentrations were analysed during the reaction time – Figure D.3. The results are indicative that Bz nitration is minimal once MNB concentration is below 0.6%.

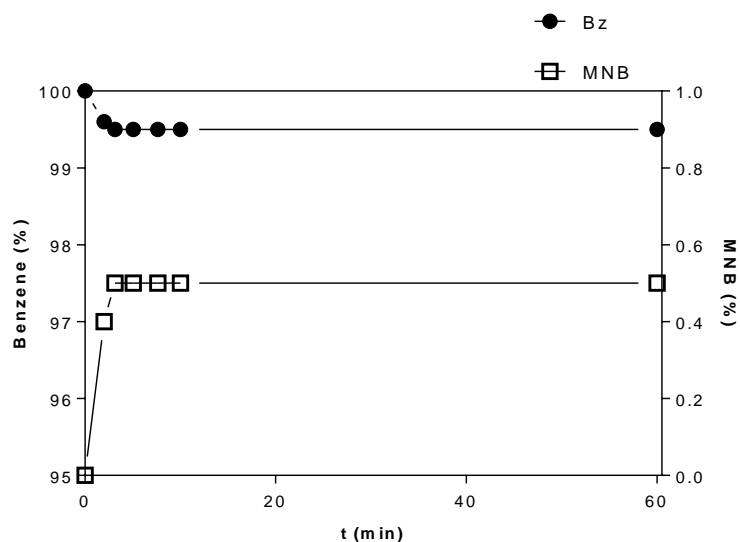


Figure D.3 – GC analysis for run E3. Reaction conditions: $T_{\text{initial}} = 15\text{ }^{\circ}\text{C}$, $\text{H}_2\text{SO}_4 = 39\text{ wt.}\%$, $\text{HNO}_3 = 2\text{ wt.}\%$.

Phenol-free benzene laboratory nitrations

In Figure D.4 are depicted some of the chromatograms obtained during test E6. As it can be seen, in the acid phase all the phenolic by-products chromatographic peaks are well spaced and resolved. Regarding the organic phase chromatogram, it is visible that TNP and 4-MNP retention times are very close to each other, but that did not invalidate the chromatographic peaks integration and identification.

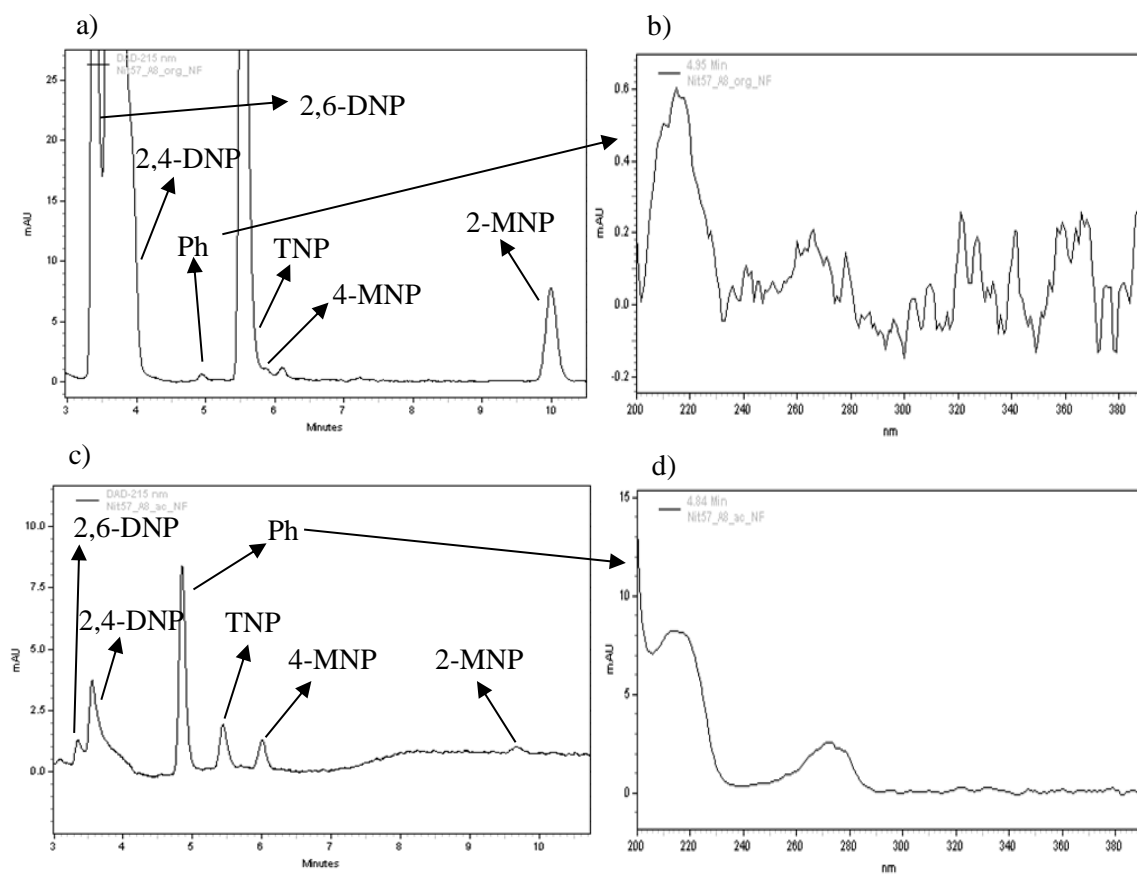


Figure D.4 – Run E6. **a)** Organic phase HPLC chromatogram. **b)** Corresponding Ph's UV-Vis spectrum. **c)** Acid phase HPLC chromatogram. **d)** Corresponding Ph's UV-Vis spectrum. Sample collected 30 minutes after the reaction start. Reaction conditions: $T_{\text{initial}} = 90\text{ }^{\circ}\text{C}$, $\text{H}_2\text{SO}_4 = 60\text{ wt.}\%$; $\text{HNO}_3 = 5\text{ wt.}\%$.

Appendix E – (Nitro)benzenesulfonic acids in nitrobenzene production

E.1. Benzenesulfonic acid identification

Aiming to clarify BSA identification two HPLC-MS analysis were performed, a first one of an industrial crude MNB sample which was then added with a BSA standard. The achieved results are depicted in Figure E.1 and show an area increase for the chromatographic peak identified as BSA (retention time ≈ 7.7 minutes). Additionally, comparing the obtained mass spectra in both analysis, it is noticeable that they display the same molecular ion. Such fact is indicative that BSA is indeed present in benzene nitration plant.

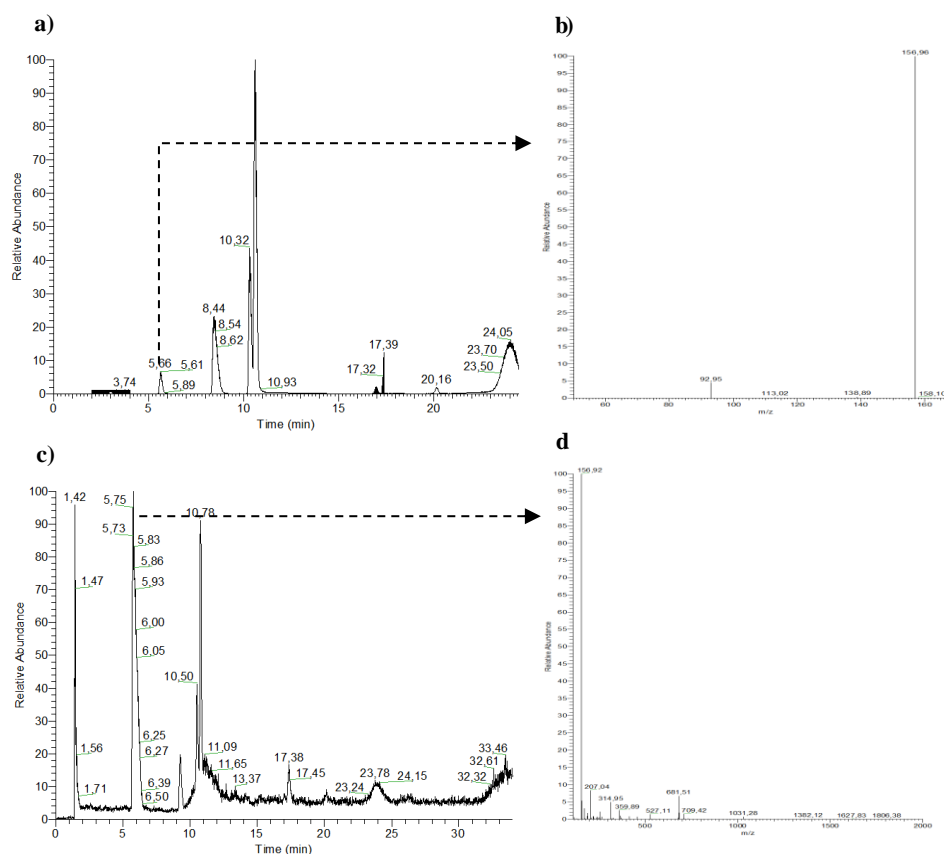


Figure E.1 – Total ion chromatogram for **a)** crude MNB sample, **c)** crude MNB sample added with BSA. Mass spectra from BSA in **b)** crude MNB sample, **d)** crude MNB sample added with BSA.